UNIVERSITY FOR DEVELOPMENT STUDIES

UNSTEADY MAGNETOHYDRODYNAMICS HEAT AND MASS TRANSFER THROUGH POROUS MEDIA

MUSAH SULEMANA

2019

UNIVERSITY FOR DEVELOPMENT STUDIES

UNSTEADY MAGNETOHYDRODYNAMICS HEAT AND MASS TRANSFER THROUGH POROUS MEDIA

BY

MUSAH SULEMANA

(M.Sc. Industrial Mathematics)

(UDS/DMS/0018/14)

THESIS SUBMITTED TO MATHEMATICS DEPARTMENT, FACULTY OF MATHEMATICAL SCIENCES, UNIVERSITY FOR DEVELOPMENT STUDIES IN PARTIAL FULFILMENT OF THE REQUIREMENTS FOR THE AWARD OF DOCTOR OF PHILOSOPHY IN MATHEMATICS

JULY, 2019

DECLARATION

Student's Declaration

I hereby declare that this thesis is the result of my own original research and that no part of it has been presented for another degree in this University or elsewhere.

Student's Signature……

Date…….

Student's Name: MUSAH SULEMANA

Supervisors' Declaration

We hereby declare that the preparation and presentation of the thesis was supervised in accordance with the guidelines on thesis laid down by the University for Development Studies.

Principal Supervisor's Signature……..

Date:…….....

Name: Prof. Yakubu Ibrahim Seini

Co-Supervisor Signature……

Date:……..

Name: Dr. Mohammed Ibrahim Daabo

Approved by

Head of Department: Dr. Kwara Nantomah

Signature…….. **Date:…….**

ABSTRACT

Unsteady heat and mass transfers are important transport phenomena that are found in many engineering and industrial applications. In such systems, the variations in the fluid flow result in variations in the heat flux for fluid-solid temperature difference. In this study, analytical and theoretical investigations of some non-linear problems arising from unsteady heat and mass transfer through porous media are considered. Analytical models are developed. These are non-linear mathematical models for unsteady boundary layer flow past a vertical plate in the presence of heat source and transverse magnetic field embedded in a porous medium; non-linear mathematical models for unsteady hydromagnetic convective heat and mass transfer past an impulsively started infinite vertical surface with Newtonian heating in porous medium; and non-linear mathematical models for unsteady hydromagnetic boundary layer flow over an exponentially stretching flat surface in a porous chemically reactive medium. These mathematical models are developed to measure the effects of unsteadiness and other physio-chemical parameters (such as radiation effects, mass diffusion, buoyancy forces, Lorentz force, velocity ratio, momentum diffusion, porous medium, chemical species, etc.) in the flow in order to understand heat and mass flow in porous media and to be able to predict related processes. These models are solved in exact form employing Laplace Transform Techniques. One major observation is that the magnetic field parameter is effective in reducing flow. The study concluded that all the controlling parameters have effects on the flow and can be used to control the flow kinematics in practice.

ACKNOWLEDGEMENTS

In preparing this thesis, I have received invaluable help from several people. The thesis owes its success to the assistance and contributions of many individuals. I wish to record my sincere gratitude to my supervisor Prof. Yakubu Ibrahim Seini, Head of Mechanical and Industrial Engineering Department, University for Development Studies, Nyankpala Campus and my co-supervisor Dr. Mohammed Ibrahim Daabo, Head of Computer Science Department, University for Development Studies, Navrongo Campus for their guidance, suggestions and encouragement. May God bless them.

My special thanks also go to Dr. Mohammed Iddrisu Muniru, Vice Dean, Faculty of Mathematical Sciences, Dr. Musah Rabiu and Dr. Baba Seidu, all of University for Development Studies, Navrongo Campus for their useful suggestions and encouragement.

I am also indebted to my parents Hajia Mariama Issahaku and Mr. Sulemana Alhassan (late) for their immense contribution in my education.

I say a big thank you to my lovely wives Mrs. Zenabu Abubakari and Mrs. Fatima Bintu Adam, my children Musah Mujaab Maltiti, Musah Zakir Wunnum, Musah Shamima Nasara, Musah Naadirah Saha and Musah Aabid Sachiri for their patience and encouragement given me to accomplish this task.

Above all, my greatest thanks go to Almighty Allah for his provision of life throughout the duration of my course of study in the University for Development Studies.

DEDICATION

This thesis is dedicated to my family and friends.

TABLE OF CONTENTS

LIST OF TABLES

LIST OF FIGURES

NOMENCLATURE

y^*	Coordinate axis normal to the plate [m]
y	Dimensionless coordinate axis normal to the plate [-]
x^*	Coordinate axis in the direction of the plate [m]
x	Dimensionless coordinate axis in the direction of the plate [-]
u^*	Velocity component in x^* direction $[ms^{-1}]$
u	Dimensionless velocity in x direction [-]
v*	Velocity component in y^*direction $[ms^{-1}]$
v	Dimensionless velocity in y direction[-]
U_0	Velocity of the plate $[ms^{-1}]$
t^*	Time (s)
t	Dimensionless time [-]
T^*	Fluid temperature near the plate $[K]$
T_w^*	Fluid temperature at the plate surface $[K]$
T_∞^*	Temperature of the free stream $[K]$
g	The acceleration due to gravity $[ms^{-2}]$
C^*	Concentration in the fluid [Kmolm^{-3}]

C_{∞}^{*}	Concentration far away from the plate [Kmolm^{-3}]
C_{w}^{*}	Concentration at the plate surface [Kmolm^{-3}]
a^{*}	Absorption parameter [-]
a	Acceleration parameter [-]
D	Chemical molecular diffusivity [$m^{-2}s^{-1}$]
C_p	Specific heat at constant pressure [$JKg^{-1}K^{-1}$]
K_c^{*}	Rate of chemical reaction [-]
K_c	Dimensionless rate of chemical reaction [-]
k^{*}	Permeability co-efficient of the porous medium [m^2]
k	Dimensionless permeability co-efficient of the porous medium [-]
q_r	Radiation heat flux [-]
Q	Heat source parameter [-]
F	Radiation parameter [-]
M	Magnetic parameter [-]
H	Heat absorption parameter [-]
A	Constant [-]
B_0	Uniform external magnetic field [Telsa]

S_0	Soret number [-]
S_c	Schmidt number [-]
P_r	Prandtl number [-]
N_u	Nusselt number [-]
Gr	Thermal Grashof number [-]
Gc	Mass Grashof number [-]
E_c	Eckert number [-]
Erf	Error function [-]
Erfc	Complementary error function [-]
β_T	Thermal expansion coefficient [K^{-1}]
β_C	Concentration expansion co-efficient [K^{-1}]
ρ	Fluid density [kgm^{-3}]
v	Kinematic viscosity [m^2s^{-1}]
$\propto$	Thermal diffusivity [m^2K^{-1}]
θ	Dimensionless temperature [-]
$\emptyset$	Dimensionless concentration [-]
μ	Dynamic viscosity [$kgm^{-1}s^{-1}$]
τ	Skin friction coefficient [-]
σ	Electrical conductivity [sm^{-1}]
K	Thermal conductivity of the fluid [$Wm^{-1}k^{-1}$]

ACRONYMS

MHD: Magnetohydrodynamics

HM: Hydromagnetic

BL: Boundary Layer

BLF: Boundary Layer Flow

L: Laplace Transform

L^{-1}: Inverse Laplace Transform

LTT: Laplace Transform Technique

LTM: Laplace Transform Method

s: Laplace transform parameter

ODEs: Ordinary Differential Equations

PDEs: Partial Differential Equations

δ: Dirac delta function

CHAPTER ONE

INTRODUCTION AND BACKGROUND STUDIES

1.0 Introduction

Heat and mass transfer occur naturally in almost all physical phenomena in life. It is argued that no meaningful work can be done without the transfer of heat and mass. In many situations, the transfer of heat and mass occur with varying time which results in unsteady processes.

Heat transfer can be defined as a process of transporting heat from a high temperature reservoir to a low temperature reservoir. In terms of the thermodynamic system, heat transfer is the movement of heat across the boundary of the system due to temperature difference between the system and the surroundings. Heat transfer can also take place within the system due to temperature differences at various points inside the system. The difference in temperature provides the potential for the heat to flow and the heat itself is called a flux, Figure 1.1.

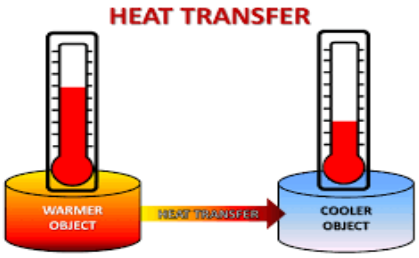

Figure 1. 1 Heat Transfer between two Objects

The effects of heat and mass transfers on unsteady flow of fluid in porous media have a wide range of engineering and industrial applications. It is commonly encountered in the flow of molten iron, recovery extraction of crude oil and in geothermal systems (Kathyayani et al., 2016). Free convection flow induced by thermal and solutal buoyancy forces acting over bodies with different geometries in a fluid saturated porous medium in the presence of magnetic field is also prevalent in many physical presence of pure air or varied and wide range of industrial applications. For example, in atmospheric flows, the presence of pure air or water is impossible because some foreign mass may be present either naturally or mixed over various geometrical bodies with air or water due to industrial emissions (Barik, 2016).

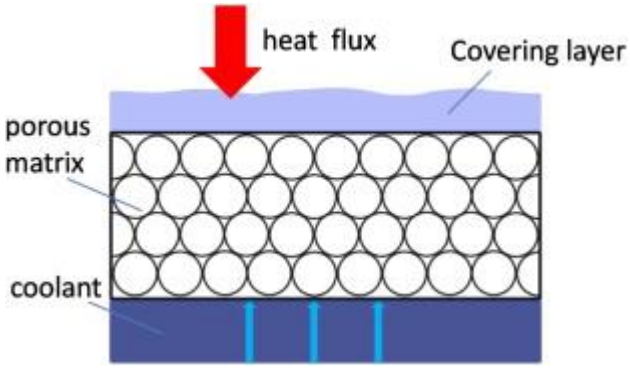

Figure 1. 2 Heat Flux through Porous Media

Also, during manufacturing processes, stretching sheets (metallic and polymer) interact with the ambient fluid thermally and mechanically. Both the kinematics of stretching

and simultaneous heating or cooling during such process has direct influences on the quality of the final products (Magyari & Keller, 1999, Ali et al., 2014).

Rout and Pattanayak (2013) indicated that MHD flow with heat and mass transfer in the presence of chemical reactions are of importance in many practical processes such as distribution of temperature and moisture over agricultural fields, energy transfer in wet tower and in the method of generating and extracting power from moving fluids.

In most cases, the processes involve unsteady flow due to the time dependence factor. Some researchers and scientist have developed different control strategies to understand the dynamics of unsteady process. However, it is a unending effort as many cases of varied conditions are still facing industry players. Unsteady boundary layer flow has become topical in recent times due to its numerous applications. It is encountered in the design and operation of heat exchangers, thermal power plants, boilers, fins, condensers, solar radiation devices, etc.

Unsteady (time-varying) heat transfer is also important in transport phenomena found in many engineering devices such as microscale cooling schemes for microprocessor chips, conventional internal combustion engines, compressors and expanders (Mathie et al., 2012). Furthermore, in many transportation processes where heat and mass transfer occur simultaneously as a result of thermal diffusion and diffusion of chemical species, the combined action of buoyancy forces occur. These processes are observed in the nuclear reactor

safety and combustion systems, solar collectors, and in metallurgical and chemical engineering processes (Barik, 2016).

The appreciation of unsteady heat and mass transfer effects is a significant factor in the development of a number of clean and renewable energy technologies (Mathie et al., 2012). The relevance of these devices in industrial or domestic settings will increase as the cost of conventional energy sources continue to rise due to the ever increasing price of oil (Darby, 1982, Adelman, 1991).

The unsteady boundary layer flow is relevant in several engineering problems like start-up processes, periodic fluid motion and in the area of convective heat and mass transfer. During unsteady flow, the boundary layer exhibits different behaviors owing to the inclusion of time dependent parameters which influence the pattern of fluid motion leading to boundary layer separation which creates complexity in the solution system. These flows exhibit other interesting phenomena which will be discussed in this study.

Many research works have reported solved problems involving two dimensional unsteady flow cases for different flow configurations. However, the solutions are often mainly restricted to similarity or self-similar ones because of the consequence of the mathematical difficulties involved in achieving the non-similarity solutions though some few research is available using the non-similar solutions. Fluid properties often vary significantly with respect to temperature in the circumstances where large or moderate temperature gradients exist across the

fluid medium. Also, different studies have been reported for variable fluid properties (Das et al., 2012, Misra et al., 2012, Ali et al., 2014).

Mass transfer from a wall slot into the boundary layer is of interest for various prospective applications together with thermal protections, energizing the inner portion of boundary layer in adverse pressure gradient and skin friction reduction on control surfaces. The effect of uniform mass transfer applied in an unsteady convection boundary layer flow with variable viscosity has also been investigated by some authors (Ali, 2006, Chin et al., 2007). The effects of porous media are however an emerging area where more research is continuing.

This study aims at developing a simple mathematical framework to understand and predict unsteady heat and mass transfer in porous media. This framework is applied to several hydromagnetic convection flows. The study builds on the works of Chaudhary and Jain (2006), Misra et al., (2012) and Chamkha et. al. (2016).

Chaudhary and Jain (2006) studied unsteady free convection boundary layer flow past an impulsively started vertical surface with Newtonian heating. The thesis extends this work to include porous medium with chemical species concentration and transverse magnetic field.

Chamkha et al. (2016) studied unsteady MHD free convection flow past an exponentially accelerated vertical plate with mass transfer, chemical and thermal radiation. This study extends their work by incorporating a nonlinear

velocity term with MHD in the temperature equation as it is of practical importance in many industrial applications.

Misra et al. (2012) studied unsteady boundary layer flow past a stretching plate and heat transfer with variable thermal conductivity. The study extends their work to include chemical reactants and permeability of the medium on a stretching surface.

1.1 Background to the Study

Unsteady flow problems are encountered in flow over helicopter blades in translational motion, flow over blades of turbines and compressors, flow over the aerodynamic surfaces of vehicles in manned flight, etc. (Chaudhary & Jain, 2006).

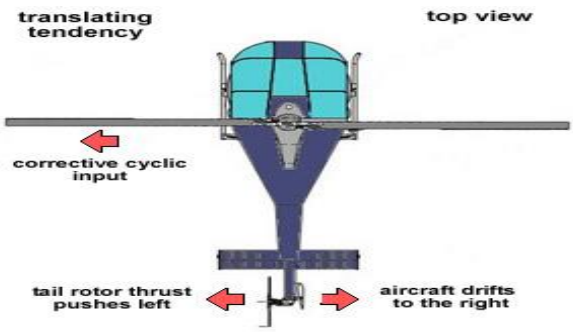

Figure 1. 3 Helicopter flight controls (source:en.Wikipedia.org)

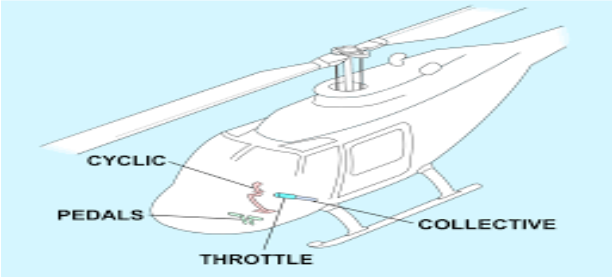

Figure 1. 4 Helicopter in translation motion (source: www.pilotfriend.com)

When an helicopter takes off, air builds around it resulting into unsteady processes. This mass flow of air needs to be determined by unsteady flow analysis so as to ensure that the helicopter attains a translational motion (Figure 1.3 & Figure 1.4). Translating motion is defined as the tendency for a single rotor helicopter to drift laterally, due to tail rotor thrust.

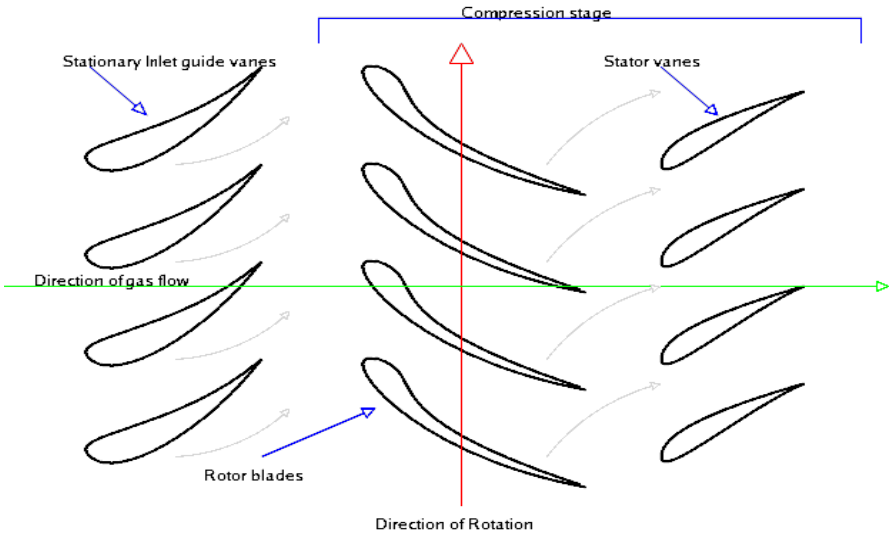

Figure1.5 Jet engine compressor design
(source: www.aerospaceengineringblog.com)

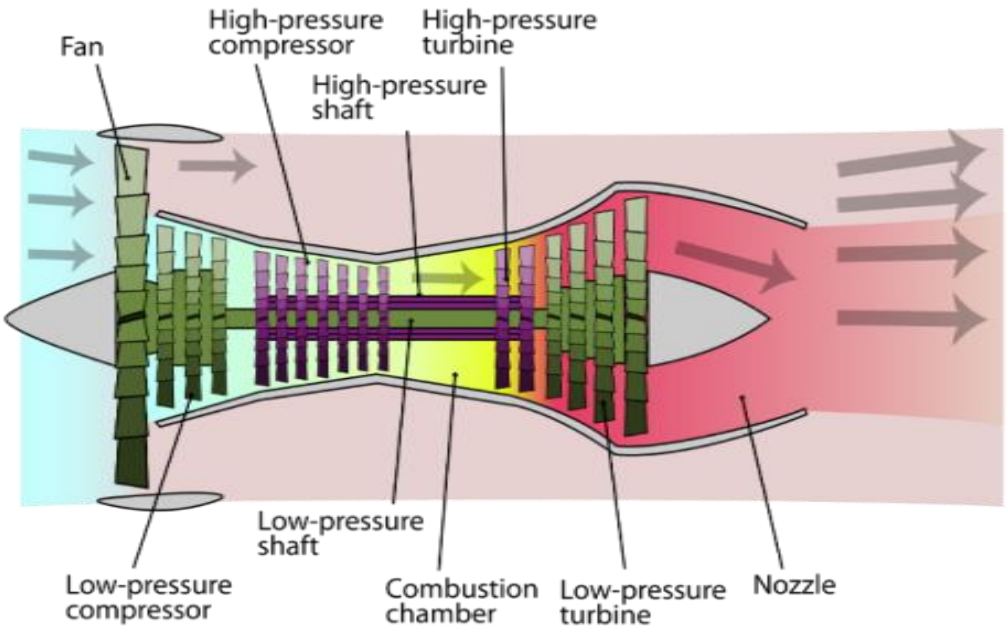

Figure 1. 6 A schematic diagram of a high bypass turbofan engine (source: turbofan-wikipedia)

In figure 1.5, the mass flow of the gas is directed toward a stationary inlet guide vanes. The rotor blades control the direction of the gas flow hence build unsteady processes that need to be determined for the compressor to function effectively.

In figure 1.6, air flows in the turbine. The non- uniform cross section of the turbine brings about unsteady processes that must be controlled.

Also, mass transfer from a wall slot into the boundary layer is of interest for various prospective applications (see figure 1.7).

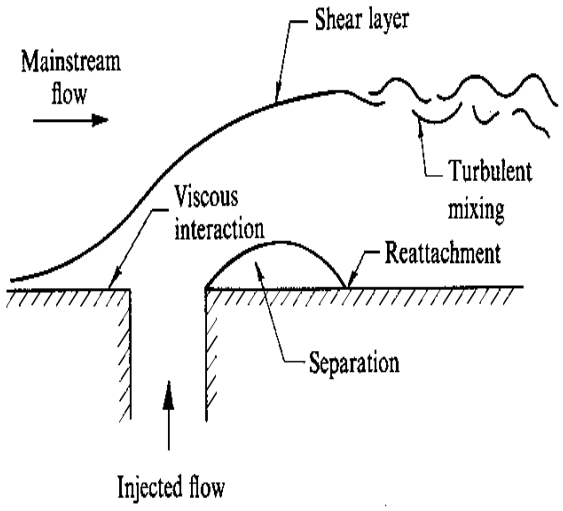

Figure 1. 7 Mass transfer from a slot to a boundary layer
(source:en.Wikipedia.org)

The injection of fluid from a wall slot into the boundary layer, viscosity interaction is experienced hence producing turbulence which results in unsteady processes.

Analytical models are developed for the unsteady heat and mass transfer problems instead of numerical methods since numerical methods make parametric investigation difficult due to the long execution time.

1.2 Categories of Flow

1.2.1 Steady flow

If a flow is such that the properties at every point in the flow do not vary over time, then the flow is said to be a steady flow. Mathematically,

$$\frac{\partial P}{\partial t} = 0$$

where P is any property like pressure, velocity or density. Thus,

$$P = P(x, y.z)$$

1.2.2 Unsteady flow

Unsteady or non-steady flow is one where the properties change over time.

That is $\frac{\partial P}{\partial t} \neq 0$ and $P = P(x, y.z, t)$

The unsteadiness in the flow field is caused either by time dependent motion of the external stream or by impulsive motion of the external stream. When the fluid motion over a body is created impulsively, the inviscid flow over the body is developed instantaneously but the viscous layer near the body is developed slowly and it becomes fully developed steady state viscous flow after certain instant of time (Chaudhary & Jain, 2006).

Unsteadiness in heat transfer introduces several effects into the heat transfer problem. The first effect is 'augmentation'; an improvement or deterioration in heat transfer performance relative to an equivalent steady problem. The other effect is 'conjugation' which occurs when the temperature fluctuations in solid domain as well as the fluid domain become important in the solution of the heat transfer problem. These two effects combined with boundary conditions make

unsteady heat transfer more challenging compared to steady problems (Mathie et al., 2012).

1.2.3 Pseudosteady Flow

Some flows, though unsteady, become steady under certain frames of reference. These are called pseudosteady flows.

Unsteady flows are undoubtedly difficult to solve while with steady flows, we have one degree of freedom less complexity.

1.2.4 Uniform and Non-uniform flow

The flow is uniform when in the flow field the velocity and other hydrodynamic parameters do not change from point to point at any instant of time. For uniform flow, the velocity is a function of time only. Thus;

$$v = v(t)$$

1.3 Heat and Mass Transfer

Heat transfer is the exchange of thermal energy between physical systems. The rate of heat transfer is dependent on the temperatures of the systems and the properties of the intervening medium through which the heat is transferred. Mass transfer is the net movement of mass from one location, usually meaning stream,

phase, fraction or component, to another. Mass transfer occurs in many processes, such as absorption, evaporation, adsorption, drying, precipitation, membrane filtration, and distillation.

1.4 Porous Media

A porous medium or a porous material is a material containing pores (voids). The skeletal portion of the material is often called the "matrix" or "frame" (figure 1.7). The pores are typically filled with a fluid (liquid or gas). The skeletal material is usually a solid, but structures like foams are often also usefully analyzed using concept of porous media.

A porous medium is most often characterised by its porosity. Other properties of the medium (e.g., permeability, tensile strength, electrical conductivity) can sometimes be derived from the respective properties of its constituents (solid matrix and fluid) and the media porosity and pores structure, but such a derivation is usually complex. Even the concept of porosity is only straightforward for a poro-elastic medium.

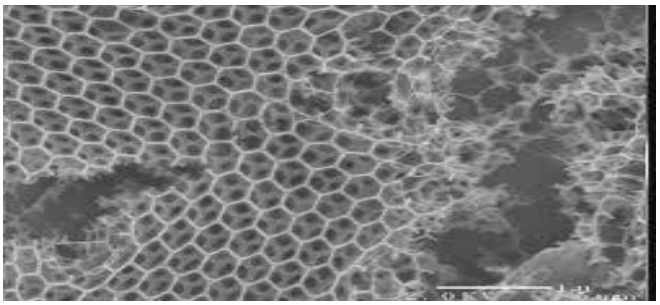

Figure 1. 8 Porous medium (source en.Wikipedia.org)

The use of porous materials as efficient and compact heat exchangers for heat dissipation is under extensive research. Amongst these, high porosity, open cell metal foams shown in Fig.1.8 has emerged as one of the most promising materials for thermal management applications where a large amount of heat needs to be transferred over a small volume. This is attributed to the high surface area to volume ratio as well as enhanced flow mixing (convection) due to the tortuosity of metal foams in Fig. 1.9. The surface area to density ratio of metal foams is roughly 1000–3000 m2/m3 (Bhaskar and Chaudhary, 2016).

Figure 1. 9 Heat transfer application of metal foam (Bhaskar and Chaudhary 2016)

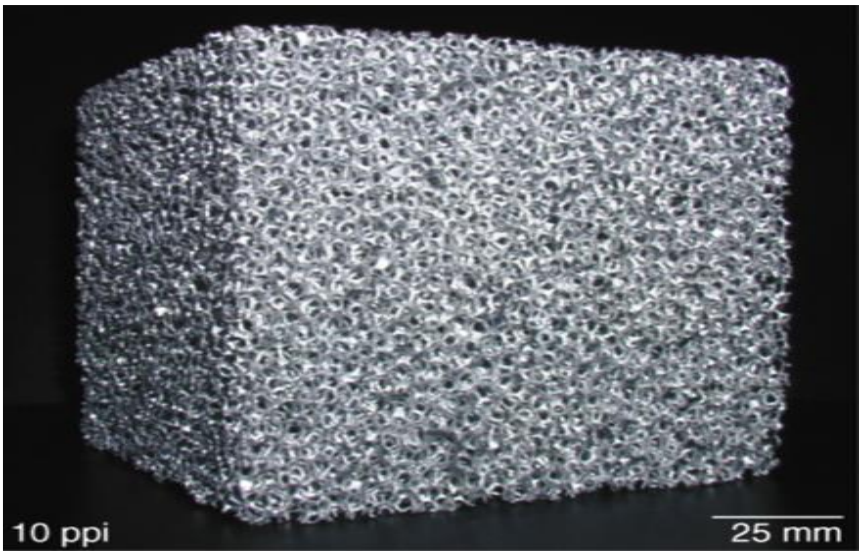

Figure 1. 10 A foam sample manufactured by sintering route (Bhaskar and Chaudhary 2016)

Natural and artificial porous materials encountered in practice are soil,

sandstone, limestone, ceramics, foam, rubber, bread, lungs, and kidneys.

Aquifers (from where water is pumped), sand filters (for purifying water), reservoirs (which yield oil or gas), packed and fluidized beds in the chemical engineering and the root zone in agricultural industry may serve as additional examples of porous media domains (Amhalhel & Furmanski, 1997).

The study of transport phenomena in porous materials has attracted considerable attention, and has been motivated by a broad range of engineering applications including:

1. Agricultural applications: e.g. fermentation process in food industries, freeze drying of food products, grain storage, soil heating to increase the growing season.

2. Environmental applications: e.g. ground water pollution, ground water systems, storage of radioactive waste, water movement in geothermal reservoirs.

3. Industrial applications: e.g. artificial freezing of ground as a structural support and as a water barrier for construction and mining purposes, crude oil production and recovery systems, porous radiant burners (PRBs), post accident heat removal (PAHR), solidification of castings, study of heat transfer phenomenon of buried electrical cables and transformer cables, fluidized bed combustion.

4. Thermal conversion and storage systems: e.g. catalytic reactors, geothermal systems, packed beds, fluidized bed, heat pipes, sensible, latent and thermo chemical energy storage systems (Amhalhel & Furmanski, 1997).

1.5 Problem statement

There are several heat and mass transfer problems already tackled in the literature. However, there are many areas in which research is continuing especially with respect to unsteady flow conditions as it is the most common flow situation in many industrial and manufacturing processes. The use of magnetic fields in flow control find applications in magneto-hydrodynamics, generators, plasma studies, nuclear technology, geothermal energy extractions, continuous coating, rolling and extrusion in manufacturing processes. The boundary layer along a film in condensation processes and the aerodynamic extrusion of plastic sheets are areas of active research. The unsteady heat and mass transfer through a porous medium is still undergoing extensive research which this study aims to contribute to.

1.6 Aim of study

The aim of the study is to investigate theoretically some nonlinear problems arising from unsteady boundary layer flow in porous media.

1.6.1 Specific Objectives

Specifically, the study will

- Develop a non-linear mathematical model for unsteady boundary layer flow past an exponentially accelerated vertical plate in the presence of transverse magnetic field and heat source embedded in a porous medium.
- Develop non-linear mathematical model for unsteady hydromagnetic convective heat and mass transfer past an impulsively started infinite vertical surface with Newtonian heating in porous medium in industrial and engineering systems.
- Develop a non-linear mathematical model for unsteady hydromagnetic boundary layer flow over an exponentially stretching flat surface in a porous chemically reactive medium.
- Provide analytical solutions for nonlinear systems of differential equations modeling boundary layer flow in porous media.
- Develop a theoretical framework for predicting the effects of controlling parameters on the velocity, thermal and concentration boundary layer thicknesses of unsteady flow.

1.7 Significance of study

Boundary layer has a pronounced effect upon any object which is immersed in a fluid. Drag on airplanes or ships and friction in pipes are common manifestations of boundary layer. There has been great interest in the study of magnetohydrodynamics (MHD) flow interaction with heat and mass transfer in any medium due to the effects of magnetic field on the boundary layer flow control and on the performance of many systems using electrically conducting fluids. Studying this type of flow is significant due to its applications in many engineering problems. Understandably, boundary layer research has become a very important branch of fluid dynamics.

1.8 Expected Contribution

This study makes the following contributions:

- Investigate the unsteady boundary layer flow in a porous medium. The study investigated some problems arising from laminar unsteady boundary layer flow interaction with heat and mass transfer in a porous medium as it finds practical application in areas such as in mechanical, mining process and chemical engineering.
- Provide information on the nature of unsteady boundary layer developed on heated porous plate in the presence of chemical contaminants.

- Serve as reference material for future works in the areas of nuclear studies, manufacturing, mining, petro-chemical, aerospace and automotive sectors.

1.9 Organization of Thesis

This thesis is organized in seven chapters. In chapter 1, the background, importance of the problem chosen and clear statement of the problem are established. A brief review of literature on heat and mass transfer as well as porous media is discussed in this chapter. The objectives of the study; significance of the study and expected contribution are also discussed in this chapter.

In chapter 2, a detail literature review on heat and mass flow in porous media; free convection over flat surfaces; hydromagnetic flow in porous media; flow control strategies as well as unsteady flow in porous media are presented.

Chapter 3 shows the development of mathematical models. The flow boundary layer equations such as the continuity equation, momentum equation, energy equation and the concentration equation are derived in this part. The dimensional partial differential equations are transformed into dimensionless equations using dimensionless variables and parameters. Laplace transform technique is employed to solve the dimensionless equations in exact form.

Chapter 4 presents unsteady boundary layer past a vertical plate in the presence of magnetic field and heat source embedded in a porous medium.

Chapter 5 deals with unsteady hydromagnetic convective heat and mass transfer past an impulsively started infinite vertical surface with Newtonian heating in a porous medium.

Chapter 6 discusses unsteady boundary layer flow over an exponentially stretching flat surface in a chemically reactive porous medium.

Summary, conclusions and recommendations are provided in chapter 7. The thesis ended in this chapter with summary of key findings, contribution to knowledge and recommendations for future research.

CHAPTER TWO

LITERATURE REVIEW

2.0 Introduction

The chapter presents a review of research on heat and mass transfer through a porous media. It highlights the various research results reported by different authors. The review focuses on flow in porous media, free convection, hydromagnetic fluid flow, unsteady flow in porous media, flow on stretching surfaces and flow control strategies. The review identifies some gaps in knowledge and presents how this thesis will address those gaps.

2.1 Overview of Heat and Mass Transfer in Porous Media

Heat and mass transfer occur simultaneously in several processes such as hot rolling, wire drawing, continuous casting, fiber drawing, evaporation of water at surfaces, drying etc. Heat and mass transfer characteristics are dependent on the thermal boundary conditions. In general, there are four common heating processes specifying the wall-to-ambient temperature distributions, prescribed surface heat flux distributions, conjugate conditions where heat is specified through a bounding surface of finite thickness and finite heat capacity. The interface temperature is not known a priori but depends on the intrinsic properties

of the system, namely the thermal conductivity of the fluid and solid (Chaudhary & Jain, 2006).

Megahed et al. (2011) investigated the effects of thermal-diffusion (Soret) and the diffusion-thermo (Dufour) effects, temperature-dependent viscosity, thermal conductivity on Falkner-Skan heat and mass transfer flow of a viscous, incompressible and electrically conducting fluid over a wedge immersed in a porous media. The results showed that the velocity profiles decrease with increasing Dufour number (or decreasing Soret number) for all η values. The temperature increases whilst the concentration decreases with increasing Dufour number (or decreasing Soret number).

Samiulhaq et al. (2012) studied radiation and porosity effects on the magnetohydrodynamic flow past an oscillating vertical plate with uniform heat flux using Laplace transforms. It was observed that the radiation parameter reduces the temperature of the fluid. Bhattacharyya (2012) conducted a research on slip effects on steady boundary layer flow and mass transfer with chemical reaction over a permeable flat plate in a porous medium using shooting method to solve the resulting equation. It was observed that the momentum boundary layer thickness is reduced for increased in permeability and suction parameters, whereas it increases with blowing parameter. The increase of velocity slip parameter reduces the momentum boundary layer thickness and also enhances

the mass transfer from the plate. Also, due to increase of mass slip, the concentration and mass transfer decreased.

Aziz et al. (2014) studied steady boundary layer slip flow along with heat and mass transfer over a flat porous plate embedded in a porous medium. The similarity variables were employed to transform the governing partial differential equations (PDEs) into ordinary differential equations (ODEs) which were solved numerically using specific method implemented in MATLAB. The results showed that an increase in permeability of porous medium increases the velocity and decreases the temperature profile. This happened due to a decreased in drag of the fluid flow. In case of heat transfer, the increase in permeability and slip parameter caused an increase in heat transfer. However for the case of increase in thermal slip parameter, there is a decrease in heat transfer. An increase in mass slip parameter causes a decrease in the concentration field.

Etwire et al. (2015) investigated the MHD thermal boundary layer flow over a flat plate with internal heat generation, viscous dissipation and convective surface boundary conditions using the fourth order Runge Kutta algorithm with a shooting method. It was realized that the velocity boundary layer thickness decreases as the magnetic field parameter increases. Also increasing the Biot number, internal heat generation parameter, Prandtl number and Brinkman number have no effect on the skin friction coefficient whilst increasing the magnetic field parameter decreases the skin friction coefficient.

Recently, Barman et al. (2017) studied heat transfer through porous media using Newton's Law of cooling and Fourier's Law. It was seen that with increases of thickness of porous layer and Reynolds number, the rate of heat transfer increases along the flow direction. All these studies dealt with steady flow. In this work, unsteady heat and mass transfer through porous media is considered.

2.2 Unsteady Flow in Porous Media

With the exception of a small number of cases involving steady flows, majority of flows in industrial and engineering applications are unsteady. Bala et al. (2012) studied the radiation effects on unsteady MHD flow past an exponentially accelerated isothermal vertical plate embedded in porous medium in the presence of heat source and chemical reaction using a crank-Nicolson's type of implicit finite difference method with a tri-diagonal matrix manipulation and an iterative procedure in the solution. Their study established a direct correlation between the Grashof number, G_r and the velocity of the flow. Rout and Pattanayak (2013) extended the problem to include variable temperature embedded in a porous medium using Laplace transform techniques and observed that the temperature of the fluid increases with increasing radiation parameters.

Chiem and Zhao (2004) conducted a research on numerical study of steady/unsteady flow and heat transfer in porous media using a characteristics-

based matrix-free implicit Finite-Volume (FV) method on unstructured grids. Hydrodynamic and heat transfer results were reported for both steady and transient flow cases. The effects of Darcy and Reynolds numbers on heat transfer augmentation and pressure loss were studied. At high Reynolds numbers the flow in the porous channel exhibits cyclic characteristics although unlike the non-porous channel flow, the cyclic vortex development is only restricted to small area behind the last solid block, while temperature changes more slowly and do not exhibit cyclic variations over a long period of time.

Mishra et al. (2015) conducted a research on numerical investigation on unsteady heat and mass transfer effect of micro-polar fluid over a stretching sheet through porous media. Similarity transformations were used to convert the governing time dependent, non-linear boundary layer equations into a system of non-linear ordinary differential equations that were solved numerically using Runge-Kutta fourth order method with shooting technique. They observed that the buoyancy force retards the fluid near the velocity boundary layer in case of opposing flow and is favourable for assisting flow. In case of assisting flow, the absence of porous matrix enhances the flow. Also, Hussanan et al. (2016) studied unsteady heat and mass transfer in a micro-polar fluid with Newtonian heating. Exact solutions were obtained using Laplace transform technique. It was observed that plate executes cosine type oscillations. Chamkha et al. (2016) studied unsteady MHD free convection flow past an exponentially accelerated vertical plate with

mass transfer, chemical and thermal radiation using Laplace transform technique. The fluid considered in their study was gray gas, absorbing/emitting radiation but non scattering medium. They concluded that the velocity increased with increase in either the acceleration coefficient 'a' or the Soret number S_0.

Uddin et al. (2015) studied similarity solution of an unsteady heat and mass transfer boundary layer flow over a continuous layer flow in a porous medium with hydromagnetic field using similarity solution coupled with shooting technique. It was realized that the velocity and temperature in the unsteady case is observed to be lesser than those of the steady case. Also, an increase in unsteadiness parameter increases the Prandtl number (Pr) and decreases the Eckert number (Ec).The heat transfer rate increases rapidly with the increase of the power law index of the surface temperature variation whereas when the magnetic parameter increases the heat transfer rate decreases.

Kathyayani et al. (2016) studied heat and mass transfer on unsteady MHD oscillatory flow of non-Newtonian fluid through porous medium in parallel plate channel. A mathematical model was developed and analyzed by using perturbation technique. The results showed that the lower the permeability the lesser the fluid speed in the entire fluid region. Also, the temperature reduces with increasing radiation parameter (F), whereas the reversal behaviour is observed throughout the fluid region with increasing Prandtl number (Pr).

In the foregone studies, it is obvious that research in unsteady magnetohydrodynamic (MHD) through porous media is continuing due to its emerging industrial relevance. This thesis therefore considers unsteady boundary layer flow past a vertical plate in the presence of transverse magnetic field and heat source embedded in porous medium which has not been documented in the literature to the best of my knowledge. The problem would be investigated using Laplace transform techniques.

2.3 Free Convection Flow on Flat Surfaces

Theoretical studies on the laminar natural convection heat transfer on flat surfaces continue to receive attention in the literature due to their industrial and technological applications. Siegel (1958) studied the unsteady free convection flow past a semi-infinite vertical plate under step-change in wall temperature or surface heat flux using the momentum integral method. He observed that the initial behaviour of the temperature and velocity fields for semi-infinite vertical flat plate is the same for double infinite vertical flat plate. Martynenko et al. (1984) extended Siegel work to include a constant temperature of the plate which is also the temperature of the surrounding stationary fluid.

Gupta et al. (1979) employed the perturbation method to investigate the free convection flow past a linearly accelerated vertical plate in the presence of viscous dissipation with Kafousias and Raptis (1981) extending it to include

mass transfer effects subject to variable suction. Arthur et al. (2015) investigated the MHD convective boundary layer flow towards a vertical surface in a porous medium with radiation, chemical reaction and internal heat generation using the Newton Raphson shooting method alongside the Fourth-order Runge - Kutta algorithm and concluded that the magnetic parameter and all the controlling parameters identified directly influence the flow around the boundary and hence can be controlled to achieve desired product characteristics.

At high temperatures, heat transfer caused by radiation is very crucial in many industrial applications such as in rocket propulsion systems, plasma physics, and in aerothermodynamics. As a result, some researchers have considered radiation effects in convection flows. It must be noted that heat transfer characteristics are dependent on the thermal boundary conditions. Hence in Newtonian heating, the rate of heat transfer from the boundary surface with finite heat capacity is proportional to the local surface temperature and this process is called conjugate convective flow. This configuration occurs in many engineering devices such as heat exchangers, fins and solar radiation devices (Chaudhary & Jain, 2006). In these cases, it is necessary to consider convective flows with Newtonian heating. Chaudhary and Jain (2006) studied the unsteady free convection boundary-layer flow past an impulsively started vertical surface with Newtonian heating using the Laplace transform techniques and observed that the increase of Prandtl number results in decrease in temperature distribution.

Narahari and Nayan (2011) considered the free convection flow past an impulsively started infinite vertical plate with Newtonian heating in the presence of thermal radiation and mass diffusion. The exact solutions in a closed-form were obtained by the Laplace transform method with an observation that the velocity increased for aiding flows but decreased for opposing flows. Radiation effects on unsteady free convection flow past a vertical plate with Newtonian heating was reported by Das et al. (2012). The governing equations were solved numerically by implicit finite difference method of Crank-Nicolson's type. It was observed that the velocity decreases near the plate and increases away from the plate with increasing Prandtl number or radiation parameter. Sharidan et al. (2014) studied the slip effects on unsteady free convective heat and mass transfer with Newtonian heating using the Laplace transform method and observed that the presence of the slip parameter reduces the fluid velocity.

Hussanan et al. (2014) studied unsteady boundary layer flow and heat transfer of a Casson fluid past an oscillating vertical plate with Newtonian heating using laplace transform technique. It was observed that velocity decreases as casson parameters increases and the thermal boundary layer thickness increases with increasing Newtonian heating parameter.

In the literature, it is obvious that most of the studies focused on radiation effects on convection flows. Heat and mass transfer of unsteady hydromagnetic convection flows with Newtonian in porous medium has not been reported. In

this thesis, it is proposed to study the unsteady hydromagnetic convective heat and mass transfer flow past an impulsively started infinite vertical plate with Newtonian heating in porous medium. This is an extension of research done by Chaudhary and Jain (2006) to include porous medium, concentration, chemical species and transverse magnetic field.

2.4 Flows on Stretching Surfaces

Fluid flow over a stretching surface has numerous applications in many engineering processes such as wire drawing, paper production, hot rolling, glass fibre production, manufacturing of plastic and rubber sheets, cooling of hot metal plates, etc. These processes require the material to be stretched and involve heat transfer between the sheet and the fluid medium. The quality of the final product largely depends on the rate at which the cooling and stretching occurs. Furthermore, the mechanical properties of the final product depend on the thermal conductivity which is assumed to vary linearly with temperature (Chaudhary and Jain, 2006).

Sakiadis (1961) pioneered the research in the boundary layer flow over a continuous solid surface moving with constant velocity. Crane (1970) extended the study of Sakiadis (1961) to the flow on an elastic sheet moving in its own plane with a velocity linear to the distance from a fixed point.

Chiam (1998) studied the boundary layer flow of viscous fluid over a porous stretching sheet and heat transfer with variable thermal conductivity using shooting method and noticed that thermal conductivity enhances the temperature of the fluid. Misra et al. (2012) extended the work of Chiam (1998) by considering the heat flow problem in two ways. That is, Prescribed Stretching Surface Temperature (PST) and Prescribed Stretching Heat Flux (PHF).

Chen (1998) studied the fluid flow and heat transfer on a stretching plate. Ishak et al. (2008) extended the work of Chen (1998) to hydromagnetic flow and heat transfer and they observed that as the magnetic field increases, the skin friction coefficient and the Nusselt number decreased.

Dandpat and Chakraborthy (2010) studied the effects of variable fluid properties on thin liquid film flow over an unsteady heated stretching sheet. It was observed that the effect of variable fluid viscosity on velocity profile of the fluid flow increases when viscosity decreases due to decrease of temperature along the stretching surface. Hsiao (2011) studied the MHD stagnation point flow of visco-elastic fluid on thermal forming stretching sheet with viscous dissipation effect and observed that the rate of heat transfer decreased with the increasing magnetic field.

Nadeem et al. (2013) discussed the fluid properties of MHD casson fluid past a linearly stretched sheet in porous medium using Runge-Kutta-Fehlberg method. They observed that the presence of the transverse magnetic field decreases the

velocity of the fluid flow. Seini (2013) studied the flow over an unsteady stretching surface with chemical reaction and non-uniform heat source using the Runge–Kutta–Fehlberg method with the shooting techniques and observed that heat and mass transfer rates as well as the skin friction coefficient increased as the unsteadiness parameter increases and decreased as the space-dependent and temperature-dependent parameters for heat source/sink increased.

Seini and Makinde (2013) studied MHD boundary layer flow due to exponential stretching surface with radiation and chemical reaction using Runge–Kutta–Fehlberg method with the shooting techniques. A nonlinear velocity term with MHD was present in the temperature equation due to the presence of the magnetic field. It was found that the rate of heat transfer at the surface decreases with increasing values of the transverse magnetic field and the radiation parameter.

Ali et al. (2014) studied heat transfer boundary layer flow past an inclined stretching sheet in presence of magnetic field using Runge-Kutta fourth-fifth (RK-45) order method along shooting technique, where the flow was generated due to linear stretching sheet. Again, a nonlinear velocity term with MHD was present in the temperature equation due to the magnetic effects in the flow. It was found that velocity profile decreases due to increase of magnetic parameter, Prandtl number and Eckert number whilst velocity increases for increasing values of Grashof number. On the other hand the temperature profile increases

in the presence of the magnetic parameter, angle of inclination, Prandtl number, Eckert number and Chandrasekhar number whilst temperature decreases for increasing Grashof number. The results have possible technological applications in liquid-based systems involving stretchable materials

Recently, Sahoo and Biswal (2015) studied MHD visco-elastic boundary layer flow past a stretching plate with heat transfer and concluded that higher Prandtl number fluid causes a fall in temperature due to low thermal diffusivity.

The focus of thesis is to investigate the unsteady boundary layer flow past a stretching plate in the presence of transverse magnetic field with heat and mass transfer in a porous medium, which is an extension of the work done by Ali et al. (2014) to include unsteady parameter, porous medium and chemical species in the flow.

2.5 Hydromagnetic Flow in Porous Media

Hassanien (1989) studied oscillatory hydromagnetic flow through a porous medium in the presence of free convection and mass transfer flow using Laplace transform technique. It was found that the velocity increases when the permeability of porous medium (k) increases. Also, the velocity increases when the concentration difference between the surface and the free stream increases whilst the magnetic parameter (M) increases the velocity decreases.

Kamel (2000) examined thermal-diffusion effect on rotating hydromagnetic flow in porous media. A complete analytical solution was obtained for the temperature, concentration and velocity fields using Laplace transformation and the method of direct integration by means of the matrix exponential (state space approach) in the case when the plate oscillates in its plane. The results showed that Prandtl number (Pr) makes the temperature distribution concentrate near the boundary layer and the flow field is greatly affected by the variation of the rotating parameter near the plate.

Ramakrishnan and Shailendhra (2011) investigated theoretically hydromagnetic flow through uniform channel bounded by porous media. The fluid flowing in the channel was assumed to be homogenous, incompressible and Newtonian. Analytical solutions were constructed for the governing equations using Beavers- Joseph slip boundary conditions. It was observed that the axial velocity of the fluid is reduced by porous parameter, Hartman number and slip parameter. It was also noticed that there was a reversal of the flow near the wall due to change in the Darcy velocity and slip velocity. Shear stress, however, shows an increasing porous parameter and a decreasing trend with the increasing Hartman number.

Norzieha et al. (2012) conducted a research on hydromagnetic rotating flow in a porous medium with slip condition and hall current. The closed form solution was obtained using Laplace transform technique. It was found that the magnetic

field and slip parameter decreased the velocity magnitude whereas permeability and Hall parameter increased it. The slip and magnetic field play an important role in retarding the growth of both the primary and secondary flows, whereas Hall parameter enhances the flow.

Chand et. al (2012) examined hydromagnetic oscillatory flow through a porous medium bounded by two vertical porous plates with heat source and Soret effect. The plates of the channel were subjected to constant injection and suction velocities. Close form solutions were obtained. The results shown that the velocity profiles increase with increasing Reynolds number (R_e) which is in confirmation with the fact that if R_e is large the inertial forces will be predominant and the effect of viscosity will confined only to the thin region adjacent to the solid surface. Also, for heavier species, i.e. increasing Schmidt number (Sc=0.22 for hydrogen and Sc=0.66 for oxygen), the velocity decreases. The temperature profile increases with increasing heat source parameter and the frequency of oscillation ω and it decreases with increasing Prandtl number (Pr).

Gireesha et al. (2015) studied numerical solution for hydromagnetic boundary layer flow and heat transfer past a stretching surface embedded in non-Darcy porous medium with fluid particle suspension. The time–dependent equations, governing the flow and heat transfer were reduced into a set of non-linear ordinary differential equations with the aid of suitable similarity transformations. The transformed equations were numerically integrated using forth- fifth order

Runge-Kutta-Fehlbeg method. It was observed that by suspending fine dust particles in the clean fluid reduces the thermal boundary layer thickness. Therefore, the dusty fluids are preferable in engineering and scientific applications involving cooling processes.

Kan et al. (2015) studied hydromagnetic flow and heat transfer over a porous oscillating stretching surface in a visco-elastic fluid with porous medium. This system was solved numerically using the finite difference scheme, in which a coordinate transformation is used to transform the semi-infinite physical space to a bounded computational domain. The study reveals that an oscillatory sheet embedded in the saturated porous medium generates oscillatory motion in the fluid. It was also found that the amplitude of the flow velocity increases with increasing visco-elastic and mass suction/injection parameters but decreases with increasing strength of the applied magnetic field. Moreover, the temperature of the fluid is a decreasing function of visco-elastic parameter, mass suction/injection parameter and Prandtl number.

2.6 Flow Control Strategies

Flow control strategies imply a small change of configuration serving an ideally large engineering benefit, like drag reduction, lift increase, mixing enhancement or noise reduction (Wikipedia, the free encyclopedia, 2017).

A new change in research in fluid dynamics is to take a step from analyzing and predicting the flow field to actively controlling it. In fluid dynamics systems, variations of flow parameters may be achieved by local perturbations using devices sensing and acting on some critically chosen parts of the flow, the process often requiring small amounts of energy. Such control devices can be used to obtain drag reduction on bodies, heat and mass transfer reduction or enhancement, increase propulsion efficiency, increase lift on wings, control of generation of sound, control of combustion instabilities etc (Engineering Archives).

In fact the ability to manipulate a flow field to effect a desired change is of immerse practical importance. Flow control is perhaps more hotly pursued by scientists and engineers than other areas in fluid mechanics (Gal-el-Hak, 1996). It might be worth recalling that a mere 10% reduction in the total drag of an aircraft translates into a saving of one billion dollars in annual fuel cost for the commercial fleet in the United States alone (Gal-el-Hak, 1996).

The science of flow control originated with Prandtl, who in a mere 8-page manuscript introduced the boundary layer theory, explaining the physics of the separation phenomena and described several experiments in which a boundary layer was controlled. Gad-el-Hak (1996) studied modern developments in flow control. The study concluded that the developments in chaos control, micro-fabrication and neural networks are making it more feasible to perform reactive

control of turbulent flows. Also, flow control is most effective when applied near the transition or separation points or near the critical regimes where flow instabilities magnify quickly.

Meunier (2009) studied stimulation and optimization of flow control strategies for Novel High-lift configurations using a Kriging-based optimization algorithm. It was found that a careful parameterization of the jet is capable of an efficient control strategy and leads to a complete reattachment of the flap flow, with considerable gains in lift and aerodynamic efficiency.

Mathelin et al. (2010) studied closed-loop fluid flow control using a low dimensional model. Their main objective was to develop a control strategy to minimize the drag of a bluff body in a 2-D flow. A reduced model was obtained using a robust statistical reduction approach and an optimal orbit in the phase space was determined using an open-loop control strategy. The non-linear reduced order model was linearized around a set of points defining a series of 'trust-regions' along the closed trajectory and the problem was put under a linear varying parameter form, allowing for the use of an efficient control law synthesis.

Sipp and Schmid (2013) examined closed-loop control of fluid flow, a review of linear approaches and tools for the stabilization of the transitional flows. Two generic flow configurations were considered: the two-dimensional flow over an open cavity, which is above a critical Reynolds number is globally unstable and

the two-dimensional flow over a backward –facing step, which is globally stable but acts as an amplifier of ambient noise sources. However, the study concluded that Galerkin-based approached is efficient for globally unstable flows, where an internal instability synchronizes the flow and makes it insensitive to external noise sources. Also, a data-based model is suitable for globally stable noise-amplifier flows.

Oruc (2017) conducted a research on strategies for the applications of flow control downstream of a bluff body. The problem is unsteady and vortical flow structure developing downstream of the body. The chaotic flow structure in the wake causes serious structural deformation on the body hence the flow is intended to be suppressed downstream of the body. It was found that suppression of vortex shedding can be achieved adopting flow control techniques such as passive or active control schemes which are effective tools for taming the flow.

CHAPTER THREE

METHODOLOGY

3.0 Introduction

In this chapter, various models such as the continuity equation, momentum equation, energy equation and concentration equation are developed. These equations are modified in subsequent chapters to model the unsteady heat and mass transfer through porous media. The governing partial differential equations are developed and transformed to dimensionless equations using suitable dimensionless parameters and variables. These dimensionless equations are solved in exact form using Laplace transform technique. The results of these models are presented graphically and quantitatively in subsequent chapters using MATLAB computer software.

3.1 Assumptions Made in Models Development

In developing the appropriate mathematical models, the following **assumptions** are made:

- The flow is unsteady.
- A magnetic field of uniform strength B_0 is applied transversely to the plate.
- The flow is assumed to be in the $x^* - axis$ direction.

- The y^* −axis is taken to be normal to the plate.
- The temperature of the plate and the ambient fluid are $T_w^*(x)$ and T_∞^* respectively. Initially, the plate and the fluid are at the same temperature T_∞^* with concentration level C_∞^* at all points.
- The fluid physical properties such as viscosity and thermal conductivity shall be assumed constant.
- Reynolds number and viscous dissipation are also assumed to be negligible.
- Since the plate is infinite along the x^* direction, all the physical variables are the functions of y^* and t^* only.
- Using Boussinesq approximation, neglecting the inertia terms, Soret and Dufour effects, under these assumptions, the boundary layer equations governing the unsteady flow process can be modeled as shown in the following sections and subsequent chapters:

3.1.1 The Continuity Equation

The continuity equation is obtained in Cartesian coordinates as (see Appendix I, A1.6)

$$\frac{\partial \rho}{\partial t^*} + \frac{\partial \rho u^*}{\partial x^*} + \frac{\partial \rho v^*}{\partial y^*} + \frac{\partial \rho w^*}{\partial z^*} = 0. \qquad (3.1)$$

Introducing the gradient operator, ∇, which in rectangular coordinates, is

$$\nabla = \frac{\partial}{\partial x^*}\hat{i} + \frac{\partial}{\partial y^*}\hat{j} + \frac{\partial}{\partial z^*}\hat{k}. \quad (3.2)$$

Therefore, the non-conservation form of the continuity equation is

$$\frac{D\rho}{Dt^*} + \rho\nabla.U^* = 0. \quad (3.3)$$

Where the velocity field, $U^* = u^*\hat{i} + v^*\hat{j} + w\hat{k}$; $\nabla.U^*$ is the divergence of the velocity and ρ is fluid density.

3.1.2 The Momentum Equation

The momentum equation is obtained from Navier-Stokes equations in conservation form (see Appendix I, A1.29) as

$$\rho\frac{DU^*}{Dt^*} = -\nabla p + \rho g + \mu\nabla^2 U^*. \quad (3.4)$$

In component form,

$$\rho\frac{Du^*}{Dt^*} = -\frac{\partial p}{\partial x^*} + \frac{\partial x^* x^*}{\partial x^*} + \frac{\partial \tau_{y^* x^*}}{\partial y^*} + \frac{\partial z^* x^*}{\partial z^*} + \rho \boldsymbol{g}_{x^*}. \quad (3.5)$$

$$\rho\frac{Dv^*}{Dt^*} = -\frac{\partial p}{\partial y^*} + \frac{\partial \tau_{x^* y^*}}{\partial x^*} + \frac{\partial \tau_{y^* y^*}}{\partial y^*} + \frac{\partial z^* y^*}{\partial z^*} + \rho \boldsymbol{g}_{y^*}. \quad (3.6)$$

$$\rho\frac{Dw^*}{Dt^*} = -\frac{\partial p}{\partial z^*} + \frac{\partial \tau_{x^* z^*}}{\partial x^*} + \frac{\partial \tau_{y^* z^*}}{\partial y^*} + \frac{\partial \tau_{z^* z^*}}{\partial z^*} + \rho \boldsymbol{g}_{z^*}. \quad (3.7)$$

where $\tau_{x^*x^*}, \tau_{y^*x^*}, \tau_{z^*x^*}, \tau_{x^*y^*}, \tau_{y^*y^*}, \tau_{z^*y^*}, \tau_{x^*z^*}, \tau_{y^*z^*}, \tau_{z^*z^*}$ are shear stress components.

Equations (3.5) - (3.7) are scalar equations and are also called Navier-Strokes equations. Since the flow is taken along the vertical surface in the upward direction, the force of gravity is crucial as it produces buoyancy effects in the flow. The atmospheric pressure is distributed equally in all directions in a free stream flow and hence can be considered negligible. The Navier-Stokes equation, in that case, reduces to

$$\rho\left(\frac{\partial u^*}{\partial t^*} + u\frac{\partial u^*}{\partial x^*} + v\frac{\partial u^*}{\partial y^*}\right) = -\frac{\partial p}{\partial x^*} + \mu\frac{\partial^2 u^*}{\partial y^{*2}} + \rho g. \tag{3.8}$$

The fluid flow experiences Lorenz force which impedes the fluid velocity due to the presence of the magnetic field. As a result, the charged particles in the fluid experienced an induced electric field, $u^* \times B_0$. Using Ohm's law and neglecting the Hall effects, the magnitude of the current density for the weakly ionized fluid is given by

$$j = \sigma(-u^* \times B_0). \tag{3.9}$$

In this thesis, a magnetic field of uniform strength B_0 is applied transversely to the plate. Also, assuming that U^* and σ are uniform, then

$$j = \sigma B_0 u^*. \tag{3.10}$$

The presence of the transverse magnetic field causes movements of a conducting material in fluid which generates electric current, j. Each unit volume of the liquid having j current and B_0 magnetic field strength experiences MHD force, $j \times B_0$ called Lorenz force which reduces the motion of the fluid flow to

$$j \times B_0 = \sigma B_0^2 u^*. \tag{3.11}$$

3.1.3 The Energy Equation

The rate of change of energy inside the fluid element for incompressible viscous fluid flow is given (see Appendix I, A1.47) by

$$\rho \frac{De^*}{Dt^*} = \rho \dot{q} + K\left(\frac{\partial^2 T^*}{\partial x^{*2}} + \frac{\partial^2 T^*}{\partial y^{*2}} + \frac{\partial^2 T^*}{\partial z^{*2}}\right) + \Phi. \tag{3.12}$$

Where

Φ is the dissipation function, which, in rectangular coordinates is

$$\Phi = 2\mu\left[\left(\frac{\partial u^*}{\partial x^*}\right)^2 + \left(\frac{\partial v^*}{\partial y^*}\right)^2 + \left(\frac{\partial w^*}{\partial z^*}\right)^2 + \frac{1}{2}\left(\frac{\partial u^*}{\partial y^*} + \frac{\partial v^*}{\partial x^*}\right)^2 + \frac{1}{2}\left(\frac{\partial u^*}{\partial z^*} + \frac{\partial w^*}{\partial x^*}\right)^2 + \frac{1}{2}\left(\frac{\partial v^*}{\partial z^*} + \frac{\partial w^*}{\partial y^*}\right)^2\right] - \lambda\left(\frac{\partial u^*}{\partial x^*} + \frac{\partial v^*}{\partial y^*} + \frac{\partial w^*}{\partial z^*}\right)^2. \tag{3.13}$$

Where

$\dot{q}$ is the rate of volumetric heat addition per unit mass,

e^* is the internal energy per unit mass of the moving fluid,

λ is the bulk viscosity coefficient and

μ the shear viscosity coefficient.

3.1.4 The Concentration Equation

In vector form, the concentration equation (see Appendix I, A1.52) is

$$\frac{\partial C^*}{\partial t^*} = div(D\ grad\ C^*). \tag{3.14}$$

$$\frac{DC^*}{Dt^*} = D\nabla^2 C^{*2} \pm \dot{r}. \tag{3.15}$$

Where C^* is the species concentration, D is the mass diffusivity and $\dot{r}$ is the rate of species generation $(+r)$ or destruction $(-r)$ which is included due to the chemical species in the fluid.

3.2 Dimensionless variables and parameters

The following dimensionless variables and parameters are used to transform the problem from dimensional equations to dimensionless equations;

$$u = \frac{u*}{U_0},\ v = \frac{v^*}{U_0},\ y = \frac{U_0 y*}{v}, Q = \frac{vQ_0}{U_0^2 \rho C_p}, \theta = \frac{T^* - T_\infty^*}{T_w^* - T_\infty^*},\ t = \frac{t^* U_0^2}{v},\ k = \frac{U_0^2 k^*}{v^2},$$

$$\emptyset = \frac{C^* - C_\infty^*}{C_w^* - C_\infty},\ P_r = \frac{\mu C_p}{k} \text{ or } P_r = \frac{v}{\propto},\quad M = \frac{\sigma B_0^2 v}{\rho U_0^2},\quad G_r = \frac{v\, g\beta_T (T_w^* - T_\infty^*)}{U_0^3},\quad G_C =$$

$$\frac{v\, g\beta_c (C_w^* - C_\infty^*)}{U_0^3} k_c = \frac{v\, k_c^*}{U_0^2},\quad S_0 = \frac{D_1 (T_w^* - T_\infty^*)}{v\,(C_w^* - C_\infty^*)},\quad H = \frac{Qv^2}{kU_0^2},\quad a = \frac{a^* v}{U_0^2},$$

$$A = \frac{U_0^2}{v}, F = \frac{16\sigma a^* v^2 T_\infty^{*3}}{K U_0^2},\ S_c = \frac{v}{D},\quad E_c = \frac{u^2}{C_p (T_w^* - T_\infty^*)} \tag{3.16}$$

3.3 Transformation of the Problem

The transformation process of the problem starts by substituting relevant dimensionless variables and parameters into the governing dimensional partial differential equations as well as the boundary conditions to obtain the

dimensionless temperature, concentration, velocity as well as skin friction, Nusselt number and Sherwood number.

3.4 Analytical Procedure

The non-linear differential equations governing the flow with their corresponding boundary conditions are solved in exact form using Laplace transform technique.

3.4.1 Laplace Transform Technique

To solve differential equations by Laplace transforms, four (4) distinct stages are observed:

- Rewrite the equation in terms of Laplace transform with one of the variables taken as a dummy variable.
- Apply the initial conditions.
- Rearrange the equation algebraically to give the transform of the solution
- Determine the inverse transform to obtain the general solution.

This procedure is used to solve the models in subsequent chapters.

CHAPTER FOUR

UNSTEADY BOUNDARY LAYER FLOW PAST A VERTICAL PLATE IN THE PRESENCE OF TRANSVERSE MAGNETIC FIELD AND HEAT SOURCE EMBEDDED IN A POROUS MEDIUM

4.1 Introduction

An investigation into the unsteady boundary layer flow past a vertical plate in the presence of transverse magnetic field and heat source embedded in a porous medium is studied. The fluid under consideration is **gray gas** which absorbs or emits heat. The governing differential equations are transformed using suitable dimensionless parameters. The dimensionless equations were solved using the Laplace transform technique and results illustrated graphically for the velocity, temperature and concentration profiles as well as the Skin friction, Sherwood number and Nusselt number. The study concludes by exploring the effects of certain controlling parameters on the flow and how these can be used to control the flow kinematics.

4.2 Mathematical Formulation of Unsteady Boundary Layer Flow Past a Vertical Plate

Consider the unsteady boundary layer flow past a vertical plate in the presence of transverse magnetic field and heat source embedded in a porous medium. In addition to the general models' assumptions in chapter three, the flow is assumed to be in the $x^* - axis$ direction which is taken along the vertical plate in the upward direction. At time $t^* > 0$, the plate is exponentially accelerated with a velocity $u^* = U_0 e^{a^* t^*}$ in its own plane and the plate temperature is raised linearly with time t and the level of concentration near the plate is raised to C_w^*. The physical system of the flow is shown in fig. 4.1.

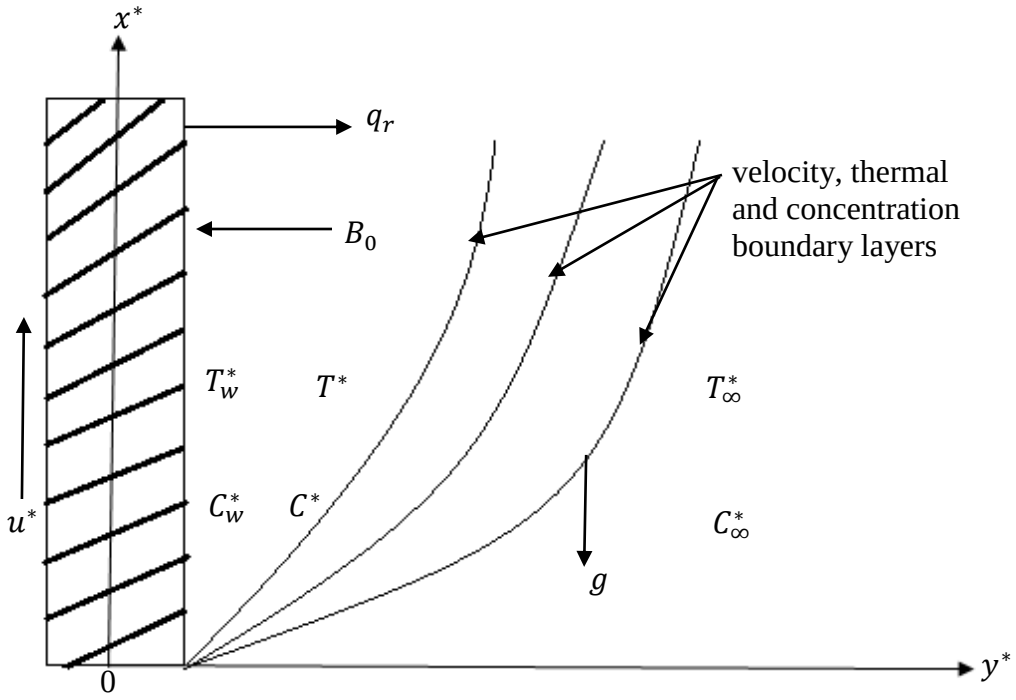

Figure 4. 1 Flow configuration and coordinate system

Under these assumptions, the boundary layer equations governing the unsteady flow process can be modeled as shown in the following sections:

4.2.1 The Continuity Equation of Unsteady Boundary Layer Flow Past a Vertical Plate

The continuity equation of fluid flow is derived in (3.3) as

$$\frac{D\rho}{Dt^*} + \rho\nabla.U^* = 0$$

Considering the substantial derivative (3.1)

$$\frac{D}{Dt^*} = \frac{\partial}{\partial t^*} + \frac{\partial}{\partial x^*} + \frac{\partial}{\partial y^*} + \frac{\partial}{\partial z^*}$$

$\frac{\partial}{\partial z^*} = 0$ since the problem is two-dimensional (2D) hence (3.1) reduces to

$$\frac{D}{Dt^*} = \frac{\partial}{\partial t^*} + \frac{\partial}{\partial x^*} + \frac{\partial}{\partial y^*} \tag{4.1}$$

With corresponding 2D velocity field, $U^* = u^* \hat{i} + v^* \hat{j}$ and its divergence $\vec{\nabla} = \frac{\partial}{\partial x^*} \hat{i} + \frac{\partial}{\partial y^*} \hat{j}$

For incompressible fluid, $\frac{D\rho}{Dt^*} = 0$ (i.e. the density following the path of a fluid element is constant) and by dividing through by ρ, (3.3) becomes $\nabla . U^* = 0$

Hence continuity equation given in equation (4.1) now simplifies to

$$\frac{\partial u^*}{\partial x^*} + \frac{\partial v^*}{\partial y^*} = 0. \tag{4.2}$$

Since the plate is infinite along the x^* − direction, all the physical variables are functions of y^* and t^* only.

Hence the continuity equation in (4.2) reduces to

$$\frac{\partial v^*}{\partial y^*} = 0. \tag{4.3}$$

4.2.2 The Momentum Equation of Unsteady Boundary Layer Flow Past a Vertical Plate

From the Navier-Stokes equation in (3.8)

$$\rho\left(\frac{\partial u^*}{\partial t^*}+u\frac{\partial u^*}{\partial x^*}+v\frac{\partial u^*}{\partial y^*}\right)=-\frac{\partial p}{\partial x^*}+\mu\frac{\partial^2 u^*}{\partial y^{*2}}+\rho g,$$

one introduces the fluid pressure, $-\frac{\partial p}{\partial x^*}=u\frac{\partial u^*}{\partial x^*}+v\frac{\partial u^*}{\partial y^*}$, thermal buoyancy, $g\beta_T(T^*-T_\infty^*)$, concentration buoyancy, $g\beta_C(C^*-C^*_\infty)$, magnetic force, $\sigma B_0^2 u^*$ and porosity term, $\frac{\nu}{k^*}u^*$ into the flow field (3.8) reduces to the momentum equation

$$\frac{\partial u^*}{\partial t^*}=\nu\frac{\partial^2 u^*}{\partial y^{*2}}+g\beta_T(T^*-T_\infty^*)+g\beta_C(C^*-C^*_\infty)-\frac{\sigma B_0^2}{\rho}u^*-\frac{\nu}{k^*}u^*. \qquad (4.4)$$

4.2.3 The Energy Equation of Unsteady Boundary Layer Flow Past a Vertical Plate

The rate of change of energy inside the fluid element for incompressible viscous fluid flow was derived in as (3.12):

$$\rho\frac{De^*}{Dt^*}=\rho\dot{q}+K\left(\frac{\partial^2 T^*}{\partial x^{*2}}+\frac{\partial^2 T^*}{\partial y^{*2}}+\frac{\partial^2 T^*}{\partial z^{*2}}\right)+\Phi$$

In (3.12), the left hand side represents the material derivative whilst the right hand is the rate of change of energy inside the fluid element.

Thus equation (3.12) can be expanded in 2D as

$$\frac{\partial T^*}{\partial t^*}+\left(u\frac{\partial T^*}{\partial x^*}+v\frac{\partial T^*}{\partial y^*}\right)=\propto\left(\frac{\partial^2 T^*}{\partial x^{*2}}+\frac{\partial^2 T^*}{\partial y^{*2}}\right)+\Phi. \qquad (4.5)$$

Since the flow is along the $x^* -$ direction, all the physical variables are functions of y^* and t^* only. Hence for the unsteady flow with magnetic field and radiative heat flux, (4.5) is modified to become

$$\frac{\partial T^*}{\partial t^*} = \alpha \frac{\partial^2 T^*}{\partial y^{*2}} - \frac{1}{\rho c_p}\frac{\partial q_r}{\partial y^*} - \frac{Q}{\rho c_p}(T^* - T^*_\infty) + \frac{\sigma B_0^{\ 2}}{\rho c_p} u^{*2}. \tag{4.6}$$

4.2.4 The Concentration Equation of Unsteady Boundary Layer Flow Past a Vertical Plate

The concentration equation was derived in (3.15) in vector form as

$$\frac{\partial C^*}{\partial t^*} = D\nabla^2 C^* \pm \dot{r}$$

In components form, (3.15) is modified to become

$$\frac{\partial C^*}{\partial t^*} = D\frac{\partial^2 C^*}{\partial y^{*2}} - K_C^{\ *}(C^* - C^*_\infty) \tag{4.7}$$

Summary of boundary layer model of flow past a vertical plate is

$$\frac{\partial v^*}{\partial y^*} = 0 \tag{4.3}$$

$$\frac{\partial u^*}{\partial t^*} = \nu \frac{\partial^2 u^*}{\partial y^{*2}} + g\beta_T (T^* - T_\infty^*) + g\beta_C (C^* - C^*_\infty) - \frac{\sigma B_0^2}{\rho} u^* - \frac{\nu}{k^*} u^* \qquad (4.4)$$

$$\frac{\partial T^*}{\partial t^*} = \alpha \frac{\partial^2 T^*}{\partial y^{*2}} - \frac{1}{\rho c_p} \frac{\partial q_r}{\partial y^*} - \frac{Q}{\rho c_p} (T^* - T^*_\infty) + \frac{\sigma B_0^{\ 2}}{\rho c_p} u^{*2} \qquad (4.6)$$

$$\frac{\partial C^*}{\partial t^*} = D \frac{\partial^2 C^*}{\partial y^{*2}} - K_C^{\ *} (C^* - C^*_\infty) \qquad (4.7)$$

All the physical variables are defined in the **Nomenclature** in page xxii.

4.2.5 Associated Boundary Conditions of Unsteady Boundary Layer Flow Past a Vertical Plate

The associated boundary conditions for the problem are necessary to obtain a complete solution. Under the assumptions of the problem, the boundary conditions governing the unsteady flow process are

$$u^* = 0,\ T^* = T_\infty^*,\ \ C^* = C_\infty^*\ for\ all\ y^* \geq 0, t^* \leq 0,$$

$$u^* = U_0 e^{a^* t^*}, T^* = T_\infty^* + (T_w^* - T_\infty^*) A t *,\ C^* = C_w^*\ \ at\ y * = 0, t * > 0, \qquad (4.8)$$

$$u^* \to 0,\ T^* \to T_\infty^*,\ C^* \to C_\infty^*\ \ as\ y * \to \infty, t * > 0.$$

4.2.6 Dimensionless Transformation of the Problem of Unsteady Boundary Layer Flow Past a Vertical Plate

The transformation of the problem starts by substituting the necessary dimensionless variables and parameters into the dimensional continuity equation, momentum equation, energy equation and the concentration equation. Thus, the dimensionless variables and parameters in (3.16) are introduced to transform the dimensional boundary layer equations (4.3), (4.4), (4.6) and (4.7) with boundary conditions (4.8) to dimensionless equations.

4.2.7 Dimensionless Continuity Equation of Unsteady Boundary Layer Flow Past a Vertical Plate

The appropriate dimensionless quantities in (3.16) for the continuity equation are as follows:

For $v = \frac{v^*}{U_0}$, one has; $\frac{\partial v^*}{\partial t^*} = \frac{U_o \partial v}{\partial t^*}$ and $\frac{\partial v^*}{\partial y^*} = \frac{U_o \partial v}{\partial y^*}$ (4.9)

For $y = \frac{U_0 y*}{v}$, one has; $y^* = \frac{vy}{U_0}$ and $\partial y^* = \frac{v}{U_0}\,\partial y$ (4.10)

$$\frac{\partial v^*}{\partial y^*} = \frac{U_o \partial v}{\partial y^*} = \frac{U_o \partial v}{\frac{v}{U_o}\partial y} = \frac{U_0^2}{v}\,\frac{\partial v}{\partial y} \tag{4.11}$$

Substituting (4.11) into (4.3) gives the dimensionless continuity equation

$$\frac{\partial v}{\partial y} = 0 \tag{4.12}$$

4.2.8 Dimensionless Momentum Equation of Unsteady Boundary Layer Flow Past a Vertical Plate

The suitable dimensionless quantities in (3.16) for the momentum equation are as follows:

$$u = \frac{u^*}{U_0} \qquad \Rightarrow u^* = U_0 u \qquad \Longrightarrow \frac{\partial u^*}{\partial t^*} = \frac{U_o \partial u}{\partial t^*} \qquad \Longrightarrow \frac{\partial u^*}{\partial y^*} = \frac{U_o \partial u}{\partial y^*}$$

$$t = \frac{t^* U_0^2}{v} \qquad \Longrightarrow t^* = \frac{v}{U_0^2}\, t \quad \Longrightarrow \partial t^* = \frac{v}{U_0^2}\, \partial t$$

$$y = \frac{U_0 y^*}{v} \quad \Longrightarrow y^* = \frac{vy}{U_0} \quad \Longrightarrow \partial y^* = \frac{v}{U_0}\, \partial y \tag{4.13}$$

Now

$$\frac{\partial u^*}{\partial t^*} = \frac{U_0 \partial u}{\partial t^*} = \frac{U_0 \partial u}{\frac{v}{U_0^2} dt} = \frac{U_0^3}{v}\, \frac{\partial u}{\partial t},$$

$$\frac{\partial u^*}{\partial y^*} = \frac{U_o \partial u}{\partial y^*} = \frac{U_o \partial u}{\frac{v}{U_o} \partial y} = \frac{U_0^2}{v}\, \frac{\partial u}{\partial y}, \tag{4.14}$$

$$\frac{\partial^2 u^*}{\partial y^{*2}} = \frac{U_0^3}{v^2}\, \frac{\partial^2 u}{\partial y^2}.$$

Using (4.13) and (4.14) in equation (4.4), produces the dimensionless momentum equation;

$$\frac{{U_o}^3}{v}\frac{\partial u}{\partial t} = v\,\frac{U_0^3}{v^2}\frac{\partial^2 u}{\partial y^2} + g\beta_T\,(T_w^* - T_\infty^*)\theta + g\beta_c(C_w^* - C_\infty^*)\emptyset - \frac{\sigma {B_o}^2}{\rho}\,uU_0 - \frac{v}{k}uU_0.$$

$$\frac{\partial u}{\partial t} = \frac{\partial^2 u}{\partial y^2} + vg\beta_T\,\frac{(T_w^* - T_\infty^*)}{U_0^3}\theta + vg\beta_c\frac{(C_w^* - C_\infty^*)}{{U_0}^3}\emptyset - \frac{\sigma {B_o}^2 v}{\rho}\,\frac{U_o u}{U_0^3} - \frac{v}{k}uU_0\frac{v}{U_0^3}$$

$$\frac{\partial u}{\partial t} = \frac{\partial^2 u}{\partial y^2} + \frac{vg\beta_T(T_w^* - T_\infty^*)}{U_0^3}\theta + \frac{vg\beta_c(C_w^* - C_\infty^*)}{{U_0}^3}\emptyset - \frac{\sigma {B_o}^2 v}{\rho U_0^2}u - \frac{v^2}{ku_0^2}u$$

$$\frac{\partial u}{\partial t} = \frac{\partial^2 u}{\partial y^2} + Gr\theta + G_c\emptyset - M_1 u \qquad (4.15)$$

(4.15) modeled the dimensionless momentum equation.

Where $M_1 = M + \frac{1}{k}$

4.2.9 Dimensionless Energy Equation of Unsteady Boundary Layer Flow Past a Vertical Plate

Using the Rosseland approximation gives

$$\frac{\partial q_r}{\partial y^*} = -4a^*\sigma(T_\infty^{*4} - T^{*4}), \qquad (4.16)$$

where a^* = Rosseland mean absorption co-efficient, σ = Stefan-Boltzmann constant and q_r = radiative heat flux.

Assuming that the temperature differences with the flow are sufficiently small such that T^{*4} is expressed as a linear function of the temperature. Then by Taylor

series expansion and neglecting the higher order terms, T^{*4} is expressed as a linear function of the temperature in the form

$$T^{*4} \approx 4T_{\infty}^{*3}T^{*} - 3T_{\infty}^{*4}. \tag{4.17}$$

Substituting (4.17) into (4.16) results in

$$\frac{\partial q_r}{\partial y^*} = -4a^*\sigma(T_{\infty}^{*4} - 4T_{\infty}^{*3}T^{*} + 3T_{\infty}^{*4})$$

$$= -4a^*\sigma(4T_{\infty}^{*4} - 4T_{\infty}^{*3}T^{*})$$

$$= -16a^*\sigma(T_{\infty}^{*4} - T_{\infty}^{*3}T^{*})$$

$$\frac{\partial q_r}{\partial y^*} = -16a^*\sigma T_{\infty}^{*3}(T_{\infty}^{*} - T^{*}) \tag{4.18}$$

The dimensionless quantities in (3.16) suitable for the energy equation are differentiated as:

$$\frac{\partial T^*}{\partial t^*} = (T_w^* - T_{\infty}^*)\frac{\partial \theta}{\partial t^*} \text{ and } \partial t^* = \frac{v}{U_0^2}\partial t$$

$$\frac{\partial T^*}{\partial t^*} = \frac{U_0^2}{v}(T_w^* - T_{\infty}^*)\frac{\partial \theta}{\partial t} \tag{4.19}$$

Similarly $\frac{\partial T^*}{\partial y^*} = (T_w^* - T_{\infty}^*)\frac{\partial \theta}{\partial y^*}$ and $\partial y^* = \frac{v}{U_0}\partial y$

$$\Longrightarrow \frac{\partial T^*}{\partial y^*} = \frac{U_0}{v}(T_w^* - T_{\infty}^*)\frac{\partial \theta}{\partial y}$$

$$\Longrightarrow \frac{\partial^2 T^*}{\partial y^{*2}} = \frac{U_0^2}{v^2}(T_w^* - T_{\infty}^*)\frac{\partial^2 \theta}{\partial y^2} \tag{4.20}$$

Putting (3.16), (4.18), (4.19) and (4.20) in (4.6)

$$\frac{U_0^2}{v}(T_w^* - T_\infty^*)\frac{\partial\theta}{\partial t} = \alpha\frac{U_0^2}{v^2}(T_w^* - T_\infty^*)\frac{\partial^2\theta}{\partial y^2} + \frac{1}{\rho C_p}16a^*\sigma T_\infty^{*3}(T_\infty^* - T^*) - \frac{Q}{\rho C_P}(T_w^* - T_\infty^*)\theta + \frac{\sigma B_0^2}{\rho C_p}u^2U_0^2,$$

$$\frac{\partial\theta}{\partial t} = \frac{\propto}{v}\frac{\partial^2\theta}{\partial y^2} + \frac{16va^*\sigma T_\infty^{*3}(T_\infty^* - T^*)}{\rho C_p U_0^2(T_w^* - T_\infty^*)} - \frac{Qv}{\rho C_P U_0^2}\theta + \frac{\sigma B_0^2 v}{\rho C_p}\frac{u^2}{(T_w^* - T_\infty^*)} \quad \text{but } P_r = \frac{v}{\propto}$$

$$= \frac{1}{P_r}\frac{\partial^2\theta}{\partial y^2} - \frac{16va^*\sigma T_\infty^{*3}(T_w^* - T_\infty^*)}{\rho C_p U_0^2(T_w^* - T_\infty^*)}\theta - \frac{Qv}{\rho C_P U_0^2}\theta + \frac{\sigma B_0^2 v}{\rho C_p}\frac{u^2}{(T_w^* - T_\infty^*)} \quad \text{but } v = \frac{\mu}{\rho}$$

$$= \frac{1}{P_r}\frac{\partial^2\theta}{\partial y^2} - \frac{16v^2a^*\sigma T_\infty^{*3}}{\mu C_p U_0^2}\theta - \frac{Qv}{\rho C_P U_0^2}\theta + \frac{\sigma B_0^2 v}{\rho C_p}\frac{u^2}{(T_w^* - T_\infty^*)} \quad \text{but } P_r = \frac{\mu C_p}{k}$$

$$= \frac{1}{P_r}\frac{\partial^2\theta}{\partial y^2} - \frac{1}{P_r}F\theta - \frac{1}{P_r}H\theta + \frac{\sigma B_0^2 v}{\rho C_p}\frac{u^2}{(T_w^* - T_\infty^*)}$$

$$= \frac{1}{P_r}\frac{\partial^2\theta}{\partial y^2} - \frac{1}{P_r}F_1\theta + \frac{\sigma B_0^2 v}{\rho U_0^2}\frac{U_0^2}{C_p(T_w^* - T_\infty^*)}\mathrm{u}^2$$

$$\frac{\partial\theta}{\partial t} = \frac{1}{P_r}\frac{\partial^2\theta}{\partial y^2} - \frac{1}{P_r}F_1\theta + ME_c u^2 \qquad \text{where } F_1 = F + H \qquad (4.21)$$

(4.21) modeled the dimensionless energy equation.

4.2.10 Dimensionless Concentration Equation of Unsteady Boundary Layer Flow Past a Vertical Plate

The appropriate dimensionless quantities in (3.16) are differentiated for the concentration equation as:

$$\frac{\partial C^*}{\partial t^*} = (C_w^* - C_\infty^*)\frac{\partial\emptyset}{\partial t^*} \text{ and } \partial t^* = \frac{v}{U_0^2}\partial t$$

$$\frac{\partial C^*}{\partial t^*} = \frac{U_0^2}{v}(C_w^* - C_\infty^*)\frac{\partial\emptyset}{\partial t} \qquad (4.22)$$

Similarly $\frac{\partial C^*}{\partial y^*} = (C_w^* - C_\infty^*)\frac{\partial \emptyset}{\partial y^*}$ and $\partial y^* = \frac{v}{U_0}\partial y$

$$\Longrightarrow \frac{\partial C^*}{\partial y^*} = \frac{U_0}{v}(C_w^* - C_\infty^*)\frac{\partial \emptyset}{\partial y}$$

$$\Longrightarrow \frac{\partial^2 C^*}{\partial y^{*2}} = \frac{U_0^2}{v^2}(C_w^* - C_\infty^*)\frac{\partial^2 \emptyset}{\partial y^2} \qquad (4.23)$$

Putting (3.16), (4.22) and (4.23) into (4.7)

$$\frac{U_0^2}{v}(C_w^* - C_\infty^*)\frac{\partial \emptyset}{\partial t} = D\frac{U_0^2}{v^2}(C_w^* - C_\infty^*)\frac{\partial^2 \emptyset}{\partial y^2} - k_c^*(C_w^* - C_\infty^*)\emptyset,$$

$$\frac{\partial \emptyset}{\partial t} = \frac{D}{v}\frac{\partial^2 \emptyset}{\partial y^2} - k_c^*\frac{v}{U_0^2}\emptyset,$$

$$\frac{\partial \emptyset}{\partial t} = \frac{1}{S_C}\frac{\partial^2 \emptyset}{\partial y^2} - k_C\emptyset. \qquad (4.24)$$

The dimensionless concentration equation is modeled in (4.24).

Now the boundary layer equations governing the unsteady flow past a vertical plate in dimensionless form are;

$\frac{\partial u}{\partial t} = \frac{\partial^2 u}{\partial y^2} + Gr\theta + G_c\emptyset - M_1 u$ in (4.15);

$\frac{\partial \theta}{\partial t} = \frac{1}{P_r}\frac{\partial^2 \theta}{\partial y^2} - \frac{1}{P_r}F_1\theta + ME_c u^2$ in (4.21);

$\frac{\partial \emptyset}{\partial t} = \frac{1}{S_C}\frac{\partial^2 \emptyset}{\partial y^2} - k_C\emptyset$ in (4.24).

4.2.11 Associated Dimensionless Boundary conditions of Unsteady Boundary Layer Flow Past a Vertical Plate

The corresponding dimensionless boundary conditions are now:

$$\begin{aligned} &u = 0, \theta = 0, \emptyset = 0 \quad for\ all \quad y \geq 0, t \leq 0; \\ &u = e^{at}, \theta = 1, \emptyset = 1 \quad at \quad y = 0, t > 0; \\ &u \to 0, \theta \to 0, \emptyset \to 0 \quad as \quad y \to \infty, t > 0. \end{aligned} \tag{4.25}$$

4.3 Analytical Solution of Unsteady Boundary Layer Flow Past a Vertical Plate

The non-linear differential equations (4.15), (4.21) and (4.24) with boundary conditions (4.25) are solved in exact form using the Laplace transform techniques.

4.3.1 Laplace Transform Technique of Unsteady Boundary Layer Flow Past a Vertical Plate

The Laplace transforms of (4.15), (4.21) and (4.24) and the boundary conditions (4.25) are given as:

In the temperature (4.21), the Laplace transform of the temperature boundary conditions is given as;

$$\begin{aligned} &\theta(y,0) = 0 \quad for\ all \quad y \geq 0,\ t \leq 0 \qquad \bar{\theta}(y,0) = 0; \\ &\theta(0,t) = 1 \ \ at \quad y = 0, t > 0 \qquad \bar{\theta}(0,s) = \frac{1}{s}; \end{aligned} \tag{4.26}$$

$\theta(y,t) \to 0 \quad as \quad y \to \infty, t > 0$. $\qquad \bar{\theta}(y,s) \to 0.$

Where s is a Laplace transform parameter.

Taking Laplace transform of (4.21) gives (See Appendix A2.3)

$$\frac{1}{P_r}\frac{\partial^2\bar{\theta}}{\partial y^2} - s\bar{\theta}(y,s) + \theta(y,0) = \frac{F_1}{P_r}\bar{\theta}(y,s) - ME_cL[u^2] .$$

But $u \neq$constant, since u is a function of space and time. i.e. $u(y,t)$.

Also from the boundary condition $\theta(y,0) = 0 \quad for\ all \quad t \leq 0$, implies

$$\frac{\partial^2\bar{\theta}}{\partial y^2} - P_r\left(s + \frac{F_1}{P_r}\right)\bar{\theta} = -P_rME_c\ L[u^2(y,t)]. \qquad (4.27)$$

The general solution of (4.27) can be written as;

$$\bar{\theta}(y,s) = \bar{\theta}_h(y,s) + \bar{\theta}_p(y,s). \qquad (4.28)$$

Where $\bar{\theta}_h\ (y,s)$ is the general solution of the homogeneous problem.

$\bar{\theta}_p(y,s)$ is any particular solution of the non-homogeneous problem.

Considering the homogeneous problem of the LHS of (4.27), the general solution (see Appendix A3.5) is

$$\bar{\theta}_h(y,s) = A(s)e^{-y\sqrt{P_rs+F_1}} + B(s)e^{y\sqrt{P_rs+F_1}} . \qquad (4.29)$$

Using method of undetermined coefficients, guessing the form of the particular solution in (4.27) to be

$\bar{\theta}_p(y,s) = A;$

$\bar{\theta}_p'(y,s) = 0;$

$\bar{\theta}_p''(y,s) = 0;$ substituting into (4.27) gives

$$0-(P_rs+F_1)A=-P_rME_c\,L[u^2(y,t)]$$

$$A=\frac{P_rME_c}{P_rs+F_1}L[u^2(y,t)]. \qquad (4.30)$$

Adding the particular solution (4.30) to (4.29) gives the general solution

$$\bar{\theta}(y,s)==A(s)e^{-y\sqrt{P_rs+F_1}}+B(s)e^{y\sqrt{P_rs+F_1}}+\frac{P_rME_c}{P_rs+F_1}L[u^2(y,t)]. \qquad (4.31)$$

Since $\theta(y,t)\to 0\ as\ \ y\to\infty, t>0 \implies \bar{\theta}(y,s)=0$ and $B(s)=0$ in (4.31).

Now (4.31) reduces to

$$\bar{\theta}(y,s)=A(s)e^{-y\sqrt{P_rs+F_1}}+\frac{P_rME_c}{P_rs+F_1}L[u^2(y,t)]. \qquad (4.32)$$

$\theta(0,t)=1 \ \ at \ \ y=0, t>0 \qquad\qquad \bar{\theta}(0,s)=\frac{1}{s}$

From (4.32), $\frac{1}{s}=A(s)+\frac{P_rME_c}{P_rs+F_1}L[u^2(y,t)]$

Thus, $\bar{\theta}(y,s)=\left(\frac{1}{s}-\frac{P_rME_c}{P_rs+F_1}L[u^2(y,t)]\right)e^{-\sqrt{P_rs+F_1}\,y}+\frac{P_rME_c}{P_rs+F_1}L[u^2(y,t)]$

$$\bar{\theta}(y,s)=\frac{1}{s}e^{-\sqrt{P_rs+F_1}\,y}+L[u^2(y,t)]P_rME_c\left(\frac{1}{P_rs+F_1}-\frac{1}{P_rs+F_1}e^{-\sqrt{P_rs+F_1}\,y}\right). \qquad (4.33)$$

Equation (4.33) is the general solution of the temperature model in Laplace domain whose inverse will be determined later when the velocity function $u^2(y,t)$ is known.

Now considering the dimensionless concentration equation (4.24) which is

$$\frac{\partial\phi}{\partial t}=\frac{1}{Sc}\frac{\partial^2\phi}{\partial y^2}-Kc\phi\,.$$

Subjected to the boundary conditions in Laplace domain:

$\emptyset(y,0) = 0 \quad for\ all \quad y \geq 0, t \leq 0 \qquad \bar{\emptyset}(y,0) =;$

$\emptyset(0,t) = 1 \ at \quad y = 0, t > 0 \qquad \bar{\emptyset}(0,s) = \frac{1}{s};$ (4.34)

$\emptyset(y,t) \to 0 \quad as \quad y \to \infty, t > 0 \qquad \bar{\emptyset}(y,s) \to 0.$

Taking Laplace of (4.24) (See Appendix (A2.4)) gives

$\frac{1}{S_c}\frac{\partial^2\bar{\emptyset}}{\partial y^2} - s\bar{\emptyset}(y,s) + \emptyset(y,0) = K_c\bar{\emptyset}.$ (4.35)

But $\emptyset(y,0) = 0$

$\frac{\partial^2\bar{\emptyset}}{\partial y^2} - S_c(s + K_c)\bar{\emptyset} = 0.$ (4.36)

Equation (4.36) is linear homogenous second order ordinary differential equation.

The general solution of the homogeneous problem in (4.36) (see Appendix A3.6) is

$\bar{\emptyset}(y,s) = A(s)e^{-y\sqrt{S_cs+S_cK_c}} + B(s)e^{y\sqrt{S_cs+S_cK_c}}.$ (4.37)

Since $\emptyset(y,t) \to 0\ as \quad y \to \infty, t > 0 \qquad \bar{\emptyset}(y,s) = 0$ and $B(s) = 0$ in (4.37).

Then (4.37) reduces to

$\bar{\emptyset}(y,s) = A(s)e^{-y\sqrt{S_cs+S_cK_c}}.$ (4.38)

But $\emptyset(0,t) = 1 \quad at \quad y = 0, t > 0 \qquad \bar{\emptyset}(0,s) = \frac{1}{s}$

From equation (4.38), $\frac{1}{s} = A(s)$

$$\overline{\emptyset}(y,s)=\frac{1}{s}e^{-\sqrt{S_c s+S_c K_c}\,y}. \qquad (4.39)$$

Standard inverse Laplace transform of (4.39) is taken from tables in Appendix II as well as the use of convolution theorem in Appendix IV. Hence the general solution of (4.39) (see convolution theorem in Appendix IV, (A4.3)) becomes

$$\emptyset(y,t)=\frac{1}{2}\left[e^{-y\sqrt{S_c K_c}}erfc\left(\frac{2t\sqrt{K_c}-y\sqrt{S_c}}{2\sqrt{t}}\right)+e^{y\sqrt{S_c K_c}}erfc\left(\frac{2t\sqrt{K_c}+y\sqrt{S_c}}{2\sqrt{t}}\right)\right] \qquad (4.40)$$

Where erf is the error function; erfc is the complementary error function.

$$erfc(x)=1-\text{erf}(x),\ erfc(0)=1, erfc(\infty)=0,\ \ erf(0)=0,$$

$$erf(\infty)=1,\ \text{erf}(z)=\frac{2}{\sqrt{\pi}}\int_0^z e^{-t^2}dt,\quad \frac{\partial}{\partial z}\text{erf}(z)=\frac{2}{\sqrt{\pi}}e^{-z^2}.$$

Equation (4.40) is general solution for the concentration profile at $t>0$.

From the dimensionless momentum equation (4.15) i.e

$$\frac{\partial u}{\partial t}=\frac{\partial^2 u}{\partial y^2}+Gr\theta+G_c\emptyset-M_1 u$$

Subject to the boundary conditions in Laplace domain as:

$$u(y,0)=0 \quad for\ all \quad y\geq 0, t\leq 0 \qquad \bar{u}(y,0)=0;$$

$$u(0,t)=e^{at} \ \ at \ \ y=0, t>0 \qquad \bar{u}(0,s)=\frac{1}{s-a}; \qquad (4.41)$$

$$u(y,t)\to 0 \quad as \quad y\to\infty, t>0 \qquad \bar{u}(y,s)\to 0.$$

Taking Laplace transform of (4.15) results in (see Appendix A2.5)

$$\frac{\partial^2 \bar{u}}{\partial y^2}-s\bar{u}+u(y,0)=-G_r\bar{\theta}-G_c\overline{\emptyset}+M_1\bar{u}.$$

But $u(y,0) = 0$

$$\frac{\partial^2 \bar{u}}{\partial y^2} - s\bar{u} = -G_r\bar{\theta} - G_c\bar{\emptyset} + M_1\bar{u}. \quad (4.42)$$

$$\frac{\partial^2 \bar{u}}{\partial y^2} - (s+M_1)\bar{u} = -G_r\bar{\theta} - G_c\bar{\emptyset}. \quad (4.43)$$

Equation (4.43) is linear non-homogenous second order ordinary differential equation.

Considering the homogeneous problem of the LHS of (4.43) the general solution is (see Appendix A3.7)

$$\bar{u}_h(y,s) = A(s)e^{-\sqrt{s+M_1}\,y} + B(s)e^{\sqrt{s+M_1}\,y}. \quad (4.44)$$

Using method of undetermined coefficients, guessing the form of the particular solution in (4.43) to be

$\bar{u}_p(y,s) = A;$

$\bar{u}_p'(y,s) = 0;$

$\bar{u}_p''(y,s) = 0;$ substituting in (4.43) gives

$0 - (s+M_1)A == -G_r\bar{\theta} - G_c\bar{\emptyset}$

$$A = \frac{G_r}{s+M_1}\bar{\theta} + \frac{G_c}{s+M_1}\bar{\emptyset}. \quad (4.45)$$

Adding the particular solution ((4.45)to (4.44) yields

$$\bar{u}(y,s) = A(s)e^{-\sqrt{s+M_1}\,y} + B(s)e^{\sqrt{s+M_1}\,y} + \frac{G_r}{s+M_1}\bar{\theta} + \frac{G_c}{s+M_1}\bar{\emptyset}. \quad (4.46)$$

Since $u(y,t) \to 0\ as \quad y \to \infty, t > 0 \qquad \bar{u}(y,s) = 0$

From (4.46), $B(s) = 0$. Now (4.46) reduces to

$$\bar{u}(y,s) = A(s)e^{-y\sqrt{s+M_1}} + \frac{G_r}{s+M_1}\bar{\theta} + \frac{G_c}{s+M_1}\bar{\emptyset}. \qquad (4.47)$$

Since $u(0,t) = e^{at} \quad at \quad y = 0, t > 0 \qquad \Longrightarrow \bar{u}(0,s) = \frac{1}{s-a}$

$$\frac{1}{s-a} = A(s) + \frac{G_r}{s+M_1}\bar{\theta} + \frac{G_c}{s+M_1}\bar{\emptyset}$$

$$\bar{u}(y,s) = \left(\frac{1}{s-a} - \frac{G_r}{s+M_1}\bar{\theta} - \frac{G_c}{s+M_1}\bar{\emptyset}\right)e^{-y\sqrt{s+M_1}} + \frac{G_r}{s+M_1}\bar{\theta} + \frac{G_c}{s+M_1}\bar{\emptyset}$$

$$\bar{u}(y,s) = \frac{1}{s-a}e^{-y\sqrt{s+M_1}} + G_r\bar{\theta}\left(\frac{1}{s+M_1} - \frac{1}{s+M_1}e^{-y\sqrt{s+M_1}}\right) + G_c\bar{\emptyset}\left(\frac{1}{s+M_1} - \frac{1}{s+M_1}e^{-y\sqrt{s+M_1}}\right). \qquad (4.48)$$

Taking inverse Laplace transform from tables in Appendix II and the use of convolution theorem in Appendix IV, the general solution of the velocity equation (4.48) (see convolution theorem in Appendix IV, (A4.6) and (A4.8)) is

$$u(y,t) = -\frac{1}{2}e^{at-y\sqrt{a+M_1}}erfc\left(\frac{2t\sqrt{a+M_1}-y}{2\sqrt{t}}\right) + \frac{1}{2}e^{at+y\sqrt{a+M_1}}erfc\left(\frac{2t\sqrt{a+M_1}+y}{2\sqrt{t}}\right) + \left(G_r\theta(y,t) + G_c\emptyset(y,t)\right)\left(e^{-M_1t} - e^{-M_1t}erfc\left(\frac{y}{2\sqrt{t}}\right)\right). \qquad (4.49)$$

Equation (4.49) is the general solution for the velocity profile at $t > 0$.

Where $M_1 = M + \frac{1}{k}$

$$\emptyset(y,t) = \frac{1}{2}\left[e^{-y\sqrt{S_cK_c}}erfc\left(\frac{2t\sqrt{K_c}-y\sqrt{S_c}}{2\sqrt{t}}\right) + e^{y\sqrt{S_cK_c}}erfc\left(\frac{2t\sqrt{K_c}+y\sqrt{S_c}}{2\sqrt{t}}\right)\right].$$

$\theta(y,t)$ is yet to be determined.

Now, knowing the general solution of the velocity model, the general solution of the temperature model can be obtained as;

From the temperature equation in (4.33) which is

$$\bar{\theta}(y,s) = \frac{1}{s}e^{-\sqrt{P_rs+F_1}\,y} + L[u^2(y,t)]P_rME_c\left(\frac{1}{P_r+F_1} - \frac{1}{P_r+F_1}e^{-\sqrt{P_rs+F_1}\,y}\right).$$

In finding the Laplace transform of the velocity function $u^2(y,t)$, the following properties of Laplace transform are used;

- $L[u^2(y,t)] \neq L[u(y,t)] \times L[u(y,t)] \neq \bar{u}^2(y,s)$.
- If the $L[u^2(y,t)] = L[u(y,t) \times u(y,t)] = \bar{u}^2(y,s)$, then

  $L^{-1}[\bar{u}^2(y,s)\,] = u^2(y,t)$.

$$\bar{\theta}(y,s) = \frac{1}{s}e^{-y\sqrt{P_rs+F_1}} + \frac{P_rME_c}{P_r+F_1}\bar{u}^2(y,s)\left(1 - e^{-y\sqrt{P_rs+F_1}}\right). \qquad (4.50)$$

Taking inverse Laplace transform from tables in Appendix II and the use of convolution theorem in Appendix IV.

The general solution of the temperature model (4.50) (see convolution theorem in Appendix IV, (A4.11) and (A4.15)) is

$$\theta(y,t) = \frac{1}{2}\left[-e^{-y\sqrt{F_1}}erfc\left(\frac{2t\sqrt{\frac{F_1}{P_r}}-y\sqrt{P_r}}{2\sqrt{t}}\right) + e^{y\sqrt{F_1}}erfc\left(\frac{2t\sqrt{\frac{F_1}{P_r}}+y\sqrt{P_r}}{2\sqrt{t}}\right)\right] +$$

$$u^2(y,t)ME_c\left(e^{-\frac{F_1}{P_r}t} - e^{-\frac{F_1}{P_r}t}erfc\left(\frac{y\sqrt{P_r}}{2\sqrt{t}}\right)\right). \quad (4.51)$$

In substituting $u^2(y,t)$ (see Appendix IV (A4.17)) in the temperature equation (4.51), the non-linear term $\theta^2(y,t)$ is considered negligible since an early assumption was made in the udy when determining the dimensionless temperature model that the temperature ifferences in the flow are sufficiently small. i.e. if $\theta(y,t)$ is small then $\theta^2(y,t)$ becomes uch smaller. This conforms in practice because, in engineering practice the emphasis is on ıe effect of sufficiently small change in physical quantities. Hence the general solution of ıe temperature model at $t > 0$ is

$$\theta(y,t) = \left[1 - ME_c e^{-\frac{F_1}{P_r}t}\left(1 - erfc\left(\frac{y\sqrt{P_r}}{2\sqrt{t}}\right)\right)\left[2G_rG_c\emptyset(y,t)e^{-2M_1t}\left(1 -\right.\right.\right.$$

$$\left.2erfc\left(\frac{y}{2\sqrt{t}}\right) + \left(erfc\left(\frac{y}{2\sqrt{t}}\right)\right)^2\right) + G_r\left(e^{-M_1t} -\right.$$

$$\left.\left.e^{-M_1t}erfc\left(\frac{y}{2\sqrt{t}}\right)\right)\left(-e^{at-y\sqrt{a+M_1}}erfc\left(\frac{2t\sqrt{a+M_1}-y}{2\sqrt{t}}\right) +\right.\right.$$

$$\left.\left.e^{at+y\sqrt{a+M_1}}erfc\left(\frac{2t\sqrt{a+M_1}+y}{2\sqrt{t}}\right)\right)\right]\left.\right]^{-1}\left[-\frac{1}{2}e^{-y\sqrt{F_1}}erfc\left(\frac{2t\sqrt{\frac{F_1}{P_r}}-y\sqrt{P_r}}{2\sqrt{t}}\right) +\right.$$

$$\left.\frac{1}{2}e^{y\sqrt{F_1}}erfc\left(\frac{2t\sqrt{\frac{F_1}{P_r}}+y\sqrt{P_r}}{2\sqrt{t}}\right) + ME_ce^{-\frac{F_1}{P_r}t}\left(1 -\right.\right.$$

$$erfc\left(\frac{y\sqrt{P_r}}{2\sqrt{t}}\right)\Bigg)\Bigg[\frac{1}{4}e^{2(at-y\sqrt{a+M_1})}\left(erfc\left(\frac{2t\sqrt{a+M_1}-y}{2\sqrt{t}}\right)\right)^2+$$

$$\frac{1}{4}e^{2(at+y\sqrt{a+M_1})}\left(erfc\left(\frac{2t\sqrt{a+M_1}+y}{2\sqrt{t}}\right)\right)^2+G_c^2\emptyset^2(y,t)e^{-2M_1t}\left(1-2erfc\left(\frac{y}{2\sqrt{t}}\right)+\right.$$

$$\left.\left(erfc\left(\frac{y}{2\sqrt{t}}\right)\right)^2\right)-\frac{1}{2}e^{2at}erfc\left(\frac{2t\sqrt{a+M_1}-y}{2\sqrt{t}}\right)erfc\left(\frac{2t\sqrt{a+M_1}+y}{2\sqrt{t}}\right)+$$

$$G_c\emptyset(y,t)\left(e^{-M_1t}-e^{-M_1t}erfc\left(\frac{y}{2\sqrt{t}}\right)\right)\left(-e^{at-y\sqrt{a+M_1}}erfc\left(\frac{2t\sqrt{a+M_1}-y}{2\sqrt{t}}\right)+\right.$$

$$\left.e^{at+y\sqrt{a+M_1}}erfc\left(\frac{2t\sqrt{a+M_1}+y}{2\sqrt{t}}\right)\right)\Bigg]\Bigg]. \qquad (4.52)$$

Where

$$\emptyset(y,t)=\frac{1}{2}\left[e^{-y\sqrt{S_cK_c}}erfc\left(\frac{2t\sqrt{K_c}-y\sqrt{S_c}}{2\sqrt{t}}\right)+e^{y\sqrt{S_cK_c}}erfc\left(\frac{2t\sqrt{K_c}+y\sqrt{S_c}}{2\sqrt{t}}\right)\right].$$

$$\theta(y,t)=b_0^{-1}\Bigg[-\frac{1}{2}e^{-y\sqrt{F_1}}erfc\left(\frac{2t\sqrt{\frac{F_1}{P_r}}-y\sqrt{P_r}}{2\sqrt{t}}\right)+\frac{1}{2}e^{y\sqrt{F_1}}erfc\left(\frac{2t\sqrt{\frac{F_1}{P_r}}+y\sqrt{P_r}}{2\sqrt{t}}\right)+$$

$$ME_ce^{-\frac{F_1}{P_r}t}\left(1-erfc\left(\frac{y\sqrt{P_r}}{2\sqrt{t}}\right)\right)\Bigg[\frac{1}{4}e^{2(at-y\sqrt{a+M_1})}\left(erfc\left(\frac{2t\sqrt{a+M_1}-y}{2\sqrt{t}}\right)\right)^2+$$

$$\frac{1}{4}e^{2(at+y\sqrt{a+M_1})}\left(erfc\left(\frac{2t\sqrt{a+M_1}+y}{2\sqrt{t}}\right)\right)^2+$$

$$e^{-2M_1t}\frac{G_c^2}{4}\left[e^{-y\sqrt{S_cK_c}}erfc\left(\frac{2t\sqrt{K_c}-y\sqrt{S_c}}{2\sqrt{t}}\right)+e^{y\sqrt{S_cK_c}}erfc\left(\frac{2t\sqrt{K_c}+y\sqrt{S_c}}{2\sqrt{t}}\right)\right]^2\left(1-\right.$$

$$2erfc\left(\frac{y}{2\sqrt{t}}\right)+\left(erfc\left(\frac{y}{2\sqrt{t}}\right)\right)^2\Bigg)-\frac{1}{2}e^{2at}erfc\left(\frac{2t\sqrt{a+M_1}-y}{2\sqrt{t}}\right)erfc\left(\frac{2t\sqrt{a+M_1}+y}{2\sqrt{t}}\right)+$$

$$\frac{G_c}{2}\left[e^{-y\sqrt{S_cK_c}}erfc\left(\frac{2t\sqrt{K_c}-y\sqrt{S_c}}{2\sqrt{t}}\right)+e^{y\sqrt{S_cK_c}}erfc\left(\frac{2t\sqrt{K_c}+y\sqrt{S_c}}{2\sqrt{t}}\right)\right]\left(e^{-M_1t}-\right.$$

$$\left.e^{-M_1t}erfc\left(\frac{y}{2\sqrt{t}}\right)\right)\left(-e^{at-y\sqrt{a+M_1}}erfc\left(\frac{2t\sqrt{a+M_1}-y}{2\sqrt{t}}\right)+\right.$$

$$\left.\left.e^{at+y\sqrt{a+M_1}}erfc\left(\frac{2t\sqrt{a+M_1}+y}{2\sqrt{t}}\right)\right)\right]. \qquad (4.53)$$

Where,

$$b_0=1-ME_ce^{-\frac{F_1}{P_r}t}\left(1-\right.$$

$$\left.erfc\left(\frac{y\sqrt{P_r}}{2\sqrt{t}}\right)\right)\left[G_rG_ce^{-2M_1t}\left[e^{-y\sqrt{S_cK_c}}erfc\left(\frac{2t\sqrt{K_c}-y\sqrt{S_c}}{2\sqrt{t}}\right)+\right.\right.$$

$$\left.e^{y\sqrt{S_cK_c}}erfc\left(\frac{2t\sqrt{K_c}+y\sqrt{S_c}}{2\sqrt{t}}\right)\right]\left(1-2erfc\left(\frac{y}{2\sqrt{t}}\right)+\left(erfc\left(\frac{y}{2\sqrt{t}}\right)\right)^2\right)+G_r\left(e^{-M_1t}-\right.$$

$$\left.e^{-M_1t}erfc\left(\frac{y}{2\sqrt{t}}\right)\right)\left(-e^{at-y\sqrt{a+M_1}}erfc\left(\frac{2t\sqrt{a+M_1}-y}{2\sqrt{t}}\right)+\right.$$

$$\left.\left.e^{at+y\sqrt{a+M_1}}erfc\left(\frac{2t\sqrt{a+M_1}+y}{2\sqrt{t}}\right)\right)\right].$$

Equation (4.53) is the general solution of the temperature profile for $t>0$. However, there is other possible solution if $\theta^2(y,t)\neq 0$ but the presence of the

discriminant, $b^2 - 4ac$ in the solution of the resulting quadratic equation makes $\theta(y,t)$ not defined for higher physical values of the controlling parameters.

4.4 Dimensionless Fluxes of Unsteady Boundary Layer Flow Past a Vertical Plate

4.4.1 The Rate of Heat Transfer Coefficient of Unsteady Boundary Layer Flow Past a Vertical Plate

Having obtained the **temperature field**, the rate of heat transfer coefficient at the vertical plate characterised by the Nusselt number can be studied. The effects of $t,, M, F, H, E_c$ and P_r on Nusselt number will be considered. In dimensionless form, the Nusselt number is given by

$$N_u = -\frac{\partial\theta}{\partial y}\Big|_{y=0} = b_0^{-2}\left[\frac{M_1 E_c}{2\sqrt{\pi^3 t^7}} G_c e^{-2M_1 t - \frac{F_1 t}{P_r}}\left(\sqrt{\pi t}(8M_1 t + 12)\right) erfc\left(\frac{2t\sqrt{K_c}}{2\sqrt{t}}\right) - \frac{\sqrt{S_c}}{\sqrt{\pi t}} G_c^2 e^{-4tK_c - 2M_1 t} + \sqrt{S_c K_c} G_c^2 e^{-2M_1 t} erfc\left(\frac{2t\sqrt{K_c}}{2\sqrt{t}}\right) + \frac{\sqrt{S_c}}{\sqrt{\pi t}} e^{-\frac{2t\sqrt{K_c}+M_1 t}{4t}} + \sqrt{S_c K_c} e^{M_1 t} erfc\left(\frac{2t\sqrt{K_c}}{2\sqrt{t}}\right)\right]. \quad (4.54)$$

4.4.2 The Rate of Mass Transfer Coefficient of Unsteady Boundary Layer Flow Past a Vertical Plate

Knowing the **concentration field,** the rate of mass transfer coefficient at the vertical plate described by the Sherwood number can be studied. The effects of t, S_c and K_c on Sherwood number will be examined. In dimensionless form, the Sherwood number is given by

$$sh = -\left(\frac{\partial \emptyset}{\partial y}\right)_{y=0} = -\frac{\sqrt{S_c}}{\sqrt{\pi t}} e^{-4tK_c} + \sqrt{S_c K_c}\left(\frac{2t\sqrt{K_c}}{2\sqrt{t}}\right). \quad (4.55)$$

4.4.3 The Skin Friction Coefficient of Unsteady Boundary Layer Flow Past a Vertical Plate

Also, having obtained the **velocity field**, it is significant to study changes in the skin friction due to the effects of the physical parameters t, F, H, M, P_r, K_c and k. In dimensionless form, the skin friction is given by

$$\tau = -\frac{\partial u}{\partial y}\Big|_{y=0} = -\frac{1}{\sqrt{\pi t}} e^{\frac{-M_1}{4}} erfc\left(\frac{2t\sqrt{\frac{F_1}{Pr}}}{2\sqrt{t}}\right) + \frac{1}{\sqrt{\pi t}} e^{\frac{-M_1}{4}} erfc\left(\frac{2t\sqrt{K_c}}{2\sqrt{t}}\right) +$$

$$\frac{1}{\sqrt{\pi t}} e^{\frac{-M_1 t}{4t^2}}\left(G_r\theta(y,t) + G_c\emptyset(y,t)\right). \quad (4.56)$$

4.5 Results and Discussion

In order to understand the physical dynamics of the problem, the effects of the controlling parameters on the Temperature (θ), Concentration$(\emptyset)$ and Velocity (u) profiles are illustrated graphically using MATLAB.

4.5.1 Graphical Results

4.5.1.1 Temperature Profiles

Fig. 4.2 illustrates the effects of Prandtl number (P_r) on the temperature profiles. Although, smaller value of P_r means increasing the thermal conductivities which

enable diffusion of more heat (Rout & Pattanayak, 2013), the presence of the magnetic field delay the convection motion of the fluid. Therefore, it is observed that decreasing P_r decreases the temperature of the fluid. Fig. 4.3, 4.4, 4.5 and 4.6 exhibit the effects of Heat absorption parameter (H), Radiation Parameter (F), Magnetic parameter (M) and Eckert number (E_c) on the temperature profiles. It is observed that increase in either H or F increases the temperature of the fluid flow. This is true because, in practice the job of thermal radiation is to increase the thermal boundary layer thickness of a fluid. However, increase in M or E_c decreases the temperature of the flow. This is as a result of the presence of magnetic field in the flow which produces Lorentz force which decays the thermal boundary layer thickness.

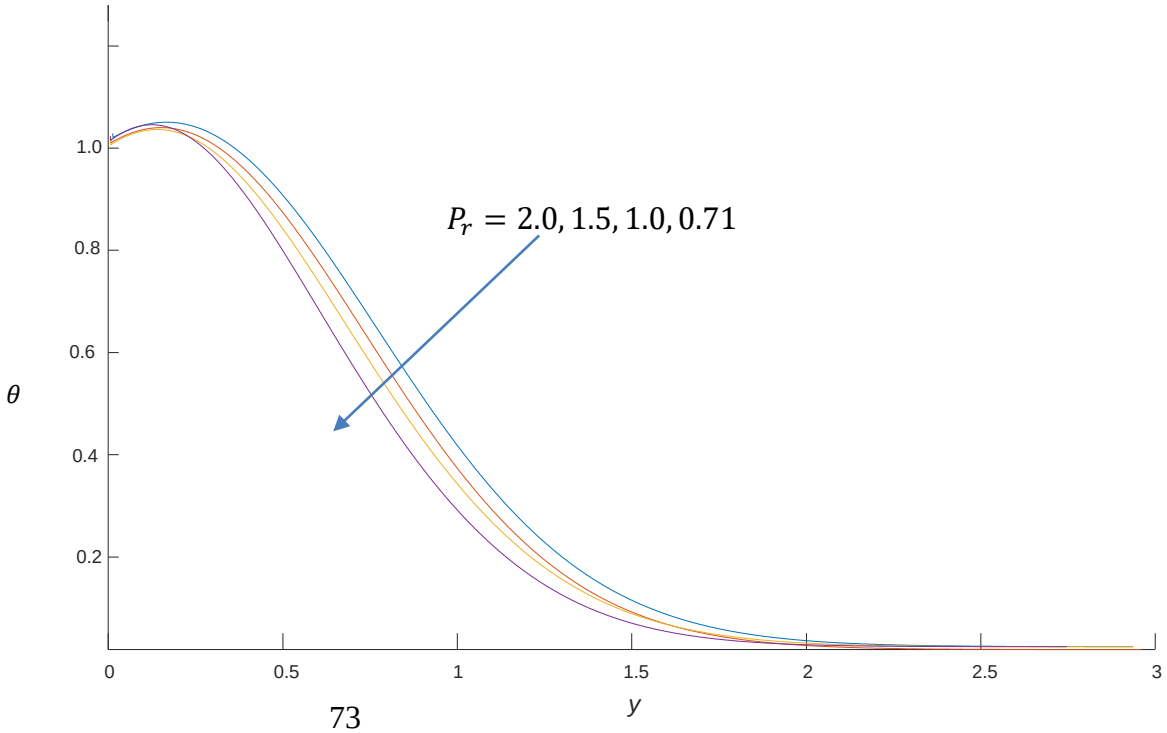

Figure 4. 2 Effects of P_r on the temperature profiles when $G_r = 5, G_c = 5$, $t = 0.2, k = 1, K_c = 1, S_c = 2.01, a = 0.2, E_c = 2, M = 2, F = 2$ and $H = 2$.

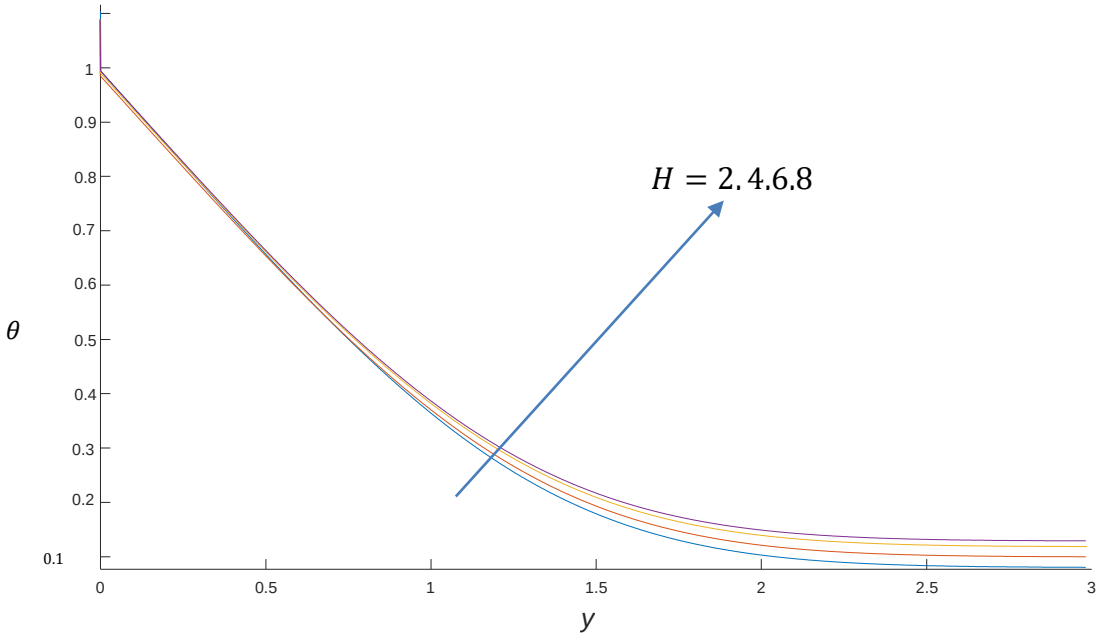

Figure 4. 3 Effects of H on the temperature profiles when $G_r = 5, G_c = 5,$ $t = 0.2, k = 1, K_c = 1, S_c = 2.01, a = 0.2, E_c = 2, M = 2, F = 2$ and $P_r = 0.71.$

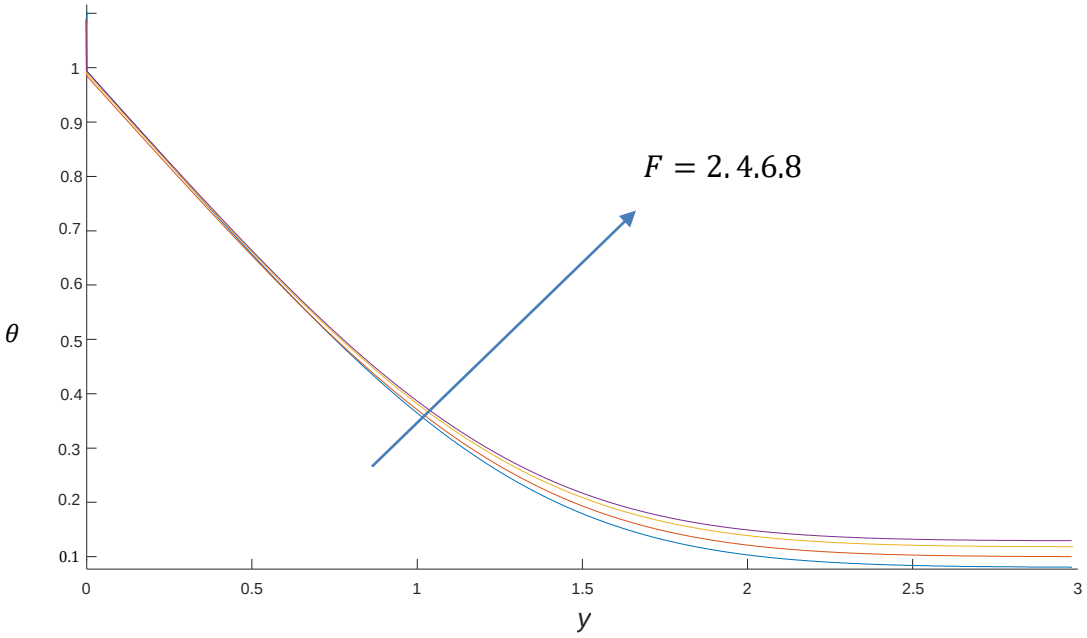

Figure 4. 4 Effects of F on the temperature profiles when $G_r = 5, G_c = 5,$ $t = 0.2, k = 1, K_c = 1, S_c = 2.01, a = 0.2, E_c = 2, M = 2, P_r = 0.71$ and $H = 2$

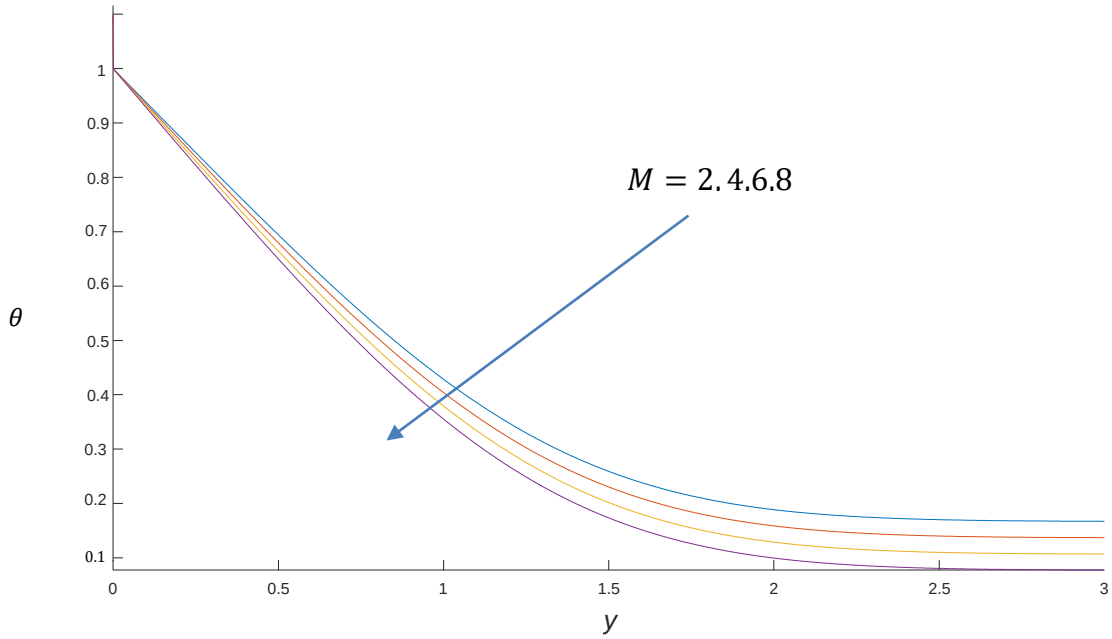

Figure 4. 5 Effects of M on the temperature profiles when $G_r = 5, G_c = 5$, $t = 0.2, k = 1, K_c = 1, S_c = 2.01, a = 0.2, E_c = 2, P_r = 0.71, F = 2$ and $H = 2$

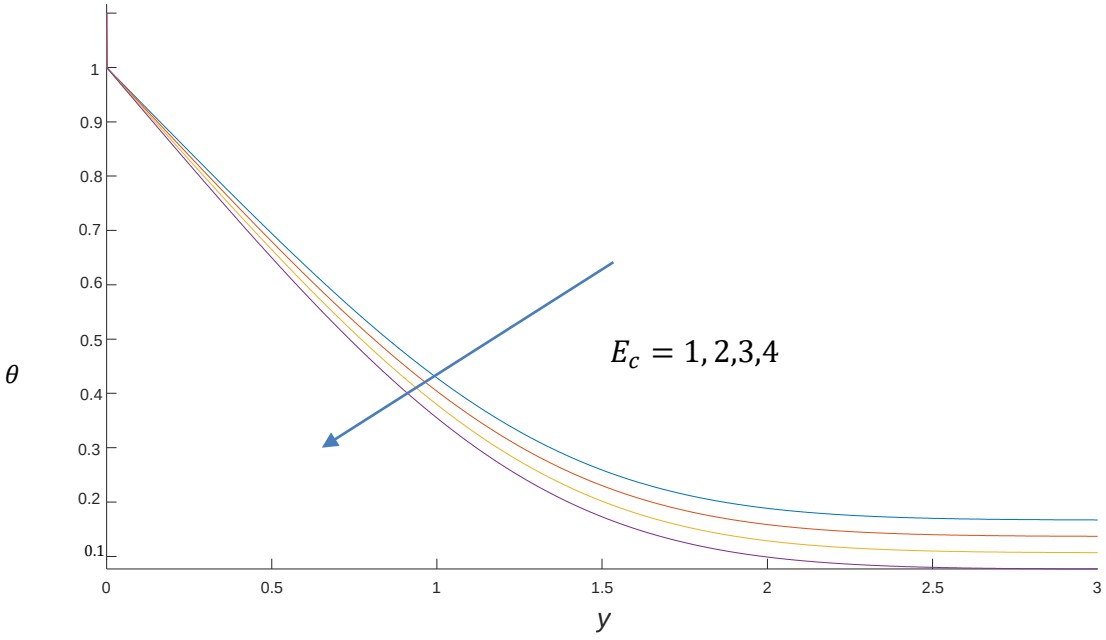

Figure 4. 6 Effects of E_c on the temperature profiles when $G_r = 5, G_c = 5$, $t = 0.2, k = 1, K_c = 1, S_c = 2.01, a = 0.2, P_r = 0.71, M = 2, F = 2$ and $H = 2$

4.5.1.2 Concentration Profiles

Fig. 4.7 and 4.8 show the effects of Chemical reaction parameter (K_c) and Schmidt number (S_c) respectively on the concentration profiles. It is observed that an increase in the chemical reaction parameter, K_c decreases the concentration boundary layer thickness. Also, it is observed that the concentration distribution increases at all points of the flow field with increasing values of S_c.

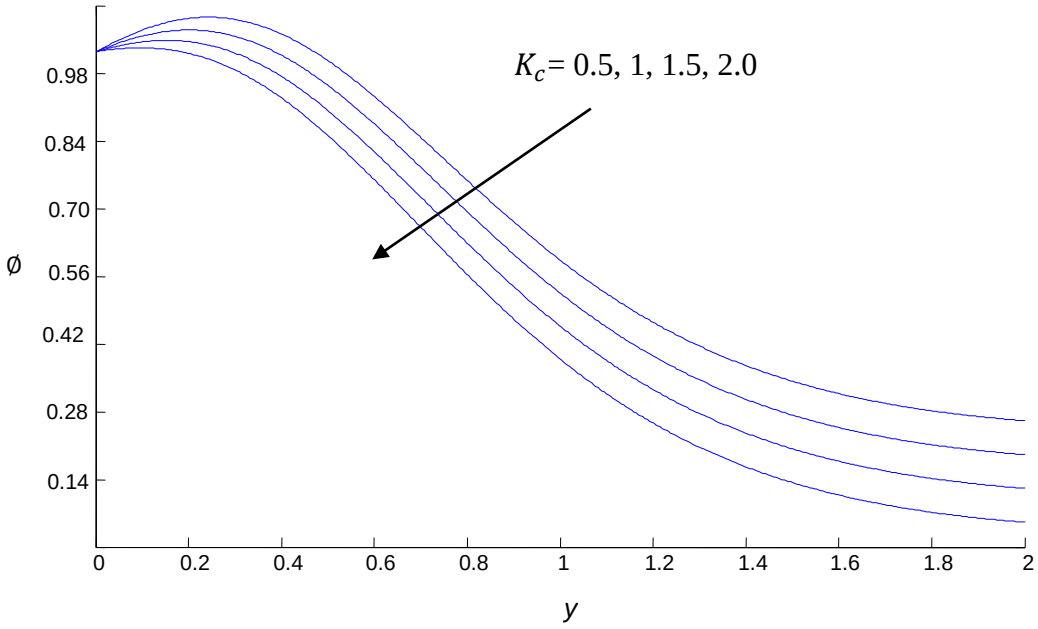

Figure 4. 7 Effects of K_c parameter on the concentration profiles when $t = 0.2$ and $S_c = 2.01$.

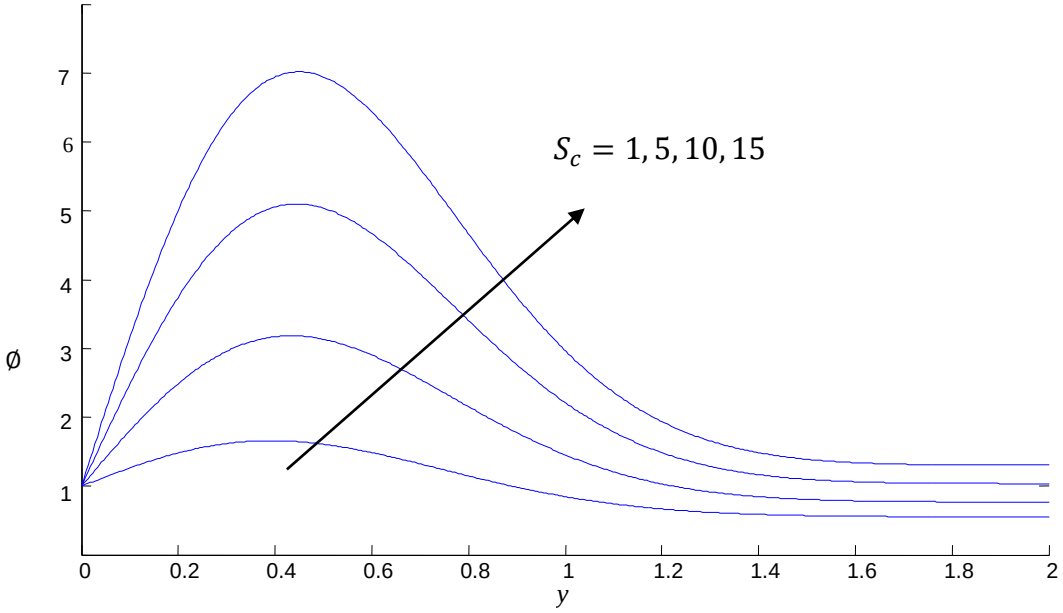

Fig. 4.8 Effects of S_c on the concentration profiles when $K_c = 1$ and $t = 0.2$.

4.5.1.3 Velocity Profiles

Fig. 4.9 – Fig. 4.14 illustrate the effects of K_c, S_c, G_c, P_r, M and G_r on the velocity profiles respectively. It is observed that an increase in either K_c, M or G_c leads to decrease in the velocity of the fluid flow whilst an increase in G_r, P_r or S_c leads to increase in the velocity of the flow as depicted in the diagrams.

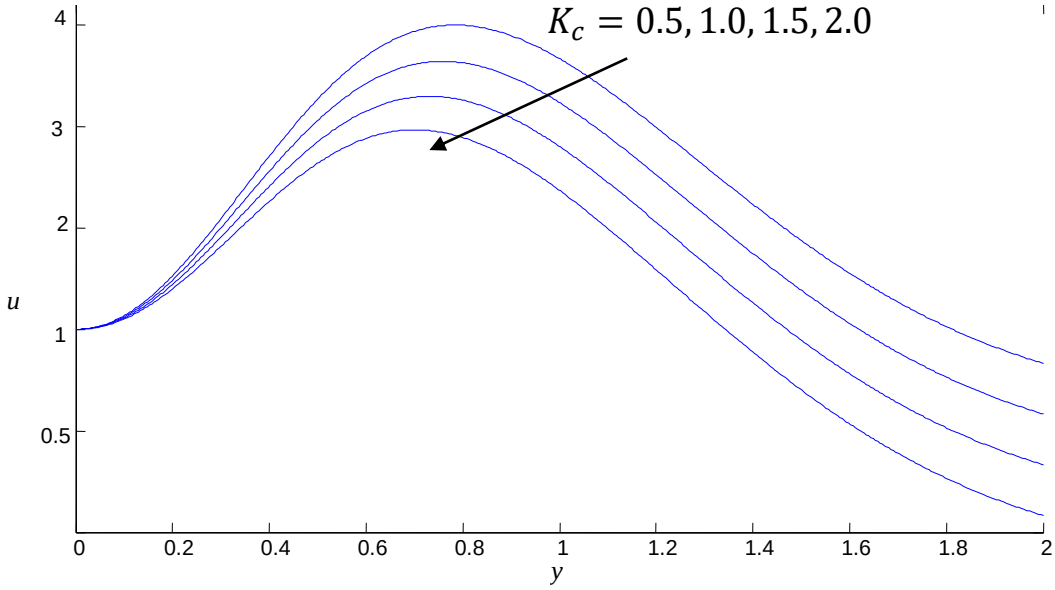

Figure 4. 9 Effects of K_c on the velocity profiles when $G_r = 5, G_c = 5, E_c = 2$ $t = 0.2, k = 1, S_c = 2.01,\ a = 0.2, P_r = 0.71, M = 2, F = 2$ and $H = 2$

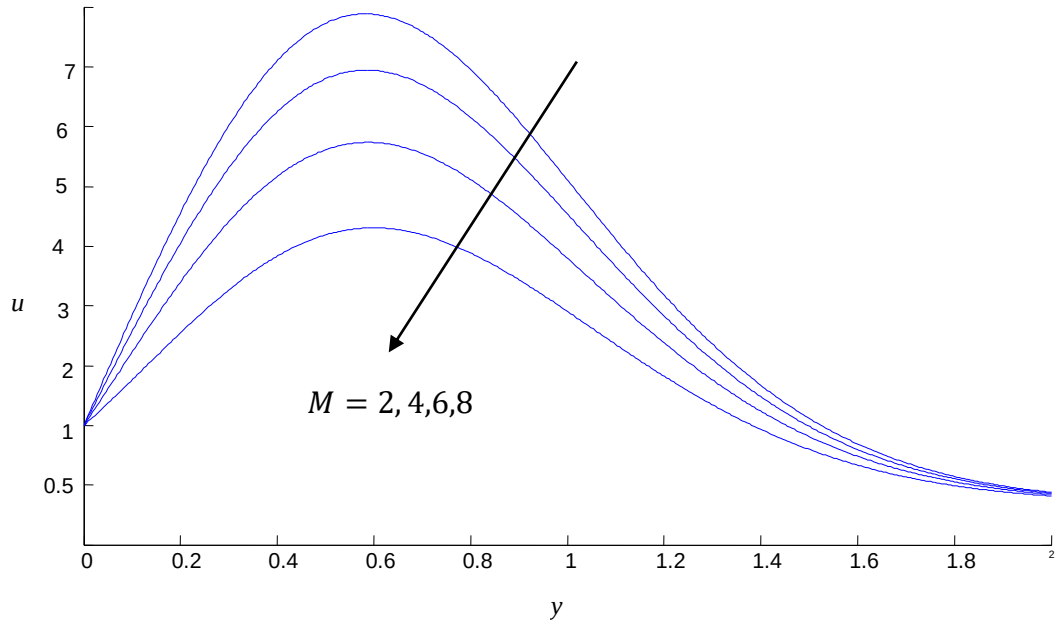

Figure 4. 10 Effects of M on the velocity profiles when $G_r = 5, G_c = 5,$ $t = 0.2, k = 1, K_c = 1, S_c = 2.01, a = 0.2, P_r = 0.71, E_c = 2, F = 2$ and $H = 2$

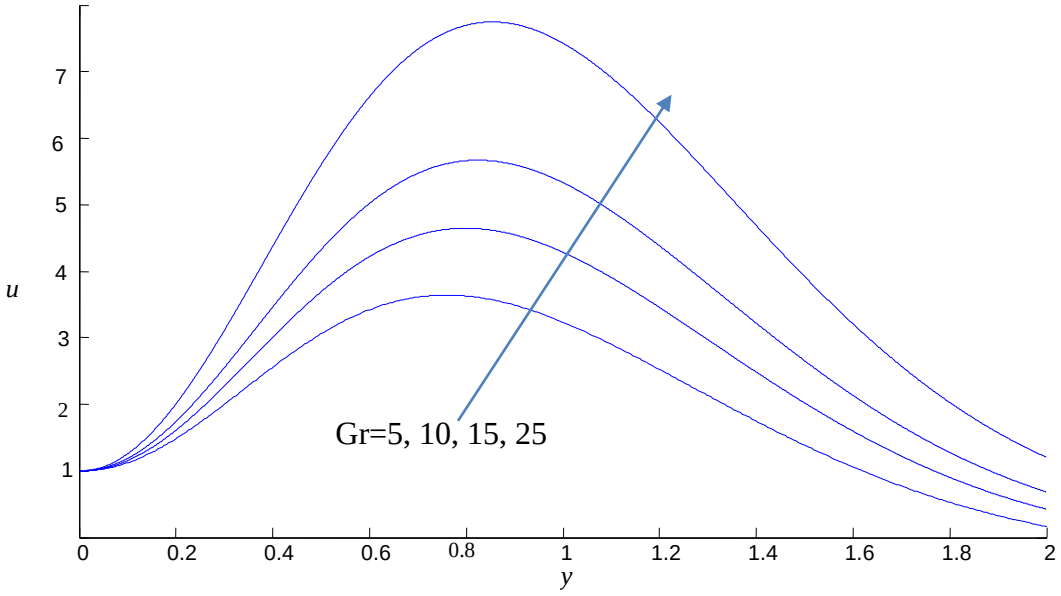

Figure 4. 11 Effects of G_r on the velocity profiles when $M = 2, G_c = 5,$ $t = 0.2, k = 1, K_c = 1, S_c = 2.01, a = 0.2, P_r = 0.71, E_c = 2, F = 2$ and $H = 2$

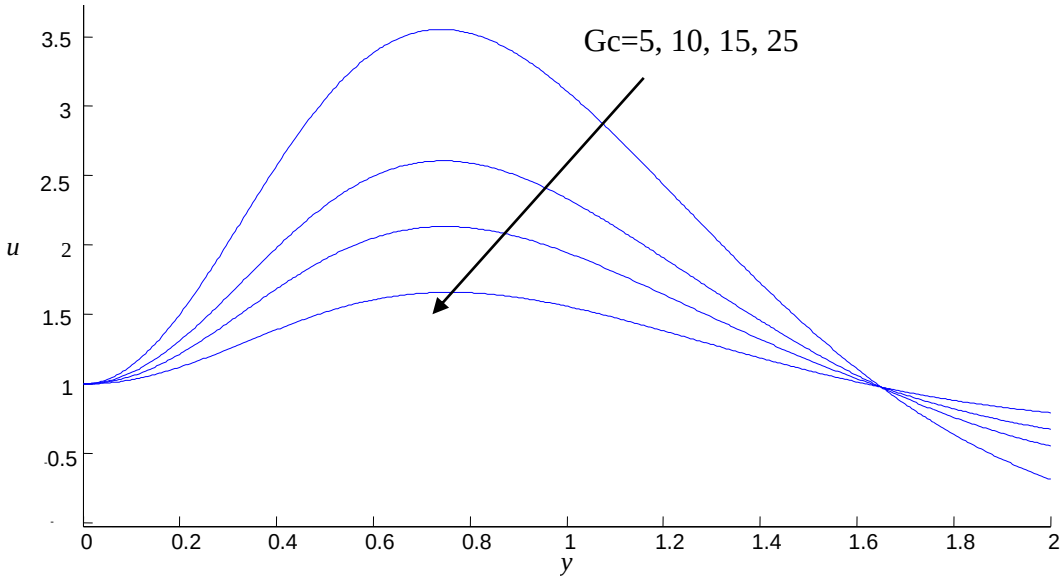

Figure 4. 12 Effects of G_c on the velocity profiles when $M = 2, G_r = 5,$ $t = 0.2, k = 1, K_c = 1, S_c = 2.01, a = 0.2, P_r = 0.71, E_c = 2, F = 2$ and $H = 2$

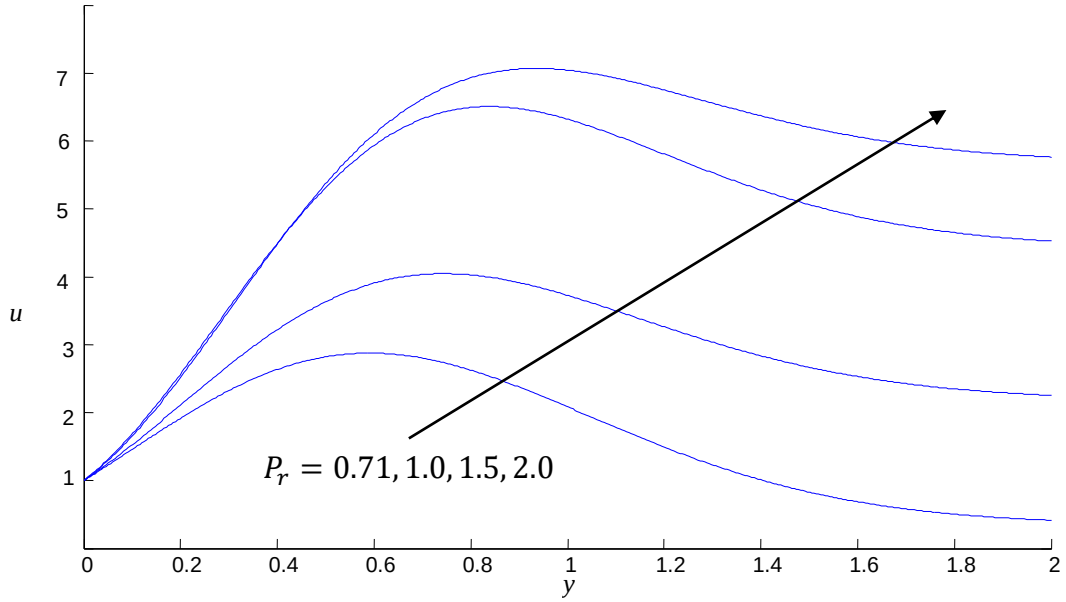

Figure 4.13 Effects of P_r of on the velocity profiles when $M = 2, G_r = 5$, $t = 0.2, k = 1, K_c = 1, S_c = 2.01, a = 0.2, G_c = 5, E_c = 2, F = 2$ and $H = 2$

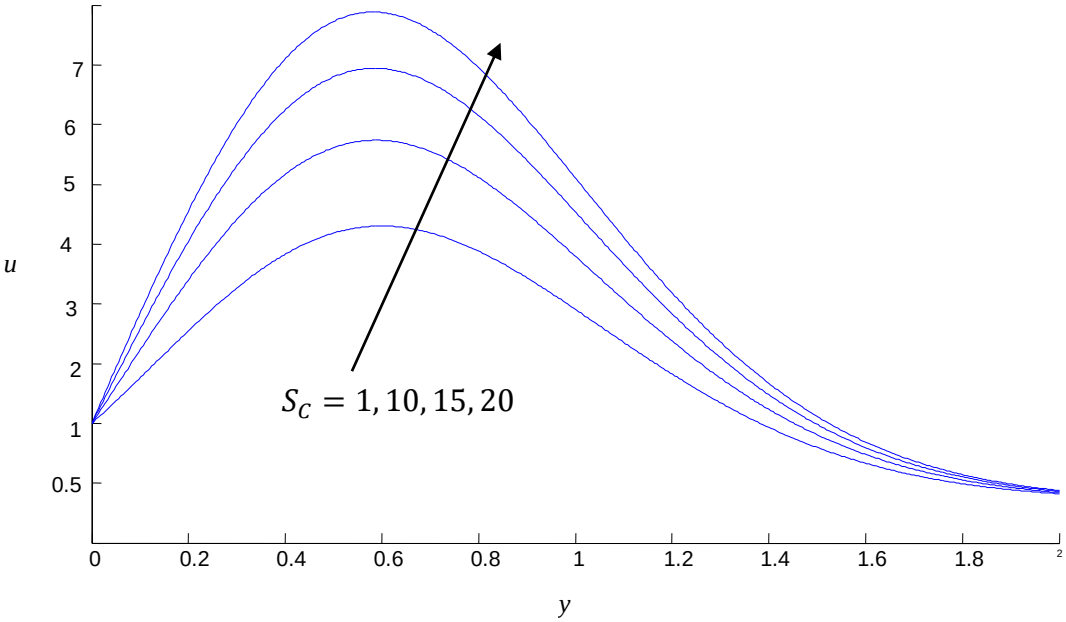

Fig. 4.14 Effects of S_c on the velocity profiles when $M = 2, G_r = 5$, $t = 0.2, k = 1, K_c = 1, P_r = 0.71, a = 0.2, G_c = 5, E_c = 2, F = 2$ and $H = 2$

4.5.1.4 Nusselt Number Profiles

Fig. 4.15, 4.16, 4.17, 4.18 and 4.19 show the effects of Prandtl number (P_r), Magnetic parameter (M), Eckert number (E_c), Radiation parameter (F) and Heat absorption parameter (H) on the Nusselt number profiles respectively. It is observed that increase in M or E_c leads to decrease in the Nusselt number whilst increase in either P_r *or* F or H leads to increase in the Nusselt number.

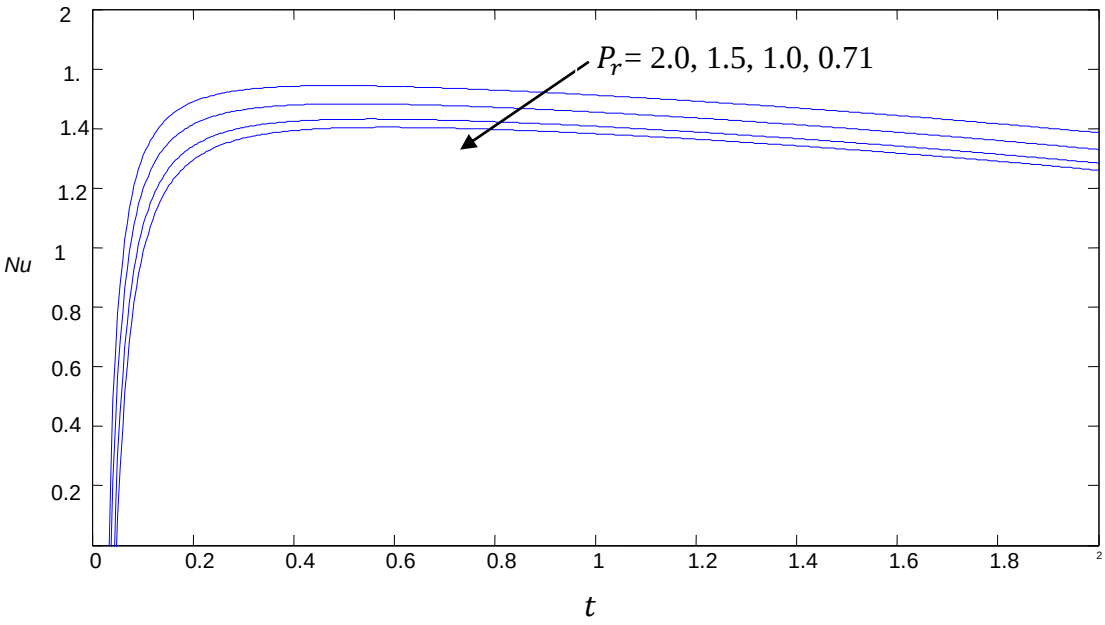

Figure 4. 15 The effects of P_r on the Nusselt number profiles when $M = 2$, $t = 0.2, k = 1, K_c = 1$, $G_c = 5, E_c = 2, F = 2$ and $H = 2$

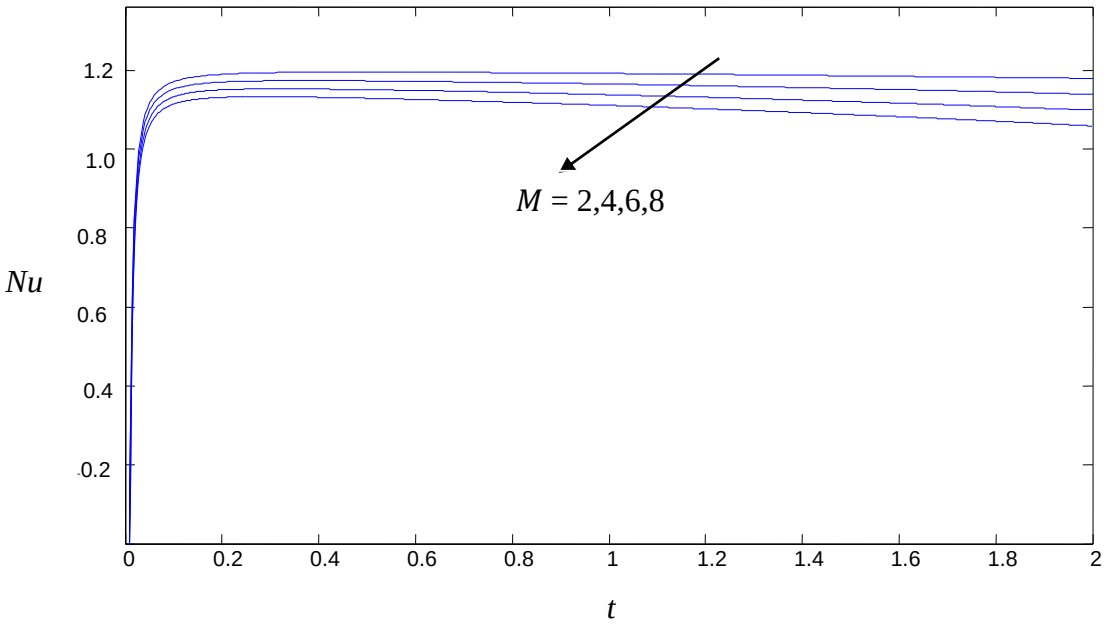

Figure 4.16 The effects of M on the Nusselt number profiles when $P_r = 0.71$, $t = 0.2, k = 1, K_c = 1,\ G_c = 5, E_c = 2, F = 2$ and $H = 2$

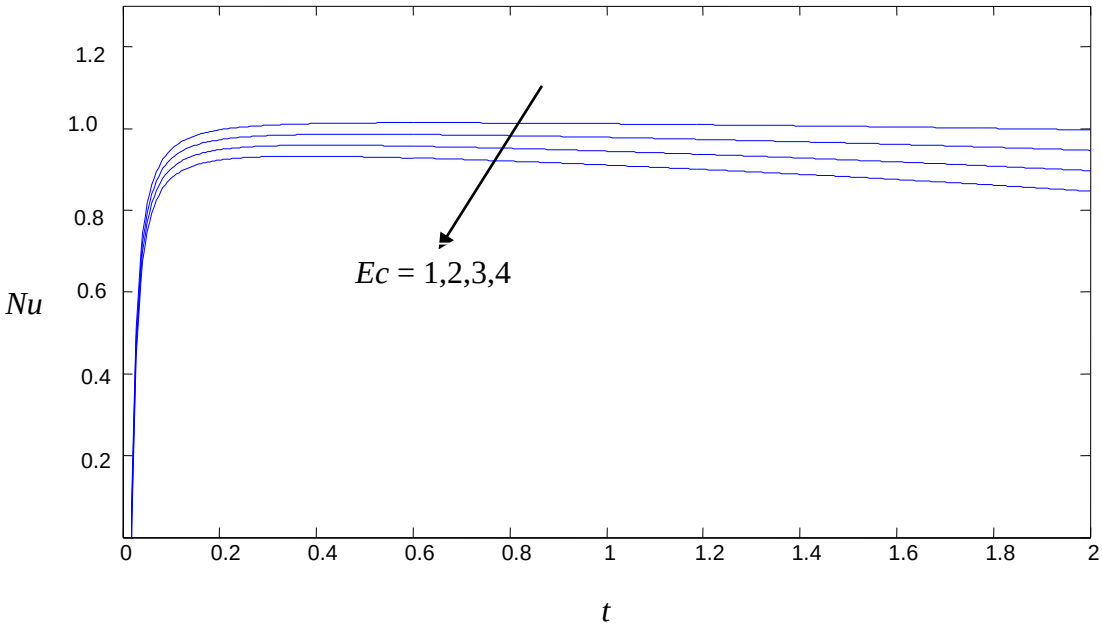

Figure 4. 17 The effects of Ec on the Nusselt number profiles when $P_r = 0.71$, $t = 0.2, k = 1, K_c = 1,\ G_c = 5,\ M = 2, F = 2$ and $H = 2$

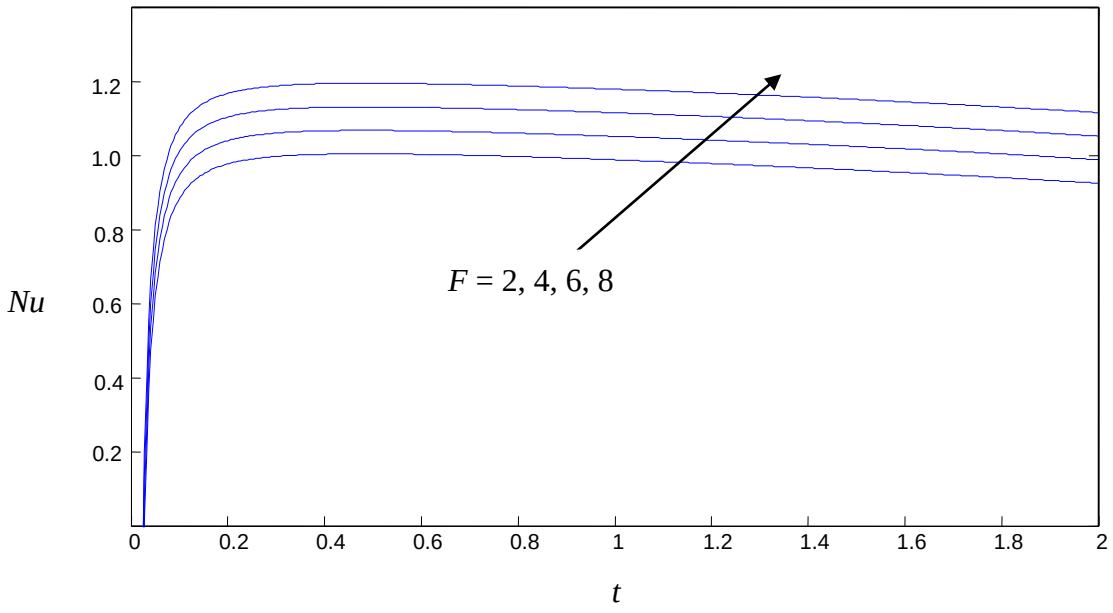

Figure 4.18 The effects of F on the Nusselt number profiles when $P_r = 0.71$, $t = 0.2, k = 1, K_c = 1,\ G_c = 5, E_c = 2, F = 2$ and $H = 2$

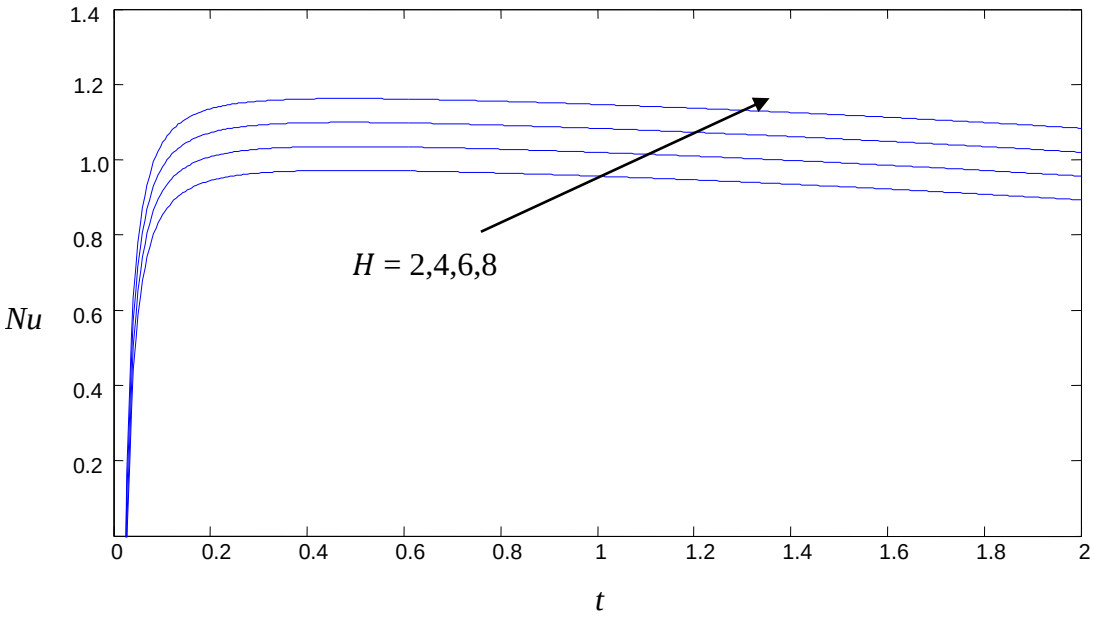

Figure 4. 19 The effects of H on the Nusselt number profiles when $P_r = 0.71$, $t = 0.2, k = 1, K_c = 1,\ G_c = 5, E_c = 2, F = 2$ and $M = 2$.

4.5.1.5 Sherwood Number Profiles

Fig. 4.20 and 4.21 show the effects of Schmidt number (*Sc*) and Chemical reaction parameter (*Kc*) on the Sherwood number profiles respectively. It is observed that an increase in *Sc* results in increase in the Sherwood Number whilst increase in *Kc* decreases the Sherwood number profile.

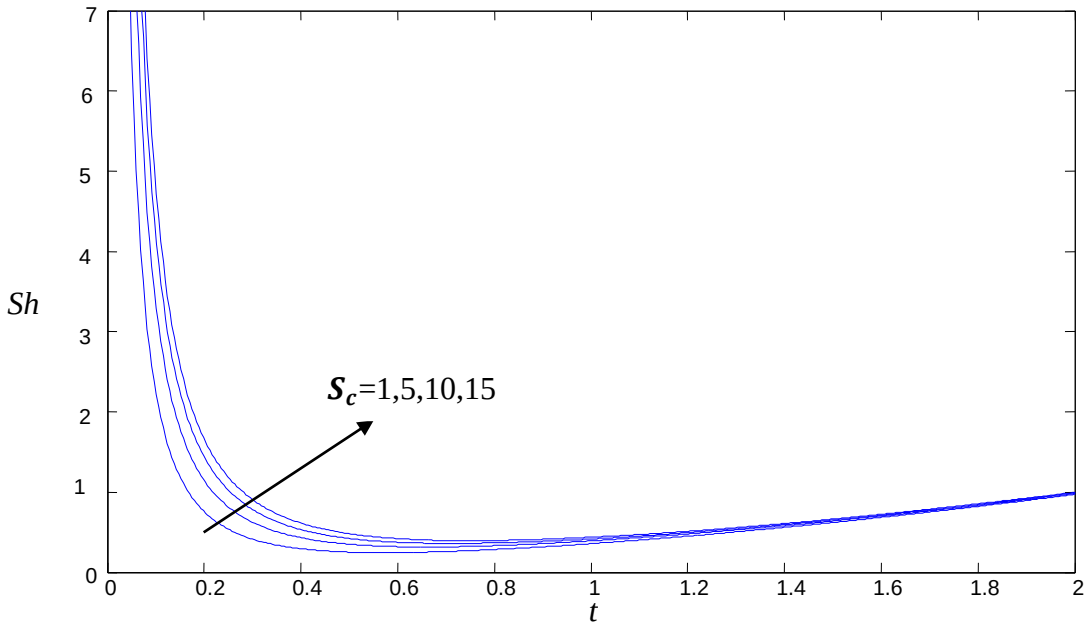

Figure 4. 20 Effects of on the Sherwood number profiles when $t = 0.2$ and $K_c = 1$.

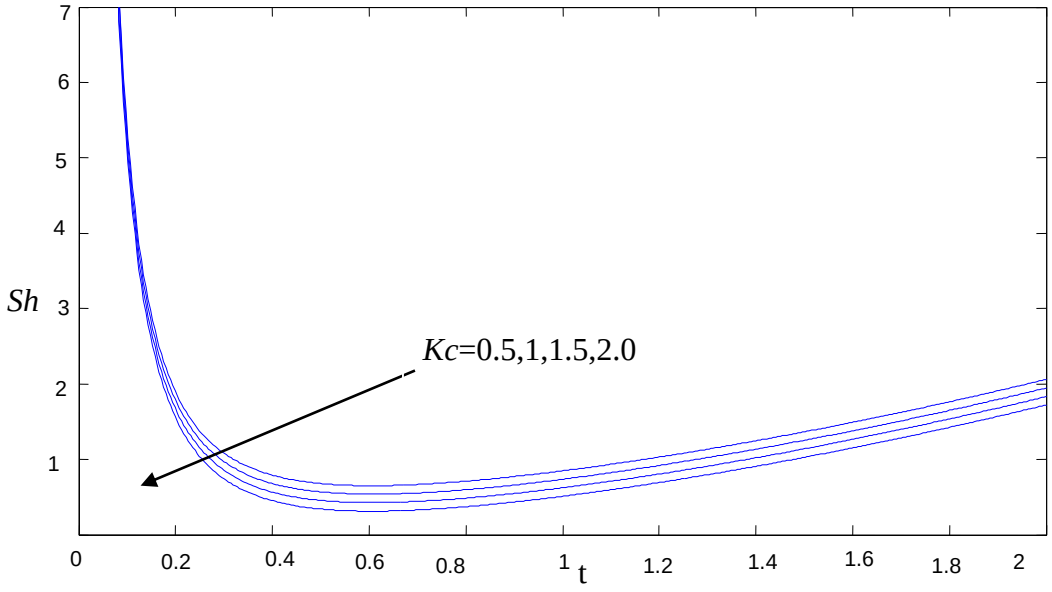

Figure 4. 21 Effects of *Kc* on the Sherwood number profiles when $t = 0.2$ and $S_c = 2.01$.

4.5.1.6 Skin Friction Profiles

Fig. 4.22 and 4.23 show the effects of permeability of porous medium (k) and Magnetic parameter (M) on the Skin Friction coefficient respectively. It is noticed that an increase in M results in decrease in the Skin Friction coefficient whilst increase in k results in increase in the Skin Friction coefficient.

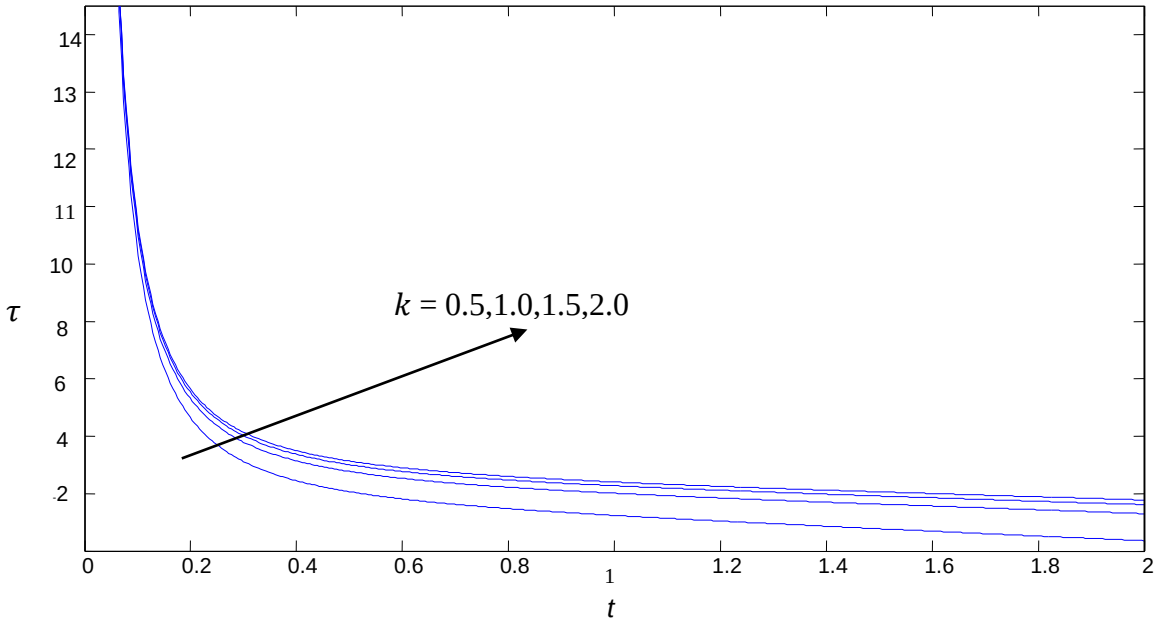

Figure 4. 22 Effects of k on the Skin Friction coefficient when $t = 0.2,\ K_c = 1, H = 2,\ F = 2, P_r = 0.71$ and $M = 2$.

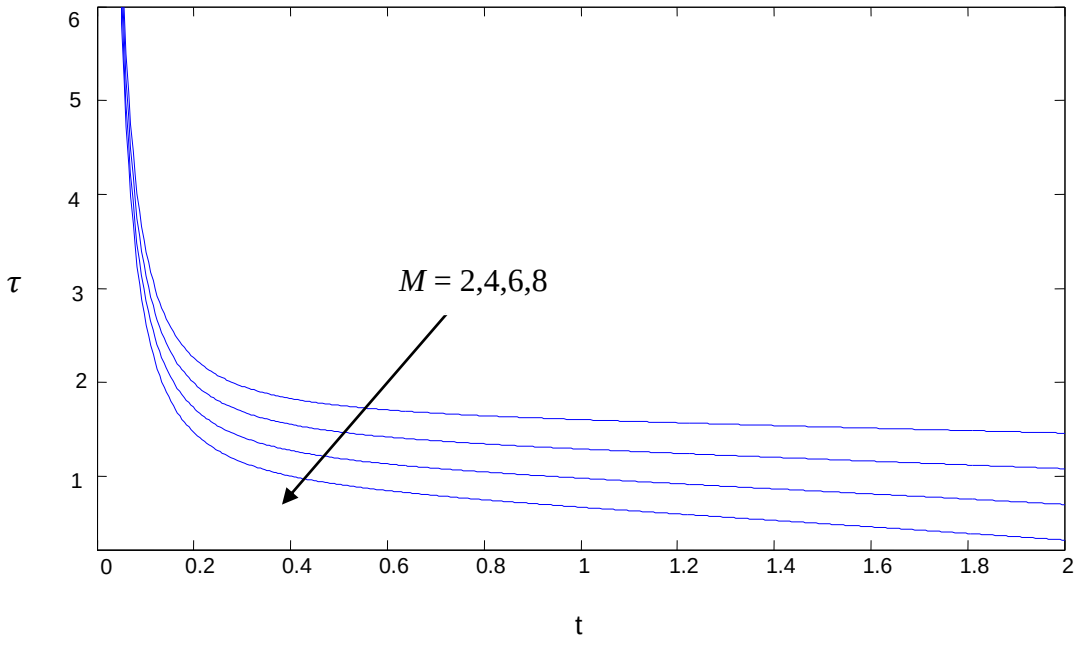

Figure 4.23 Effects of M on the Skin Friction coefficient profiles when $t = 0.2,\ K_c = 1, H = 2,\ F = 2, P_r = 0.71$ and $k = 1$.

4.5.2 Numerical Results

Table 4.1-4.3 show the behaviour of **skin friction coefficient, $-\boldsymbol{u}'(\mathbf{0})$, Sherwood number**, $-\emptyset'(\mathbf{0})$ and **Nusselt number**, $-\boldsymbol{\theta}'(\mathbf{0})$ for various values of time (t), magnetic parameter (M), dimensionless chemical reaction parameter (K_c), Eckert number (E_c), Eckert number (E_c), Schmidt number (S_c), Prandtl number (P_r), radiation parameter (F), dimensionless permeability of porous medium and heat absorption coefficient (H). From Table 4.1, it is noted that the skin friction coefficient, $-u'(0)$ decreases for increasing values of t, M, P_r and k_c but increases with increasing values of k, F and H. From Table 4.2, Sherwood number, $-\emptyset'(0)$ decreases with increasing values of t and k_c but increases with increasing values of S_c. From Table 4.3, Nusselt number , $-\theta'(0)$ decreases with increasing values of t, M, E_c but increases with increasing values of and $Pr, F, G_c, K_c$and S_c.

In order to measure the accuracy of the results obtained, comparison of the present study is made with results of Chamkha *et al.* (2016) which shown a good agreement in Table 4.4.

Table 4. 1:The Skin friction coefficient, -u' (0) at the wall, for various values of t, M, k, F, H, P_r and K_c.

t	M	k	F	H	P_r	K_c	$-u'(0)$
0.2	1.0	1.0	1.0	1.0	1.0	1.0	0.1194
0.4	1.0	1.0	1.0	1.0	1.0	1.0	0.0894
0.6	1.0	1.0	1.0	1.0	1.0	1.0	0.0671
0.2	1.5	1.0	1.0	1.0	1.0	1.0	0.1053
0.2	2.0	1.0	1.0	1.0	1.0	1.0	0.0930
0.2	2.5	1.0	1.0	1.0	1.0	1.0	0.0820
0.2	1.0	2	1.0	1.0	1.0	1.0	0.1353
0.2	1.0	4	1.0	1.0	1.0	1.0	0.1440
0.2	1.0	6	1.0	1.0	1.0	1.0	0.1469
0.2	1.0	1.0	2	1.0	1.0	1.0	0.1942
0.2	1.0	1.0	2.5	1.0	1.0	1.0	0.2222
0.2	1.0	1.0	3	1.0	1.0	1.0	0.2458

0.2	1.0	1.0	1.0	**2**	1.0	1.0	0.1942
0.2	1.0	1.0	1.0	**2.5**	1.0	1.0	0.2222
0.2	1.0	1.0	1.0	**3**	1.0	1.0	0.2458
0.2	1.0	1.0	1.0	1.0	**0.71**	1.0	0.1826
0.2	1.0	1.0	1.0	1.0	**1.0**	1.0	0.1194
0.2	1.0	1.0	1.0	1.0	**1.5**	1.0	0.0473
0.2	1.0	1.0	1.0	1.0	1.0	**0.2**	0.3108
0.2	1.0	1.0	1.0	1.0	1.0	**0.4**	0.2434
0.2	1.0	1.0	1.0	1.0	1.0	**0.6**	0.1937

Table 4. 2:Sherwood number, -∅' (0) at the wall, for various values of t, S_c and K_c.

t	S_c	K_c	$-\emptyset'(0)$
0.2	1.0	1.0	1.0141
0.4	1.0	1.0	0.8126
0.6	1.0	1.0	0.8047
0.2	**0.2**	1.0	0.4535
0.2	**0.4**	1.0	0.6414
0.2	**0.6**	1.0	0.7855
0.2	1.0	**0.2**	1.1645
0.2	1.0	**0.4**	1.0950
0.2	1.0	**0.6**	1.0490

Table 4. 3:The Local Nusselt number, -θ' (0) at the wall, for various values of $t, M, E_c, G_c, F, P_r, K_c, S_c$ when $k = 1$ and $H = 1$

t	M	E_c	G_c	F	P_r	K_c	S_c	$-\theta'(0)$
0.2	1	1	1	1	1	1	1	1.7623
0.4	1	1	1	1	1	1	1	0.6154
0.6	1	1	1	1	1	1	1	0.2877
0.2	2	1	1	1	1	1	1	0.6075
0.2	4	1	1	1	1	1	1	0.0482
0.2	6	1	1	1	1	1	1	0.0037
0.2	1	0.2	1	1	1	1	1	1.0574
0.2	1	0.4	1	1	1	1	1	0.7049
0.2	1	0.6	1	1	1	1	1	0.3525
0.2	1	1	5	1	1	1	1	0.6611
0.2	1	1	7	1	1	1	1	0.6943
0.2	1	1	9	1	1	1	1	1.3111
0.2	1	1	1	2	1	1	1	0.000052
0.2	1	1	1	4	1	1	1	0.0056
0.2	1	1	1	6	1	1	1	0.6075
0.2	1	1	1	1	0.71	1	1	0.0898

0.2	1	1	1	1	1.0	1	1	0.6075
0.2	1	1	1	1	1.2	1	1	0.3251
0.2	1	1	1	1	1	0.2	1	0.0458
0.2	1	1	1	1	1	0.4	1	0.1192
0.2	1	1	1	1	1	0.6	1	0.2338
0.2	1	1	1	1	1	1	2	0.3372
0.2	1	1	1	1	1	1	3	0.4107
0.2	1	1	1	1	1	1	4	0.4778

Table 4. 4:Comparison of results for a reduced Nusselt number (-θ(0)) when $M = E_c = 0$.

Pr	**Chamkha *et al.*(2012)**	**Present study**
0.71	**0.5694**	**0.5689**
1.0	0.6295	0.6294
3.0	0.6727	0.6718
10	0.9978	0.9967

4.6 Conclusion

The MHD unsteady boundary layer flow in the presence heat generation in porous medium has been investigated. The non-linear partial differential equations have been modeled and transformed to dimensionless differential equations using the dimensionless variables. The Laplace transform techniques were employed to solve the resulting dimensionless differential equations directly and results illustrated graphically. From the results obtained, the following conclusions can be drawn:

1. The thermal boundary layer thickness diminishes with the magnetic parameter (M) or Eckert number (Ec) but increases with the Prandtl number (Pr) or the heat absorption parameter (H) or the radiation parameter (F).
2. The concentration boundary layer thickness increases with the Schmidt number (S_c) whilst the chemical reaction parameter (K_c) causes a reduction in the species concentration in the fluid.
3. The velocity of flow decreases with increase in either Chemical reaction parameter (K_c) or Magnetic parameter (M) or Mass Grashof number (Gc) but increases with an increase in Grashof number (Gr) or Schmidt number (Sc).
4. The Nusselt number decreases in either Magnetic parameter (M) or Eckert number (Ec) but increases with increase in the Prandtl number (Pr) or Radiation parameter (F) or Heat absorption parameter (H).

5. The Sherwood number decreases with time (t) or the chemical reaction parameter (Kc) but increases with the Schmidt number (Sc).
6. The Skin Friction coefficient decreases with increase in time (t), Magnetic parameter (M), Prandtl number (Pr), Chemical reaction parameter (Kc) but increases with increase in Permeability of porous medium (k), Radiation parameter (F) and Heat absorption parameter (H).

CHAPTER FIVE

UNSTEADY HYDROMAGNETIC CONVECTIVE HEAT AND MASS TRANSFER PAST AN IMPULSIVELY STARTED INFINITE VERTICAL SURFACE WITH NEWTONIAN HEATING IN A POROUS MEDIUM

5.1 Introduction

In this chapter, unsteady hydromagnetic convective heat and mass transfer past an impulsively started infinite vertical surface with Newtonian heating in a porous medium is studied. **Three (3) fluids** are considered in this study namely **air**, **electrolyte solution** and **water.** These fluids physical Prandtl numbers (air (Pr = 0.71), electrolyte solution (Pr = 1.0) and water (Pr = 7.0)) in practice are used for the analysis. The governing differential equations are transformed using suitable dimensionless parameters. The dimensionless equations are solved using the Laplace transform techniques and results are illustrated graphically for the velocity, temperature and concentration profiles. Numerical results are also provided for the Nusselt number, Skin friction and Sherwood number.

5.2 Mathematical Formulation of Unsteady Hydromagnetic Convective Heat and Mass Transfer

Consider the unsteady hydromagnetic convective heat and mass transfer past an impulsively started infinite vertical surface with Newtonian heating. In addition to the models' assumptions, the flow is assumed to be in the $x^* - axis$ direction which is taken along the plate in the vertical upward direction. At time $t^* > 0$, the plate is subjected to an impulsive motion in vertically upward direction with a uniform velocity U_0 and at a temperature T_w^* and the concentration level near the plate is raised to C_w^* . The physical system of the flow is shown in Fig. 5.1.

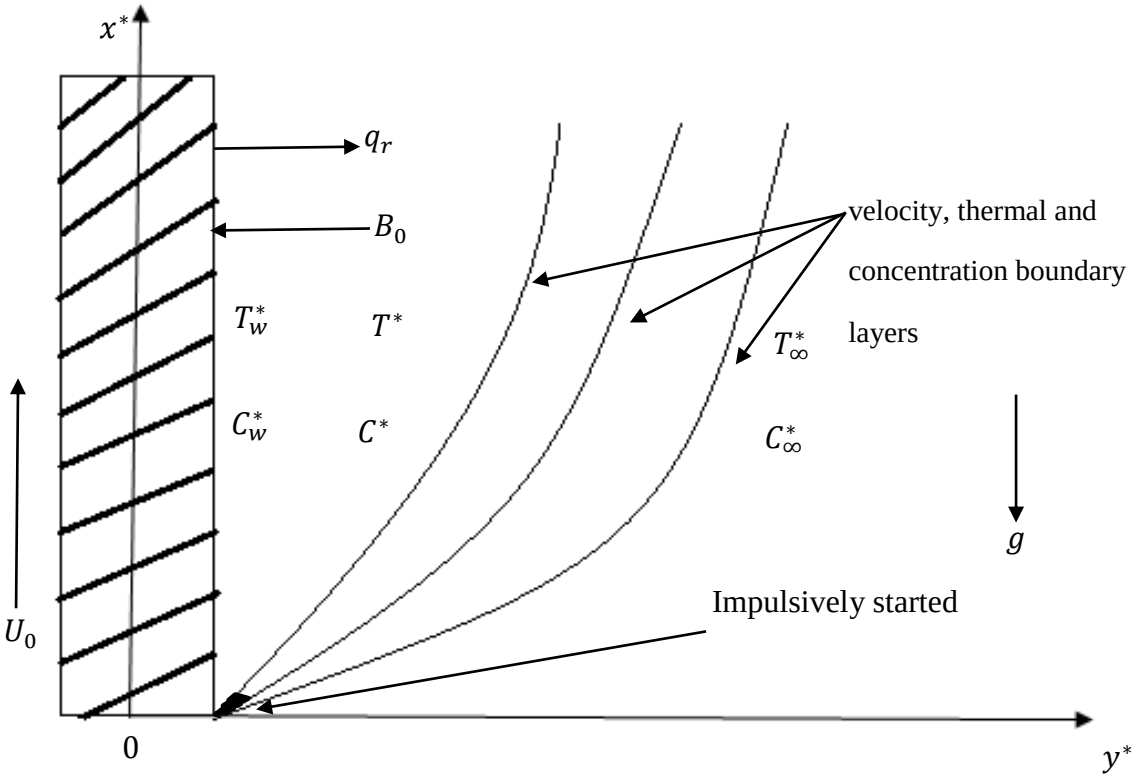

Figure 5. 1 Flow configuration and coordinate system

The boundary layer equations governing the unsteady flow process can be modeled as shown in the following sections:

5.2.1 The Continuity Equation of Unsteady Hydromagnetic Convective Heat and Mass Transfer

Since the plate is infinitely along the $x^* -$ direction, all the physical variables are functions of y^* and t^* only aand hence the continuity equation was derived in (4.3) as

$$\frac{\partial v^*}{\partial y^*} = 0$$

5.2.2 The Momentum Equation of Unsteady Hydromagnetic Convective Heat and Mass Transfer

The momentum equation was derived in (3.8) as

$$\rho\left(\frac{\partial u^*}{\partial t^*} + u\frac{\partial u^*}{\partial x^*} + v\frac{\partial u^*}{\partial y^*}\right) = -\frac{\partial p}{\partial x^*} + \mu\frac{\partial^2 u^*}{\partial y^{*2}} + \rho g$$

Introducing the fluid pressure, $-\frac{\partial p}{\partial x^*} = u\frac{\partial u^*}{\partial x^*} + v\frac{\partial u^*}{\partial y^*}$, thermal buoyancy, $g\beta_T(T^* - T_\infty^*)$, concentration buoyancy, $g\beta_C(C^* - C^*_\infty)$ and magnetic force, $\sigma B_0^2 u^*$ into the flow field in (3.8) reduces to the momentum equation

$$\frac{\partial u^*}{\partial t^*} = \nu\frac{\partial^2 u^*}{\partial y^{*2}} + g\beta_T(T^* - T_\infty^*) + g\beta_C(C^* - C^*_\infty) - \frac{\sigma B_0^{\,2}}{\rho}u^* \qquad (5.1)$$

5.2.3 The Energy Equation of Unsteady Hydromagnetic Convective Heat and Mass Transfer

In (3.12), the energy equation was derived as

$$\frac{\partial T^*}{\partial t^*} + \left(u\frac{\partial T^*}{\partial x^*} + v\frac{\partial T^*}{\partial y^*} + w\frac{\partial T^*}{\partial z^*}\right) = \propto \left(\frac{\partial^2 T^*}{\partial x^{*2}} + \frac{\partial^2 T^*}{\partial y^{*2}} + \frac{\partial^2 T^*}{\partial z^{*2}}\right) + \Phi$$

Since the flow is along the x^*- direction, all the physical variables are the functions of y^* and t^* only. Hence for the unsteady flow with magnetic field and radiative heat flux, (3.12) is modified to become

$$\rho C_p \frac{\partial T*}{\partial t*} = k\frac{\partial^2 T*}{\partial y*^2} - \frac{\partial q_r}{\partial y*} + \sigma B_0^2 u^{*2} \qquad (5.2)$$

5.2.4 The Concentration Equation of Unsteady Hydromagnetic Convective Heat and Mass Transfer

The concentration equation was derived in vector form in (3.15) as

$$\frac{\partial C^*}{\partial t^*} = D\nabla^2 C^* + \dot{r}$$

In component form, (3.15) is modified to become

$$\frac{\partial C*}{\partial t*} = D\frac{\partial^2 C*}{\partial y*^2} - K_C(C*-C*_\infty) \quad \text{(as in (4.7)) .}$$

Now the boundary layer equations governing the unsteady flow process modeled in dimensional form are

$\frac{\partial v^*}{\partial y^*} = 0$ (as in (4.3)).

$$\frac{\partial u^*}{\partial t^*} = \nu \frac{\partial^2 u^*}{\partial y^{*2}} + g\beta_T (T^* - T_\infty^*) + g\beta_C (C^* - C^*_\infty) - \frac{\sigma B_0^{\,2}}{\rho} u^* \ . \qquad (5.1)$$

$$\rho C_p \frac{\partial T^*}{\partial t^*} = k \frac{\partial^2 T^*}{\partial y^{*2}} - \frac{\partial q_r}{\partial y^*} + \sigma B_0^2 u^{*2}. \qquad (5.2)$$

$$\frac{\partial C^*}{\partial t^*} = D \frac{\partial^2 C^*}{\partial y^{*2}} - K_C (C^* - C^*_\infty) \cdot$$

5.2.5 Associated Boundary Conditions of Unsteady Hydromagnetic Convective Heat and Mass Transfer

Under the assumptions of the problem, the boundary conditions governing the unsteady flow process are

$$u^* = 0,\ T^* = T_\infty^*\ C^* = C_\infty^*\ \ for\ all\ \ y^* \geq 0,\ t^* \leq 0;$$

$$u^* = U_0, T^* = T_w^*,\ C^* = C_w^*\ \ at\ y^* = 0,\ t^* > 0; \qquad (5.3)$$

$$u^* \to 0,\ T^* \to T_\infty^*,\ C^* \to C_\infty^*\ \ as\ y^* \to \infty\ , t^* > 0.$$

5.2.6 Dimensionless Transformation of Unsteady Hydromagnetic Convective Heat and Mass Transfer

The dimensionless temperature, concentration, velocity as well as skin friction, Nusselt number and Sherwood number are obtained using the following dimensionless parameters.

5.2.7 The Dimensionless Variables of Unsteady Hydromagnetic Convective Heat and Mass Transfer

The dimensionless equalities in (3.16) similar to dimensionless parameters used by Narahari *et al.* (2011), Sharidan *et al.* (2014), Chaudhary *et al.* (2006) are introduced.

5.2.8 Dimensionless Continuity Equation of Unsteady Hydromagnetic Convective Heat and Mass Transfer

The dimensionless continuity equation was derived in (4.12) as

$$\frac{\partial v}{\partial y} = 0.$$

5.2.9 The Dimensionless Momentum Equation of Unsteady Hydromagnetic Convective Heat and Mass Transfer

Substituting the partial derivatives of the dimensionless quantities for the momentum equation in (4.9), (4.13) and (4.14) into (5.1) give

$$\frac{{U_o}^3}{v}\frac{\partial u}{\partial t} = v\,\frac{U_0^3}{v^2}\frac{\partial^2 u}{\partial y^2} + g\beta_T\,(T_w^* - T_\infty^*)\theta + g\beta_c(C_w^* - C_\infty^*)\emptyset - \frac{\sigma {B_o}^2}{\rho}\,uU_0\,,$$

$$\frac{\partial u}{\partial t} = \frac{\partial^2 u}{\partial y^2} + vg\beta_T\,\frac{(T_w^* - T_\infty^*)}{U_0^3}\theta + vg\beta_c\frac{(C_w^* - C_\infty^*)}{{U_0}^3}\emptyset - \frac{\sigma {B_o}^2 v}{\rho}\,\frac{U_o u}{U_0^3},$$

$$\frac{\partial u}{\partial t} = \frac{\partial^2 u}{\partial y^2} + \frac{vg\beta_T(T_w^* - T_\infty^*)}{U_0^3}\theta + \frac{vg\beta_c(C_w^* - C_\infty^*)}{{U_0}^3}\emptyset - \frac{\sigma {B_o}^2 v}{\rho U_0^2}u\,,$$

$$\frac{\partial u}{\partial t} = \frac{\partial^2 u}{\partial y^2} + Gr\theta + G_c\emptyset - Mu. \quad (5.4)$$

5.2.10 The Dimensionless Energy Equation of Unsteady Hydromagnetic Convective Heat and Mass Transfer

Using Rosseland approximation in (4.18) and by substituting the partial derivatives of the dimensionless quantities for the energy equation (4.19) and (4.20) into (5.2) gives

$$\frac{U_0^2}{v}(T_w^* - T_\infty^*)\frac{\partial\theta}{\partial t} = \frac{v}{P_r}\frac{U_0^2}{v^2}(T_w^* - T_\infty^*)\frac{\partial^2\theta}{\partial y^2} + \frac{1}{\rho C_p}16a^*\sigma T_\infty^{*3}(T_\infty^* - T^*) + \frac{\sigma B_0^2}{\rho C_p}u^2U_{0,}^2$$

$$\frac{\partial\theta}{\partial t} = \frac{1}{P_r}\frac{\partial^2\theta}{\partial y^2} + \frac{16va^*\sigma T_\infty^{*3}(T_\infty^* - T^*)}{\rho C_p U_0^2(T_w^* - T_\infty^*)} + \frac{\sigma B_0^2}{\rho C_p}u^2U_0^2\frac{v}{U_0^2(T_w^* - T_\infty^*)},$$

$$= \frac{1}{P_r}\frac{\partial^2\theta}{\partial y^2} - \frac{16va^*\sigma T_\infty^{*3}(T_w^* - T_\infty^*)}{\rho C_p U_0^2(T_w^* - T_\infty^*)}\theta + \frac{\sigma B_0^2}{\rho C_p}u^2U_0^2\frac{v}{U_0^2(T_w^* - T_\infty^*)} \quad \text{since} \quad v = \frac{\mu}{\rho},$$

$$= \frac{1}{P_r}\frac{\partial^2\theta}{\partial y^2} - \frac{16v^2a^*\sigma T_\infty^{*3}}{\mu C_p U_0^2}\theta + \frac{\sigma B_{0v}^2}{\rho U_0^2}\frac{U_0^2}{C_p(T_w^* - T_\infty^*)}u^2,$$

$$= \frac{1}{P_r}\frac{\partial^2\theta}{\partial y^2} - \frac{16v^2a^*\sigma T_\infty^{*3}}{P_r k U_0^2}\theta + ME_c u^2,$$

$$= \frac{1}{P_r}\frac{\partial^2\theta}{\partial y^2} - \frac{1}{P_r}F\theta + ME_c u^2,$$

$$= \frac{1}{P_r}\left(\frac{\partial^2\theta}{\partial y^2} - F\theta\right) + ME_c u^2. \quad (5.5)$$

5.2.11 The Dimensionless Concentration Equation of Unsteady Convective Heat and Mass Transfer

Since the concentration boundary layer equation is the same as in (4.7), by substituting the partial derivatives of the dimensionless quantities for the concentration equation in (4.22) and (4.23) into (4.7) resulted in

$\frac{\partial \emptyset}{\partial t} = \frac{1}{S_C}\frac{\partial^2 \emptyset}{\partial y^2} - k_C \emptyset$ (see (4.24)).

Now the boundary layer equations governing the unsteady flow process modeled in dimensionless form are (5.4), (5.5) and (4.24).

5.2.12 Associated Dimensionless Boundary Conditions of Unsteady Hydromagnetic Convective Heat and Mass Transfer

The corresponding boundary conditions in dimensionless form are

$$\begin{aligned} &u = 0 \quad \theta = 0 \quad \emptyset = 0 \text{ for all } y \geq 0, t \leq 0; \\ &u = 1 \quad \theta = 0, \quad \emptyset = 1 \text{ for all } y = 0, t > 0; \\ &u \to 0 \quad \theta \to 0 \quad \emptyset \to 0 \text{ as } y \to \infty, t > 0. \end{aligned} \tag{5.6}$$

5.3 Analytical Solution of Unsteady Hydromagnetic Convective Heat and Mass Transfer

The non-linear differential equations (5.4), (5.5) and (4.24) with boundary conditions (5.6) are solved in exact form using Laplace transform technique as shown below.

5.3.1 Laplace Transform Technique of Unsteady Hydromagnetic Convective Heat and Mass Transfer

In the energy model (5.5) subject to the boundary conditions in (5.6)

In Laplace domain, the boundary conditions can be written as:

$$\begin{aligned} &\theta(y,0)=0 \quad for\ all \quad y\geq 0, t\leq 0 && \bar{\theta}(y,0)=0;\\ &\theta(0,t)=0 \quad at \quad y=0, t>0 && \bar{\theta}(0,s)=0; \\ &\theta(y,t)\to 0 \quad as \quad y\to\infty, t>0 && \bar{\theta}(y,s)\to 0. \end{aligned} \tag{5.7}$$

Taking Laplace transform of (5.5) results in

$$\frac{1}{P_r}\frac{\partial^2\bar{\theta}}{\partial y^2}-s\bar{\theta}(y,s)+\theta(y,0)=\frac{F}{P_r}\bar{\theta}(y,s)-ME_cL[u^2]\,. \tag{5.8}$$

Also from the boundary condition $\theta(y,0)=0 \quad for\ all \quad t\leq 0$, implies

$$\frac{\partial^2\bar{\theta}}{\partial y^2}-P_r\left(s+\frac{F}{P_r}\right)\bar{\theta}=-P_rME_c\,L[u^2(y,t)]. \tag{5.9}$$

Considering the homogeneous problem of the LHS of (5.9), the general solution is

$$\bar{\theta}_h(y,s) = A(s)e^{-y\sqrt{P_r s+F}} + B(s)e^{y\sqrt{P_r s+F}}. \quad (5.10)$$

Using method of undetermined coefficients, guessing the form of the particular solution in (5.9) to be

$\bar{\theta}_p(y,s) = A;$

$\bar{\theta}_p'(y,s) = 0;$

$\bar{\theta}_p''(y,s) = 0$; substituting in (5.9) gives

$$0 - (P_r s + F)A = -P_r ME_c\, L[u^2(y,t)]$$

$$A = \frac{P_r ME_c}{P_r s+F} L[u^2(y,t)]. \quad (5.11)$$

Adding the particular solution (5.11) to (5.10) gives the general solution

$$\bar{\theta}(y,s) == A(s)e^{-y\sqrt{P_r s+F}} + B(s)e^{y\sqrt{P_r s+F}} + \frac{P_r ME_c}{P_r s+F} L[u^2(y,t)]. \quad (5.12)$$

Since $\theta(y,t) \to 0\ as\ \ y \to \infty, t > 0 \implies \bar{\theta}(y,s) = 0$ and $B(s) = 0$ in (5.12).

Now (5.12) reduces to

$$\bar{\theta}(y,s) = A(s)e^{-y\sqrt{P_r s+F}} + \frac{P_r ME_c}{P_r s+F} L[u^2(y,t)]. \quad (5.13)$$

$\theta(0,t) = 0 \quad at \quad y = 0, t > 0 \qquad\qquad \bar{\theta}(0,s) = 0$

From (5.13), $0 = A(s) + \frac{P_r ME_c}{P_{rs}+F} L[u^2(y,t)]$

$$\bar{\theta}(y,s) = -L[u^2(y,t)]P_r ME_c \frac{e^{-y\sqrt{P_r s+F}}}{P_r s+F} + L[u^2(y,t)]P_r ME_c \frac{1}{P_r s+F}. \quad (5.14)$$

$$\bar{\theta}(y,s) = \bar{u}^2(y,s)P_r ME_c \left(\frac{1}{P_r s+F} - \frac{1}{P_r s+F} e^{-y\sqrt{P_r s+F}}\right). \quad (5.15)$$

Equation (5.15) is the solution of the temperature model in Laplace domain.

Again, the velocity term is coupled in the temperature equation, the general solution of the velocity equation is obtained upon which the general solution of the temperature equation can be determined.

Now considering the dimensionless concentration equation (4.24) which is

$$\frac{\partial \phi}{\partial t} = \frac{1}{Sc}\frac{\partial^2 \phi}{\partial y^2} - Kc\phi .$$

Subjected to the boundary conditions in Laplace domain:

$\emptyset(y,0) = 0 \quad for\ all \quad y,t \le 0 \qquad \bar{\emptyset}(y,0) = 0;$

$\emptyset(0,t) = 1 \ \ at \quad y = 0, t > 0 \qquad \bar{\emptyset}(0,s) = \frac{1}{s};$

$\emptyset(y,t) \to 0 \quad as \quad y \to \infty, t > 0 \qquad \bar{\emptyset}(y,s) \to 0.$

Also, since the concentration boundary conditions is the same as in (4.34), the general solution of the concentration profile at $t > 0$ (see (4.40)) is

$$\emptyset(y,t) = \frac{1}{2}\left[e^{-y\sqrt{S_cK_c}}erfc\left(\frac{2t\sqrt{K_c}-y\sqrt{S_c}}{2\sqrt{t}}\right) + e^{y\sqrt{S_cK_c}}erfc\left(\frac{2t\sqrt{K_c}+y\sqrt{S_c}}{2\sqrt{t}}\right)\right].$$

Similarly, in momentum model (5.4) subject to the boundary conditions in (5.6). In Laplace domain, the momentum boundary conditions can be written as:

$u(y,0) = 0 \quad for\ all \quad y \ge 0, t \le 0 \qquad \bar{u}(y,0) = 0;$

$u(0,t) = 1 \ \ at \ \ y = 0, t > 0 \qquad \bar{u}(0,s) = \frac{1}{s};$ (5.16)

$u(y,t) \to 0 \ \ as \ \ y \to \infty, t > 0 \qquad \bar{u}(y,s) \to 0.$

Taking Laplace transform of (5.4) results in

$\frac{\partial^2 \bar{u}}{\partial y^2} - s\bar{u} + u(y,0) = -G_r\bar{\theta} - G_c\bar{\emptyset} + M\bar{u}.$

But $u(y,0) = 0$

$\frac{\partial^2 \bar{u}}{\partial y^2} - s\bar{u} = -G_r\bar{\theta} - G_c\bar{\emptyset} + M\bar{u}.$ (5.17)

$\frac{\partial^2 \bar{u}}{\partial y^2} - (s+M)\bar{u} = -G_r\bar{\theta} - G_c\bar{\emptyset}.$ (5.18)

Equation (5.18) is linear non-homogenous second order ordinary differential equation.

Considering the homogeneous problem of the LHS of (5.18) the general solution is

$\bar{u}_h(y,s) = A(s)e^{-y\sqrt{s+M}} + B(s)e^{y\sqrt{s+M}}.$ (5.19)

Using method of undetermined coefficients, guessing the form of the particular solution in (5.18) to be

$\bar{u}_p(y,s) = A;$

$\bar{u}_p'(y,s) = 0;$

$\bar{u}_p''(y,s) = 0;$ substituting in (5.18) gives

$0 - (s+M)A == -G_r\bar{\theta} - G_c\bar{\emptyset}$

$$A = \frac{G_r}{s+M}\bar{\theta} + \frac{G_c}{s+M}\bar{\emptyset}. \qquad (5.20)$$

Adding the particular solution (5.20) to (5.19) yields

$$\bar{u}(y,s) = A(s)e^{-y\sqrt{s+M}} + B(s)e^{y\sqrt{s+M}} + \frac{G_r}{s+M}\bar{\theta} + \frac{G_c}{s+M}\bar{\emptyset}. \qquad (5.21)$$

Since $u(y,t) \to 0 \; as \quad y \to \infty, t > 0 \qquad \bar{u}(y,s) = 0$

From (5.21), $B(s) = 0$. Now (2.21) reduces to

$$\bar{u}(y,s) = A(s)e^{-y\sqrt{s+M}} + \frac{G_r}{s+M}\bar{\theta} + \frac{G_c}{s+M}\bar{\emptyset}. \qquad (5.22)$$

Since $u(0,t) = 1 \quad at \quad y = 0, t > 0 \qquad \Longrightarrow \bar{u}(0,s) = 1$

$$1 = A(s\,) + \frac{G_r}{s+M}\bar{\theta} + \frac{G_c}{s+M}\bar{\emptyset}$$

$$\bar{u}(y,s) = \left(1 - \frac{G_r}{s+M}\bar{\theta} - \frac{G_c}{s+M}\bar{\emptyset}\right)e^{-y\sqrt{s+M}} + \frac{G_r}{s+M}\bar{\theta} + \frac{G_c}{s+M}\bar{\emptyset}$$

$$\bar{u}(y,s) = e^{-y\sqrt{s+M}} + G_r\bar{\theta}\left(\frac{1}{s+M} - \frac{1}{s+M}e^{-y\sqrt{s+M}}\right) + G_c\bar{\emptyset}\left(\frac{1}{s+M} - \frac{1}{s+M}e^{-y\sqrt{s+M}}\right). \qquad (5.23)$$

Taking inverse Laplace transform of (5.23), the general solution (see convolution theorem in Appendix IV, (A4.4) and (A4.8)) is

$$u(y,t) = \frac{ye^{-\frac{y^2}{4t}-tM}}{2\sqrt{\pi t^3}} + G_r\theta(y,t)\left(e^{-Mt} - e^{-Mt}erfc\left(\frac{y}{2\sqrt{t}}\right)\right) +$$

$$G_c\emptyset(y,t)\left(e^{-Mt} - e^{-Mt}erfc\left(\frac{y}{2\sqrt{t}}\right)\right).$$

$$u(y,t) = \frac{ye^{-\frac{y^2}{4t}-tM}}{2\sqrt{\pi t^3}} + \left(G_r\theta(y,t) + G_c\emptyset(y,t)\right)\left(e^{-Mt} - e^{-Mt}erfc\left(\frac{y}{2\sqrt{t}}\right)\right). \quad (5.24)$$

Equation (5.24) is the general solution for the velocity profile at $t > 0$.

Now, knowing the general solution of the velocity model, the general solution of the temperature model can be obtained as;

From the temperature equation in (5.15) which is

$$\bar{\theta}(y,s) = \bar{u}^2(y,s)P_rME_c\left(\frac{1}{P_rs+F} - \frac{1}{P_rs+F}e^{-y\sqrt{P_rs+F}}\right).$$

Taking inverse Laplace transform of (5.15) from tables in Appendix II and the use of convolution theorem in Appendix IV, the general solution (see, convolution theorem in Appendix IV, (A4.12) and (A4.15)) is

$$\theta(y,t) = u^2(y,t)ME_c\left(e^{-\frac{F}{P_r}t} - e^{-\frac{F}{P_r}t}erfc\left(\frac{y\sqrt{P_r}}{2\sqrt{t}}\right)\right). \quad (5.25)$$

In substituting $u^2(y,t)$ (see Appendix IV, (A4.19)) in the temperature equation (5.25), the non-linear term $\theta^2(y,t)$ is considered negligible since the temperature differences in the flow are sufficiently small. Hence, the general solution of the temperature model is

$$\theta(y,t)=\left[1-ME_c e^{-\frac{F}{P_r}t}\left(1-erfc\left(\frac{y\sqrt{P_r}}{2\sqrt{t}}\right)\right)\left[\frac{ye^{-\frac{y^2}{4t}-tM}}{\sqrt{\pi t^3}}G_r\left(e^{-Mt}-\right.\right.\right.$$

$$\left.\left.\left.e^{-Mt}erfc\left(\frac{y}{2\sqrt{t}}\right)\right)+2G_rG_c\emptyset(y,t)e^{-2Mt}\left(1-erfc\left(\frac{y}{2\sqrt{t}}\right)\right)^2\right]\right]^{-1}\left[ME_c e^{-\frac{F}{P_r}t}\left(1-\right.\right.$$

$$\left.\left.erfc\left(\frac{y\sqrt{P_r}}{2\sqrt{t}}\right)\right)\left[\frac{y^2e^{-\frac{y^2}{2t}-2tM}}{4\pi t^3}+\frac{ye^{-\frac{y^2}{4t}-tM}}{\sqrt{\pi t^3}}G_c\emptyset(y,t)\left(e^{-Mt}-e^{-Mt}erfc\left(\frac{y}{2\sqrt{t}}\right)\right)+\right.\right.$$

$$\left.\left.G_c^2\emptyset^2(y,t)e^{-2Mt}\left(1-erfc\left(\frac{y}{2\sqrt{t}}\right)\right)^2\right]\right]. \qquad (5.26)$$

But $\emptyset(y,t)=\frac{1}{2}\left[e^{-y\sqrt{S_cK_c}}erfc\left(\frac{2t\sqrt{K_c}-y\sqrt{S_c}}{2\sqrt{t}}\right)+e^{y\sqrt{S_cK_c}}erfc\left(\frac{2t\sqrt{K_c}+y\sqrt{S_c}}{2\sqrt{t}}\right)\right]$.

$$\theta(y,t)=a_0^{-1}\left[ME_c e^{-\frac{F}{P_r}t}\left(1-erfc\left(\frac{y\sqrt{P_r}}{2\sqrt{t}}\right)\right)\left[\frac{y^2e^{-\frac{y^2}{2t}-2tM}}{4\pi t^3}+\right.\right.$$

$$\frac{ye^{-\frac{y^2}{4t}-tM}}{2\sqrt{\pi t^3}}G_c\left[e^{-y\sqrt{S_cK_c}}erfc\left(\frac{2t\sqrt{K_c}-y\sqrt{S_c}}{2\sqrt{t}}\right)+e^{y\sqrt{S_cK_c}}erfc\left(\frac{2t\sqrt{K_c}+y\sqrt{S_c}}{2\sqrt{t}}\right)\right]\left(e^{-Mt}-\right.$$

$$\left.e^{-Mt}erfc\left(\frac{y}{2\sqrt{t}}\right)\right)+\frac{1}{2}G_c^2e^{-2Mt}\left[e^{-y\sqrt{S_cK_c}}erfc\left(\frac{2t\sqrt{K_c}-y\sqrt{S_c}}{2\sqrt{t}}\right)+\right.$$

$$\left.\left.e^{y\sqrt{S_cK_c}}erfc\left(\frac{2t\sqrt{K_c}+y\sqrt{S_c}}{2\sqrt{t}}\right)\right]\left(1-erfc\left(\frac{y}{2\sqrt{t}}\right)\right)^2\right]\right]. \qquad (5.27)$$

Where

$$a_0 = 1 - ME_c e^{-\frac{F}{P_r}t}\left(1 - erfc\left(\frac{y\sqrt{P_r}}{2\sqrt{t}}\right)\right)\left[\frac{ye^{-\frac{y^2}{4t}-tM}}{\sqrt{\pi t^3}}G_r\left(e^{-Mt} - e^{-Mt}erfc\left(\frac{y}{2\sqrt{t}}\right)\right) + G_r G_c e^{-2Mt}\left[e^{-y\sqrt{S_c K_c}}erfc\left(\frac{2t\sqrt{K_c}-y\sqrt{S_c}}{2\sqrt{t}}\right) + e^{y\sqrt{S_c K_c}}erfc\left(\frac{2t\sqrt{K_c}+y\sqrt{S_c}}{2\sqrt{t}}\right)\right]\left(1 - erfc\left(\frac{y}{2\sqrt{t}}\right)\right)^2\right].$$

Equation (5.27) is the general solution of the temperature profile for $t > 0$.

Other possible solution exist for $\theta^2(y,t) \neq 0$ but limited in application in practice due to the presence of the discriminant in the solution of the resulting quadratic equation which makes $\theta(y,t)$ not defined for higher values of the controlling parameters.

Knowing the temperature model, other possible solutions exist for the velocity model in (5.24) as follows.

5.3.2 Other Possible Solutions for velocity model

Since Prandtl number is ratio of momentum diffusivity to thermal diffusivity of the fluid, $P_r = 1$ refers to those fluids whose momentum and thermal boundary layer thickness are of magnitude of the same order, and the temperature $\theta(y,t)$

solution in (5.26) is valid for all values of P_r except $P_r = 0$, which is not practically possible. Other possible solutions of the velocity model are:

Case 1. When $P_r = 1$ and $S_c = 1$

$$u(y,t) = \frac{ye^{-\frac{y^2}{4t}-tM}}{2\sqrt{\pi t^3}} + \left[\left[1 - ME_c e^{-Ft}\left(1 - erfc\left(\frac{y}{2\sqrt{t}}\right)\right)\left[\frac{ye^{-\frac{y^2}{4t}-tM}}{\sqrt{\pi t^3}} G_r\left(e^{-Mt} - e^{-Mt}erfc\left(\frac{y}{2\sqrt{t}}\right)\right) + G_r G_c e^{-2Mt}\left[e^{-y\sqrt{K_c}}erfc\left(\frac{2t\sqrt{K_c}-y}{2\sqrt{t}}\right) + e^{y\sqrt{K_c}}erfc\left(\frac{2t\sqrt{K_c}+y}{2\sqrt{t}}\right)\right]\left(1 - erfc\left(\frac{y}{2\sqrt{t}}\right)\right)^2\right]\right]^{-1}\left[ME_c e^{-Ft}\left(1 - erfc\left(\frac{y}{2\sqrt{t}}\right)\right)\left[\frac{y^2 e^{-\frac{y^2}{2t}-2tM}}{4\pi t^3} + \frac{ye^{-\frac{y^2}{4t}-tM}}{2\sqrt{\pi t^3}}\left[e^{-y\sqrt{K_c}}erfc\left(\frac{2t\sqrt{K_c}-y}{2\sqrt{t}}\right) + e^{y\sqrt{K_c}}erfc\left(\frac{2t\sqrt{K_c}+y}{2\sqrt{t}}\right)\right]\left(e^{-Mt} - e^{-Mt}erfc\left(\frac{y}{2\sqrt{t}}\right)\right) + \frac{1}{2}G_c^2 e^{-2Mt}\left[e^{-y\sqrt{K_c}}erfc\left(\frac{2t\sqrt{K_c}-y}{2\sqrt{t}}\right) + e^{y\sqrt{K_c}}erfc\left(\frac{2t\sqrt{K_c}+y}{2\sqrt{t}}\right)\right]\left(1 - erfc\left(\frac{y}{2\sqrt{t}}\right)\right)^2\right] + \frac{1}{2}\left[e^{-y\sqrt{K_c}}erfc\left(\frac{2t\sqrt{K_c}-y}{2\sqrt{t}}\right) + e^{y\sqrt{K_c}}erfc\left(\frac{2t\sqrt{K_c}+y}{2\sqrt{t}}\right)\right]\left(e^{-Mt} - e^{-Mt}erfc\left(\frac{y}{2\sqrt{t}}\right)\right)\right]. \quad (5.28)$$

Case 2. When $P_r = 1$ and $S_c \neq 1$

$$u(y,t)=\frac{ye^{-\frac{y^2}{4t}-tM}}{2\sqrt{\pi t^3}}+\left[\left[1-ME_ce^{-Ft}\left(1-\right.\right.\right.$$

$$\left.\left.\left.erfc\left(\frac{y}{2\sqrt{t}}\right)\right)\left[\frac{ye^{-\frac{y^2}{4t}-tM}}{\sqrt{\pi t^3}}G_r\left(e^{-Mt}-e^{-Mt}erfc\left(\frac{y}{2\sqrt{t}}\right)\right)+\right.\right.\right.$$

$$G_rG_ce^{-2Mt}\left[e^{-y\sqrt{S_cK_c}}erfc\left(\frac{2t\sqrt{K_c}-y\sqrt{S_c}}{2\sqrt{t}}\right)+e^{y\sqrt{S_cK_c}}erfc\left(\frac{2t\sqrt{K_c}+y\sqrt{S_c}}{2\sqrt{t}}\right)\right]\left(1-\right.$$

$$\left.\left.\left.\left.erfc\left(\frac{y}{2\sqrt{t}}\right)\right)^2\right]\right]^{-1}\left[ME_ce^{-Ft}\left(1-erfc\left(\frac{y}{2\sqrt{t}}\right)\right)\left[\frac{y^2e^{-\frac{y^2}{2t}-2tM}}{4\pi t^3}+\right.\right.\right.$$

$$\left.\left.\left.\frac{ye^{-\frac{y^2}{4t}-tM}}{2\sqrt{\pi t^3}}\left[e^{-y\sqrt{S_cK_c}}erfc\left(\frac{2t\sqrt{K_c}-y\sqrt{S_c}}{2\sqrt{t}}\right)+e^{y\sqrt{S_cK_c}}erfc\left(\frac{2t\sqrt{K_c}+y\sqrt{S_c}}{2\sqrt{t}}\right)\right]\left(e^{-Mt}-\right.\right.\right.$$

$$\left.\left.\left.e^{-Mt}erfc\left(\frac{y}{2\sqrt{t}}\right)\right)+\frac{1}{2}G_c^2e^{-2Mt}\left[e^{-y\sqrt{S_cK_c}}erfc\left(\frac{2t\sqrt{K_c}-y\sqrt{S_c}}{2\sqrt{t}}\right)+\right.\right.\right.$$

$$\left.\left.\left.\left.e^{y\sqrt{S_cK_c}}erfc\left(\frac{2t\sqrt{K_c}+y\sqrt{S_c}}{2\sqrt{t}}\right)\right]\left(1-erfc\left(\frac{y}{2\sqrt{t}}\right)\right)^2\right]\right]+\right.$$

$$\left.\frac{1}{2}\left[e^{-y\sqrt{S_cK_c}}erfc\left(\frac{2t\sqrt{K_c}-y\sqrt{S_c}}{2\sqrt{t}}\right)+e^{y\sqrt{S_cK_c}}erfc\left(\frac{2t\sqrt{K_c}+y\sqrt{S_c}}{2\sqrt{t}}\right)\right]\right]\left(e^{-Mt}-\right.$$

$$\left.e^{-Mt}erfc\left(\frac{y}{2\sqrt{t}}\right)\right). \qquad (5.29)$$

5.3.3 Dimensionless Fluxes of Unsteady Hydromagnetic Convective Heat and Mass Transfer

5.3.3.1 The Rate of Heat Transfer Coefficient of Unsteady Hydromagnetic Convective Heat and Mass Transfer

Having obtained the **temperature field**, the rate of heat transfer coefficient at the impulsively started infinite vertical plate in terms of the Nusselt number can be studied. In dimensionless form, the Nusselt number is given by

$$N_u = -\frac{\partial\theta}{\partial y}\Big|_{y=0} = a_0^{-2}\left[\frac{ME_c}{2\sqrt{\pi^3 t^7}}G_c e^{-2Mt-\frac{Ft}{Pr}} erfc\left(\frac{2t\sqrt{K_c}}{2t}\right) - \frac{\sqrt{S_c}}{\sqrt{\pi t}}G_c^2 e^{-4tK_c-2Mt} + \sqrt{S_c K_c}G_c^2 e^{-2Mt} erfc\left(\frac{2t\sqrt{K_c}}{2\sqrt{t}}\right) + \frac{\sqrt{S_c}}{\sqrt{\pi t}}e^{-\frac{2t\sqrt{K_c}+Mt}{4t}} + \sqrt{S_c K_c}e^{Mt} erfc\left(\frac{2t\sqrt{K_c}}{2\sqrt{t}}\right)\right]. \quad (5.30)$$

5.3.3.2 The Rate of Mass Transfer Coefficient of Unsteady Hydromagnetic Convective Heat and Mass Transfer

Knowing the **concentration field,** the rate of mass transfer coefficient at the impulsively started infinite vertical plate in terms of the Sherwood number can be studied. In dimensionless form, the Sherwood number is given by

$$sh = -\left(\frac{\partial\emptyset}{\partial y}\right)_{y=0} = -\frac{\sqrt{S_c}}{\sqrt{\pi t}}e^{-4tK_c} + \sqrt{S_c K_c}\left(\frac{2t\sqrt{K_c}}{2\sqrt{t}}\right). \quad (5.31)$$

5.3.3.3 The Skin Friction Coefficient of Unsteady Hydromagnetic Convective Heat and Mass Transfer

Also, having obtained the **velocity field**, it is significant to study changes in the skin friction due to the effects of the physical parameters t, K_c and M. In dimensionless form, the skin friction is given by

$$\tau = -\frac{\partial u}{\partial y}\Big|_{y=0} = \frac{1}{2\sqrt{\pi t^3}} e^{\frac{-1}{16Mt}} - \frac{e^{-Mt}}{2\sqrt{\pi t}} erfc\left(\frac{2t\sqrt{K_c}}{2\sqrt{t}}\right) + \frac{1}{\sqrt{\pi t}} e^{\frac{-Mt}{4t^2}}\big(G_r\theta(y,t) + G_c\emptyset(y,t)\big). \quad (5.32)$$

5.4 Results and Discussion

In order to determine the effects of the physical parameters such as $t, P_r, S_c, G_r, G_C, M, E_c$ and K_c on the hydromagnetic convection flow, the numeric values of the temperature field, concentration field and velocity field were computed and shown in the figures. Three (3) fluids were considered in this study namely **air**, **electrolyte solution** and **water**. The values of the Prandtl number (P_r) are taken as 0.71 (for air), 1.0 (for electrolyte solution) and 7.0 (for water) and the values of the Schmidt number (S_c) are taken as 0.24 (air), 0.67 (electrolyte solution) and 0.62 (water), which are the physical values of P_r and S_c of these fluids. However, the value Sc = 0.67 (electrolyte solution) is used in the analysis since in electrolyte solutions the Sc is usually large.

5.4.1 Graphical Results

5.4.1.1 Temperature Profiles

Fig. 5.2a shows the effect of the Prandtl number on the temperature profile for electrolyte solution (Pr=1.0), air (Pr=0.71) and water (Pr=7.0). Although, smaller Prandtl numbers give greater thermal boundary layer thickness (Chaudhary, *et al.* (2006) and Narahari *et al.* (2011), however, the present of the magnetic field delay the convection motion. Since the molecules of water are closer to each other than air, they get heated or charged up faster than air in the presence of magnetic field hence the reverse process occurred. Therefore, it is observed that the thermal boundary layer thickness is greater for water (Pr = 7.0) as compared to air (Pr =0.71) and electrolyte solution (Pr = 1.0). Thus, the temperature falls more rapidly for air than water and electrolyte solution. Also, the thermal boundary layer thickness decreases with increase in time.

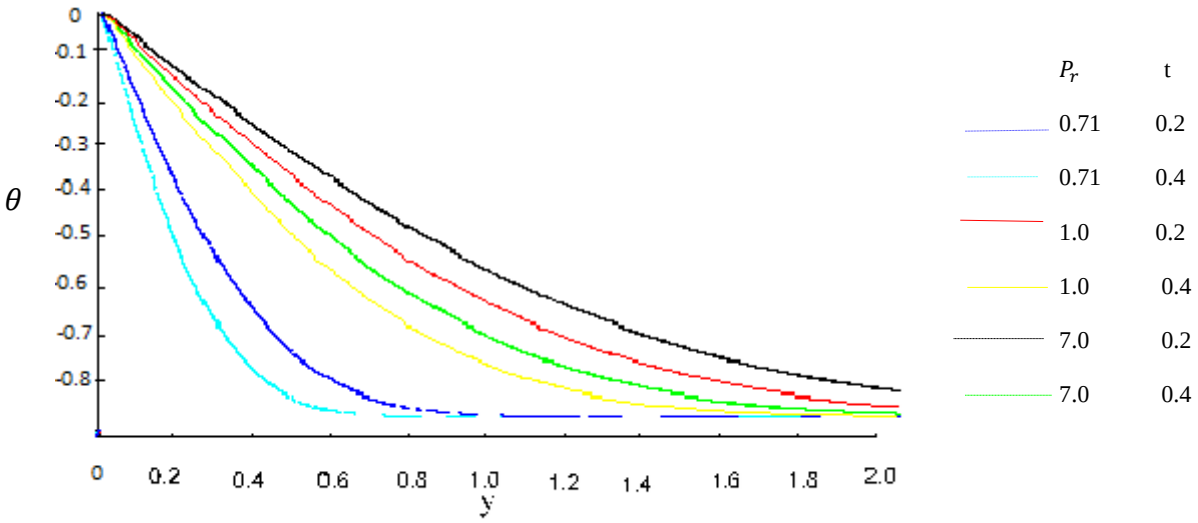

Figure 5. 2a (Present study in the presence of magnetic field). Temperature profile for electrolyte solution (P_r=1.0), air (P_r=0.71) and water (P_r=7.0) when $G_r = 5, G_c = 5, K_c = 1, S_c = 2.01, E_c = 2, M = 2$ and $F = 2$.

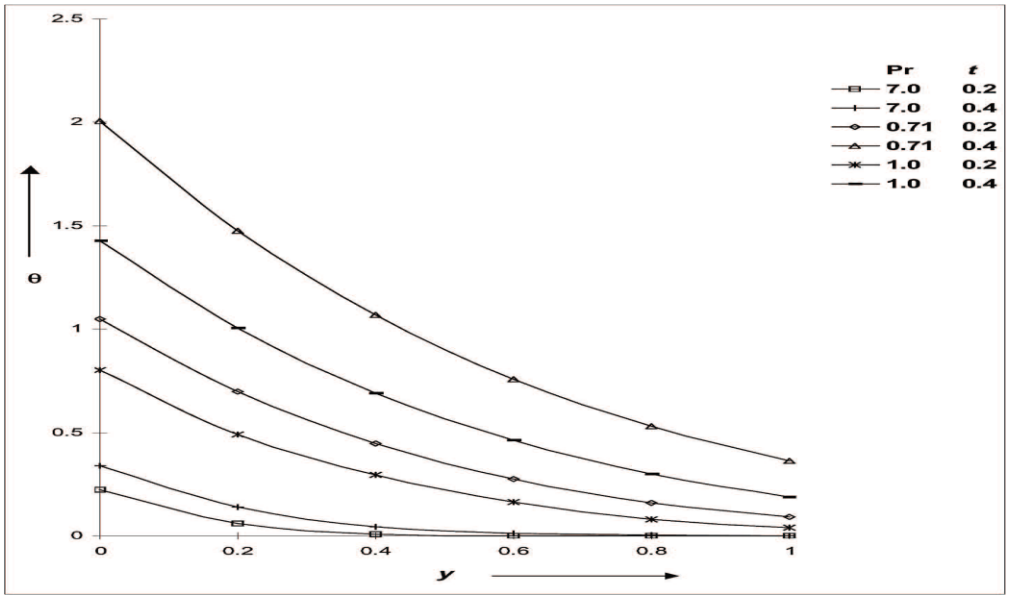

Figure 5. 2b:Chaudhary et al. (2006). Temperature profile (In the absence of Magnetic field)

Fig. 5.3, 5.4 and 5.5 represent the effect of Eckert number Ec on the temperature profile for electrolyte solution (*Pr =1.0*), air (*Pr = 0.71*) and water (*Pr = 7.0*) respectively. It is observed that as the time passes, the temperature falls for the positive values of *Ec* whilst for the negative values of *Ec* the reverse occurred.

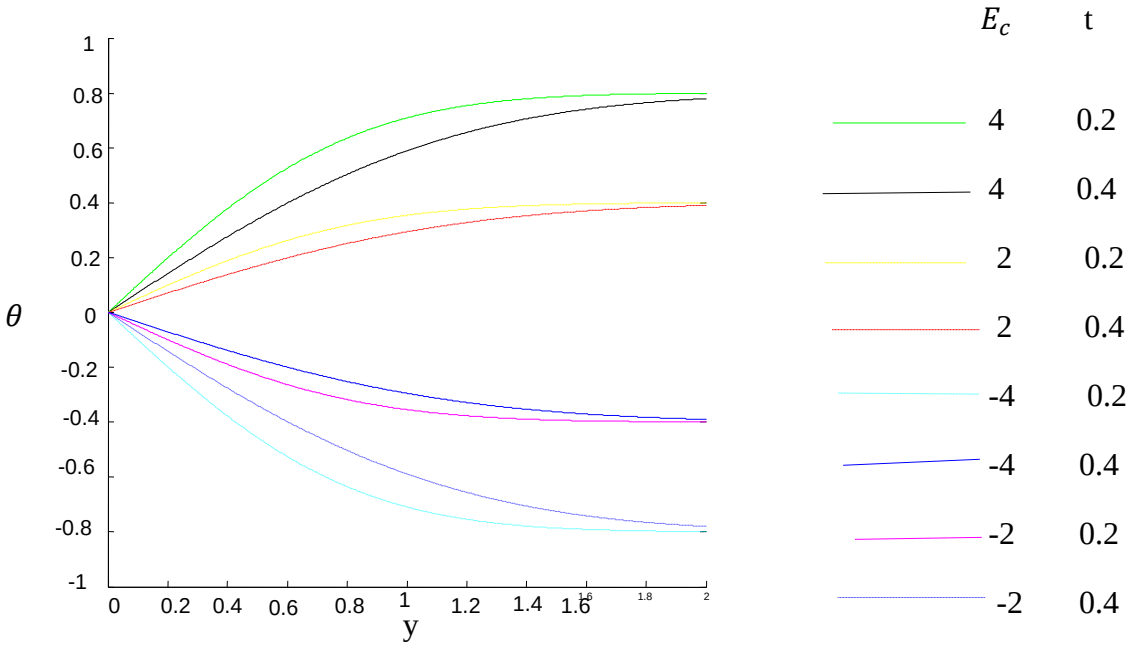

Figure 5. 3 Temperature profile of the effect of E_c on the electrolyte solution (Pr=1.0) when $G_r = 5, G_c = 5, K_c = 1, S_c = 2.01, M = 2$ and $F = 2$.

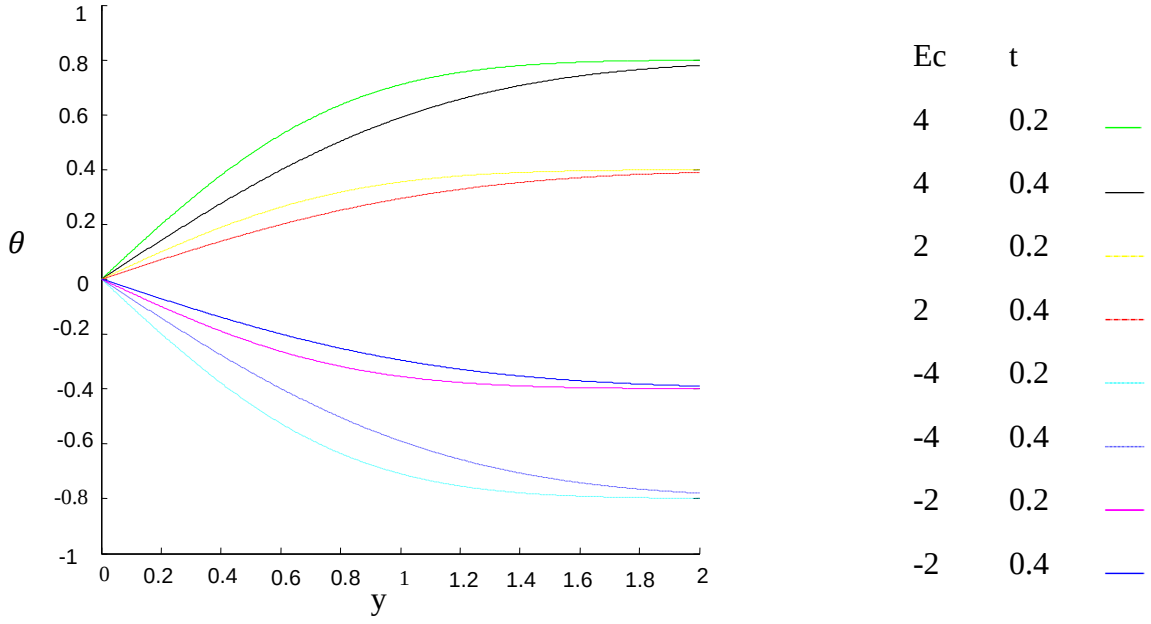

Figure 5. 4 Temperature profile of the effect of E_c on air (Pr=0.71) when $G_r = 5, G_c = 5, K_c = 1, S_c = 2.01, M = 2$ and $F = 2$.

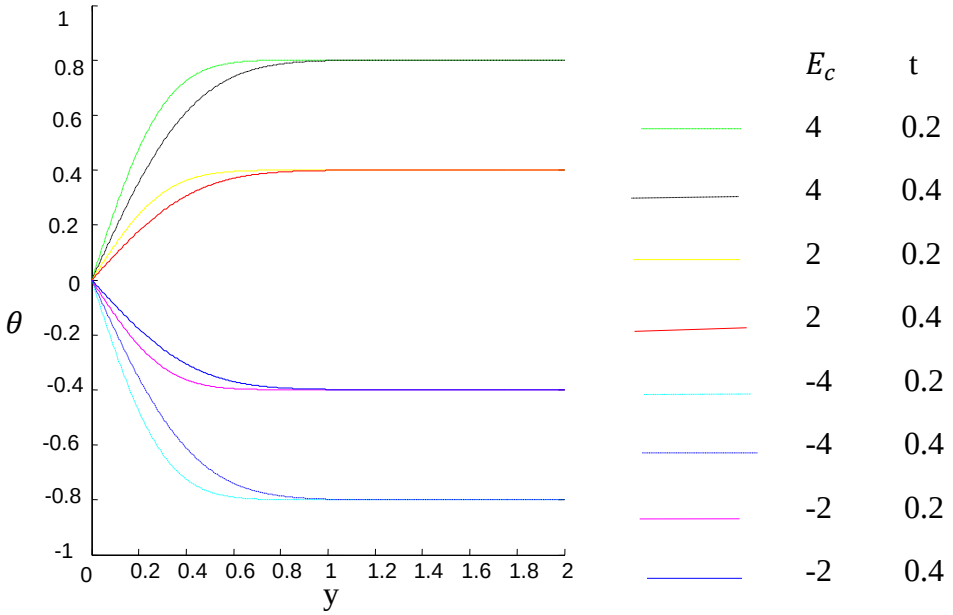

Figure 5. 5 Temperature profile of the effect of E_c on water (Pr=7.0) when $G_r = 5, G_c = 5, K_c = 1, S_c = 2.01, M = 2$ and $F = 2$.

Fig. 5.6 illustrates the effect of the magnetic parameter M on the temperature profile for electrolyte solution (*Pr =1.0*), air (*Pr = 0.71*) and water (*Pr =7.0*). It is noticed that the thermal boundary layer thickness is greater for water (*Pr =7.0*) than electrolyte solution (*Pr =1.0*) and air (*Pr = 0.71*) as the magnetic parameter *M* increases.

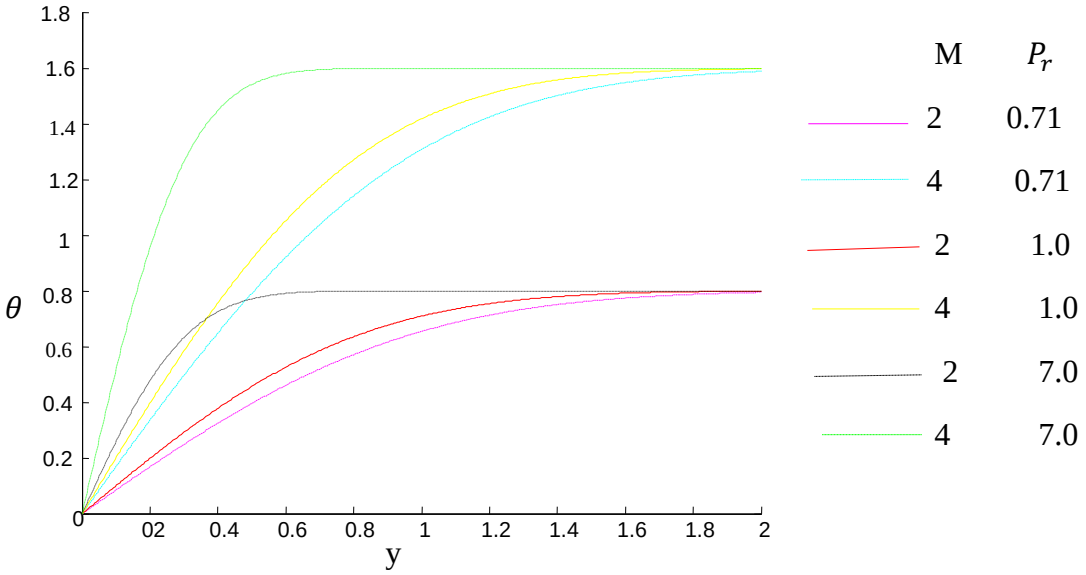

Figure 5. 6 Temperature profile of the effect of *M* on electrolyte solution (Pr=1.0), air (Pr=0.71) and water (Pr=7.0) when $G_r = 5, G_c = 5, K_c = 1, S_c = 2.01, E_c = 2, F = 2,$ and $t = 0.2$.

5.4.1.2 Concentration Profiles

Fig. 5.7 shows the effect of the Schmidt number *Sc* on the concentration profile for electrolyte solution (*Sc* = 0.67), air (*Sc* = 0.24) and water (*Sc* = 0.62). It is realized that concentration is high for electrolyte solution (*Sc* = 0.67) as compared to water (*Sc* = 0.62) and air (*Sc* = 0.24). However, the concentration decreases faster for electrolyte solution (*Sc* = 0.67) as compared to water (*Sc* = 0.62) and air (*Sc* = 0.24) as time passes.

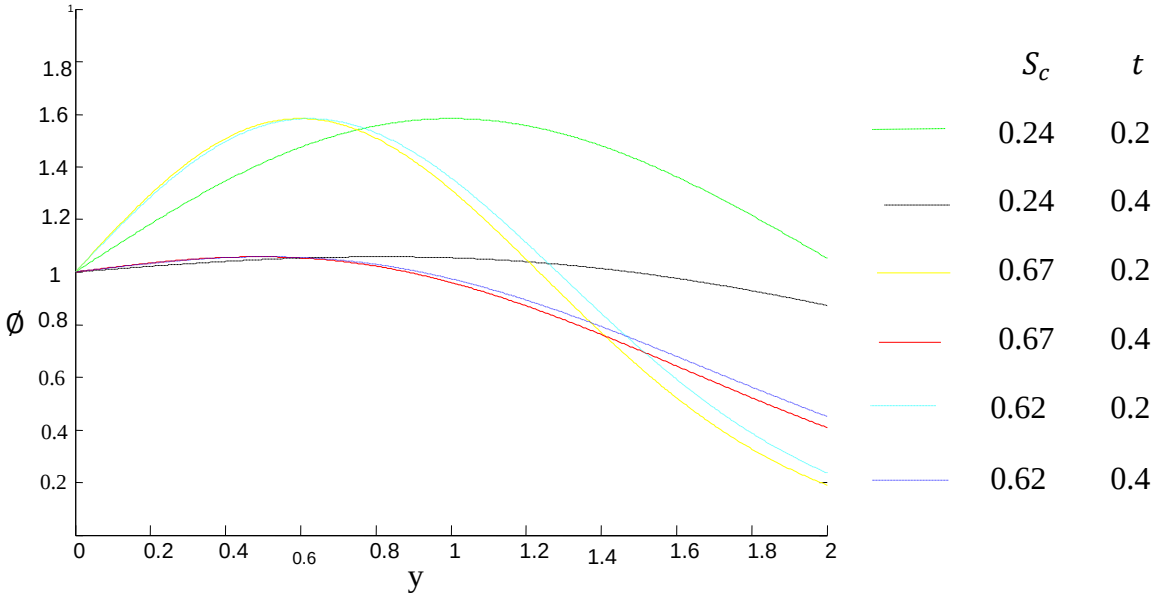

Figure 5. 7 Concentration profile for air (*Sc* = 0.24), electrolyte solution (*Sc* = 0.67) and water (*Sc* = 0.62) when *Kc* = 1.

In fig. 5.8, the effect of rate of chemical reaction *Kc* on air (*Sc* = 0.24), electrolyte solution (*Sc* = 0.67) and water (*Sc* = 0.62) is considered. Again, concentration is high for electrolyte solution (*Sc* = 0.67) as compared to water (*Sc* = 0.62) and air (*Sc* = 0.24). Also, as time goes on, concentration decreases faster for electrolyte solution (*Sc* =0.67) as compared to water (*Sc* = 0.62) and air (*Sc* = 0.24).

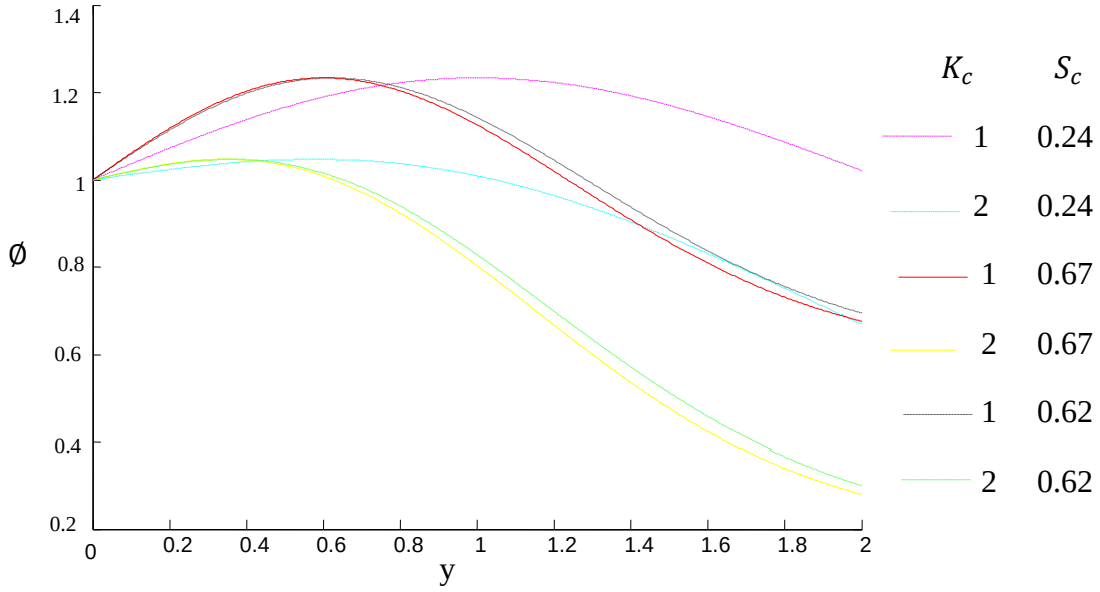

Figure 5. 8 Concentration profile of the effect of Rate of Chemical reaction (*Kc*) on air (*Sc* = 0.21), electrolyte solution (*Sc* = 0.67) and water (*Sc* = 0.62) when *t*=0.2.

5.4.1.3 Velocity Profiles

Fig. 5.9 illustrates velocity profile for air (*Pr = 0.71*), electrolyte solution (*Pr = 1.0*) and water (*Pr = 7.0*). It is noticed that increase in velocity is greater for water (*Pr = 7.0*) as compared to electrolyte solution (*Pr = 1.0*) and air (*Pr = 0.71*). The velocity however, decreases for all the three (3) fluids as time passes.

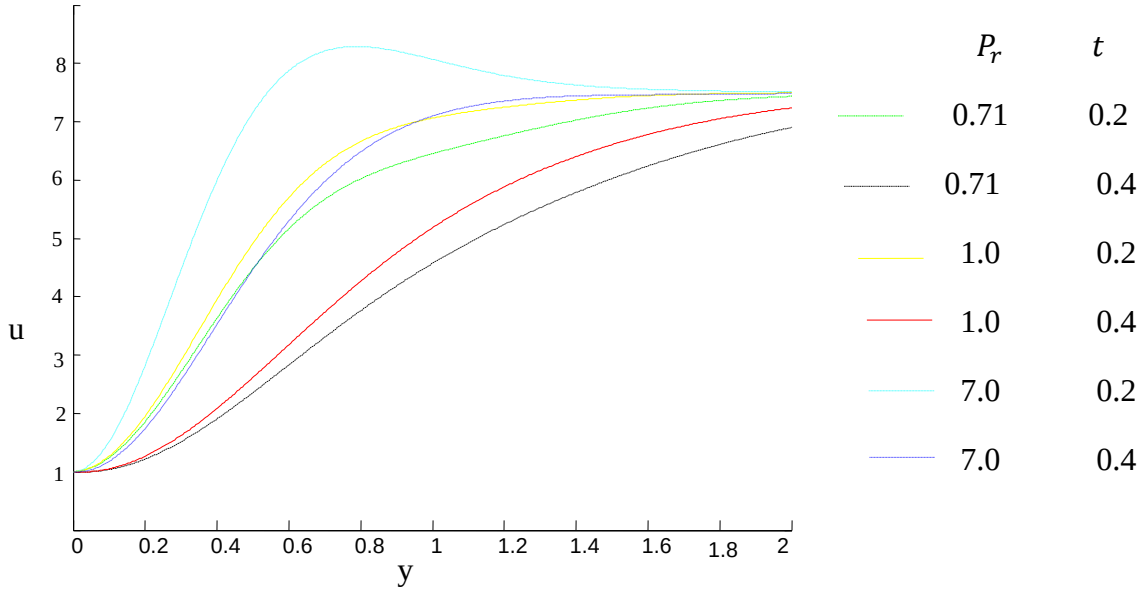

Figure 5. 9 Velocity profile for air (Pr=0.71), electrolyte solution (Pr=1.0) and water (Pr = 7.0) when $G_r = 5, G_c = 5, K_c = 1, S_c = 2.01, E_c = 2, M = 2$ and $F = 2$.

Fig. 5.10a, 5.11a and 5.12a represent the effect of Grashof number Gr on the velocity profile for electrolyte solution (*Pr = 1.0*), air (*Pr = 0.71*) and water (*Pr = 7.0*) respectively. Though, the effect of an increase in Grashof number is to raise the velocity values. Due to the presence of the magnetic field, it is observed that as time goes on, the velocity decreases for positive values of Gr but increases for negative values of Gr. However, the velocity remains positive for $G_r > 0$ and negative for $G_r < 0$.

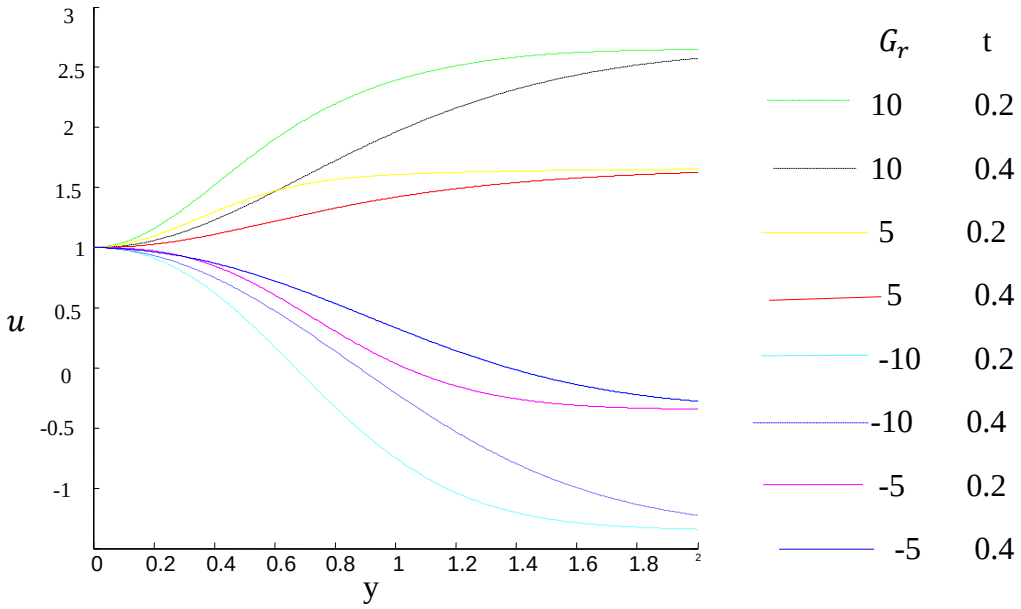

Figure 5. 10a Velocity profile of the effect of Grashof number Gr on electrolyte solution (Pr=1.0) in the present of magnetic field when $G_c = 5, K_c = 1, S_c = 2.01$, $E_c = 2, M = 2$ and $F = 2$. [Present study].

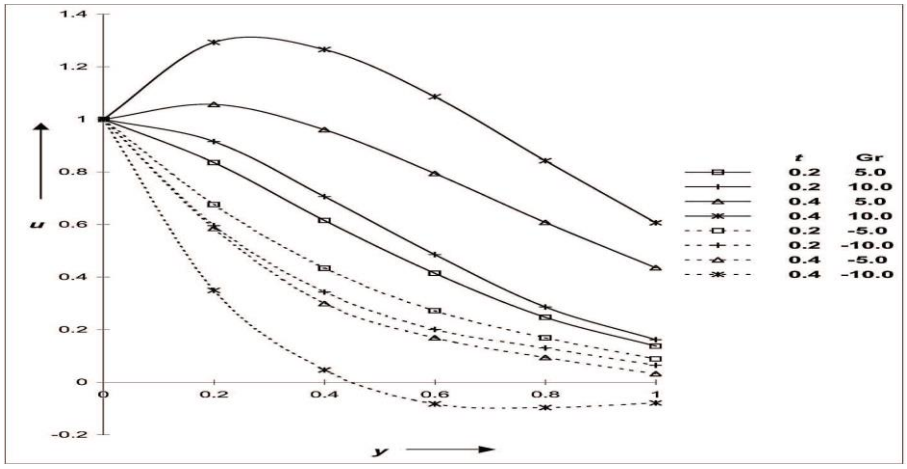

Fig. 5.10b **Chaudhary *et al.* (2006). Velocity profile for electrolyte solution Pr=1.0 (In the absence of Magnetic field)**

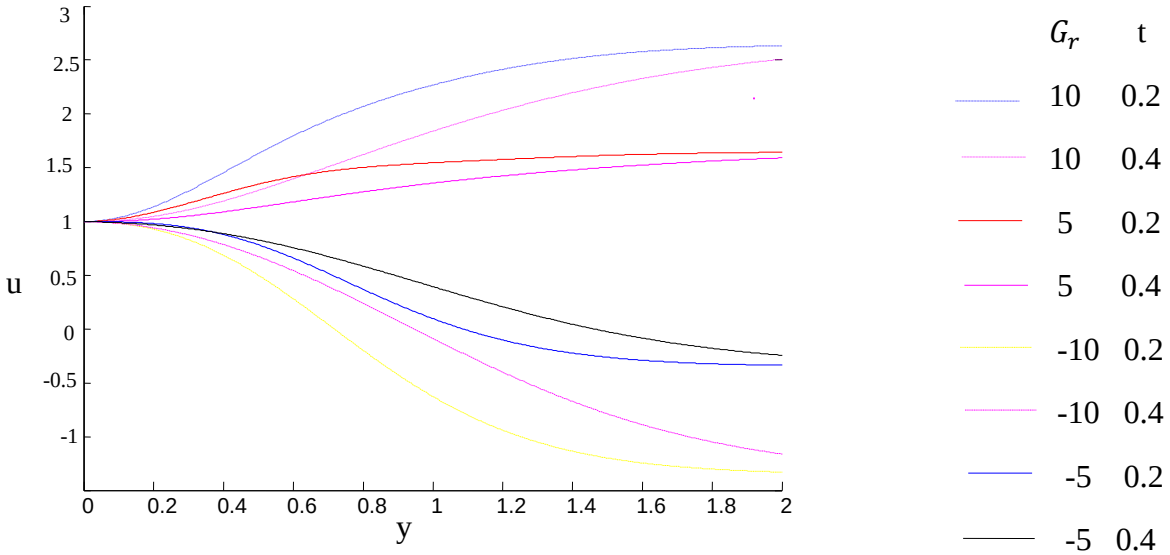

Figure 5. 11a Velocity profile of the effect of *Gr* on air (Pr = 0.71) in the present of magnetic field when $G_c = 5, K_c = 1, S_c = 2.01$, $E_c = 2, M = 2$ and $F = 2$. [Present study].

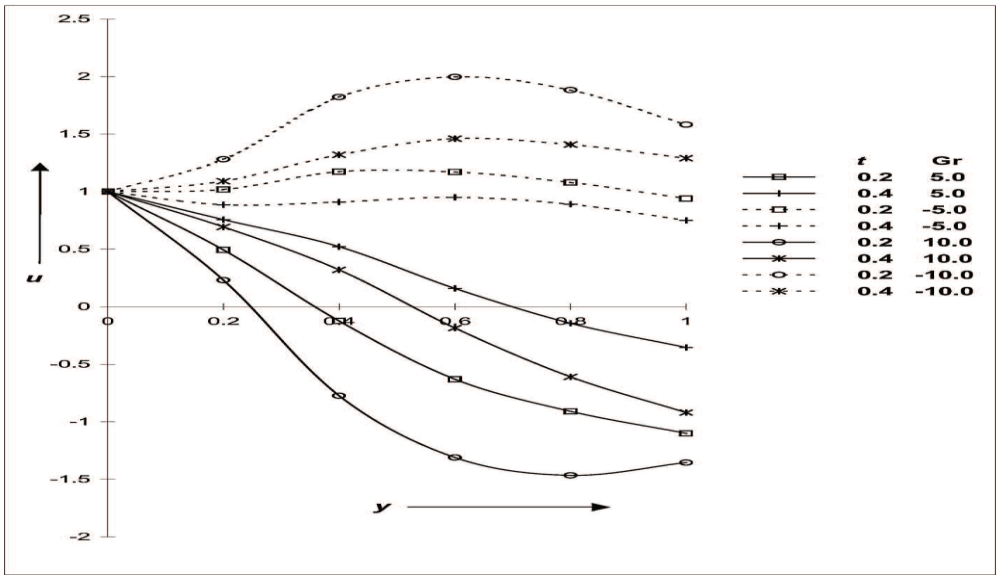

Fig. 5.11b **Chaudhary *et al.* (2006). Velocity profile for air *Pr = 0.71***

(In the absence of Magnetic field).

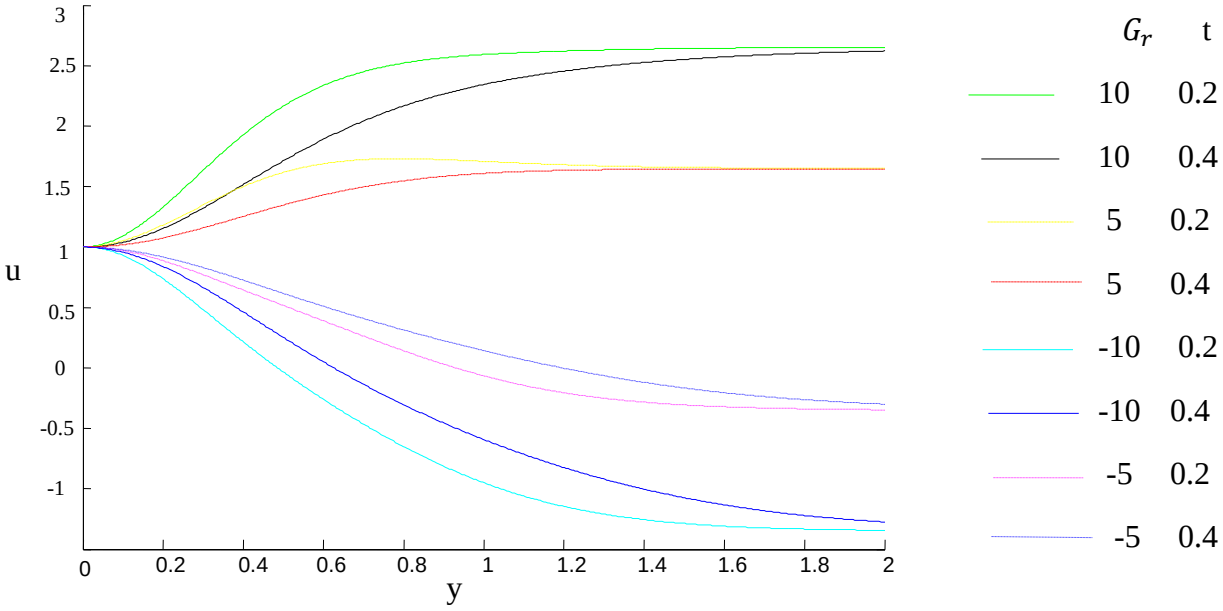

Figure 5. 12a (Present study). Velocity profile of the effect of *Gr* on water (Pr = 7.0) in the present of magnetic field when $G_c = 5, K_c = 1, S_c = 2.01$, $E_c = 2, M = 2$ and $F = 2$.

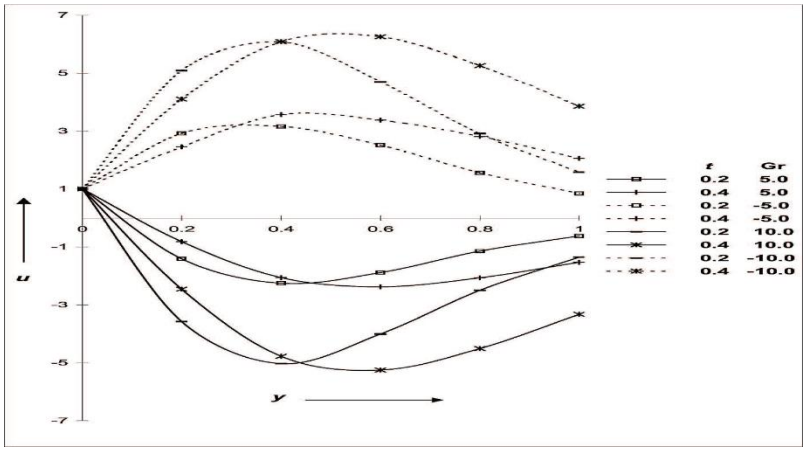

Fig. 5.12b **Chaudhary *et al.* (2006). Velocity profile for water *Pr = 7.0* (In the absence of Magnetic field)**

Fig. 5.13, 5.14 and 5.15 show the effect of mass Grashof number Gc on the velocity profile for electrolyte solution (Pr=1.0), air (Pr=0.71) and water (Pr=7.0) respectively. It is noticed that the velocity decreases as time goes on. However, the velocity increases for $G_r < 0$ and decreases for $G_r > 0$.

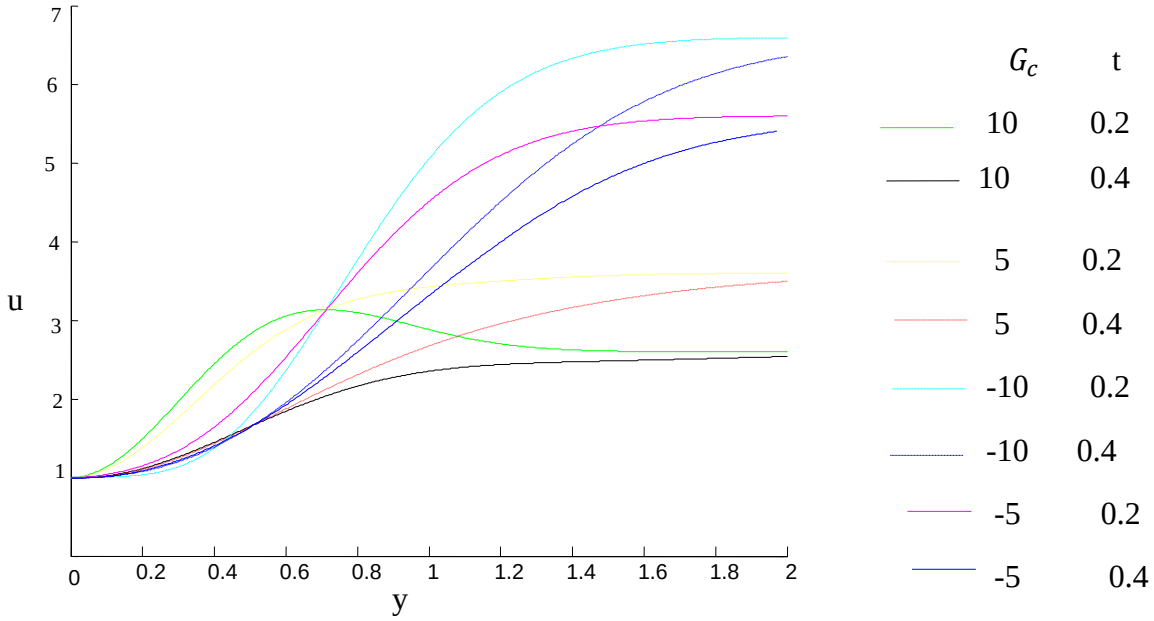

Figure 5. 13 Velocity profile of the effect of *Gc* on electrolyte solution (Pr=1.0) when $G_r = 5, K_c = 1, S_c = 2.01$, $E_c = 2, M = 2$ and $F = 2$.

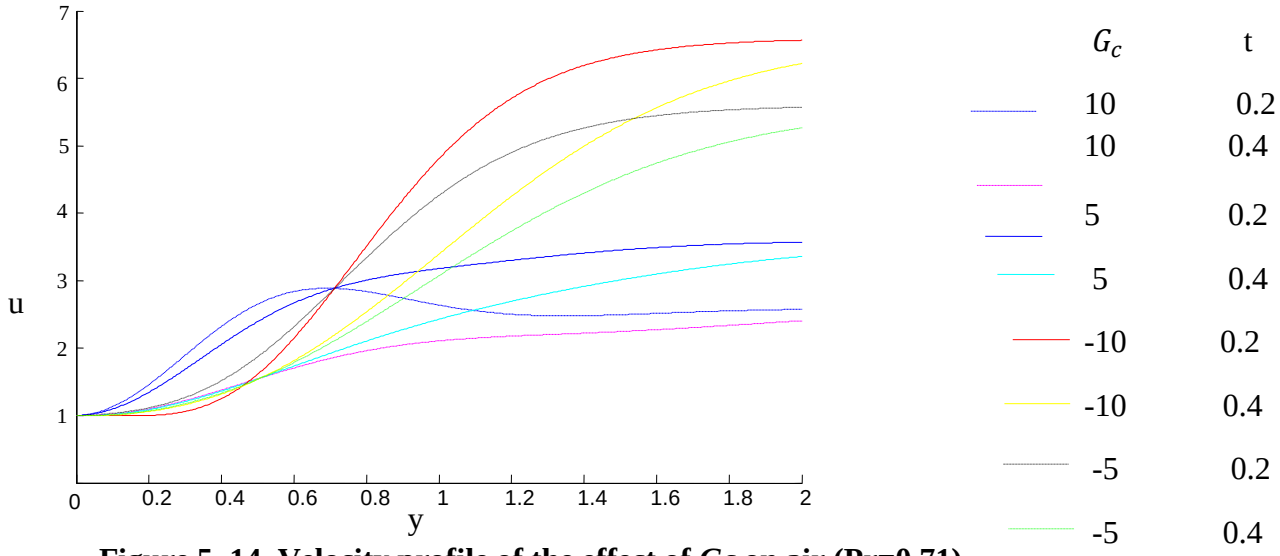

Figure 5. 14 Velocity profile of the effect of *Gc* on air (Pr=0.71) when $G_r = 5, K_c = 1, S_c = 2.01$, $E_c = 2, M = 2$ and $F = 2$.

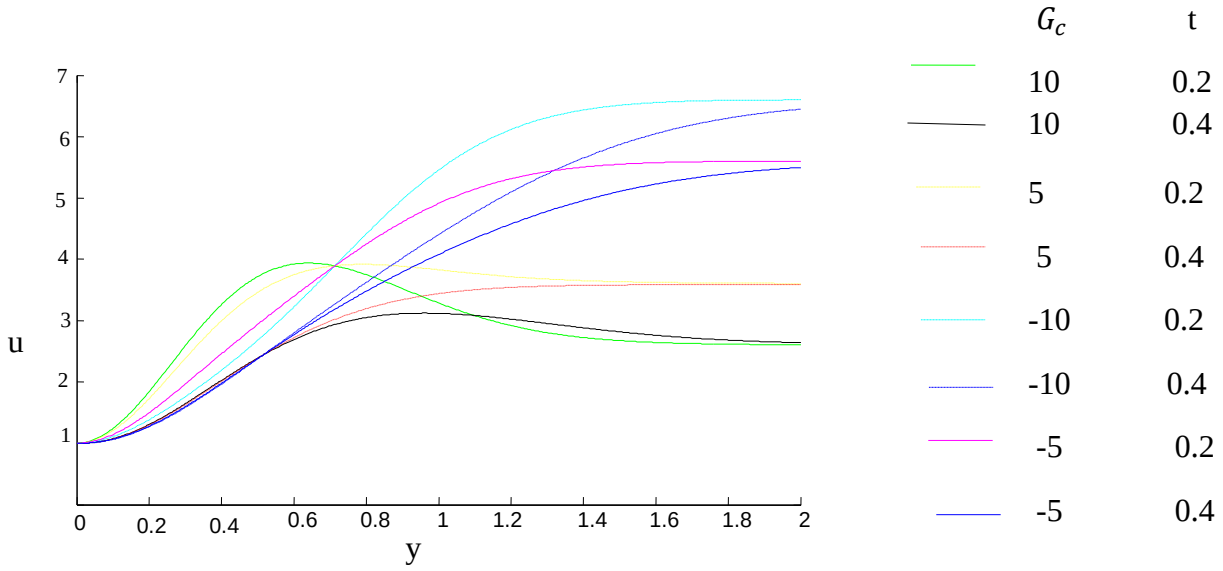

Figure 5. 15 Velocity profile of the effect of *Gc* on water (Pr=7.0) when $G_r = 5, K_c = 1, S_c = 2.01$, $E_c = 2, M = 2$ and $F = 2$.

In Fig. 5.16, the effect of the magnetic parameter, *M* on the velocity profile for electrolyte solution (Pr = 1.0), air (Pr = 0.71) and water (Pr = 7.0) is considered. It revealed that the velocity increases for all the three (3) fluids as the magnetic parameter M increases. However, the increase in velocity of water (Pr = 7.0) is greater as compared to air (Pr = 0.71) and electrolyte solution (Pr = 1.0).

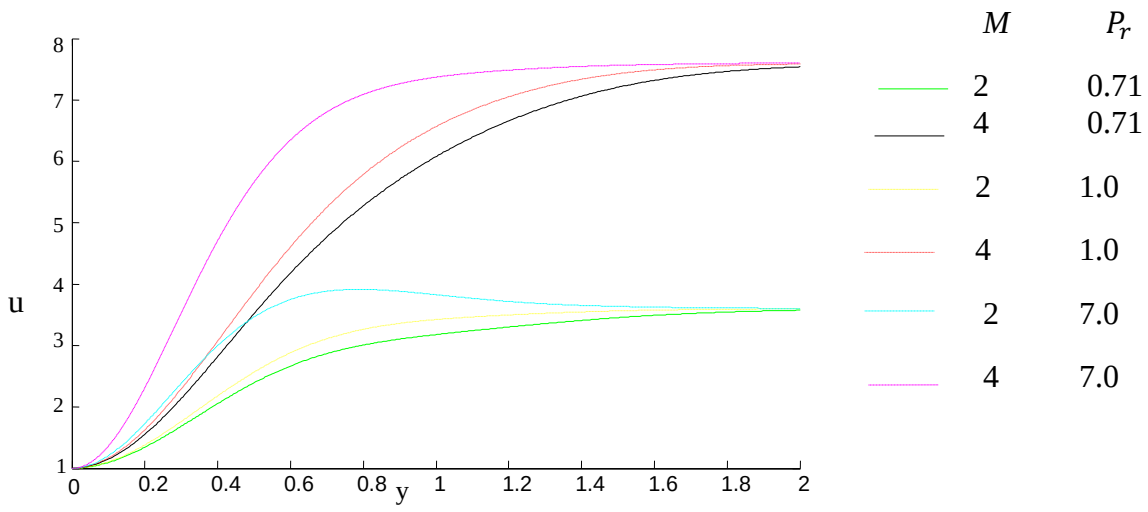

Figure 5. 16 Velocity profile of the effect *M* on electrolyte solution (Pr = 1.0), air (Pr = 0.71) and water (Pr = 7.0) when $G_c = 5, K_c = 1,\ S_c = 2.01,\ E_c = 2,\ G_r = 2$ and $F = 2$.

Fig. 5.17 illustrates the effect of the Eckert number on the velocity profile for electrolyte solution (Pr=1.0), air (Pr=0.71) and water (Pr=7.0). The velocity increases with increase in Eckert number for all the fluids. However, the velocity increased is greater for water (Pr=7.0) than air (Pr=0.71) and electrolyte solution (Pr=1.0).

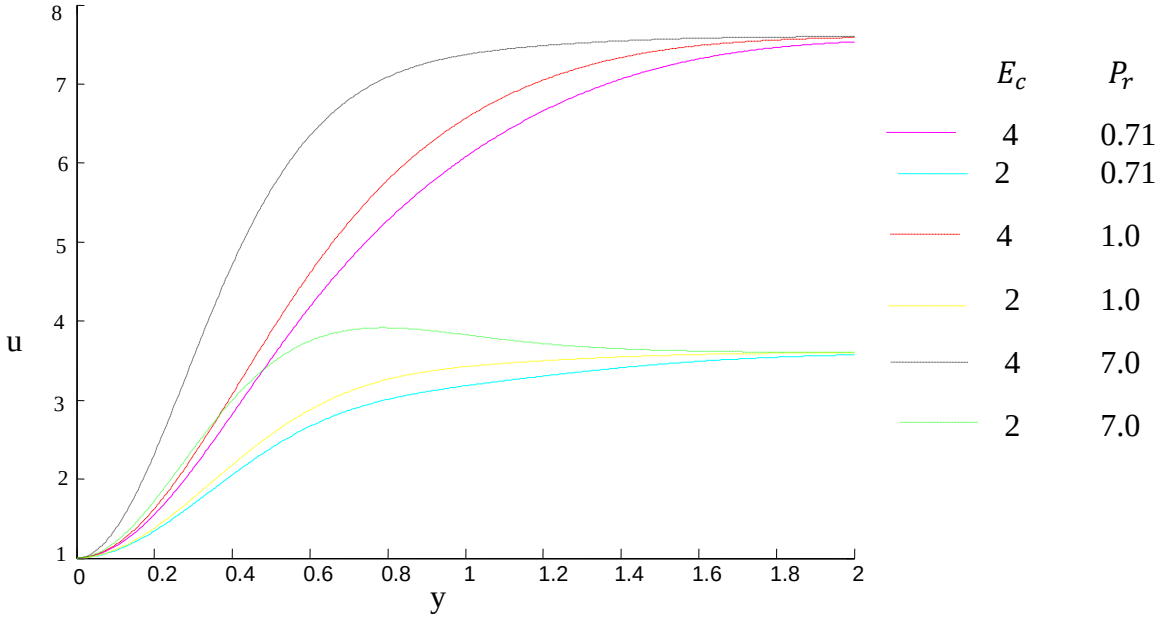

Figure 5. 17 Velocity profile of the effect of E_c on electrolyte solution (Pr = 1.0), air (Pr = 0.71) and water (Pr = 7.0) when $G_c = 5, K_c = 1,\ S_c = 2.01,\ M = 2,\ G_r = 2$ and $F = 2$.

In Fig. 5.18, the effect of the rate of chemical reaction Kc on the velocity profile for electrolyte solution (Pr = 1.0), air (Pr = 0.71) and water (Pr = 7.0) is determined. It is noticed that the velocity decreases with increase in the rate of chemical reaction, *Kc*.

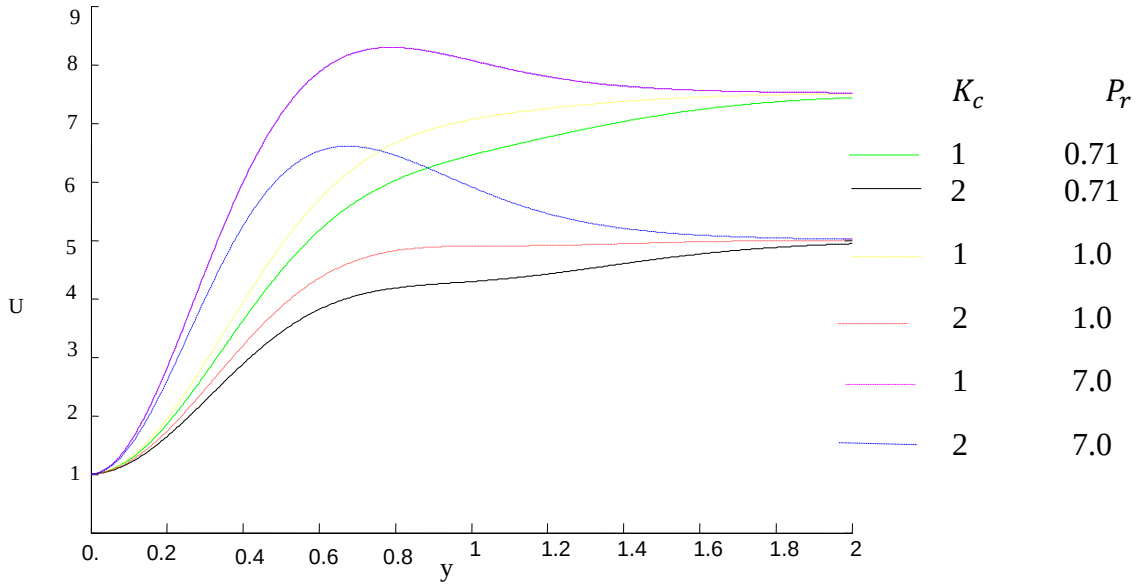

Figure 5. 18 Velocity profile of the effect of *Kc* on air (Pr = 0.71), electrolyte solution (Pr = 1.0) and water (Pr = 7.0) when $G_c = 5, E_c = 2$, $S_c = 2.01$, $M = 2$, $G_r = 2$ and $F = 2$.

5.4.2 Numerical Results

5.4.2 Numerical Results

Table 5.1-5.3 show the behaviour of **skin friction coefficient, $-u'(0)$, Sherwood number**, $-\emptyset'(0)$ and **Nusselt number**, $-\theta'(0)$ for various values of time (t), magnetic parameter (M), Eckert number (E_c), dimensionless chemical reaction parameter (K_c), Schmidt number (S_c), radiation parameter (F), thermal Grashof number (G_c) and mass Grashof number (G_c). From Table 5.1, it is noted that the skin friction coefficient, $-u'(0)$ decreases for increasing values of t and M but increases for increasing values of k_c. From Table 5.2, Sherwood number, $-\emptyset'(0)$ decreases with increasing values of t or k_c but

increases for increase values of S_c. From Table 5.3, Nusselt number , $-\theta'(0)$ dereases with increasing values of t, M, E_c but increases with increasing values G_c F, P_r, K_c and S_c.

Table 5. 1:The Skin friction coefficient, -u' (0) at the wall, for various values of t, M and K_c.

t	M	K_c	$-u'(0)$
0.2	1.0	1.0	2.0352
0.4	1.0	1.0	0.8428
0.6	1.0	1.0	0.4923
0.2	0.2	1.0	1.5786
0.2	0.4	1.0	1.1371
0.2	0.6	1.0	0.3417
0.2	1.0	0.2	1.9060
0.2	1.0	0.4	1.9515
0.2	1.0	0.6	1.9851

Table 5. 2: Sherwood number, -∅' (0) at the wall, for various values of t, S_c and K_c.

t	S_c	K_c	$-\emptyset'(0)$
0.2	1.0	1.0	1.0141
0.4	1.0	1.0	0.8126
0.6	1.0	1.0	0.8047
0.2	**0.2**	1.0	0.4535
0.2	**0.4**	1.0	0.6414
0.2	**0.6**	1.0	0.7855
0.2	1.0	**0.2**	1.1645
0.2	1.0	**0.4**	1.0950
0.2	1.0	**0.6**	1.0490

Table 5. 3:The Local Nusselt number, -θ' (0) at the wall, for various values of $t, M, E_c, G_c, F, P_r, K_c$ and S_c.

t	M	E_c	G_c	F	P_r	K_c	S_c	$-\theta'(0)$
0.2	1	1	1	1	1	1	1	2.8484
0.4	1	1	1	1	1	1	1	2.0236
0.6	1	1	1	1	1	1	1	0.2977
0.2	1.5	1	1	1	1	1	1	0.6260
0.2	2	1	1	1	1	1	1	0.5888
0.2	2.5	1	1	1	1	1	1	0.5280
0.2	1	1.5	1	1	1	1	1	1.071
0.2	1	2	1	1	1	1	1	0.8570
0.2	1	2.5	1	1	1	1	1	0.6427
0.2	1	1	5	1	1	1	1	1.6648
0.2	1	1	7	1	1	1	1	1.6652
0.2	1	1	9	1	1	1	1	1.8120
0.2	1	1	1	2	1	1	1	0.2529
0.2	1	1	1	4	1	1	1	0.3123
0.2	1	1	1	6	1	1	1	0.3856
0.2	1	1	1	1	0.71	1	1	0.4096

0.2	1	1	1	1	1	1	1	0.4285
0.2	1	1	1	1	7	1	1	0.4690
0.2	1	1	1	1	1	0.2	1	0.2816
0.2	1	1	1	1	1	0.4	1	0.3412
0.2	1	1	1	1	1	0.6	1	0.3814
0.2	1	1	1	1	1	1	2	0.6593
0.2	1	1	1	1	1	1	3	0.9176
0.2	1	1	1	1	1	1	4	1.2131

5.5 Conclusion

Unsteady hydromagnetic convective heat and mass transfer with Newtonian heating in a porous medium has been investigated. The governing non-linear partial differential equations have been derived and transformed into dimensionless differential equations using the dimensionless variables. Laplace transform technique was used to solve the dimensionless differential equations and results shown graphically. The following conclusions can be drawn from the results obtained:

1. In the presence of magnetic field, the thermal boundary layer thickness is greater for water (Pr = 7.0) as compared to air (Pr =0.71) and electrolyte solution (Pr = 1.0) but diminishes with increase in time.
2. Concentration is high for electrolyte solution (Sc=0.67) as compared to water (Sc=0.62) and air (0.24) but diminishes faster for electrolyte solution (Sc=0.67) as compared to water (Sc=0.62) and air (0.24) as time passes.
3. The velocity increases with increase in Eckert number (Ec), Magnetic parameter (M) but decreases with increase in rate of chemical reaction (Kc) for all the three (3) fluids.
4. Though, the effect of an increase in Grashof number is to raise the velocity values. Due to the presence of the magnetic field, it is observed that as time goes on, the velocity decreases for positive values of Gr but increases for negative values of Gr. However, the velocity remains positive for $G_r > 0$ and negative for $G_r < 0$.

.

CHAPTER SIX

UNSTEADY HYDROMAGNETIC BOUNDARY LAYER FLOW OVER AN EXPONENTIALLY STRETCHING FLAT SURFACE IN A CHEMICALLY REACTIVE POROUS MEDIUM

6.1 Introduction

Unsteady boundary layer flow past a stretching surface in the presence of magnetic field with heat and mass transfer in a porous medium is studied. The fluid under consideration is **quiescent** viscous incompressible fluid. The boundary layer equations are transformed into dimensionless equations. The dimensionless equations are solved in exact form using the Laplace transform techniques and results are shown graphically for the velocity, thermal boundary layer thicknesses and concentration boundary layer thicknesses. Also, numerical values are obtained for the skin friction coefficient, Sherwood number as well as the Nusselt number.

6.2 Mathematical Formulation of Unsteady Hydromagnetic Boundary Layer Flow over a Flat Surface

Consider an unsteady boundary layer flow past a stretching surface with heat and mass transfer in a porous medium, where x^* −axis is along the stretching plate. In addition to the models' assumptions, at time $t^* > 0$, the surface is moving

continuously with the velocity $u^* = U_w(x) = U_0(1 - e^{-at})$ in the positive x^* −direction and the plate temperature is raised linearly with t^* and the level of concentration near the plate is raised to C_w^*. The physical system of the flow is shown in fig. 6.1.

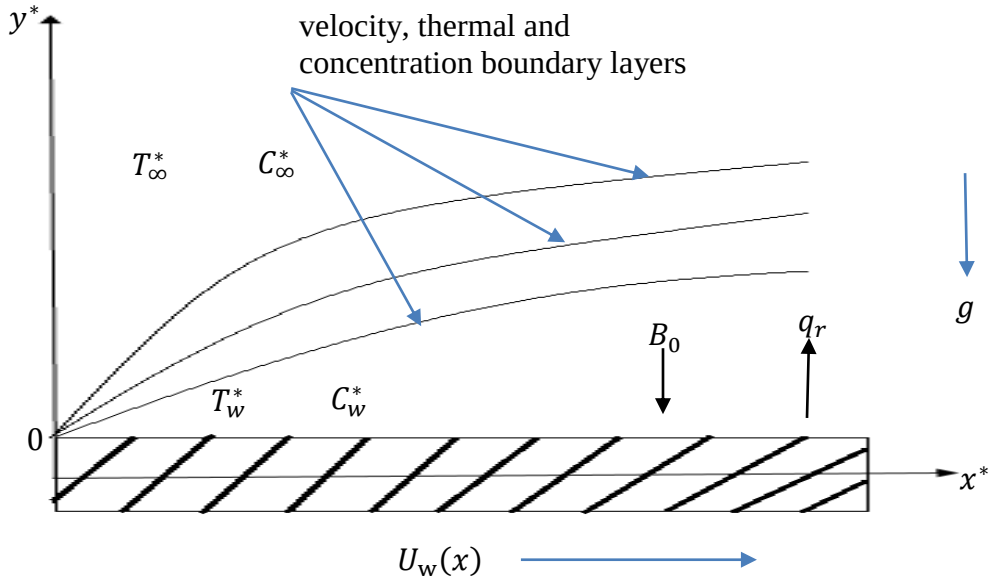

Figure 6. 1 Flow configuration and coordinate system

Under these assumptions, the governing boundary layer equations are:

6.2.1 The Continuity Equation of Unsteady Hydromagnetic Boundary Layer Flow over a Flat Surface

The continuity equation was derived in (4.2) as

$$\frac{\partial u^*}{\partial x^*} + \frac{\partial v^*}{\partial y^*} = 0$$

6.2.2 The Momentum Equation of Unsteady Hydromagnetic Boundary Layer Flow over a Flat Surface

The momentum equation was derived in (3.8) as

$$\rho\left(\frac{\partial u^*}{\partial t^*}+u\frac{\partial u^*}{\partial x^*}+v\frac{\partial u^*}{\partial y^*}\right)=-\frac{\partial p}{\partial x^*}+\mu\frac{\partial^2 u^*}{\partial y^{*2}}+\rho g$$

Introducing the fluid pressure, $-\frac{\partial p}{\partial x^*}=u\frac{\partial u^*}{\partial x^*}+v\frac{\partial u^*}{\partial y^*}$, thermal buoyancy, $g\beta_T(T^*-T_\infty^*)$, concentration buoyancy, $g\beta_C(C^*-C^*_\infty)$, magnetic force, $\sigma B_0^2 u^*$ and the porosity term, $\frac{\nu}{k^*}u^*$ into the flow field in (3.8) reduces to the momentum equation

$$\frac{\partial u^*}{\partial t^*}-V\frac{\partial u^*}{\partial y^*}=\nu\frac{\partial^2 u^*}{\partial y^{*2}}+g\beta_T(T^*-T_\infty^*)+g\beta_C(C^*-C^*_\infty)-\frac{\sigma B_0^2}{\rho}u^*-\frac{\nu}{k^*}u^* \tag{6.1}$$

6.2.3 The Energy Equation of Unsteady Hydromagnetic Boundary Layer Flow over a Flat Surface

The energy was derived in (3.12) as

$$\frac{\partial T^*}{\partial t^*}+\left(u\frac{\partial T^*}{\partial x^*}+v\frac{\partial T^*}{\partial y^*}+w\frac{\partial T^*}{\partial z^*}\right)=\propto\left(\frac{\partial^2 T^*}{\partial x^{*2}}+\frac{\partial^2 T^*}{\partial y^{*2}}+\frac{\partial^2 T^*}{\partial z^{*2}}\right)+\Phi$$

Since temperature field varies with regard to y^*only, so $\frac{\partial T^*}{\partial x^*}=0$.

Hence for the unsteady flow with magnetic field and radiative heat flux, (3.12) is modified to become

$$\frac{\partial T*}{\partial t*} - V\frac{\partial T*}{\partial y*} = \alpha\frac{\partial^2 T*}{\partial y*^2} + \frac{\nu}{c_p}\left(\frac{\partial u^*}{\partial y^*}\right)^2 + \left(\frac{\nu}{k^* c_p} + \frac{\sigma B_0{}^2}{\rho c_p}\right)u^{*2} + \frac{1}{\rho c_p}\frac{\partial q_r}{\partial y*} - \frac{Q}{\rho c_p}(T* - T*_\infty)$$

(6.2)

6.2.4 The Concentration Equation of Unsteady Hydromagnetic Boundary Layer Flow over a Flat Surface

The concentration equation was derived in (3.15) in vector form as

$$\frac{\partial c^*}{\partial t^*} = D\nabla^2 C^* + \dot{r}$$

In components form, (3.15) is modified to become

$$\frac{\partial C*}{\partial t*} - V\frac{\partial c^*}{\partial y^*} = D\frac{\partial^2 C*}{\partial y*^2} - K_C{}^*(C* - C*_\infty) \qquad (6.3)$$

6.2.5 Associated Boundary Conditions of Unsteady Hydromagnetic Boundary Layer Flow over a Flat Surface

The associated boundary conditions are

$$\begin{aligned} &y^* \geq 0, t^* \leq 0: && u^* = 0, \quad \mathrm{v}^* = 0 \quad T^* = T^*_\infty, C^* = C^*_\infty, \\ &y^* = 0, t^* > 0: && u^* = U_\mathrm{w}(x) = U_0(1 - e^{-at}), \quad T^* = T^*_w,\ C^* = C^*_w, \\ &y^* \to \infty, t^* > 0: && u^* \to 0,\ T^* \to T^*_\infty,\ C^* \to C^*_\infty. \end{aligned} \qquad (6.4)$$

6.2.6 Transformation of Unsteady Hydromagnetic Boundary Layer Flow over a Flat Surface

6.2.6.1 The Dimensionless Variables of Unsteady Hydromagnetic Boundary Layer Flow over a Flat Surface

The following dimensionless variables and parameters similar to (3.16) are introduced:

$$u=\frac{u^*}{V}, y=\frac{y^*V}{\upsilon}, t=\frac{t^*V^2}{\upsilon}, M=\frac{\sigma B_0^2\upsilon}{\rho V^2}, Gr=\frac{\upsilon g\beta_T(T_w^*-T_\infty^*)}{V^3}, Gc=\frac{\upsilon g\beta_C(C_w^*-C_\infty^*)}{V^3},$$
$$\Pr=\frac{\upsilon}{\alpha}, \theta=\frac{T^*-T_\infty}{T_w^*-T_\infty^*}, \phi=\frac{C^*-C_\infty^*}{C_w^*-C_\infty^*}, Da=\frac{V^2k^*}{\upsilon^2}, Ec=\frac{V_2}{c_p(T_\infty^*-T_\infty^*)}, Sc=\frac{\upsilon}{D}, \lambda=\frac{U_0}{V},$$
$$Q=\frac{\upsilon Q}{V^2\rho c_p}, F=\frac{16\sigma a^*\upsilon^2T_\infty^{*3}}{k^*U_0^2}$$

(6.5)

All the physical variables are defined in the Nomenclature

6.2.6.2 Dimensionless Continuity Equation of Unsteady Hydromagnetic Boundary Layer Flow over a Flat Surface

The suitable dimensionless quantities in (6.5) for the continuity equation in (4.2) are differentiated as:

$$u=\frac{u^*}{V} \qquad \Rightarrow u^*=\mathrm{V}v \qquad \Rightarrow \frac{\partial u^*}{\partial x^*}=\mathrm{V}\frac{\partial u}{\partial x^*}$$

$$\Rightarrow \frac{\partial u^*}{\partial y^*}=\mathrm{V}\frac{\partial u}{\partial y^*}$$

$$\Rightarrow \frac{\partial u^*}{\partial t^*} = \mathrm{V}\frac{\partial u}{\partial t^*}$$

$$v = \frac{v^*}{V} \qquad \Rightarrow v^* = \mathrm{Vv} \qquad \Rightarrow \frac{\partial v^*}{\partial t^*} = \mathrm{V}\frac{\partial v}{\partial t^*}$$

$$\Rightarrow \frac{\partial v^*}{\partial y^*} = \mathrm{V}\frac{\partial v}{\partial y^*}$$

$$y = \frac{Vy^*}{v} \qquad \Longrightarrow y^* = \frac{v}{V}y \qquad \Longrightarrow \partial y^* = \frac{v}{V}\,\partial y$$

$$x = \frac{Vx^*}{v} \qquad \Longrightarrow x^* = \frac{v}{V}x \qquad \Longrightarrow \partial x^* = \frac{v}{V}\,\partial x$$

$$t = \frac{t^*V^2}{v} \qquad \Longrightarrow t^* = \frac{v}{V^2}t \qquad \Longrightarrow \partial t^* = \frac{v}{V^2}\,\partial t$$

(6.6)

Now

$$\frac{\partial v^*}{\partial y^*} = \mathrm{V}\frac{\partial v}{\partial y^*} = \frac{V^2}{\mathrm{v}}\frac{\partial v}{\partial y}$$

$$\frac{\partial u^*}{\partial x^*} = \mathrm{V}\frac{\partial u}{\partial x^*} = \frac{V^2}{\mathrm{v}}\frac{\partial u}{\partial x}$$

(6.7)

Substituting (6.7) in continuity equation (4.2) gives

$$\frac{\partial u}{\partial x} + \frac{\partial v}{\partial y} = 0 \qquad (6.8)$$

(6.8) models the dimensionless continuity equation.

6.2.6.3 The Dimensionless Momentum Equation of Unsteady Hydromagnetic Boundary Layer Flow over a Flat Surface

Similarly,

$$\frac{\partial u^*}{\partial t^*} = \mathrm{V}\frac{\partial u}{\partial t^*} = \frac{V^3}{\mathrm{v}}\frac{\partial u}{\partial t}$$

$$\frac{\partial u^*}{\partial y^*} = \mathrm{V}\frac{\partial u}{\partial y^*} = \frac{V^2}{\mathrm{v}}\frac{\partial u}{\partial y}$$

$$\frac{\partial^2 u^*}{\partial y^{*2}} = \frac{V^3}{v^2}\frac{\partial^2 u}{\partial y^2} \tag{6.9}$$

Substituting (6.5) and (6.9) in the momentum model (6.1) give

$$\frac{V^3}{\mathrm{v}}\frac{\partial \mathrm{u}}{\partial \mathrm{t}} - \mathrm{v}\frac{V^2}{\mathrm{v}}\frac{\partial u}{\partial y} = v\frac{V^3}{v^2}\frac{\partial^2 u}{\partial y^2} + g\beta_T\,(T_w^* - T_\infty^*)\theta + \; g\beta_c(C_w^* - C_\infty^*)\emptyset - \frac{\sigma B_0^2}{\rho}\mathrm{uV} -$$

$$\frac{v}{\mathrm{k}}\mathrm{uv}$$

$$\frac{\partial \mathrm{u}}{\partial \mathrm{t}} - \frac{\partial u}{\partial y} = \frac{\partial^2 u}{\partial y^2} + \mathrm{v}g\beta_T\frac{(T_w^* - T_\infty^*)}{V^3}\theta + \; vg\beta_c\frac{(C_w^* - C_\infty^*)}{V^3}\emptyset - \frac{\sigma B_0^2 v}{\rho V^2}\mathrm{u} - \frac{v^2}{\mathrm{k}V^2}u$$

$$\frac{\partial \mathrm{u}}{\partial \mathrm{t}} - \frac{\partial u}{\partial y} = \frac{\partial^2 u}{\partial y^2} + G_r\theta + \; G_c\emptyset - M_1 u \tag{6.10}$$

where $M_1 = M + \frac{1}{K}$

Equation (6.10) models the dimensionless momentum equation.

6.2.6.4 The Dimensionless Energy Equation of Unsteady Hydromagnetic Boundary Layer Flow over a Flat Surface

The appropriate dimensionless quantities in (6.5) for the energy equation are differentiated as:

$$\frac{\partial T^*}{\partial t^*} = (T_w^* - T_\infty^*)\frac{\partial \theta}{\partial t^*} \text{ and } \partial t^* = \frac{v}{V^2}\partial t$$

$$\Longrightarrow \frac{\partial T^*}{\partial t^*} = \frac{V^2}{v}(T_w^* - T_\infty^*)\frac{\partial \theta}{\partial t}$$

$$\frac{\partial T^*}{\partial y^*} = (T_w^* - T_\infty^*)\frac{\partial \theta}{\partial y^*} \text{ and } \partial y^* = \frac{v}{\mathrm{V}}\partial y$$

$$\Longrightarrow \frac{\partial T^*}{\partial y^*} = \frac{\mathrm{V}}{v}(T_w^* - T_\infty^*)\frac{\partial \theta}{\partial y}$$

$$\Longrightarrow \frac{\partial^2 T^*}{\partial y^{*2}} = \frac{V^2}{v^2}(T_w^* - T_\infty^*)\frac{\partial^2 \theta}{\partial y^2} \tag{6.11}$$

Substituting (6.5), (6.11) and Roseland approximation (4.18) in (6.2)

$$\frac{V^2}{v}(T_w^* - T_\infty^*)\frac{\partial \theta}{\partial t} - \mathrm{v}\frac{\mathrm{V}}{v}(T_w^* - T_\infty^*)\frac{\partial \theta}{\partial y} = \frac{v}{P_r}\frac{V^2}{v^2}(T_w^* - T_\infty^*)\frac{\partial^2 \theta}{\partial y^2} + \frac{v}{C_p}\left(\frac{V^2}{v}\frac{\partial u}{\partial y}\right)^2 +$$

$$\frac{v}{k^* C_p}V^2u^2 + \frac{\sigma B_0^2}{\rho C_p}V^2u^2 + \frac{1}{\rho C_p}16a^*\sigma T_\infty^{*3}(T_\infty^* - T^*) - \frac{Q}{\rho C_p}(T_w^* - T_\infty^*)\theta$$

But $v = \frac{\mu}{\rho}$

$$\frac{\partial \theta}{\partial t} - \frac{\partial \theta}{\partial y} = \frac{1}{P_r}\frac{\partial^2 \theta}{\partial y^2} + \frac{V^2}{C_p(T_w^* - T_\infty^*)}\left(\frac{\partial u}{\partial y}\right)^2 + \frac{v^2}{k^* C_p V^2 (T_w^* - T_\infty^*)}V^2u^2 +$$

$$\frac{\sigma B_{0\mathrm{v}}^2}{\rho V^2}\frac{V^2}{C_p(T_w^* - T_\infty^*)}u^2 + \frac{1}{\mu C_p V^2 (T_w^* - T_\infty)}16a^* v^2 \sigma T_\infty^{*3}(T_{\mathrm{w}}^* - T_\infty^*)\theta - \frac{Qv}{\rho C_p V^2}\theta$$

But $P_r = \frac{\mu C_p}{K^*}$

$$\frac{\partial \theta}{\partial t} - \frac{\partial \theta}{\partial y} = \frac{1}{P_r}\frac{\partial^2 \theta}{\partial y^2} + E_c\left(\frac{\partial u}{\partial y}\right)^2 + E_c M_1 u^2 - \frac{1}{P_r}F\theta - H\theta$$

$$\frac{\partial \theta}{\partial t} - \frac{\partial \theta}{\partial y} = \frac{1}{P_r}\frac{\partial^2 \theta}{\partial y^2} + E_c\left(\frac{\partial u}{\partial y}\right)^2 + E_c M_1 u^2 - \frac{1}{P_r}F_1\theta \qquad (6.12)$$

where $F_1 = F + H$

The dimensionless energy equati0n is modeled in (6.12)

6.2.6.5 The Dimensionless Concentration Equation of Unsteady Hydromagnetic Boundary Layer Flow over a Flat Surface

The suitable dimensionless quantities in (6.5) for the concentration equation are differentiated as

$\frac{\partial C^*}{\partial t^*} = (C_w^* - C_\infty^*)\frac{\partial \emptyset}{\partial t^*}$ and $\partial t^* = \frac{v}{V^2}\partial t$

$$\Longrightarrow \frac{\partial C^*}{\partial t^*} = \frac{V^2}{v}(C_w^* - C_\infty^*)\frac{\partial \emptyset}{\partial t}$$

Similarly $\frac{\partial C^*}{\partial y^*} = (C_w^* - C_\infty^*)\frac{\partial \emptyset}{\partial y^*}$ and $\partial y^* = \frac{v}{\mathrm{V}}\partial y$

$$\Longrightarrow \frac{\partial C^*}{\partial y^*} = \frac{\mathrm{V}}{v}(C_w^* - C_\infty^*)\frac{\partial \emptyset}{\partial y}$$

$$\Longrightarrow \frac{\partial C^{*2}}{\partial y^{*2}} = \frac{V^2}{v^2}(C_w^* - C_\infty^*)\frac{\partial^2 \emptyset}{\partial y^2} \qquad (6.13)$$

Putting (6.5) and (6.13) in (6.3)

$$\frac{V^2}{v}(C_w^* - C_\infty^*)\frac{\partial \emptyset}{\partial t} - \mathrm{V}\frac{V}{v}(C_w^* - C_\infty^*)\frac{\partial \emptyset}{\partial t} = D\frac{V^2}{v^2}(C_w^* - C_\infty^*)\frac{\partial^2 \emptyset}{\partial y^2} - k_c^*(C_w^* - C_\infty^*)\emptyset$$

$$\frac{\partial \emptyset}{\partial t} - \frac{\partial \emptyset}{\partial y} = \frac{D}{v}\frac{\partial^2 \emptyset}{\partial y^2} - k_c^*\frac{v}{\mathrm{V}}\emptyset$$

$$\frac{\partial \emptyset}{\partial t} - \frac{\partial \emptyset}{\partial y} = \frac{1}{S_C}\frac{\partial^2 \emptyset}{\partial y^2} - k_C\emptyset \qquad (6.14)$$

Equation (6.14) models the dimensionless concentration.

6.2.6.6 Associated Dimensionless Boundary Conditions of Unsteady Hydromagnetic Boundary Layer Flow over a Flat Surface

The dimensionless momentum, energy and concentration equations in (6.10), (6.12) and (6.14) respectively are subjected to the boundary conditions in dimensionless form as

$$u = 0,\ \theta = 0,\ \phi = 0,\ \ for\ \ \mathrm{y} \geq 0,\ t \leq 0$$

$$u = \lambda(1 - e^{-mt}),\ \ \theta = 1,\ \ \phi = 1,\ \text{for all}\ \ y = 0,\ t > 0$$

$$u \to 0, \theta \to 0, \phi \to 0,\ \ as\ \ y \to \infty,\ \ t > 0 \qquad (6.15)$$

6.3 Analytical Solution of Unsteady Hydromagnetic Boundary Layer Flow over a Flat Surface

The coupled differential equations (6.10), (6.12) and (6.14) with boundary conditions (6.15) are solve in exact form using Laplace transform technique as shown below.

6.3.1 Laplace Transform Technique of Unsteady Hydromagnetic Boundary Layer Flow over a Flat Surface

In energy model (6.12) subject to the boundary conditions in (6.15).

In Laplace domain, the boundary conditions for the energy equation can be written as:

$$\begin{aligned} &\theta(y,0)=0 \quad for\ all\ \ y\geq 0, t\leq 0 && \bar{\theta}(y,0)=0;\\ &\theta(0,t)=1 \quad at\ \ y=0, t>0 && \bar{\theta}(0,s)=\frac{1}{s};\\ &\theta(y,t)\to 0 \quad as\ \ y\to\infty, t>0 && \bar{\theta}(y,s)\to 0. \end{aligned} \tag{6.16}$$

Taking Laplace transform of both sides of (6.12) results in

$$\frac{\partial^2\bar{\theta}}{\partial y^2}+P_r\frac{\partial\bar{\theta}}{\partial y}-P_r(s+\frac{F_1}{P_r})\bar{\theta}=-P_rE_cL\left[\left(\frac{\partial u(y,t)}{\partial y}\right)^2\right]-P_rM_1E_c\bar{u}^2(y,s). \tag{6.17}$$

Considering the homogeneous problem in the LHS of (6.17) the general solution is (see Appendix IV (A3.11)).

$$\bar{\theta}_h(y,s)=A(s)\mathrm{e}^{\frac{-P_r-\sqrt{P_r^2+4(P_rs+F_1)}}{2}y}+B(s)\mathrm{e}^{\frac{-P_r+\sqrt{P_r^2+4(P_rs+F_1)}}{2}y} \tag{6.18}$$

Guessing the form of the particular solution to be

$\bar{\theta}_p(y,s) = A;$

$\bar{\theta}_p{}'(y,s) = 0;$

$\bar{\theta}_p{}''(y,s) = 0;$ substituting all in (6.17) gives

$$0 + 0 - (P_r s + F_1)A = -P_r E_c L\left[\left(\frac{\partial u(y,t)}{\partial y}\right)^2\right] - P_r M_1 E_c \bar{u}^2(y,s)$$

$$A = \frac{P_r E_c L\left[\left(\frac{\partial u(y,t)}{\partial y}\right)^2\right]}{P_r s + F_1} + \frac{P_r M_1 E_c \bar{u}^2(y,s)}{P_r s + F_1} \qquad (6.19)$$

Adding the particular solution (6.19) to (6.18) gives

$$\bar{\theta}(y,s) = A(s)\mathrm{e}^{\frac{-P_r - \sqrt{P_r^2 + 4(P_r s + F_1)}}{2}y} + B(s)\mathrm{e}^{\frac{-P_r + \sqrt{P_r^2 + 4(P_r s + F_1)}}{2}y} +$$

$$\frac{P_r E_c L\left[\left(\frac{\partial u(y,t)}{\partial y}\right)^2\right]}{P_r s + F_1} + \frac{P_r M_1 E_c \bar{u}^2(y,s)}{P_r s + F_1}. \qquad (6.20)$$

Since $\theta(\mathrm{y},t) \to 0$, $as \;\; y \to \infty, t > 0,\;\; \bar{\theta}(\mathrm{y},s) = 0$ an $B(s) = 0$. Now (6.20) reduces to

$$\bar{\theta}(y,s) = A(s)\mathrm{e}^{\frac{-P_r - \sqrt{P_r^2 + 4(P_r s + F_1)}}{2}y} + \frac{1}{P_r s + F_1} P_r E_c L\left[\left(\frac{\partial u(y,t)}{\partial y}\right)^2\right] +$$

$$\frac{1}{P_r s + F_1} P_r M_1 E_c \bar{u}^2(y,\ s) \qquad (6.21)$$

From the boundary conditions $\theta(0,t)=1 \quad at \ y=o, \ t>0 \qquad \bar{\theta}(0,s)=\frac{1}{s}$ put in (6.21) gives

$$\frac{1}{s}=A(s)+\frac{P_rE_cL\left[\left(\frac{\partial u(y,t)}{\partial y}\right)^2\right]}{P_rs+F_1}+\frac{P_rM_1E_c\bar{u}^2(y,s)}{P_rs+F_1}. \tag{6.22}$$

Put (6.22) in (6.21).

$$\bar{\theta}(y,s)=\left(\frac{1}{s}-\frac{P_rE_cL\left[\left(\frac{\partial u(y,t)}{\partial y}\right)^2\right]}{P_rs+F_1}-\frac{P_rM_1E_c\bar{u}^2(y,s)}{P_rs+F_1}\right)e^{\frac{-P_r-\sqrt{P_r^2+4(P_rs+F_1)}}{2}y}+$$

$$\frac{P_rE_cL\left[\left(\frac{\partial u(y,s)}{\partial y}\right)^2\right]}{P_rs+F_1}+\frac{P_rM_1E_c\bar{u}^2(y,s)}{P_rs+F_1}. \tag{6.23}$$

$$\bar{\theta}(y,s)=\frac{1}{s}e^{\frac{-P_r-\sqrt{P_r^2+4(P_rs+F_1)}}{2}y}+L\left[\left(\frac{\partial u(y,t)}{\partial y}\right)^2\right]P_rE_c\left(\frac{1}{P_rs+F_1}-\right.$$

$$\left.\frac{1}{P_rs+F_1}e^{\frac{-P_r-\sqrt{P_r^2+4(P_rs+F_1)}}{2}y}\right)+\bar{u}^2(y\ s)P_rM_1E_c\left(\frac{1}{P_rs+F_1}-\right.$$

$$\left.\frac{1}{P_rs+F_1}e^{\frac{-P_r-\sqrt{P_r^2+4(P_rs+F_1)}}{2}y}\right). \tag{6.24}$$

In the concentration model (6.14) subject to the boundary conditions in (6.15),

in Laplace domain, the boundary conditions for the dimensionless concentration can be written as

$$\emptyset(y,0)=0 \quad for\ all\ \ t\le 0 \qquad \bar{\emptyset}(y,0)=0\ ;$$

$$\emptyset(0,t)=1 \quad at\ \ y=0, t>0 \qquad \bar{\emptyset}(0,s)=\frac{1}{s}\ ; \tag{6.25}$$

$$\emptyset(y,t)\to 0 \quad as \quad y\to\infty, t>0 \qquad \bar{\emptyset}(y,s)\to 0.$$

Taking Laplace transform of both sides of (6.14) gives

$$\frac{1}{S_c}\frac{\partial^2\bar{\emptyset}}{\partial y^2}-s\bar{\emptyset}(y,s)+\emptyset(y,0)+\frac{\partial\bar{\emptyset}}{\partial y}=K_c\bar{\emptyset}\,(y,s) \tag{6.26}$$

But $\emptyset(y,0)=0.$

$$\frac{\partial^2\bar{\emptyset}}{\partial y^2}+S_c\frac{\partial\bar{\emptyset}}{\partial y}-S_c(s+K_c)\bar{\emptyset}=0. \tag{6.27}$$

Equation (6.27) is linear second order homogeneous differential equation.

Considering the homogeneous problem of (6.27) the general solution (see Appendix III, (A3.15)) is

$$\bar{\emptyset}(y,s)=A(s)e^{\frac{-S_c-\sqrt{S_c^2+4(S_cs+S_cK_c)}}{2}y}+B(s)e^{\frac{-S_c+\sqrt{S_c^2+4(S_cs+S_cK_c)}}{2}y}. \tag{6.28}$$

Since $\emptyset(y,t)\to 0\ as\quad y\to\infty, t>0 \quad\Longrightarrow \bar{\emptyset}(y,s)=0$, in (6.28), $B(s)=0$

Now (6.28) reduces to

$$\bar{\emptyset}(y,s)=A(s)e^{\frac{-S_c-\sqrt{S_c^2+4(S_cs+S_cK_c)}}{2}y} \tag{6.29}$$

$$\emptyset(0,t)=1 \quad at \quad y=0, t>0 \qquad \Longrightarrow \bar{\emptyset}(0,s)=\frac{1}{s}$$

In (6.29), $\frac{1}{s}=A(s)$

$$\overline{\emptyset}(y,s)=\frac{1}{s}e^{\frac{-S_c-\sqrt{S_c^2+4(S_cs+S_cK_c)}}{2}y.} \qquad (6.30)$$

Taking inverse Laplace Transform, from tables in Appendix II and the use of convolution theorem in Appendix IV, the general solution of the concentration equation (6.30) $at\ t>0$ (see convolution theorem in Appendix IV, (A4.23)) is

$$\emptyset(y,t)=\frac{1}{2}e^{\frac{-yS_c-y\sqrt{S_c^2+4S_cK_c}}{2}}\left(-erfc\left(\frac{t\sqrt{S_c+4K_c}-y\sqrt{S_c}}{2\sqrt{t}}\right)+\right.$$

$$\left.e^{y\sqrt{S_c^2+4S_cK_c}}erfc\left(\frac{t\sqrt{S_c+4K_c}+y\sqrt{S_c}}{2\sqrt{t}}\right)\right). \qquad (6.31)$$

Similarly, in the momentum model (6.10) subject to the boundary conditions in (6.15).

In Laplace domain, the boundary conditions for the dimensionless momentum equation can be written as:

$$u(y,0)=0 \quad for\ all\ t\le 0 \qquad \bar{u}(y,0)=0;$$

$$u(0,t)=\lambda\,(1-e^{-mt})\ \text{at}\ \ y=0,\ t>0 \qquad \bar{u}(0,s)=\frac{\lambda}{s}-\frac{\lambda}{s+m}; \qquad (6.32)$$

$$u(y,t)\to 0 \quad as \quad y\to\infty, t>0 \qquad \bar{u}(y,s)\to 0.$$

Taking Laplace transform of (6.10) gives

$$\frac{\partial^2\bar{u}}{\partial y^2} - s\bar{u} + u(y,0) + \frac{\partial\bar{u}}{\partial y} = -G_r\bar{\theta} - G_c\bar{\emptyset} + M_1\bar{u}. \quad (6.33)$$

But $u(y,0) = 0$

$$\frac{\partial^2\bar{u}}{\partial y^2} + \frac{\partial\bar{u}}{\partial y} - (s + M_1)\bar{u} = -G_r\bar{\theta} - G_c\bar{\emptyset}. \quad (6.34)$$

Considering the homogeneous problem in the LHS of (6.34) the general solution is

$$\bar{u}_h(y,s) = A(s)\mathrm{e}^{\frac{-1-\sqrt{1+4(s+M_1)}}{2}\mathrm{y}} + B(s)\mathrm{e}^{\frac{-1+\sqrt{1+4(s+M_1)}}{2}\mathrm{y}}. \quad (6.35)$$

Guessing the form of the particular solution to be

$\bar{u}_p(y,s) = A;$

$\bar{u}_p{}'(y,s) = 0;$

$\bar{u}_p{}''(y,s) = 0;$ substituting all in (6.34) gives

$$0 + 0 - (s + M_1)A = -G_r\bar{\theta} - G_c\bar{\emptyset}. \quad (6.36)$$

Adding the particular solution (6.36) to (6.35) gives the general solution

$$\bar{u}(y,s) = A(s)\mathrm{e}^{\frac{-1-\sqrt{1+4(s+M_1)}}{2}\mathrm{y}} + B(s)\mathrm{e}^{\frac{-1+\sqrt{1+4(s+M_1)}}{2}\mathrm{y}} + \frac{G_r\bar{\theta}}{s+M_1} + \frac{G_c\bar{\emptyset}}{s+M_1}. \quad (6.37)$$

Since $u(\mathrm{y},t) \to 0$ as $y \to \infty, t > 0 \implies \bar{u}(\mathrm{y},s) = \mathrm{o}$ and $B(s) = 0$ in (6.37)

Now (6.37) reduces to

$$\bar{u}(y,s) = A(s)\mathrm{e}^{\frac{-1-\sqrt{1+4(s+M_1)}}{2}\mathrm{y}} + \frac{G_r\bar{\theta}}{s+M_1} + \frac{G_c\bar{\emptyset}}{s+M_1} \quad (6.38)$$

But $u(0,t) = \lambda(1 - e^{-mt})$ at $y = 0,\ t > 0 \quad \bar{u}(0,s) = \frac{\lambda}{s} - \frac{\lambda}{s+m}$

$$A(s) = \frac{\lambda}{s} - \frac{\lambda}{s+m} - \frac{G_r\bar{\theta}}{s+M_1} - \frac{G_c\bar{\emptyset}}{s+M_1}. \quad (6.39)$$

Puttting (6.39) in (6.38) gives

$$\bar{u}(y,s) = \left(\frac{\lambda}{s} - \frac{\lambda}{s+m}\right)e^{\frac{-1-\sqrt{1+4(s+M_1)}}{2}y} + G_r\bar{\theta}\left(\frac{1}{s+M_1} - \frac{1}{s+M_1}e^{\frac{-1-\sqrt{1+4(s+M_1)}}{2}y}\right) +$$

$$G_c\bar{\emptyset}\left(\frac{1}{s+M_1} - \frac{1}{s+M_1}e^{\frac{-1-\sqrt{1+4M_1}}{2}y}\right). \quad (6.40)$$

Taking inverse Laplace Transform, from tables in Appendix II and the use of convolution theorem in Appendix IV, the general solution of the velocity model (6.40) $at\ t > 0$ (see convolution theorem in Appendix IV, (A4.25), (A4.29) and (A4.32)) is

$$u(y,t) = \frac{\lambda}{2}e^{\frac{-y-y\sqrt{1+4M_1}}{2}}\left[-erfc\left(\frac{-y+t\sqrt{1+4M_1}}{2\sqrt{t}}\right) +\right.$$

$$\left.e^{y\sqrt{1+4M_1}}erfc\left(\frac{y+t\sqrt{1+4M_1}}{2\sqrt{t}}\right)\right] -$$

$$\frac{\lambda}{2}e^{\frac{-y-y\sqrt{1+4(m+M_1)+1}}{2}-mt}\left[-erfc\left(\frac{-y+t\sqrt{-4(m+M_1)+1}}{2\sqrt{t}}\right) +\right.$$

$$\left.e^{y\sqrt{-4(m+M_1)+1}}erfc\left(\frac{y+t\sqrt{-4(m+M_1)+1}}{2\sqrt{t}}\right)\right] + (G_r\theta(y,t) + G_c\emptyset(y,t))\left[e^{-M_1t} +\right.$$

$$\left.\frac{1}{2}e^{-M_1t-y}erfc\left(\frac{t-y}{2\sqrt{t}}\right) - \frac{1}{2}e^{-M_1t}\text{erfc}\left(\frac{t+y}{2\sqrt{t}}\right)\right]. \quad (6.41)$$

Where

$$\emptyset(y,t) = \frac{1}{2}e^{\frac{-yS_c - y\sqrt{S_c^2+4S_cK_c}}{2}}\left(-erfc\left(\frac{t\sqrt{S_c+4K_c}-y\sqrt{S_c}}{2\sqrt{t}}\right)+\right.$$

$$\left.e^{y\sqrt{S_c^2+4S_cK_c}}erfc\left(\frac{t\sqrt{S_c+4K_c}+y\sqrt{S_c}}{2\sqrt{t}}\right)\right).$$

Equation (6.41) is the general solution for the velocity profile at $t > 0$.

Now, knowing the general solution of the velocity model, the general solution of the temperature model can be obtained as;

From the temperature equation in (6.24) which is

$$\bar{\theta}(y,s) = \frac{1}{s}\mathrm{e}^{\frac{-P_r-\sqrt{P_r^2+4(P_rs+F_1)}}{2}\mathrm{y}} + \left(\frac{\partial u(y,s)}{\partial y}\right)^2 P_rE_c\left(\frac{1}{P_rs+F_1} - \right.$$

$$\left.\frac{1}{P_rs+F_1}\ \mathrm{e}^{\frac{-P_r-\sqrt{P_r^2+4(P_rs+F_1)}}{2}\mathrm{y}}\right) + \bar{u}^2(y,s)P_rM_1E_c\left(\frac{1}{P_rs+F_1} - \right.$$

$$\left.\frac{1}{P_rs+F_1}\mathrm{e}^{\frac{-P_r-\sqrt{P_r^2+4(P_rs+F_1)}}{2}\mathrm{y}}\right).$$

In finding the Laplace transform of the velocity function $\left(\frac{\partial u(y,t)}{\partial y}\right)^2$, the following properties of Laplace transform are used;

- If the $L\left[\left(\frac{\partial u(y,t)}{\partial y}\right)^2\right] = \left(\frac{\partial u(y,s)}{\partial y}\right)^2$, then $L^{-1}\left[\left(\frac{\partial u(y,s\ )}{\partial y}\right)^2\right] = \left(\frac{\partial u(y,t)}{\partial y}\right)^2$.

Taking inverse Laplace transform of the temperature equation (6.24) from tables in Appendix II and the use of convolution theorem in Appendix IV, the general solution (see, convolution theorem in Appendix IV, (A4.12), (A4.35) and (A4.38)) is

$$\theta(y,t) = -\frac{1}{2}e^{\frac{-P_r}{2}-y\sqrt{4F_1+P_r^2}}erfc\left(\frac{t\sqrt{\frac{4F_1}{P_r}+P_r}-y\sqrt{P_r}}{2\sqrt{t}}\right)+$$

$$\frac{1}{2}e^{\frac{-P_r}{2}+y\sqrt{F_1+\frac{1}{4}P_r^2}}erfc\left(\frac{t\sqrt{\frac{4F_1}{P_r}+P_r}+y\sqrt{P_r}}{2\sqrt{t}}\right)+\left(\frac{\partial u(y,t)}{\partial y}\right)^2 P_r E_c\left[\frac{1}{P_r}e^{\frac{-F_1 t}{P_r}}+\right.$$

$$\left.\frac{1}{2P_r}e^{\frac{-F_1}{P_r}+yP_r}erfc\left(\frac{t\sqrt{P_r}-y\sqrt{P_r}}{2\sqrt{t}}\right)-\frac{1}{2}e^{\frac{-F_1}{P_r}+2yP_r}erfc\left(\frac{t\sqrt{P_r}+y\sqrt{P_r}}{2\sqrt{t}}\right)\right]+$$

$$u^2(y,t)P_r E_c M_1\left[\frac{1}{P_r}e^{\frac{-F_1 t}{P_r}}+\frac{1}{2P_r}e^{\frac{-F_1}{P_r}+yP_r}erfc\left(\frac{t\sqrt{P_r}-y\sqrt{P_r}}{2\sqrt{t}}\right)-\right.$$

$$\left.\frac{1}{2}e^{\frac{-F_1}{P_r}+2yP_r}erfc\left(\frac{t\sqrt{P_r}+y\sqrt{P_r}}{2\sqrt{t}}\right)\right]. \qquad (6.42)$$

Where $u^2(y,t)$ and $\left(\frac{\partial u(y,t)}{\partial y}\right)^2$ are shown in (Appendix IV, (A4.39) and (A4.41) respectively).

In substituting $u^2(y,t)$ and $\left(\frac{\partial u(y,t)}{\partial y}\right)^2$ (see Appendix IV, (A4.39) and (A4.41)) in the temperature equation (6.24), the non-linear term $\theta^2(y,t)$ is

considered negligible due to the temperature differences in the flow being sufficiently small. Therefore, the general solution of the temperature model for $t > 0$ is

$$\theta(y,t) = b_1^{-1}\left[-\frac{1}{2}e^{\frac{-P_r}{2}-y\sqrt{4F_1+P_r^2}}erfc\left(\frac{t\sqrt{\frac{4F_1}{P_r}+P_r}-y\sqrt{P_r}}{2\sqrt{t}}\right)+\right.$$

$$\frac{1}{2}e^{\frac{-P_r}{2}+y\sqrt{F_1+\frac{1}{4}P_r^2}}erfc\left(\frac{t\sqrt{\frac{4F_1}{P_r}+P_r}+y\sqrt{P_r}}{2\sqrt{t}}\right)+b_2P_rE_c\left[\frac{1}{P_r}e^{\frac{-F_1t}{P_r}}+\right.$$

$$\frac{1}{2P_r}e^{\frac{-F_1}{P_r}+yP_r}erfc\left(\frac{t\sqrt{P_r}-y\sqrt{P_r}}{2\sqrt{t}}\right)-\frac{1}{2}e^{\frac{-F_1}{P_r}+2yP_r}erfc\left(\frac{t\sqrt{P_r}+y\sqrt{P_r}}{2\sqrt{t}}\right)\Big]+$$

$$b_3P_rE_cM_1\left(\frac{1}{P_r}e^{\frac{-F_1t}{P_r}}+\frac{1}{2P_r}e^{\frac{-F_1}{P_r}+yP_r}erfc\left(\frac{t\sqrt{P_r}-y\sqrt{P_r}}{2\sqrt{t}}\right)-\right.$$

$$\left.\left.\frac{1}{2}e^{\frac{-F_1}{P_r}+2yP_r}erfc\left(\frac{t\sqrt{P_r}+y\sqrt{P_r}}{2\sqrt{t}}\right)\right)\right]. \qquad (6.43)$$

Where

$$b_1 = 1 - P_rE_c\left[\frac{1}{P_r}e^{\frac{-F_1t}{P_r}}+\frac{1}{2P_r}e^{\frac{-F_1}{P_r}+yP_r}erfc\left(\frac{t\sqrt{P_r}-y\sqrt{P_r}}{2\sqrt{t}}\right)-\right.$$

$$\left.\frac{1}{2}e^{\frac{-F_1}{P_r}+2yP_r}erfc\left(\frac{t\sqrt{P_r}+y\sqrt{P_r}}{2\sqrt{t}}\right)\right]\left[\frac{1}{2\sqrt{\pi t}}e^{\frac{-M_1t-(t-y)^2}{4t-y}}-\frac{1}{2}erfc\left(\frac{t-y}{2\sqrt{t}}\right)e^{-M_1t-y}+\right.$$

$$\left.\frac{1}{2\sqrt{\pi t}}e^{\frac{-M_1t-(t-y)^2}{4t-y}}\right]^4\left[-\frac{\lambda}{2\sqrt{\pi t}}e^{\frac{-y-y\sqrt{1+4M_1}}{2}-\frac{\left(-y+t\sqrt{4M_1+1}\right)^2}{4t}}-\frac{\lambda}{4}(-1-\right.$$

$$\sqrt{4M_1+1})\mathrm{e}^{\frac{-\mathrm{y}-\mathrm{y}\sqrt{1+4M_1}}{2}}erfc\left(\frac{-y+t\sqrt{4M_1+1}}{2\sqrt{t}}\right)-\frac{\lambda}{2\sqrt{\pi t}}\mathrm{e}^{\frac{-\mathrm{y}+\mathrm{y}\sqrt{1+4M_1}}{2}-\frac{(y+t\sqrt{4M_1+1})^2}{4t}}+$$

$$\frac{\lambda}{4}(-1+\sqrt{4M_1+1})\mathrm{e}^{\frac{-\mathrm{y}+\mathrm{y}\sqrt{1+4M_1}}{2}}erfc\left(\frac{y+t\sqrt{4M_1+1}}{2\sqrt{t}}\right)\Bigg]\Bigg[\frac{\lambda}{4}(-1-$$

$$\sqrt{1-4(m+M_1)})\mathrm{e}^{\frac{-2\mathrm{mt}-\mathrm{y}-\mathrm{y}\sqrt{1-4(m+M_1)}}{2}}erfc\left(\frac{-y+t\sqrt{1-4(m+M_1)}}{2\sqrt{t}}\right)+$$

$$\frac{\lambda}{2\sqrt{\pi t}}\mathrm{e}^{\frac{-2\mathrm{mt}-\mathrm{y}-\mathrm{y}\sqrt{1-4(m+M_1)}}{2}-\frac{(-y+t\sqrt{1-4(m+M_1)})^2}{4t}}+$$

$$\frac{\lambda}{2\sqrt{\pi t}}\mathrm{e}^{\frac{-2\mathrm{mt}-\mathrm{y}+\mathrm{y}\sqrt{1-4(m+M_1)}}{2}-\frac{(y+t\sqrt{1-4(m+M_1)})^2}{4t}}-\frac{\lambda}{4}(-1+$$

$$\sqrt{1-4(m+M_1)})\mathrm{e}^{\frac{-2\mathrm{mt}-\mathrm{y}+\mathrm{y}\sqrt{1-4(m+M_1)}}{2}}erfc\left(\frac{y+t\sqrt{1-4(m+M_1)}}{2\sqrt{t}}\right)\Bigg]-$$

$$2P_rE_cM_1G_rG_c\emptyset(y,t)\left[\frac{1}{P_r}e^{\frac{-F_1t}{P_r}}+\frac{1}{2P_r}e^{\frac{-F_1}{P_r}+yP_r}erfc\left(\frac{t\sqrt{P_r}-y\sqrt{P_r}}{2\sqrt{t}}\right)-\right.$$

$$\left.\frac{1}{2}e^{\frac{-F_1}{P_r}+2yP_r}erfc\left(\frac{t\sqrt{P_r}+y\sqrt{P_r}}{2\sqrt{t}}\right)\right]\Bigg[-\frac{1}{4}(-2e^{-M_1t}-e^{-M_1t-y})^2\left(-erfc\left(\frac{t-y}{2\sqrt{t}}\right)+\right.$$

$$\left.erfc\left(\frac{t+y}{2\sqrt{t}}\right)\right)^2\Bigg]\frac{\lambda}{2}\mathrm{e}^{\frac{-\mathrm{y}-\mathrm{y}\sqrt{1+4M_1}}{2}}\left[-erfc\left(\frac{-\mathrm{y}+\mathrm{t}\sqrt{1+4M_1}}{2\sqrt{t}}\right)+\right.$$

$$\left.e^y\sqrt{1+4M_1}erfc\left(\frac{\mathrm{y}+\mathrm{t}\sqrt{1+4M_1}}{2\sqrt{t}}\right)\right]\left[\frac{2e^{-M_1t}-e^{-M_1t-y}}{2}\left(-erfc\left(\frac{t-y}{2\sqrt{t}}\right)+erfc\left(\frac{t+y}{2\sqrt{t}}\right)e^y\right)\right]$$

$$\frac{\lambda}{2}\mathrm{e}^{\frac{-2\mathrm{mt}-\mathrm{y}-\mathrm{y}\sqrt{-4(m+M_1)+1}}{2}}\left[-erfc\left(\frac{-\mathrm{y}+\mathrm{t}\sqrt{-4(m+M_1)+1}}{2\sqrt{t}}\right)+\right.$$

$$\left.e^y\sqrt{-4(m+M_1)+1}erfc\left(\frac{\mathrm{y}+\mathrm{t}\sqrt{-4(m+M_1)+1}}{2\sqrt{t}}\right)\right]\left[\frac{2e^{-M_1t}-e^{-M_1t-y}}{2}\left(-erfc\left(\frac{t-y}{2\sqrt{t}}\right)+\right.\right.$$

$$\left.\left.erfc\left(\frac{t+y}{2\sqrt{t}}\right)e^y\right)\right].$$

The terms $b_2$and b_3 are shown (see Appendix IV).

There exist other possible solution for $\theta^2(y,t) \neq 0$ but limited in application in practice due to the presence of the discriminant in the solution of the resulting quadratic equation which makes $\theta(y,t)$ not defined for higher values of the controlling parameters.

6.3.2 Dimensionless Fluxes of Unsteady Hydromagnetic Boundary Layer Flow over a Flat Surface

6.3.2.1 The Rate of Heat Transfer Coefficient of Unsteady Hydromagnetic Boundary Layer Flow over a Flat Surface

Having obtained the **temperature field**, the rate of heat transfer coefficient at the flat surface in terms of the Nusselt number can be studied. The effects of t, M, F, H, E_c and P_r on Nusselt number will be considered. In dimensionless form, the Nusselt number is given by

$$N_u = -\frac{\partial\theta}{\partial y}\Big|_{y=0}$$

$$= b_1^{-2}\left[\frac{1}{4}P_r\sqrt{4F_1+P_r^2}erfc\left(\frac{t\sqrt{\frac{4F_1}{P_r}+P_r}}{2\sqrt{t}}\right)-\frac{1}{2}erfc\left(\frac{t\sqrt{\frac{4F_1}{P_r}+P_r}}{2\sqrt{t}}\right)-\right.$$

$$\frac{\lambda t(8(m+M_1)-1)}{4\sqrt{\pi t^3}}e^{-\frac{t^2(4m+4M_1-1)^2}{4t}}+\frac{1}{4}P_rE_c\lambda^2\left(\sqrt{M_1+1}-1\right)efrc\left(\frac{4M_1t+t}{2\sqrt{t}}\right)^2+$$

$$\left.\frac{2}{\sqrt{\pi}}e^{-\frac{(4M_1t-t)^2}{4t}}\right]. \qquad (6.43)$$

6.3.2.2 The Rate of Mass Transfer Coefficient of Unsteady Hydromagnetic Boundary Layer Flow over a Flat Surface

Knowing the **concentration field,** the rate of mass transfer coefficient at the flat surface in terms of the Sherwood number can be studied. The effects of t, S_c and K_c on Sherwood number will be examined. In dimensionless form, the Sherwood number is given by

$$sh = -\left(\frac{\partial\emptyset}{\partial y}\right)_{y=0}$$

$$= \frac{1}{4}\left(S_c+\sqrt{S_c(4K_c+S_c)}\right)erfc\left(\frac{t\sqrt{4K_c+S_c}}{2\sqrt{t}}\right)-\frac{\sqrt{S_c}}{8\sqrt{\pi t}}e^{-t^2(4K_c+S_c)}+$$

$$\left(-\frac{1}{4}\left(-S_c+\sqrt{S_c(4K_c+S_c)}\right)+\sqrt{S_c(4K_c+S_c)}\right)erfc\left(\frac{t\sqrt{4K_c+S_c}}{2\sqrt{t}}\right)-\frac{\sqrt{S_c}}{\sqrt{\pi t}}\left(\frac{1}{2}+\right.$$

$$\left.y\sqrt{4K_cS_c+S_c^2}\right)e^{\frac{-t^2(4K_c+S_c)}{4t}}. \qquad (6.44)$$

6.3.2.3 Skin Friction Coefficient of Unsteady Hydromagnetic Boundary Layer Flow over a Flat Surface

Also, having obtained the **velocity field**, it is significant to study changes in the skin friction due to the effects of the physical parameters $t, M, H, E_c, P_r, K_c, G_r$ and G_c. In dimensionless form, the skin friction is given by

$$\tau = -\frac{\partial u}{\partial y}\Big|_{y=0} = \frac{\lambda}{4}\left(\left(1+\sqrt{4M_1}\right)erfc\left(\frac{\sqrt{4M_1+1}}{2\sqrt{t}}\right) - \frac{2}{\sqrt{\pi t}}e^{\frac{(4M_1+1)}{4t}}\right) + \left(\frac{\lambda}{4}\left(-1-\sqrt{4M_1+1}\right)+\sqrt{4M_1+1}\right)erfc\left(\frac{\sqrt{4M_1+1}}{2\sqrt{t}}\right) - \frac{\lambda}{2\sqrt{\pi t}}e^{\frac{(4M_1+1)}{4t}} + \frac{\lambda}{2\sqrt{\pi t}}e^{-\frac{t^2(1-4(m+M_1))}{4t}} + \frac{\lambda}{4}\left(-1-\sqrt{4(m+M_1)+2}\right)erfc\left(\frac{t\sqrt{1-4(m+M_1)}}{2\sqrt{t}}\right) - \left(\frac{\lambda}{4}\left(-1-\sqrt{4(m+M_1)+2}\right)+\sqrt{1-4(m+M_1)}\right)erfc\left(\frac{\sqrt{1-4(m+M_1)}}{2\sqrt{t}}\right) + \frac{1}{\sqrt{\pi t}}e^{-\frac{t^2(1-4(m+M_1))}{4t}}\left(\frac{\lambda}{2}-mt\right) + \left(G_r\theta(y,t)+G_c\emptyset(y,t)\right)\left[\left(\frac{1}{2}\frac{1}{\sqrt{\pi t}}e^{-\frac{-t^2}{4t}} - \frac{1}{2}erfc\left(\frac{t}{2\sqrt{t}}\right)\right)e^{-M_1 t} - \frac{1}{2}\frac{1}{\sqrt{\pi t}}e^{\frac{-M_1 t-t^2}{4t}}\right] + \left(G_r\frac{\partial\theta}{\partial y}+G_c\frac{\partial\emptyset}{\partial y}\right)e^{-M_1 t}. \quad (6.45)$$

6.4 Results and Discussion

To understand the physical dynamics of the problem, the effects of the controlling parameters on the Temperature (θ), Concentration$(\emptyset)$ and Velocity (u) profiles are illustrated graphically using MATLAB.

6.4.1 Graphical Results

6.4.1.1 Temperature Profiles

Fig. 6.2 illustrates the effects of time (t) on the temperature profiles. It is observed as time passes, the temperature of the fluid decreases. Fig. 6.3, 6.4 and 6.5 exhibit the effects of Prandtl number (Pr), Magnetic parameter (M) and Eckert number (Ec), respectively on the temperature profiles. It is also observed that increase in either Magnetic parameter (M) or Eckert number (Ec) decreases the temperature of the fluid whilst decrease in Pr decreases the temperature.

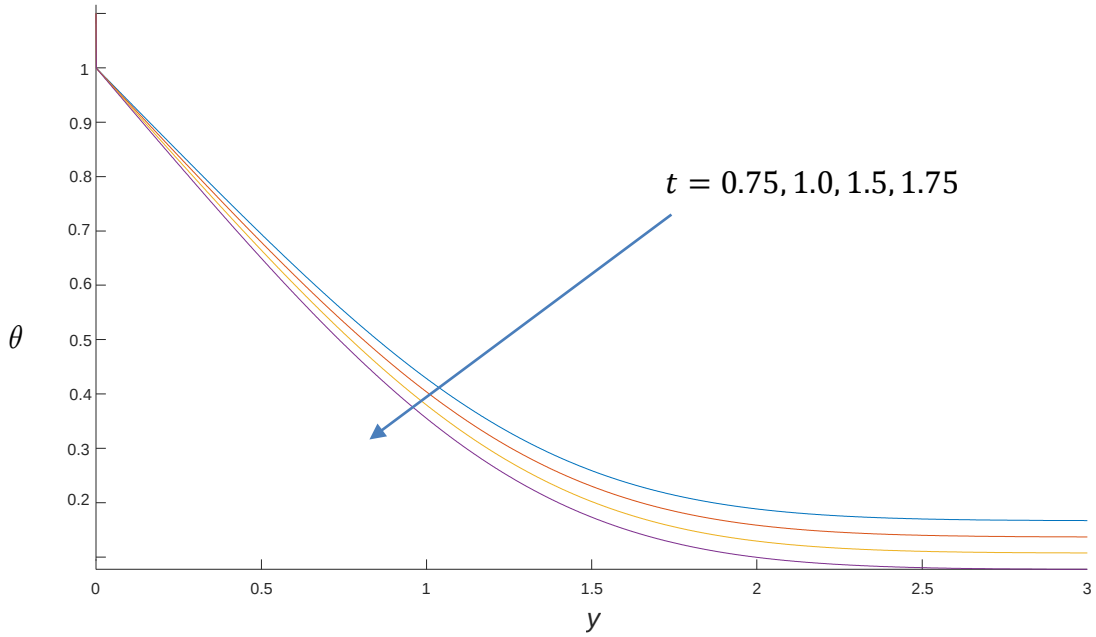

Figure 6. 2 Temperature field for different instance of time t when M=2, Ec=2 Pr=0.71, H=2, F=1 k=1, m=1, Gr=5, Gc=5 Kc=1, Sc=2.01 and ↘=1

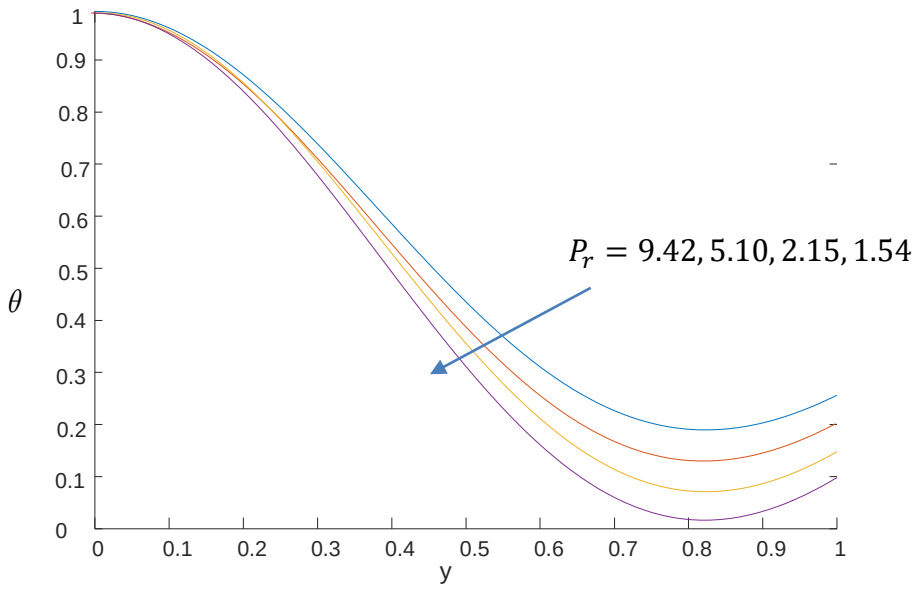

Figure 6. 3 Temperature field for different values of Prandtl number Pr when M=2, Ec=2, t=0.2, H=2, F=1, k=1, m=1, Kc=1, Gc=5, Gr=5, Sc=2.01 and ⅄=1

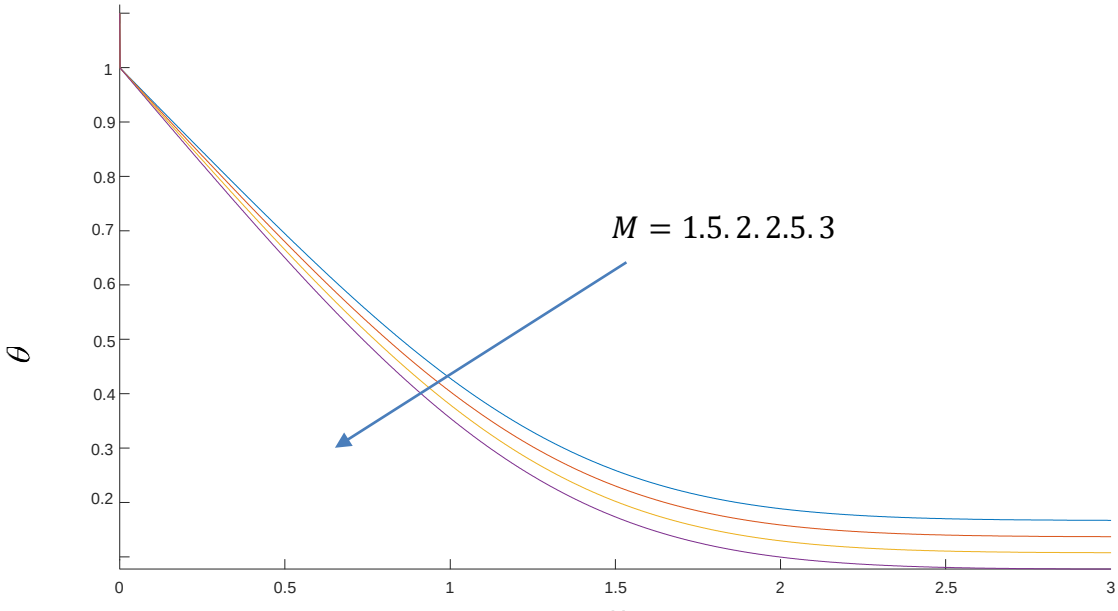

Figure 6.4 Temperature field for different values of magnetic parameters, M when t=0.2, Pr=0.71, Ec=2, H=2, F=1, Gc=5, Gr=5, Kc=1, Sc=2.01, k=1, m=1 and ⅄=1

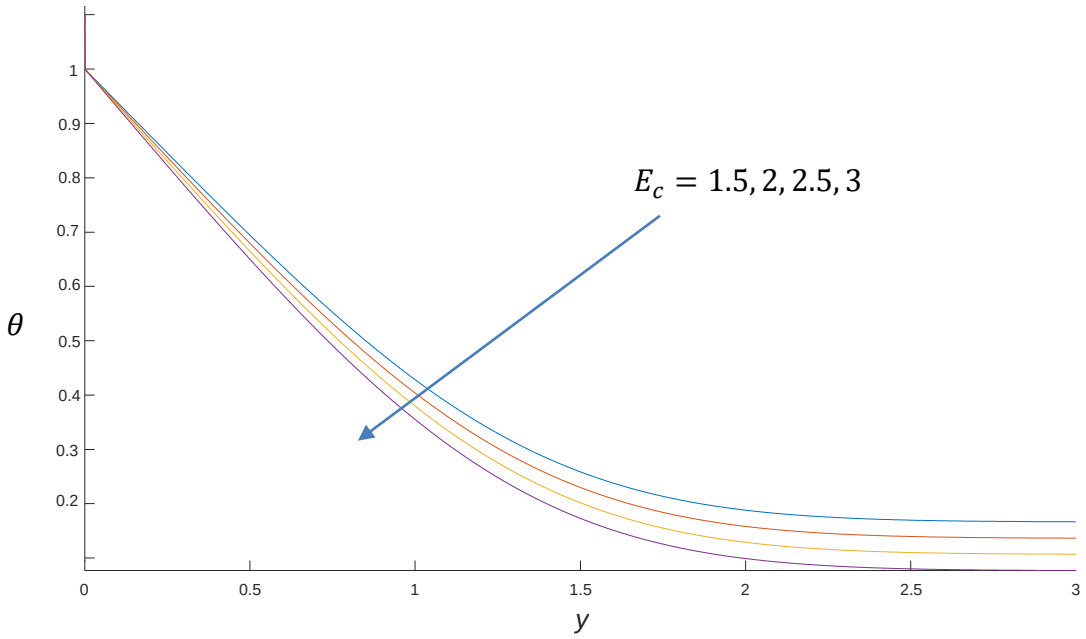

Figure 6. 5 Temperature field for different values of Eckert number Ec when M=2, Pr=0.7, t=0.2, H=2, F=1, k=1, m=1, Gr=5, Gc=5, Kc=1, Sc=2.01 and ↘=1.

Fig.6.6 and Fig. 6.7 show the effects of Radiation parameter and Heat (F) absorption parameter (H) on the temperature profile respectively. It is noticed that increase in either F or H increases the thermal boundary thickness of the fluid.

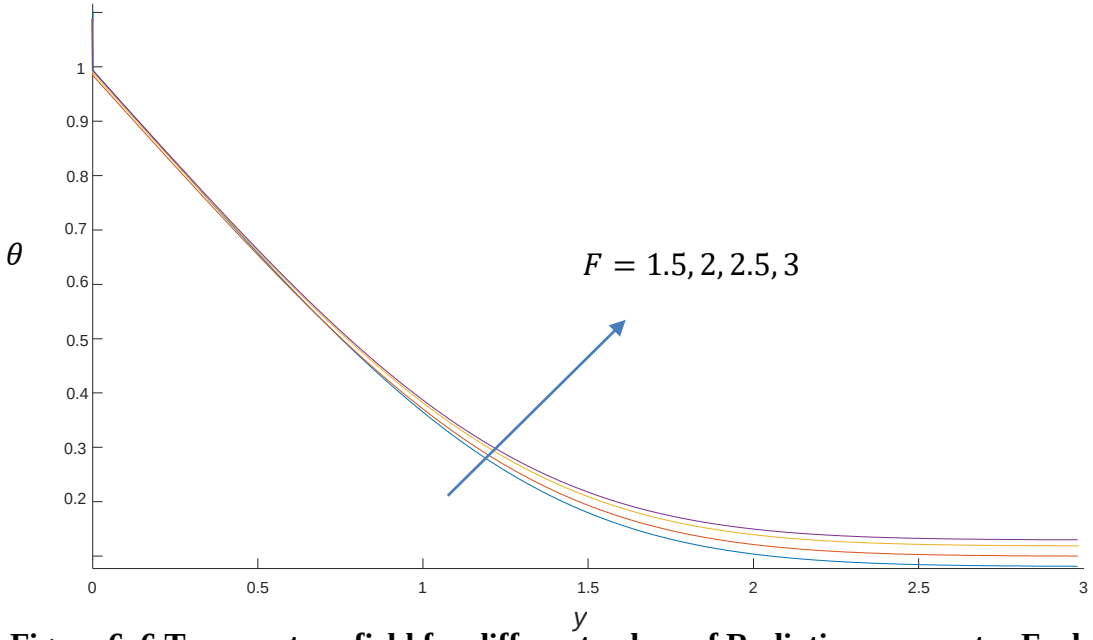

Figure 6. 6 Temperature field for different values of Radiation parameter F when M=2, Pr=0.71, t=0.2, M=2, Ec=2, H=2 , Gr=5, Gc=5, Kc=1, Sc=2.01, m=1 and ⅄=1

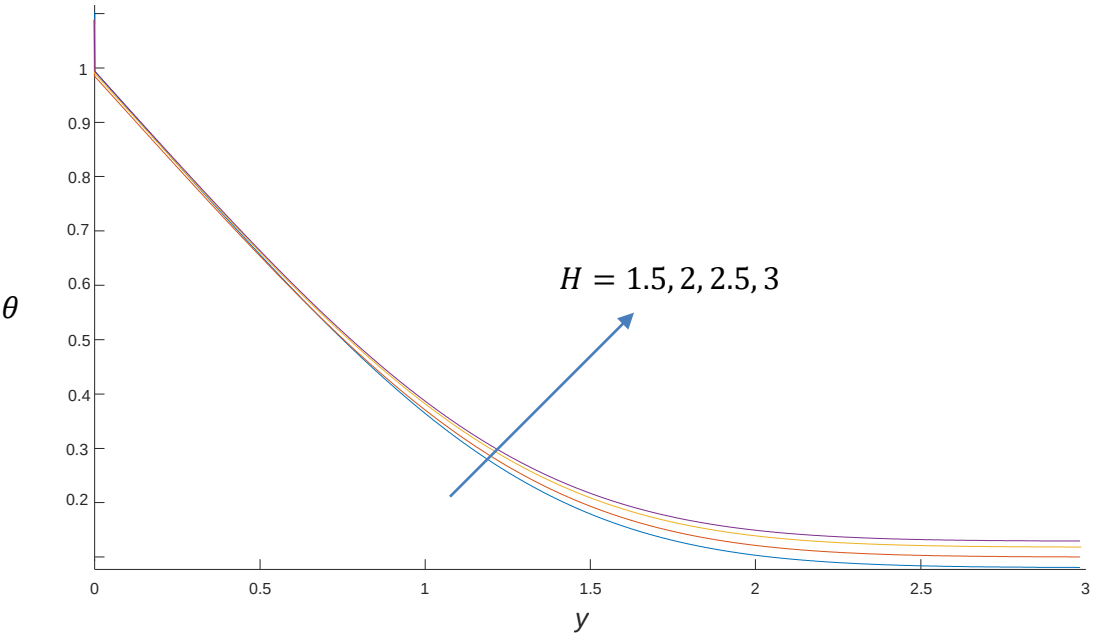

Figure 6.7 Temperature field for different values of Heat absorption parameter H when M=2, Pr=0.71, t=0.2, M=2, Ec=2, F=1, Gr=5, Gc=5, m=1, Sc=2.01, Kc=1and ⅄=1

6.4.1.2Concentration Profiles

In Fig. 6.8, 6.9 and 6.10, the effects of t, Sc and Kc on the concentration profiles respectively are considered. It is observed that as time passes, the concentration of the fluid decreases hence reduction in permeability of the porous medium. However, increase in either Sc or Kc increases the concentration of the flow, however at the twist of the flow the concentration decreases for further increase in values of Sc due to the unsteadiness in the flow. Also, in the case of concentration field for the different values of Kc, the fluid converged at termination point as depicted in the diagram.

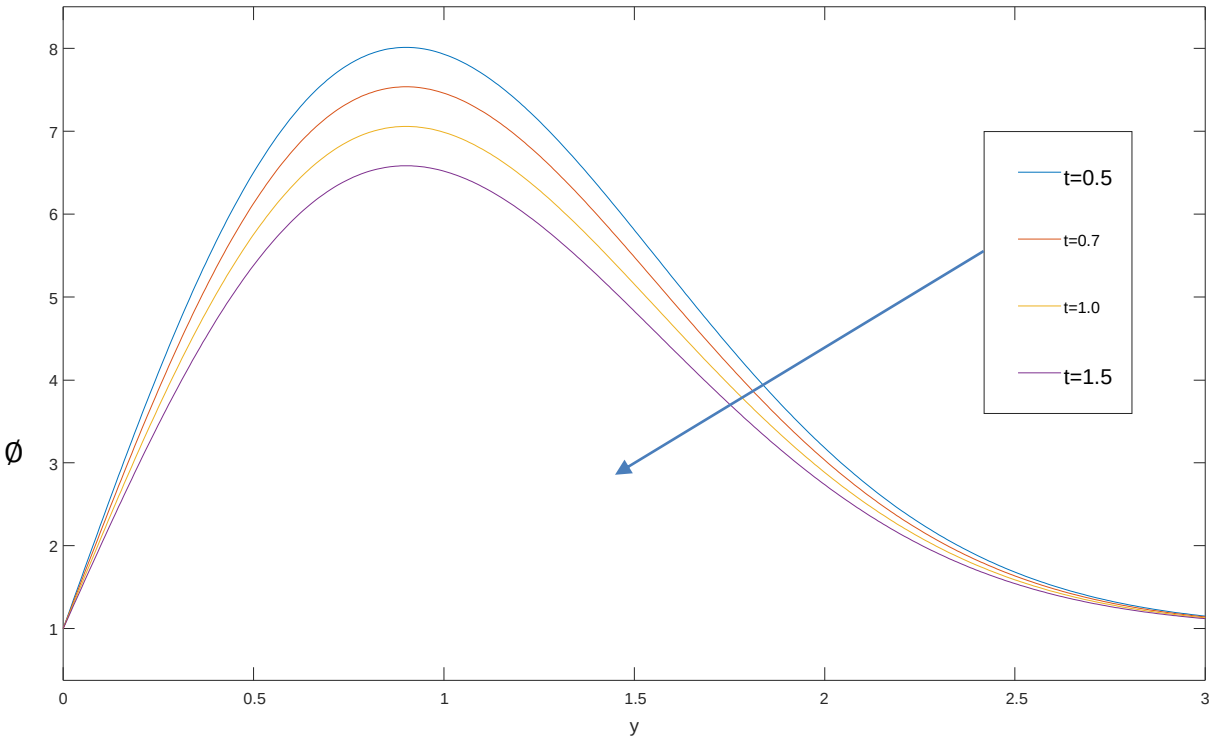

Figure 6.8 Concentration field for different values of time t when *Sc=2.01, Kc=1.5.*

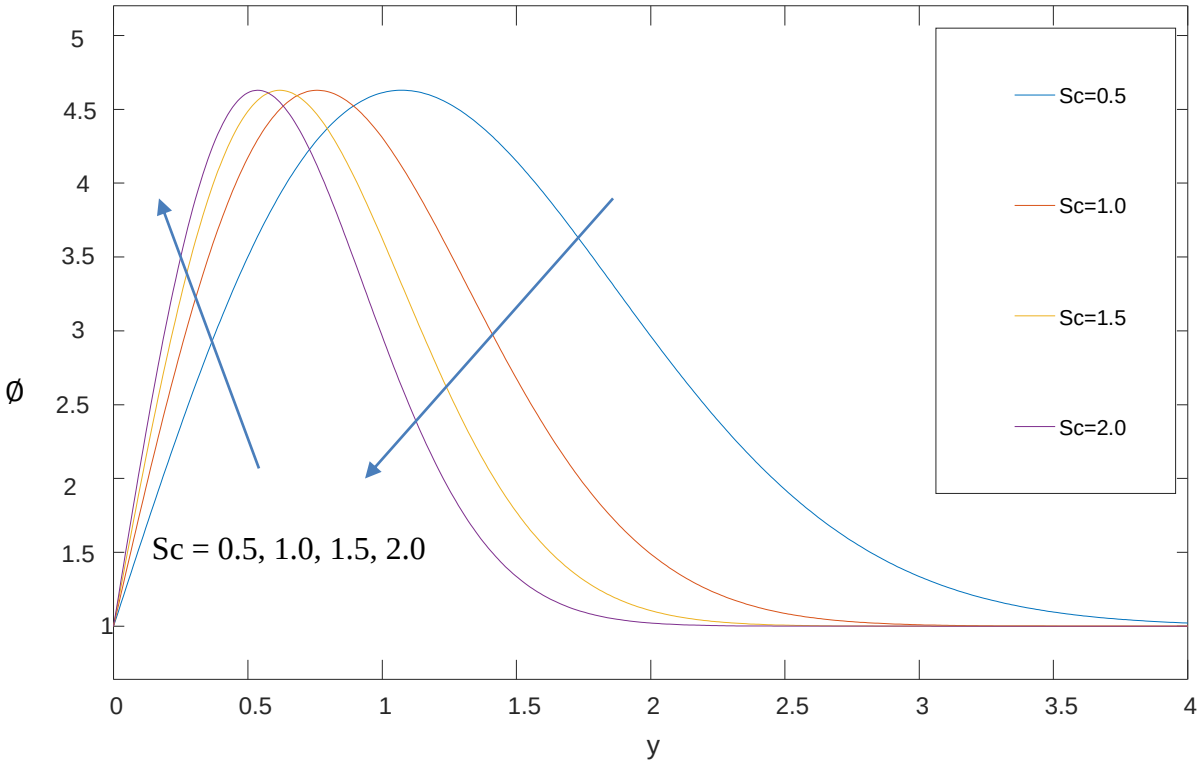

Figure 6. 9 Concentration field for different values of *Sc when t=0.2 and Kc=1*

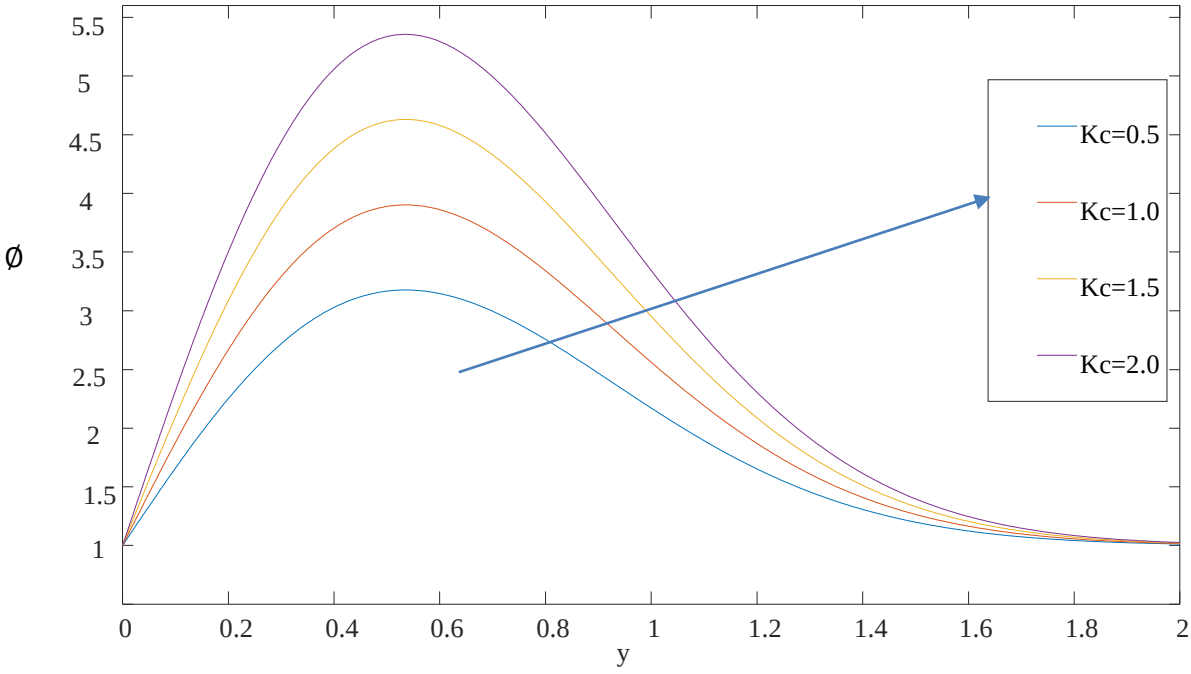

Figure 6.10 Concentration field for different values of Kc when Sc=2.01 and t=0.2

6.4.1.3 Velocity Profiles

Fig. 6.11 – Fig. 6.13 illustrate the effects of Gr, Gc and M on the velocity profiles respectively. Though with an increase in the of values of Gr, the flow is accelerated due to the intensity in the buoyancy force influencing the velocity within the boundary layer to increase however, in fig. 6.11, the velocity of the fluid decreases with increase in Grashof number Gr due to the presence of the magnetic field which delays the convection motion of the fluid. Similarly, in fig. 6.12, an increased in Gc led to decrease in the velocity of the flow but both fluids converged at termination point as depicted in the diagrams. This is in good agreement with **Ali et al. (2014).** Also, in Fig. 6.13, an increase in M decreases the velocity of the flow. This true in practice because magnetic field retards a free convective flow.

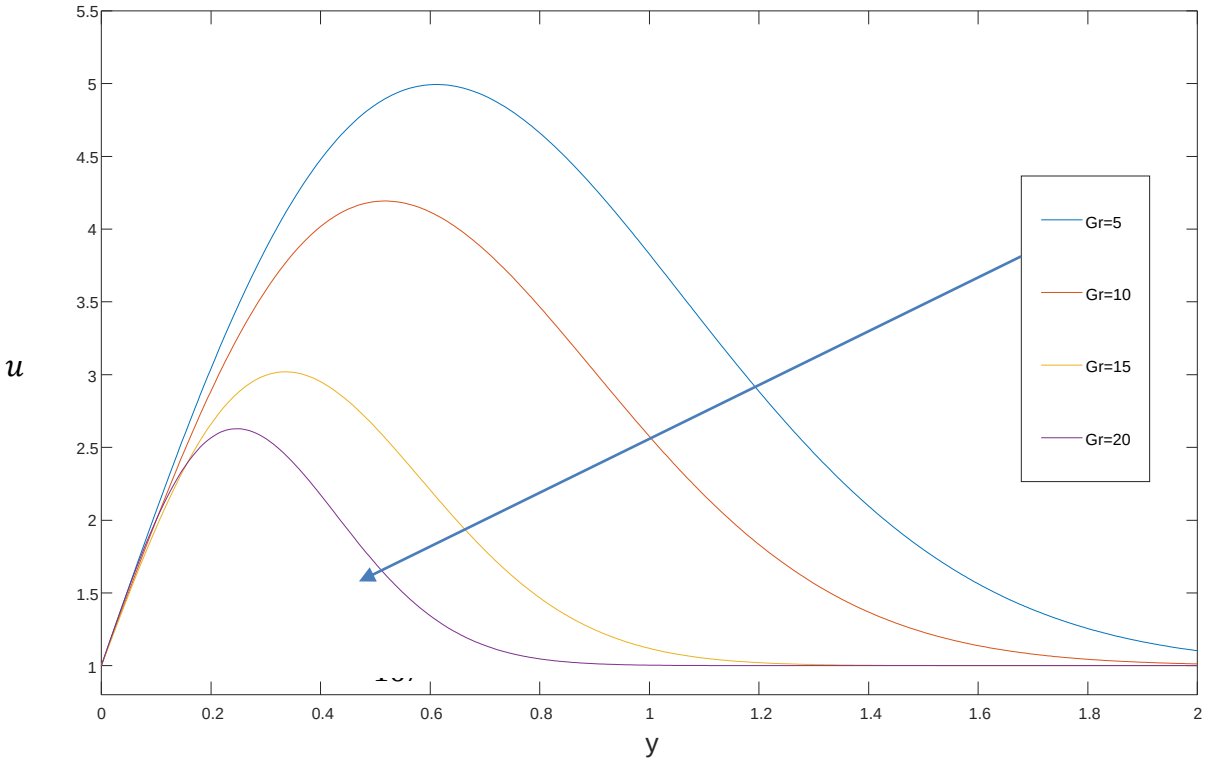

Figure 6.11:Velocity field for different values of Thermal Grashof number Gr when t=0.75, M=2, Ec=2, k=1, Kc=1.5, Gc=5, Pr=0.71, Ec=2, Sc=2.01, F=1, H=2, m=1 and ⅄=1

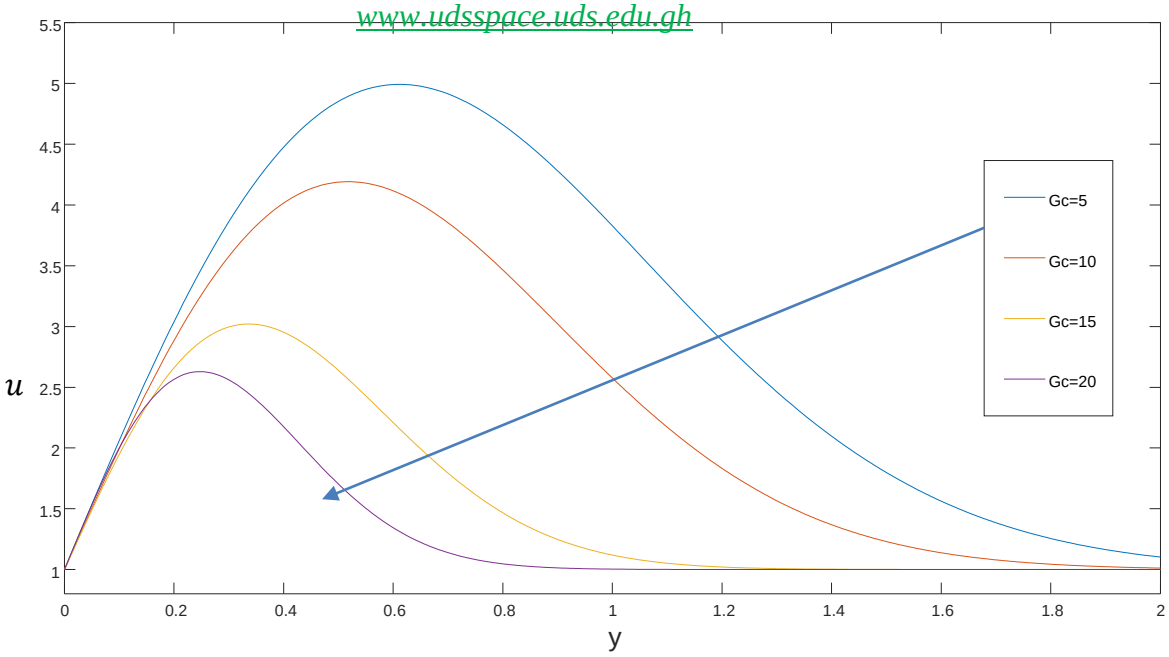

Figure 6.12:Velocity field for different values of Mass Grashof number Gc when t=0.75, M=2, Ec=2, k=1, Kc=1.5, Gr=5, Pr=0.71, Ec=2, Sc=2.01, F=1, H=2, m=1 and ↖=1

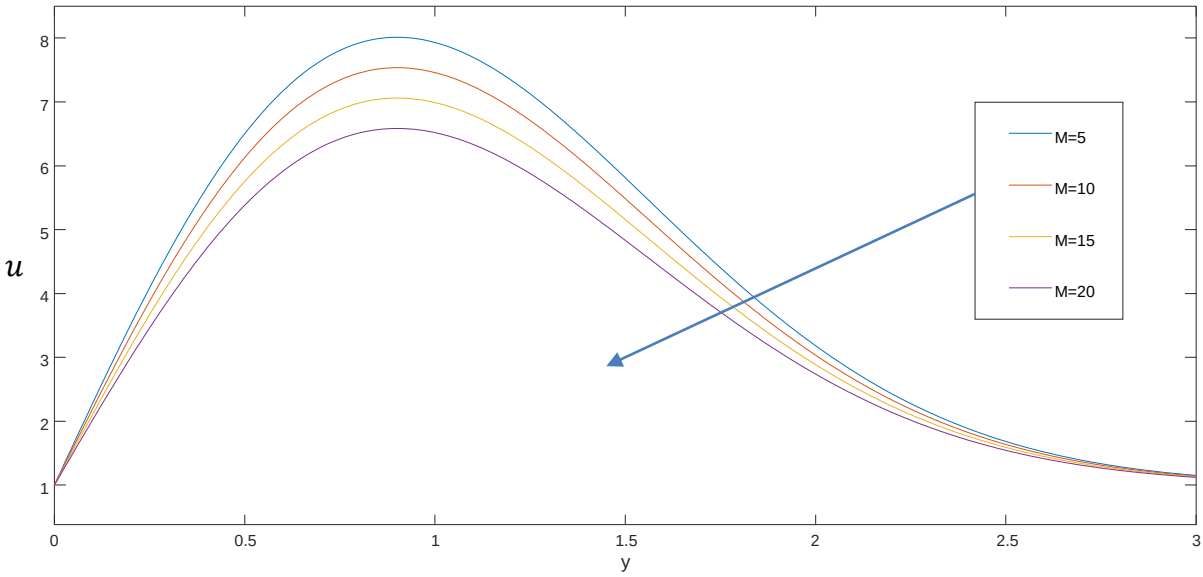

Figure 6.13:Velocity field for different values of Magnetic parameter M when t=0.75, Ec=2, k=1, Kc=1.5,Gr=5, Gc=5, Pr=0.71, Ec=2, Sc=2.01, F=1, H=2, m=1 and ↖=1

6.5 Numerical Results

Table 6.1-6.3 show the behaviour of **skin friction coefficient, $-\boldsymbol{u}'(\mathbf{0})$, Sherwood number**, $-\emptyset'(\mathbf{0})$ and **Nusselt number**, $-\boldsymbol{\theta}'(\mathbf{0})$ for various values of time (t), magnetic parameter (*M*), Eckert number (*Ec*), dimensionless chemical reaction parameter (*kc*), Schmidt number (*Sc*), prandtl number (*Pr*), dimensionless permeability coefficient of the porous medium (k), Heat absorption parameter (*H*), radiation parameter (*F*), thermal Grashof number (*Gr*), Mass Grashof number (*Gc*) . From Table 6.1, it is noted that the skin friction coefficient, $-u'(0)$ decreases for increasing values of $t, M, E_c, P_r,$ G_r and G_c but increases for increasing values of $H, F,$ $S_{c,}$ k_c, k and F. From Table 6.2, Sherwood number, $-\emptyset'(0)$ decreases with increasing values of t but increases for increase values of S_c and k_c .From Table 6.3, Nusselt number , $-\theta'(0)$ decreases with increasing values of t, M, E_c, Gr, Gc and P_r but increases with increase values of $H, k, Kc,$ *Sc* and *F*. Also in Table 6.4, order to measure the accuracy of the results obtained, a comparison is made with Misra *et al*. (2012) which shown a good agreement.

Table 6. 1: The Skin friction coefficient, -u' (0) at the wall, for various of *t, M, H, Ec, Pr, Kc, Gr, k, F , Gc* when *m* = 1 *and* λ=1.

t	M	H	E_c	P_r	G_r	G_c	S_c	k_c	k	F	$-u'(0)$
0.2	1.0	1.0	1.0	1.0	1.0	1.0	1.0	1.0	1.0	1.0	1.5561
0.4	1.0	1.0	1.0	1.0	1.0	1.0	1.0	1.0	1.0	1.0	0.5533
0.2	1.5	1.0	1.0	1.0	1.0	1.0	1.0	1.0	1.0	1.0	1.5511
0.2	2.0	1.0	1.0	1.0	1.0	1.0	1.0	1.0	1.0	1.0	1.5458
0.2	1.0	0.2	1.0	1.0	1.0	1.0	1.0	1.0	1.0	1.0	1.3038
0.2	1.0	0.4	1.0	1.0	1.0	1.0	1.0	1.0	1.0	1.0	1.3669
0.2	1.0	1.0	1.5	1.0	1.0	1.0	1.0	1.0	1.0	1.0	1.5458
0.2	1.0	1.0	2.0	1.0	1.0	1.0	1.0	1.0	1.0	1.0	1.5354
0.2	1.0	1.0	1.0	0.71	1.0	1.0	1.0	1.0	1.0	1.0	1.6276
0.2	1.0	1.0	1.0	1.0	1.0	1.0	1.0	1.0	1.0	1.0	1.5561
0.2	1.0	1.0	1.0	1.0	0.5	1.0	1.0	1.0	1.0	1.0	2.0188
0.2	1.0	1.0	1.0	1.0	1.5	1.0	1.0	1.0	1.0	1.0	1.0934

0.2	1.0	1.0	1.0	1.0	1.0	0.5	1.0	1.0	1.0	1.0	1.8715
0.2	1.0	1.0	1.0	1.0	1.0	1.5	1.0	1.0	1.0	1.0	1.2408
0.2	1.0	1.0	1.0	1.0	1.0	1.0	2.0	1.0	1.0	1.0	1.8174
0.2	1.0	1.0	1.0	1.0	1.0	1.0	2.5	1.0	1.0	1.0	1.9227
0.2	1.0	1.0	1.0	1.0	1.0	1.0	1.0	0.1	1.0	1.0	1.2723
0.2	1.0	1.0	1.0	1.0	1.0	1.0	1.0	0.2	1.0	1.0	1.3038
0.2	1.0	1.0	1.0	1.0	1.0	1.0	1.0	1.0	0.2	1.0	1.5147
0.2	1.0	1.0	1.0	1.0	1.0	1.0	1.0	1.0	0.4	1.0	1.5406
0.2	1.0	1.0	1.0	1.0	1.0	1.0	1.0	1.0	0.2	0.2	1.3038
0.2	1.0	1.0	1.0	1.0	1.0	1.0	1.0	1.0	0.4	0.4	1.3669

Table 6. 2: Sherwood number, -∅' (0) at the wall, for various values of *t, Sc and Kc.*

t	S_C	K_c	$-\emptyset'(0)$
0.2	0.5	0.5	0.3345
0.4	0.5	0.5	0.1183
0.2	0.24	0.5	0.2318
0.2	0.62	0.5	0.3725
0.2	0.5	0.4	0.3122
0.2	0.5	0.6	0.3568

Table 6.3: The Local Nusselt number, -θ' (0) at the wall, for various of *t, M, H, Ec, Pr, Kc, Gr, k, F, Gc* when , *m = 1* and λ = 1.

t	M	H	E_c	P_r	G_r	G_c	S_c	k_c	k	F	-θ' (0)
0.2	1.0	1.0	1.0	1.0	1.0	1.0	1.0	1.0	1.0	1.0	0.9254
0.4	1.0	1.0	1.0	1.0	1.0	1.0	1.0	1.0	1.0	1.0	0.3103
0.2	1.5	1.0	1.0	1.0	1.0	1.0	1.0	1.0	1.0	1.0	0.9233
0.2	2.0	1.0	1.0	1.0	1.0	1.0	1.0	1.0	1.0	1.0	0.9150
0.2	1.0	0.2	1.0	1.0	1.0	1.0	1.0	1.0	1.0	1.0	0.6731
0.2	1.0	0.4	1.0	1.0	1.0	1.0	1.0	1.0	1.0	1.0	0.7362
0.2	1.0	1.0	1.5	1.0	1.0	1.0	1.0	1.0	1.0	1.0	0.9212
0.2	1.0	1.0	2.0	1.0	1.0	1.0	1.0	1.0	1.0	1.0	0.9047
0.2	1.0	1.0	1.0	0.71	1.0	1.0	1.0	1.0	1.0	1.0	0.9254
0.2	1.0	1.0	1.0	1.0	1.0	1.0	1.0	1.0	1.0	1.0	1.0004
0.2	1.0	1.0	1.0	1.0	0.5	1.0	1.0	1.0	1.0	1.0	0.7362
0.2	1.0	1.0	1.0	1.0	1.5	1.0	1.0	1.0	1.0	1.0	0.6731

0.2	1.0	1.0	1.0	1.0	1.0	0.5	1.0	1.0	1.0	1.0	0.9308
0.2	1.0	1.0	1.0	1.0	1.0	1.5	1.0	1.0	1.0	1.0	0.9284
0.2	1.0	1.0	1.0	1.0	1.0	1.0	2.0	1.0	1.0	1.0	0.6342
0.2	1.0	1.0	1.0	1.0	1.0	1.0	2.5	1.0	1.0	1.0	0.8421
0.2	1.0	1.0	1.0	1.0	1.0	1.0	1.0	0.1	1.0	1.0	0.8463
0.2	1.0	1.0	1.0	1.0	1.0	1.0	1.0	0.2	1.0	1.0	0.9120
0.2	1.0	1.0	1.0	1.0	1.0	1.0	1.0	1.0	0.2	1.0	0.5924
0.2	1.0	1.0	1.0	1.0	1.0	1.0	1.0	1.0	0.4	1.0	0.7801
0.2	1.0	1.0	1.0	1.0	1.0	1.0	1.0	1.0	0.2	0.2	0.8332
0.2	1.0	1.0	1.0	1.0	1.0	1.0	1.0	1.0	0.4	0.4	0.9036

Table 6. 4:Comparison of wall temperature gradient, -θ' (0) for different values of *Pr* when *M=0* and *Ec=0.*

Pr	Misra *et al.* (2012)	Present study
0.71	0.2754	0.2746
1.0	0.2811	0.2803
2.0	0.3173	0.3171
3.0	0.3492	0.3490

6.6 Conclusion

A hydromagnetic unsteady boundary layer flow past an exponentially stretching surface in a chemically reactive porous medium has been investigated. The non-linear partial differential equations have been modeled and transformed to dimensionless differential equations using the dimensionless variables. The Laplace transform techniques are employed to solve the resulting dimensionless differential equations directly and results illustrated graphically. From the results obtained, the following conclusions can be drawn:

1. The thermal boundary layer thickness diminishes with time, magnetic parameter and Eckert number but increases with the Prandtl number, radiation parameter and the heat absorption parameter.
2. The concentration boundary layer thickness decreases along with time whilst increasing with the Schmidt number and the rate of chemical reaction in the fluid. However, at the twist of the flow, the Schmidt number causes a reduction in the species concentration in the fluid.
3. The velocity decreases with increasing values of the thermal Grashof number, the mass Grashof number and the magnetic parameter.

CHAPTER SEVEN

SUMMARY, CONCLUSIONS AND RECOMMENDATIONS

7.1 Summary

Unsteady MHD heat and mass transfer through porous media has been investigated. There are several heat and mass transfer problems already tackled in the literature. However, there are many areas in which research is continuing especially with respect to unsteady flow conditions as it is the most common flow situation in many industrial and manufacturing processes. The aim of the study was to investigate theoretically some nonlinear problems arising from unsteady boundary layer flow in porous media. The specific objectives of the study were to develop a:

- non-linear mathematical model for unsteady boundary layer flow past an exponentially accelerated vertical plate in the presence of heat source and transverse magnetic field embedded in a porous medium.
- non-linear mathematical model for unsteady hydromagnetic convective heat and mass transfer past an impulsively started infinite vertical surface with Newtonian heating in porous medium.
- non-linear mathematical model for unsteady hydromagnetic boundary layer flow over an exponentially stretching flat surface in a porous chemically reactive medium.

The non-linear partial differential equations had been modelled and transformed to dimensionless differential equations using the dimensionless variables. The Laplace transform techniques were employed to solve the resulting dimensionless differential equations directly and results illustrated graphically using MATLAB.

7.2 Conclusions

Base on the results obtained, the following conclusions can be drawn:

- A theoretical framework has been developed and used to predict the influence of various controlling parameters on the velocity, thermal and concentration boundary layers.
- The magnetic field parameter is effective in reducing the flow as it introduces an induced force known as the Lorenz force which tends to attract charged particles.
- For an exponentially stretching surface, the magnetic field parameter leads to decreasing thermal boundary layer thickness whilst the effect of increasing the radiation parameter leads to increasing thermal boundary layer thickness.
- Although, low Prandtl numbers give greater thermal boundary layer thickness, the presence of the magnetic field delay the convection motion.

Hence the thermal boundary layer thickness is greater for large Prandtl numbers such as water (Pr = 7.0) as compared to air (Pr = 0.71) and electrolyte solution (Pr = 1.0) but decreases with time.

- Concentration is high for large values of Schmidt numbers such as electrolyte solution (Sc = 0.67) compared to water (Sc = 0.62) and air (Sc = 0.24) but diminished faster for electrolyte solution of high Schmidt number with time. This relates well with physical situation because Schmidt number physically relates to the relative thickness of hydrodynamic layer and mass-transfer boundary layer.

7.4 Contribution to Knowledge and Recommendations

The study made the following novel contributions:

- Water, air and electrolytes cool objects differently. Hence a choice of fluid will determine the level of cooling to achieve.
- Magnetic field strengths can be used to influence the kinematics of flow.
- Heat transfer in porous media can be controlled with system parameters to achieve a desired product.

Future research can be considered in the following areas:

- Unsteady boundary layer flow interaction with heat and mass transfer in a circular conduits.

- Chemically reactive unsteady flow in a nuclear reactor
- Unsteady MHD boundary layer flow on curved surfaces as is encountered in aircraft wing design and other industrial machinery.

The research is also recommended for

- practical applications in unsteady processes in the areas such as mechanical, electrical, automobile, mining, manufacturing, chemical engineering etc since most of these industrial processes are time dependent.
- information on the nature of unsteady boundary layer developed on heated porous plate in the presence of chemical contaminants.
- engineering systems or devices that require magnetic systems.
- Serve as reference material for future works in the areas of nuclear studies, manufacturing, mining, petro-chemical, aerospace and automotive sectors.
- More importantly, the exact solutions obtained in the study will serve as accuracy standards for approximate methods.

REFERENCES

Adelman M. A. (1991). User cost in oil production, Resources and Energy, 13(3), 217-240.

Ali M. (2007). The effect of variable viscosity on mixed convection heat transfer along a vertical moving surface, Int. J. of thermal sciences, vol.45, 60-69.

Ali M., Abdul -Alim M.D. and Alam M. S. (2014). Heat transfer boundary layer flow past an inclined stretching sheet in the presence of magnetic field, Int. J. of Advancements in Reseach & Technology, vol 3 (5), 34-40.

Amhalhel G. A. and Furmanski P. (1997). Problems of Modeling Flow and heat transfer in porous media, Institute of Heat Engineering Nr 85, 1-34.

Anderson J. D. (2009). Governing equations of fluid dynamics, Computational Fluid Dynamics, 3rd ed., Springer-Verlag Berlin Heidelbeg.

Arthur E. M., Ayando T. and Seini Y. I (2015). MHD convective boundary layer flow towards a vertical surface in a porous medium with radiation, chemical reaction and internal heat generation, Frontiers in Heat and Mass Transfer(FHMT),6,21,1-10.

Aziz A., Siddiqque J. I. and Aziz T., (2014). Steady boundary layer slip flow along with heat and Mass transfer over a flat porous plate embedded in a porous medium, PLos ONE (12): e1145444.http://doi.org/10.1371/journal. 0114544.

Bala P.A.R., Bhaskar N.R. and Suneetha S. (2012). Effects on MHD flow past an exponentially accelerated isothermal vertical plate embedded in porous medium in the presence of heat source and chemical reaction, Journal of Applied Fluid Mechanics, 5(3) 119-126.

Bhaskar B. S. and Chaudhary S. K. (2016). Review of fluid flow and heat transfer through porous media heat exchangers, International Journal of New Innovations in Engineering and Technology, 6(2), 28-42.

Barik, R.N. (2016). Heat and mass transfer on unsteady MHD flow through an accelerated isothermal vertical plate embedded in porous medium in the presence of heat source and chemical reaction, European Journal of advances in Engineering and Technology 3(1):56-61.

Barman P. C., Das A. and Islam M. R. (2017). Heat transfer through porous media 4(2), 3642-3645.

Bhattacharyya K. (2012). Slip effects on boundary layer flow and mass transfer with chemical reaction over a permeable flat plate in a porous medium, Frontiers in heat and mass transfer, 3, 043006, Doi: 10.5098/ hmt.v3.4.

Chamkha, A.J., Raju, M.C., Sudhakar, R.T. and Varma S.V.K. (2016). Unsteady MHD free convection flow past an exponentially accelerated vertical plate with mass transfer, chemical and thermal radiation. Int. J. of Microscale and Nanoscale thermal 5(1), 57-75.

Chand K., Kumar R. and Sharma S. (2012). Hydromagnetic oscillatory flow through a porous medium bounded by two vertical porous plates with heat source and soret effect, Advances in Applied Science Research, 3(4), 2169-2178.

Chaudhary, R. C. and Jain, P. (2006). Unsteady free convection boundary layer flow past an impulsively started vertical surface with Newtonian heating, Rom. Joun. Phys., vol.51, Nos. 9-10, pp.911-925

Chen C. H. (1998) Laminar mixed convection adjacent to vertical, continuously stretching sheets. J. of Heat and Mass transfer, 33, pp.471-476

Chiam T. C. (1998) Heat transfer in a fluid with variable thermal conductivity over a linearly stretching sheet. Acta Mechanica 129, 63-72.

Chiem K. S. and Zhao Y. (2004), Numerical study of steady/unsteady flow and heat transfer in porous media, International Journal of Heat and Fluid Flow, 25(6), 1015-1033.

Chin E. K., Naza R., Arifin N. and Pop I. (2007). Effect of variable viscosity on mixed convection boundary layer flow over a vertical surface embedded in a porous medium, Int. communication in heat and mass transfer, vol.34, 464-473.

Crane L. J. (1970) Flow past a stretching plate. Journal of Applied Mathematics and Physics (ZAMP) 21:645-647, doi: 10.1007/BF01587695.

Dandpat, B. S. and Chakraborthy, S. (2010) Effects of variable fluid properties on unsteady thin film flow over a non-linear stretching sheet. Int. J. of Heat and Mass transfer, 53, pp.5757-5763.

Darby M. R. (1982), The price of oil and world inflation and recession, The American Economic Review, 72(4), 738-751.

Das S., Mandal C. and Jana R. N (2012), Radiation effects on unsteady free convection flow past a vertical plate with Newtonian heating, Int. J. of Computer Applications, vol. 41-No.13, p.36-41.

Etwire, C. J., Seini, Y. I., and Azure D. A. (2015). MHD Thermal Boundary Layer Flow over a Flat Plate with Internal Heat Generation, Viscous Dissipation and Convective Surface Boundary Conditions. International Journal of Emerging Technology and Advanced Engineering 5(5), 335-342 .

Gad-el- Hak M. (1996) Modern developments in flow control, Applied Mechanics Reviews, vol. 49, 365-379.

Gireesha B.J, Mahanthesh B., Manjunatha P. T. and Gorla R. S. R. (2015) Numerical solution for hydromagnetic boundary layer flow and heat transfer past a stretching surface embedded in non-Darcy porous medium, Journal of the Nigerian Mathematical Society, 34, 267-285.

Gupta, A.S, Pop, I. and Soundalgekar, V.G. (1979). Free convection flow past a linearly accelerated vertical plate on the presence of viscous dissipation heat. Rev. Roum. sci. Techn. Mec Apl. 24, 561-568.

Hassanien I. A. (1989), Oscillatory hydromagnetic flow through a porous medium in the presence of free convection and mass transfer flow, Astrophysics and Space Science, Kluwer Academic publishers, 151, 73-80.

Hsiao K. L. (2011) MHD stagnation point visco-elastic fluid flow and heat transfer on a thermal forming stretching sheet with viscous dissipation, Canadian Journal of Chemical Engineering 89, 1228-1235.

Hussanan, A., Salleh, M.Z., Khan, I. and Tahar R.M (2014). Unsteady boundary layer flow and heat transfer of a Casson fluid past an oscillating vertical plate with Newtonian heating. Plos One,9(10),e108763.

Hussanan, A., Salleh, M.Z., Khan, I. and Tahar R.M (2016). Heat and mass transfer in a micropolar fluid with Newtonian heating: an exact analysis. Neural Computing and Applications. DOI10.1007/s00521-016-2516-0.

Intaglietta M. (2017), Heat and Diffusion equation in space and time, http://www.isn.ucsd.edu/courses/beng221/lectures.

Ishak A., Nazar R. and Pop I. (2008) Hydromagnetic flow and heat transfer adjacent to a stretching vertical sheet, Journal of Heat and Mass, 44, pp.921-927.

Kafousias, N.G and Raptis, A.A. (1981). Mass transfer effects subject to variable suction or injection. Rev. Roum. Sci. Techn. Mec. Apl. 26, 11-22.

Kamel M. H. (2000) Thermal-diffusion effect on rotating hydromagnetic flow in porous media, Mechanics and Mechanical Engineering International Journal, 4(2), 150-164.

Kan S. U., Ali N. and Abbas Z. (2015) Hydromagnetic flow and heat transfer over a porous oscillating stretching surface in a viscoelastic fluid with porous medium, PLoS ONE 10(12), 1-18.

Kathyayani G., Sambasivudu P. and Badu D. M. P. (2016) Effects of heat and mass transfer on unsteady MHD flow of fluid in porous media, International Journal of Science and Research, 5(9), 112-118.

Magyari E. and Keller B. (1999), Heat and mass transfer in the boundary layers on an exponentially stretching continuous surface, J. Phys. D: Appl. Phys. 32, 577-585.

Martynenko O. G., Berezovsky A. A. and Sakovishin, Y. A. (1984) Laminar free convection from a vertical plate. Int. J. of Heat and Mass Transfer, vol. 27, pp. 869–881.

Marthie R., Nakamura H. and Markides (2012), Augmentation in unsteady conjugate heat transfer part-II , International Journal of Heat and Mass transfer, vol 56, 819-833.

Mathelin L., Turki M. A., Pastur L. and Kandil H. A (2010) Closed-loop fluid flow control using a low dimensional model, Mathematical and Computer modelling 52(2010), 1161-1168.

Megahed A. A., Afify A. A. and Mosbah A. (2011) Similarly solution for Steady MHD Falkner – Skan heat and mass transfer flow over a wedge in porous media considering Thermal-diffusion and Diffusion-thermo effects with variable viscosity and thermal conductivity, Int. J. of Applied Math. and Phys. 3(1), 119-129.

Meunier M. (2009) Stimulation and optimization of flow control strategies for Novel High-lift configurations, AIAA Journal, 47(5), 1-8, Doi:10.2514/1.38245.

Misra M., Ahmad N. and Siddiqui Z. U. (2012) ,Unsteady boundary layer flow past a stretching plate and heat transfer with variable thermal conductivity, World Journal of Mechanics, Scientific Research, vol.2, 35-41.

Mishra S. R., Mohanty B. and Pattanayak H. B. (2015), Numerical investigation on unsteady heat and mass transfer effect of micropolar fluid over a stretching sheet through porous media, Alexandria Engineering Journal, 54, 223-232.

Nadeem S., Haq R., Akbar N.S. and Khan N. H. (2013) MHD three-dimensional Casson fluid flow past a porous linearly stretching sheet, Alexendra Engineering Journal 52, 577-582.

Narahari, M. and Nayan, M. (2011), Free convection flow past an impulsively started infinite vertical plate with Newtonian heating in the presence of thermal radiation and mass diffusion, Turkish J. of Eng. And Env. Sci., 35.

Norzieha M., Farhad A., Sharidan S., Khan I. and Samiulhaq (2012), Hydromagnetic rotating flow in a porous medium with slip condition and hall current, International Journal of Physical Sciences 7(10), 1540-1548.

Oruc V. (2017) Strategies for the applications of flow control downstream of a bluff body, Flow Measurement and Instrumentation, volume 53, part B, 215-220.

Ramakrishnan K. and Shailendhra K. (2011). Hydromagnetic flow through uniform channel bounded by porous media, Appl. Math. Mech. –Engl. Ed.,32(7), 837-846.

Rout B. R. and Pattanayak (2013). Chemical reaction and radiation effect on MHD flow past an exponentially accelerated vertical plate in presence of heat source with variable temperatre embedded in a porous medium, Mathematical theoy and Modeling, 3(8), 18-26.

Saad, T. (2009) Derivative of the continuity equation in Cartesian coordinates: http://pleasemakeanote.blogspot.com/2009/02/derivation-continuity-equation-in-html.

Sahoo A. C., Biswal T. (2015) MHD Visco-elastic boundary layer flow past a stretching plate with heat transfer. IJETMAS vol. 3(9), 11-18.

Sakiadis B. C. (1961) Boundary layer behaviour on continuous solid surfaces, AIChJ, 26-28.

Samiulhaq, Constantin F., Ilyas k., Fard A. and Sharidan S., (2012) Radiation and Porosity Effects on the Magnetohydrodynamic Flow Past an Oscillating Vertical Plate with Uniform Heat Flux, Z. Naturforsch. 67a, 572 – 580 (2012) / DOI: 10.5560/ZNA.2012-0070.

Seini Y. I. (2013). Flow over unsteady stretching surface with chemical reaction and non-uniform heat source. J. Eng. Manuf. Technol. 1 (2013) 24-35

Seini Y. I. and Makinde O. D. (2013). MHD Boundary Layer Flow due to Exponential Stretching Surface with Radiation and Chemical Reaction, Mathematical Problems in Engineering Volume 2013, Article ID 163614, 1-7 pages.

Sharidan S., Abid H., Khan I. and Salleh M.Z (2014), Slip effects on unsteady free convective heat and mass transfer flow with Newtonian heating, Thermal science 142-143.

Siegel, R. (1958), Transient free convection from a vertical flat plate, Transactions of the American Societies of Mechanical Engineers, vol.80, pp. 347–359 .

Sipp D. and Schmid P. (2013) Closed-loop control of fluid flow, a review of linear approaches and tools for the stabilization of transitional flows, Onera Journal, AerospaceLab, issue 6, 1-11.

Uddin M. J., Ali M. D., Uddin M. N. and Zahed N. M. (2015) Similarly solutions of unsteady convective boundary layer flow along isothermal vertical plate with porous medium, Open Journal of Fluid Dynamics, vol. pp. 391-406.

APPENDIX I

MODELS' DERIVATIONS

DERIVATION OF CONTINUITY EQUATION

The continuity equation is an expression of a fundamental mass conservation. All fluid particles that flow into any fluid region must flow out. Consider a cubical control volume inside a fluid in figure A1.1. All fluid that is accumulated inside the control volume + all fluid that is flowing into the control volume must be equal to the amount of fluid flowing out of the control volume. Thus Accumulation + Flow In = Flow Out

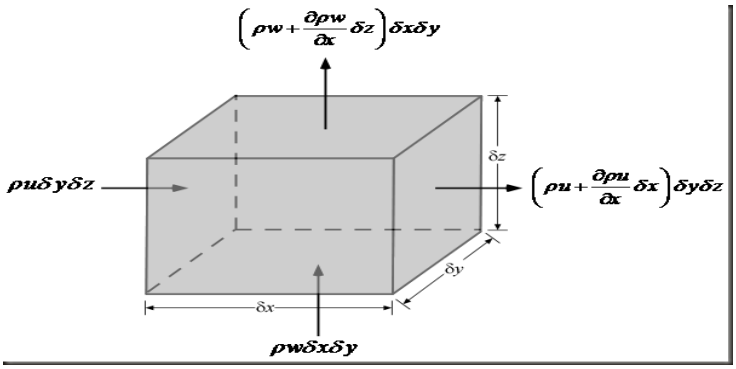

Figure A1.1 Mass flux through each of the six faces of a control volume of fluid (Saad, 2009)

Introducing '*' on the variables in figure A1.1 for uniqueness of variables and parameters already used in the study. The mass of the control volume at some time t^* is

$$M_{t^*} = \rho \delta x^* \delta y^* \delta z^* \quad \text{(A1.1)}$$

The time rate of change of mass in the control volume is

$$\frac{\partial \rho}{\partial t^*} \delta x^* \delta y^* \delta z^* \quad \text{(A1.2)}$$

Now we can compute the net flow through the control volume faces. Starting with the x direction, the net flow is

$$\left(\rho u^* + \frac{\partial \rho u^*}{\partial x^*} \delta x^*\right) \delta y^* \delta z^* - \rho u^* \delta y^* \delta z^* = \frac{\partial \rho u^*}{\partial x^*} \delta x^* \delta y^* \delta z^* \quad \text{(A1.3)}$$

Similarly, the net flow through the y and z faces are respectively

$$\frac{\partial \rho v^*}{\partial y^*} \delta x^* \delta y^* \delta z^* \quad \text{(A1.4)}$$

$$\frac{\partial \rho w^*}{\partial z^*} \delta x^* \delta y^* \delta z^* \quad \text{(A1.5)}$$

Mass conservation requires that the net flow through the control volume is zero. By adding up the resulting net flow and dividing by the volume of the fluid element ($\delta x^* \delta y^* \delta z^*$), the continuity equation is obtained in Cartesian coordinates as

$$\frac{\partial \rho}{\partial t^*} + \frac{\partial \rho u^*}{\partial x^*} + \frac{\partial \rho v^*}{\partial y^*} + \frac{\partial \rho w^*}{\partial z^*} = 0 \quad \text{(A1.6)}$$

DERIVATION OF MOMENTUM EQUATION

The derivation of the momentum equation relies heavily on the Newton's 2nd Law of motion. Consider a moving fluid element in figure A1.2 below

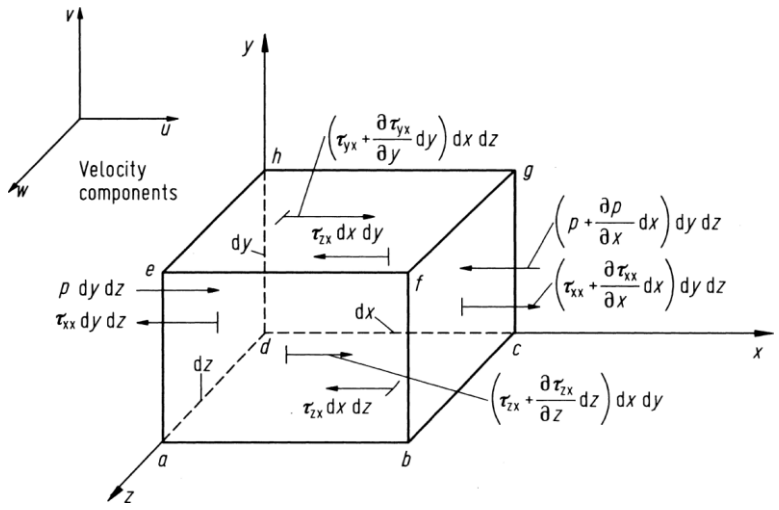

Figure A1. 2 Infinitesimally small moving fluid element showing only the forces in the x direction (Anderson, 2009)

Introducing '*' on the variables in figure A1.2 for uniqueness of variables and parameters already used in the study. The Newton's 2nd law, when applied to the moving fluid element says that the net force on the fluid element equals its mass times the acceleration of the element. This is a vector relation, and hence can be split into three scalar relations along the x^*, y^*, and z^*-axes.

Consider the x^* −component of Newton's 2nd law

$$F_{x^*} = ma_{x^*} \qquad \text{(A1.7)}$$

This means that a moving fluid experiences forces whose magnitude depends on the acceleration in its direction of motion. These forces are made up of body forces and surface forces.

Denoting the body force per unit mass acting on the fluid by g and its x^*-component by g_{x^*}, the volume of the fluid element is $(dx^*dy^*dz^*)$ hence

$$\left\{\begin{matrix} Body\ force\ on\ the\ fluid\ element \\ acting\ in\ the\ x^*-direction \end{matrix}\right\} = \rho g_{x^*}(dx^*dy^*dz^*) \qquad \text{(A1.8)}$$

On the face $abcd$, the only force due to shear stress $\tau_{y^*x^*}dx^*dz^*$ acts in the negative x^*direction whilst the shear force $\left[\tau_{y^*x^*} + \left(\partial\tau_{y^*x^*}/\partial y^*\right)dy^*\right]dx^*dz^*$ acts in the positive x^*-direction on the face $efgh$ which is at a distance of dy above the face $abcd$. Similarly, on the face $dcgh$, $\tau_{z^*x^*}dx^*dy^*$ acts in the negative x^*- direction whereas on the face $abfe$, $[\tau_{z^*x^*} + (\partial\tau_{z^*x^*}/\partial z^*)dz^*]dx^*dy^*$ acts in the positive x^*-direction. On the face $adhe$, which is perpendicular to the x^*-aixs, the forces in the x^*-direction are the pressure force pdx^*dz^* which acts in the direction into the fluid element and $\tau_{x^*x^*}dx^*dy^*$ which is in the negative x^*-direction. In contrast, on the face $bcgf$, the pressure force $[p + (\partial p/\partial x^*)dx^*]dy^*dz^*$ presses inward on the fluid element in the negative x^*-direction and there is a suction due to the viscous normal stress which tries to pull the element to the right in the positive x^*-direction with a force equal to $[\tau_{x^*x^*} + (\partial\tau_{x^*x^*}/\partial x^*)dx^*]dy^*dz^*$. Hence for the moving fluid element

$$\begin{Bmatrix} Net\ surface\ force \\ in\ the\ x^* - \text{direction} \end{Bmatrix} = \left[p - \left(p + \frac{\partial p}{\partial x^*}\partial x^*\right)\right] dy^* dz^* + \left[\left(\tau_{x^*x^*} + \frac{\partial \tau_{x^*x^*}}{\partial x^*}\partial x^*\right) - \tau_{x^*x^*}\right] dy^* dz^* + \left[\left(\tau_{y^*x^*} + \frac{\partial \tau_{y^*x^*}}{\partial y^*}\partial y^*\right) - \tau_{y^*x^*}\right] dx^* dz^* + \left[\left(\tau_{z^*x^*} + \frac{\partial \tau_{z^*x^*}}{\partial z^*}\partial z^*\right) - \tau_{z^*x^*}\right] dx^* dy^* \quad \text{(A1.9)}$$

Where $\tau_{y^*x^*}$ and $\tau_{z^*x^*}$ are the shear stress components. $\tau_{x^*x^*}$ is the normal stress in the $x^* -$ direction.

The total force in the x^* −direction (F_{x^*}) is the sum of (A1.8) and (A1.9). Simplifying terms give

$$F_x = \left(-\frac{\partial p}{\partial x^*} + \frac{\partial \tau_{x^*x^*}}{\partial x^*} + \frac{\partial \tau_{y^*x^*}}{\partial y^*} + \frac{\partial \tau_{z^*x^*}}{\partial z^*}\right) dx^* dy^* dz^* + \rho g_{x^*}(dx^* dy^* dz^*) \quad \text{(A1.10)}$$

Now considering the RHS of (A1.7), the mass of the fluid element is fixed and is given by

$$m = \rho dx^* dy^* dz^* \quad \text{(A1.11)}$$

Also, the acceleration of the fluid element is the time rate of change of its velocity and is given by the substantial derivative

$$a_{x^*} = \frac{Du^*}{Dt^*} \quad \text{(A1.12)}$$

Substituting all terms into (A1.7) result in

$$\rho \frac{Du^*}{Dt^*} = -\frac{\partial p}{\partial x^*} + \frac{\partial \tau_{x^*x^*}}{\partial x^*} + \frac{\partial \tau_{y^*x^*}}{\partial y^*} + \frac{\partial \tau_{z^*x^*}}{\partial z^*} + \rho g_{x^*} \quad \text{(A1.13)}$$

Equation (A1.13) is the x^*-component form of the momentum equation for a viscous flow. Similarly, the y^* and z^* components can be obtained respectively as

$$\rho \frac{Dv^*}{Dt^*} = -\frac{\partial p}{\partial y^*} + \frac{\partial \tau_{x^*y^*}}{\partial x^*} + \frac{\partial \tau_{y^*y^*}}{\partial y^*} + \frac{\partial \tau_{z^*y^*}}{\partial z^*} + \rho g_{y^*} \qquad \text{(A1.14)}$$

$$\rho \frac{Dw^*}{Dt^*} = -\frac{\partial p}{\partial z^*} + \frac{\partial \tau_{x^*z^*}}{\partial x^*} + \frac{\partial \tau_{y^*z^*}}{\partial y^*} + \frac{\partial \tau_{z^*z^*}}{\partial z^*} + \rho g_{z^*} \qquad \text{(A1.15)}$$

where $\tau_{x^*x^*}, \tau_{y^*x^*}, \tau_{z^*x^*}, \tau_{x^*y^*}, \tau_{y^*y^*}, \tau_{z^*y^*}, \tau_{x^*z^*}, \tau_{y^*z^*}, \tau_{z^*z^*}$ are shear stress components.

Since the fluid element is moving with the flow, equations (A1.13) - (A1.15) are in non-conservation form. They are scalar equations, and are called the *Navier-Stokes equations* in honour of the two men, the Frenchman M. Navier and the Englishman G. Stokes, who independently obtained the equations in the first half of the nineteenth century (source en.Wikipedia.org).

The Navier-Stokes equations can be obtained in conservation form in terms of the substantial derivative as

$$\rho \frac{Du^*}{Dt^*} = \rho \frac{\partial u^*}{\partial t^*} + \rho U^*.\nabla u^* \qquad \text{(A1.16)}$$

Expanding the following derivative

$$\frac{\partial(\rho u^*)}{\partial t^*} = \rho \frac{\partial u^*}{\partial t^*} + u^* \frac{\partial \rho}{\partial t^*} \qquad \Rightarrow \rho \frac{\partial u^*}{\partial t^*} = \frac{\partial(\rho u^*)}{\partial t^*} - u^* \frac{\partial \rho}{\partial t^*} \qquad \text{(A1.17)}$$

The vector identity for the divergence of the product of scalar times a vector is

$$U^*.(\rho u^* U^*) = u^* \nabla.(\rho U^*) + (\rho U^*).\nabla u^*$$

$$\rho U^*.\nabla u^* = U^*.(\rho u^* U^*) - u^* \nabla.(\rho U^*) \quad \text{(A1.18)}$$

Substituting gives

$$\rho \frac{Du^*}{Dt^*} = \frac{\partial(\rho u^*)}{\partial t^*} - u^* \frac{\partial \rho}{\partial t^*} - u^* \nabla.(\rho U^*) + U^*.(\rho u^* U^*)$$

$$\rho \frac{Du^*}{Dt^*} = \frac{\partial(\rho u^*)}{\partial t^*} - u^* \left(\frac{\partial \rho}{\partial t^*} + \nabla.(\rho U^*) \right) + U^*.(\rho u^* U^*) \quad \text{(A1.19)}$$

The term $\frac{\partial \rho}{\partial t^*} + \nabla.(\rho U^*)$ is the continuity equation in (3.3), hence it is zero.

Thus, (A1.19) reduces to

$$\rho \frac{Du^*}{Dt^*} = \frac{\partial(\rho u^*)}{\partial t^*} + U^*.(\rho u^* U^*) \quad \text{(A1.20)}$$

This yield for the x* direction

$$\frac{\partial(\rho u^*)}{\partial t^*} + U^*.(\rho u^* U^*) = -\frac{\partial p}{\partial x^*} + \frac{\partial \tau_{x^* x^*}}{\partial x^*} + \frac{\partial \tau_{y^* x^*}}{\partial y^*} + \frac{\partial \tau_{z^* x^*}}{\partial z^*} + \rho g_{x^*} \quad \text{(A1.21)}$$

Similarly, for the y* and z* directions,

$$\frac{\partial(\rho v^*)}{\partial t^*} + U^*.(\rho v^* U^*) = -\frac{\partial p}{\partial y^*} + \frac{\partial \tau_{x^* y^*}}{\partial x^*} + \frac{\partial \tau_{y^* y^*}}{\partial y^*} + \frac{\partial \tau_{z^* y^*}}{\partial z^*} + \rho g_{y^*} \quad \text{(A1.22)}$$

$$\frac{\partial(\rho w^*)}{\partial t^*} + U^*.(\rho w^* U^*) = -\frac{\partial p}{\partial z^*} + \frac{\partial \tau_{x^* z^*}}{\partial x^*} + \frac{\partial \tau_{y^* z^*}}{\partial y^*} + \frac{\partial \tau_{z^* z^*}}{\partial z^*} + \rho g_{z^*} \quad \text{(A1.23)}$$

Equations (A1.21) – (A1.23) are the Navier-Stokes equations in conservation form. In the late seventeenth century, Sir Isaac Newton observed that the shear stress, τ, in a fluid was proportional to the time rate of strain, i.e. velocity gradients. Such fluids are called *Newtonian fluids*. In virtually all practical aerodynamics problems, the fluid can be assumed to be Newtonian. For such fluids, Stokes (1845) obtained:

$$\tau_{x^*x^*} = \lambda\nabla.U^* + 2\mu\frac{\partial u^*}{\partial x^*}; \qquad \tau_{y^*y^*} = \lambda\nabla.U^* + 2\mu\frac{\partial v^*}{\partial y^*}$$

$$\tau_{z^*z^*} = \lambda\nabla.U^* + 2\mu\frac{\partial w^*}{\partial z^*}; \qquad \tau_{x^*y^*} = \tau_{y^*x^*} = \mu\left(\frac{\partial v^*}{\partial x^*} + \frac{\partial u^*}{\partial y^*}\right)$$

$$\tau_{x^*z^*} = \tau_{z^*x^*} = \mu\left(\frac{\partial u^*}{\partial z^*} + \frac{\partial w^*}{\partial x^*}\right); \quad \tau_{y^*z^*} = \tau_{z^*y^*} = \mu\left(\frac{\partial w^*}{\partial y^*} + \frac{\partial v^*}{\partial z^*}\right) \qquad \text{(A1.24)}$$

Where $\lambda = -\frac{2}{3}\mu$ (A1.25)

The complete Navier- Stokes equations in conservation form is thus obtained as

$$\frac{\partial(\rho u^*)}{\partial t^*} + \frac{\partial(\rho u^{*2})}{\partial x^*} + \frac{\partial(\rho u^* v^*)}{\partial y^*} + \frac{\partial(\rho u^* w^*)}{\partial z^*} = -\frac{\partial p}{\partial x^*} + \frac{\partial}{\partial x^*}\left(\lambda\nabla.U^* + 2\mu\frac{\partial u^*}{\partial x^*}\right) + \frac{\partial}{\partial y^*}\left[\mu\left(\frac{\partial v^*}{\partial x^*} + \frac{\partial u^*}{\partial y^*}\right)\right] + \frac{\partial}{\partial z^*}\left[\mu\left(\frac{\partial u^*}{\partial z^*} + \frac{\partial w^*}{\partial x^*}\right)\right] + \rho g_{x^*}$$

(A1.26)

$$\frac{\partial(\rho v^*)}{\partial t^*} + \frac{\partial(\rho u^* v^*)}{\partial x^*} + \frac{\partial(\rho v^{*2})}{\partial y^*} + \frac{\partial(\rho v^* w^*)}{\partial z^*} = -\frac{\partial p}{\partial y^*} + \frac{\partial}{\partial x^*}\left[\mu\left(\frac{\partial v^*}{\partial x^*} + \frac{\partial u^*}{\partial y^*}\right)\right] + \frac{\partial}{\partial y^*}\left(\lambda\nabla.U^* + 2\mu\frac{\partial v^*}{\partial y^*}\right) + \frac{\partial}{\partial z^*}\left[\mu\left(\frac{\partial w^*}{\partial y^*} + \frac{\partial v^*}{\partial z^*}\right)\right] + \rho g_{y^*}$$

(A1.27)

$$\frac{\partial(\rho w^*)}{\partial t^*} + \frac{\partial(\rho u^* w^*)}{\partial x^*} + \frac{\partial(\rho v^* w^*)}{\partial y^*} + \frac{\partial(\rho w^{*2})}{\partial z^*} = -\frac{\partial p}{\partial z^*} + \frac{\partial}{\partial x^*}\left[\mu\left(\frac{\partial u^*}{\partial z^*} + \frac{\partial w^*}{\partial x^*}\right)\right] + \frac{\partial}{\partial y^*}\left[\mu\left(\frac{\partial w^*}{\partial y^*} + \frac{\partial v^*}{\partial z^*}\right)\right] + \frac{\partial}{\partial z^*}\left(\lambda\nabla.U^* + 2\mu\frac{\partial w^*}{\partial z^*}\right) + \rho g_{z^*} \qquad \text{(A1.28)}$$

In general, Navier- Stokes equation in conservation form is

$$\rho\frac{DU^*}{Dt^*} = -\nabla p + \rho g + \mu\nabla^2 U^* \qquad \text{(A1.29)}$$

DERIVATION OF ENERGY EQUATION

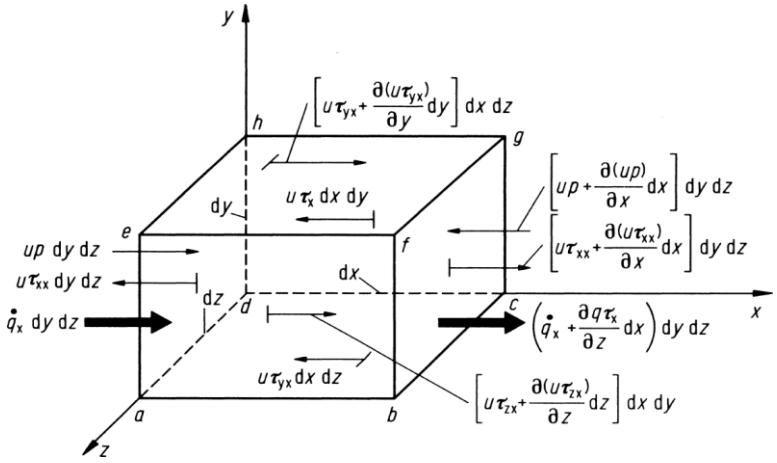

Figure A1. 3 Energy fluxes associated with infinitesimally small moving fluid element showing only fluxes in the x*- direction (Anderson, 2009).

The energy equation is derived from the first law of thermodynamics, which, when applied to moving fluid element in figure A1.3 becomes:

$$\left\{\begin{matrix}Rate\ of\ change\ of\\ energy\ inside\ the\\ fluid\ element\end{matrix}\right\}=\left\{\begin{matrix}Net\ flux\ of\\ heat\ into\\ the\ element\ (\end{matrix}\right\}+\left\{\begin{matrix}Rate\ of\ work\ done\ on\\ the\ element\ due\ to\ body\\ and\ surface\ forces\end{matrix}\right\}$$

Let A, B and C denote the respective terms above.

$$\Rightarrow \qquad A = B + C \tag{A1.30}$$

Introducing '*' on the variables in figure A1.3 for uniqueness of variables and parameters. Evaluate C, i.e. the rate of work done on the moving fluid element due to body and surface forces. The rate of work done by the body force acting on the fluid element is equal to the product of the force and the component of velocity in the direction of the force. Thus,

$$\rho g.U^*(dx^*dy^*dz^*) \qquad \text{(A1.31)}$$

To obtain the net rate of work done on the fluid element by the surface forces, the forces in the positive x^*- direction are considered to do positive work and the forces in the negative x^*- direction do negative work. Hence, comparing the pressure forces on face $adhe$ and $bcgf$, the net rate of work done by pressure in the x^*- direction is

$$\left[u^*p - \left(u^*p + \frac{\partial(u^*p)}{\partial x^*}\partial x^*\right)\right]dy^*dz^* = -\frac{\partial(u^*p)}{\partial x^*}dx^*dy^*dz^* \qquad \text{(A1.32)}$$

Similarly, the net rate of work done by the shear stresses in the x^*- direction on faces $abcd$ and $efgh$ is

$$\left[\left(u^*\tau_{y^*x^*} + \frac{\partial\left(u^*\tau_{y^*x^*}\right)}{\partial y^*}\partial y^*\right) - u^*\tau_{y^*x^*}\right]dx^*dz^* = \frac{\partial\left(u^*\tau_{y^*x^*}\right)}{\partial y^*}dx^*dy^*dz^*$$

(A1.33)

For all the surface forces in the x^*- direction, the net rate of work done on the moving fluid element is

$$\left[-\frac{\partial(u^*p)}{\partial x^*} + \frac{\partial(u^*\tau_{x^*x^*})}{\partial x^*} + \frac{\partial\left(u^*\tau_{y^*x^*}\right)}{\partial y^*} + \frac{\partial(u^*\tau_{z^*x^*})}{\partial z^*}\right]dx^*dy^*dz^* \qquad \text{(A1.34)}$$

Similar expressions can be obtained for surface forces in the y^* and z^*- directions. Hence the net rate of work done on the moving fluid element due to body and surface forces is given as

$$C = \{sum\ of\ the\ suface\ forces\} + \{sum\ of\ the\ body\ forces\}$$

$$= \left[-\left(\frac{\partial(u^* p)}{\partial x^*} + \frac{\partial(v^* p)}{\partial y^*} + \frac{\partial(w^* p)}{\partial z^*} \right) + \frac{\partial(u^* \tau_{x^* x^*})}{\partial x^*} + \frac{\partial\left(u^* \tau_{y^* x^*}\right)}{\partial y^*} + \frac{\partial(u^* \tau_{z^* x^*})}{\partial z^*} + \right.$$

$$\frac{\partial\left(v^* \tau_{x^* y^*}\right)}{\partial x^*} + \frac{\partial\left(v^* \tau_{y^* y^*}\right)}{\partial y^*} + \frac{\partial\left(v^* \tau_{z^* y^*}\right)}{\partial z^*} + \frac{\partial(w^* \tau_{x^* z^*})}{\partial x^*} + \frac{\partial\left(w^* \tau_{y^* z^*}\right)}{\partial y^*} +$$

$$\left. \frac{\partial(w^* \tau_{z^* z^*})}{\partial z^*} \right] dx^* dy^* dz^* + \rho g . U^* dx^* dy^* dz^* \qquad \text{(A1.35)}$$

In (A1.30), B is the net flux of heat into the element. This heat flux is due to two factors namely:

(i) the volumetric heating such as absorption or emission of radiation and

(ii) heat transfer across the surface due to temperature gradients, i.e. thermal conduction.

Defining $\dot{q}$ as the rate of volumetric heat addition per unit mass, noting that the mass of the moving fluid element is $\rho dx^* dy^* dz^*$ gives

$$\left\{ \begin{matrix} Volumetric\ heating \\ of\ the\ element \end{matrix} \right\} = \rho \dot{q} \rho dx^* dy^* dz^* \qquad \text{(A1.36)}$$

The heat transferred by thermal conduction into the moving fluid element across the face $adhe$ is $\dot{q}_{x^*} dy^* dz^*$. The heat transferred out of the element across face $bcgf$ is $[\dot{q}_{x^*} + (\partial \dot{q}_{x^*} / \partial x^*) dx^*] dy^* dz^*$. Therefore the net heat transferred in the x^*- direction into the fluid element by thermal conduction is

$$\left[\dot{q}_{x^*} - \left(\dot{q}_{x^*} + \frac{\partial(\dot{q}_{x^*})}{\partial x^*} \partial x^* \right) \right] dy^* dz^* = - \frac{\partial(\dot{q}_{x^*})}{\partial x^*} dx^* dy^* dz^* \qquad \text{(A1.37)}$$

Similar equations can be obtained for heat transfer in y^* and z^* directions across other faces. Hence

$$\left\{\begin{matrix} Heating\ of\ the \\ fluid\ element\ by \\ thermal\ conduction \end{matrix}\right\} = -\left(\frac{\partial \dot{q}_{x^*}}{\partial x^*} + \frac{\partial \dot{q}_{y^*}}{\partial y^*} + \frac{\partial \dot{q}_{z^*}}{\partial z^*}\right) dx^* dy^* dz^* \qquad \text{(A1.38)}$$

Thus,

$$B = \left[p\dot{q} - \left(\frac{\partial \dot{q}_{x^*}}{\partial x^*} + \frac{\partial \dot{q}_{y^*}}{\partial y^*} + \frac{\partial \dot{q}_{z^*}}{\partial z^*}\right)\right] dx^* dy^* dz^* \qquad \text{(A1.39)}$$

But heat transferred by thermal conduction is proportional to the local temperature gradient

$$\dot{q}_{x^*} = -K\frac{\partial T^*}{\partial x^*};\quad \dot{q}_{y^*} = -K\frac{\partial T^*}{\partial y^*};\quad \dot{q}_{z^*} = -K\frac{\partial T^*}{\partial z^*} \qquad \text{(A1.40)}$$

Thus,

$$B = \left[p\dot{q} + \frac{\partial}{\partial x^*}\left(K\frac{\partial T^*}{\partial x^*}\right) + \frac{\partial}{\partial y^*}\left(K\frac{\partial T^*}{\partial y^*}\right) + \frac{\partial}{\partial z^*}\left(K\frac{\partial T^*}{\partial z^*}\right)\right] dx^* dy^* dz^* \qquad \text{(A1.41).}$$

The time rate of change of energy of the fluid element was denoted by A. The total energy of the moving fluid per unit mass is the sum of its internal energy per unit mass, e^*, and its kinetic energy per unit mass, $V^{*2}/2$. The total energy is $(e^* + V^{*2}/2)$ and the mass of the fluid is $\rho dx^* dy^* dz^*$. The time rate of change of energy per unit mass is given by

$$A = \rho\frac{D}{Dt^*}\left(e^* + \frac{V^{*2}}{2}\right) dx^* dy^* dz^* \qquad \text{(A1.42)}$$

Hence the final form of the energy equation is obtained to be

$$\rho\frac{D}{Dt^*}\left(e^* + \frac{V^{*2}}{2}\right) = \rho\dot{q} + \frac{\partial}{\partial x^*}\left(K\frac{\partial T^*}{\partial x^*}\right) + \frac{\partial}{\partial y^*}\left(K\frac{\partial T^*}{\partial y^*}\right) + \frac{\partial}{\partial z^*}\left(K\frac{\partial T^*}{\partial z^*}\right) - \frac{\partial(u^*p)}{\partial x^*} -$$

$$\frac{\partial(v^*p)}{\partial y^*} - \frac{\partial(w^*p)}{\partial z^*} + \frac{\partial(u^*\tau_{x^*x^*})}{\partial x^*} + \frac{\partial\left(u^*\tau_{y^*x^*}\right)}{\partial y^*} + \frac{\partial(u^*\tau_{z^*x^*})}{\partial z^*} + \frac{\partial\left(v^*\tau_{x^*y^*}\right)}{\partial x^*} + \frac{\partial\left(v^*\tau_{y^*y^*}\right)}{\partial y^*} +$$

$$\frac{\partial\left(v^*\tau_{z^*y^*}\right)}{\partial z^*} + \frac{\partial(w^*\tau_{x^*z^*})}{\partial x^*} + \frac{\partial\left(w^*\tau_{y^*z^*}\right)}{\partial y^*} + \frac{\partial(w^*\tau_{z^*z^*})}{\partial z^*} + \rho g_{x^*}.U^* \qquad \text{(A1.43)}$$

This is the non-conservation form of the energy equation in terms of the total energy. In terms of internal energy, e^*, the energy equation is obtained as:

$$\rho\frac{De^*}{Dt^*} = \rho\dot{q} + \frac{\partial}{\partial x^*}\left(K\frac{\partial T^*}{\partial x^*}\right) + \frac{\partial}{\partial y^*}\left(K\frac{\partial T^*}{\partial y^*}\right) + \frac{\partial}{\partial z^*}\left(K\frac{\partial T^*}{\partial z^*}\right) - p\left(\frac{\partial u^*}{\partial x^*} + \frac{\partial v^*}{\partial y^*} + \frac{\partial w^*}{\partial z^*}\right) +$$

$$\tau_{x^*x^*}\frac{\partial u^*}{\partial x^*} + \tau_{y^*x^*}\frac{\partial u^*}{\partial y^*} + \tau_{z^*x^*}\frac{\partial u^*}{\partial z^*} + \tau_{x^*y^*}\frac{\partial v^*}{\partial x^*} + \tau_{y^*y^*}\frac{\partial v^*}{\partial y^*} + \tau_{z^*y^*}\frac{\partial v^*}{\partial z^*} +$$

$$\tau_{x^*z^*}\frac{\partial w^*}{\partial x^*} + \tau_{y^*z^*}\frac{\partial w^*}{\partial y^*} + \tau_{z^*z^*}\frac{\partial w^*}{\partial z^*} \qquad \text{(A1.44)}$$

Equation (A1.44) can be expressed totally in terms of the flow field variables by replacing the viscous stress terms $\tau_{x^*y^*}, \tau_{x^*z^*,}$ etc. with their equivalent expressions say $\tau_{x^*y^*} = \tau_{y^*x^*,}\ \tau_{x^*z^*} = \tau_{z^*x^*,}\tau_{y^*z^*} = \tau_{z^*y^*}$ resulting in

$$\rho\frac{De^*}{Dt^*} = \rho\dot{q} + \frac{\partial}{\partial x^*}\left(K\frac{\partial T^*}{\partial x^*}\right) + \frac{\partial}{\partial y^*}\left(K\frac{\partial T^*}{\partial y^*}\right) + \frac{\partial}{\partial z^*}\left(K\frac{\partial T^*}{\partial z^*}\right) - p\left(\frac{\partial u^*}{\partial x^*} + \frac{\partial v^*}{\partial y^*} + \frac{\partial w^*}{\partial z^*}\right) +$$

$$\tau_{x^*x^*}\frac{\partial u^*}{\partial x^*} + \tau_{y^*y^*}\frac{\partial v^*}{\partial y^*} + \tau_{z^*z^*}\frac{\partial w^*}{\partial z^*} + \tau_{y^*x^*}\left(\frac{\partial u^*}{\partial y^*} + \frac{\partial v^*}{\partial x^*}\right) + \tau_{z^*x^*}\left(\frac{\partial u^*}{\partial z^*} + \frac{\partial w^*}{\partial x^*}\right) +$$

$$\tau_{z^*y^*}\left(\frac{\partial v^*}{\partial z^*} + \frac{\partial w^*}{\partial y^*}\right) \qquad \text{(A1.45)}$$

Substituting (A1.44) into (A1.45) gives

$$\rho\frac{De^*}{Dt^*} = \rho\dot{q} + \frac{\partial}{\partial x^*}\left(K\frac{\partial T^*}{\partial x^*}\right) + \frac{\partial}{\partial y^*}\left(K\frac{\partial T^*}{\partial y^*}\right) + \frac{\partial}{\partial z^*}\left(K\frac{\partial T^*}{\partial z^*}\right) - p\left(\frac{\partial u^*}{\partial x^*} + \frac{\partial v^*}{\partial y^*} + \frac{\partial w^*}{\partial z^*}\right) +$$

$$\lambda\left(\frac{\partial u^*}{\partial x^*} + \frac{\partial v^*}{\partial y^*} + \frac{\partial w^*}{\partial z^*}\right)^2 + \mu\left[2\left(\frac{\partial u^*}{\partial x^*}\right)^2 + 2\left(\frac{\partial v^*}{\partial y^*}\right)^2 + 2\left(\frac{\partial w^*}{\partial z^*}\right)^2 + \left(\frac{\partial u^*}{\partial y^*} + \frac{\partial v^*}{\partial x^*}\right)^2 +\right.$$

$$\left.\left(\frac{\partial u^*}{\partial z^*} + \frac{\partial w^*}{\partial x^*}\right)^2\left(\frac{\partial v^*}{\partial z^*} + \frac{\partial w^*}{\partial y^*}\right)^2\right]. \qquad \text{(A1.46)}$$

Equation (A1.46) is a form of the energy equation completely in terms of the flow field variables.

Hence the rate of change of energy inside the fluid element for incompressible viscous fluid flow is

$$\rho\frac{De^*}{Dt^*} = \rho\dot{q} + K\left(\frac{\partial^2 T^*}{\partial x^{*2}} + \frac{\partial^2 T^*}{\partial y^{*2}} + \frac{\partial^2 T^*}{\partial z^{*2}}\right) + \Phi \qquad \text{(A1.47)}$$

DERIVATION OF CONCENTRATION EQUATION

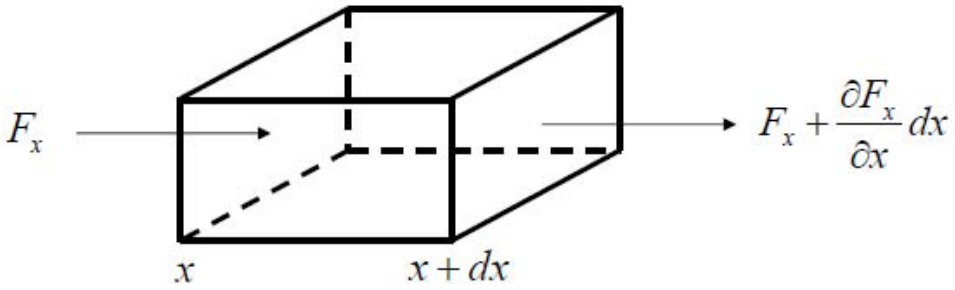

Figure A1.4 Flux balance along the x-direction in a region of space described in Cartesian (Intaglietta, 2017)

The concentration equation of a fluid is derived on the principles of species conservation in a mixture as well as Fick's Law.

The Fick's Law

Consider figure A1.4 above, introducing '*' on the variables for uniqueness of variables and parameters already used in the study. Fick's law states that the flux of the diffusing material F_{x^*} in x^*- direction is proportional to the negative gradient of the mass concentration C^* in the same direction:

$$F_{x^*} = -D\frac{dC^*}{dx^*} \tag{A1.47}$$

where D is the mass diffusion coefficient. This coefficient may be constant or a function of time, location and concentration.

In figure A1.4, assuming fluxes occur only in the x^*- direction, then

$$\left\{\begin{matrix}the\ flux\ of\ material\\ through\ the\ face\ of\\ element\ of\ volume\ x^*\end{matrix}\right\}-\left\{\begin{matrix}the\ flux\\ through\\ the\ face\\ x^*+dx^*\end{matrix}\right\}=\left\{\begin{matrix}the\ rate\ at\ which\\ the\ concentration\\ changes\ in\ the\ volume\end{matrix}\right\}$$

$$\Rightarrow F_{x^*}-\left(F_{x^*}+\frac{\partial F_{x^*}}{\partial x^*}dx^*\right)=\frac{\partial C^*}{\partial t^*}=-\frac{\partial F_{x^*}}{\partial x^*}$$

(A1.48)

Now considering the fluxes in all directions yield

$$\frac{\partial C^*}{\partial t^*}+\frac{\partial F_{x^*}}{\partial x^*}+\frac{\partial F_{y^*}}{\partial y^*}+\frac{\partial F_{z^*}}{\partial z^*}=0 \quad \text{(A1.49)}$$

$$\frac{\partial C^*}{\partial t^*}=\frac{\partial}{\partial x^*}\left(D\frac{\partial C^*}{\partial x^*}\right)+\frac{\partial}{\partial y^*}\left(D\frac{\partial C^*}{\partial y^*}\right)+\frac{\partial}{\partial z^*}\left(D\frac{\partial C^*}{\partial z^*}\right) \quad \text{(A1.50)}$$

In vector form, (A1.50) is expressed as

$$\frac{\partial C^*}{\partial t^*}=div(D\ grad\ C^*) \quad \text{(A1.51)}$$

$$\frac{DC^*}{Dt^*}=D\nabla^2C^{*2}{}_{\pm}\dot{r} \quad \text{(A1.52)}$$

APPENDIX II

LAPLACE TRANSFORMS

Considering the energy model in (4.21);

$$\frac{\partial\theta}{\partial t} = \frac{1}{P_r}\frac{\partial^2\theta}{\partial y^2} - \frac{1}{P_r}F_1\theta + ME_c u^2$$

The Laplace transform is

$$\frac{1}{P_r}L\left[\frac{\partial^2\theta}{\partial y^2}\right] - L\left[\frac{\partial\theta}{\partial t}\right] = \frac{1}{P_r}F_1 L[\theta] - ME_c L[u^2]$$

Taking $L\left[\frac{1}{P_r}\frac{\partial^2\theta}{\partial y^2}\right]$, using the definition of Laplace transform

Taking $L\left[\frac{1}{P_r}\frac{\partial^2\theta}{\partial y^2}\right] = \int_0^\infty \frac{1}{P_r}\frac{\partial^2\theta}{\partial y^2}e^{-st}\,\partial t$

$$= \frac{1}{P_r}\frac{\partial^2}{\partial y^2}\int_0^\infty \theta(y,t)e^{-st}\,\partial t$$

But $\int_0^\infty \theta(y,t)e^{-st}\,\partial t = \bar{\theta}(y,s).$

$$L\left[\frac{1}{P_r}\frac{\partial^2\theta}{\partial y^2}\right] = \frac{1}{P_r}\frac{\partial^2\bar{\theta}}{\partial y^2} \qquad \text{(A2.1)}$$

Also, taking $L\left[\frac{\partial\theta}{\partial t}\right]$. Let $\frac{\partial\theta}{\partial t} = \theta_t(y,t)$

$$L\frac{\partial\theta}{\partial t} = L\big(\theta_t(y,t)\big) = e^{-st}\theta(y,t)|_0^\infty + s\int_0^\infty \theta(y,t)e^{-st}\,\partial t$$

$$= s\bar{\theta}(y,s) - \theta(y,0). \qquad \text{(A2.2)}$$

Gathering the bits together

$$\Rightarrow \frac{1}{P_r}\frac{\partial^2\bar{\theta}}{\partial y^2} - s\bar{\theta}(y,s) + \theta(y,0) = \frac{1}{P_r}F_1\bar{\theta}(y,s) - ME_c L[u^2(y,\ t]. \quad \text{(A2.3)}$$

Similarly, the other models can be expressed in Laplace transforms as:

In the dimensionless concentration model (4.24), the Laplace transform is

$$\frac{1}{S_c}\frac{\partial^2\bar{\emptyset}}{\partial y^2} - s\bar{\emptyset}(y,s) + \emptyset(y,0) = K_c\bar{\emptyset}(y,s). \qquad \text{(A2.4)}$$

Also, in the dimensionless momentum model (4.15), the Laplace transform is

$$\frac{\partial^2\bar{u}}{\partial y^2} - \bar{u} + u(y,0) = -G_r\bar{\theta} - G_c\bar{\emptyset} + M_1\bar{u} \qquad \text{(A2.5)}$$

Table of Laplace Transforms

$f(t)$ for $t \geq 0$	$\hat{f} = L(f(t)) = \int_0^\infty e^{-st} f(t)dt$
1	$\frac{1}{s}$
e^{at}	$\frac{1}{s-a}$
t^n	$\frac{n!}{s^{n+1}} (n = 0,1,\dots)$
t^a	$\frac{\Gamma(a+1)}{s^{a+1}} (a > 0)$
$\sin bt$	$\frac{b}{s^2+b^2}$
$\cos bt$	$\frac{s}{s^2+b^2}$
$\sinh bt$	$\frac{b}{s^2-b^2}$
$\cosh bt$	$\frac{s}{s^2-b^2}$

$f'(t)$	$sL(f) - f(0)$
$f''(t)$	$s^2L(f) - sf(0)$ $- f'(0)$
$t^n f(t)$	$(-1)^n \frac{d^n F}{ds^n}(s)$
$e^{at} f(t)$	$L(f)(s-a)$
$u(t-a) = \begin{cases} 0 & t \le a \\ 1 & t > a \end{cases}$	$\frac{e^{-as}}{s}$
$u(t-a)f(t-a)$	$e^{-as}L(f)(s)$
$u(t-a)g(t)$	$e^{-as}L\big(g(t+a)\big)(s)$
$\delta(t-1)$	e^{-as}
$(f*g)(t)$ $= \int_0^t f(t-\tau)\, g(\tau) d\tau$	$L(f*g) = L(f)L(g)$

Table of Special Laplace Transforms

$f(t)$ for $t \geq 0$	$\hat{f} = L(f(t)) = \int_0^\infty e^{-st} f(t)dt$
$\frac{e^{-a^2/(4t)}}{\sqrt{\pi t}}$	$\frac{e^{-a\sqrt{s}}}{\sqrt{s}}$
$\frac{ae^{-a^2/(4t)}}{2\sqrt{\pi t^3}}$	$e^{-a\sqrt{s}}$
$erf(t)$	$\frac{e^{s^2/4}erfc(s/2)}{s}$
$erfc\left(\frac{a}{2\sqrt{t}}\right)$	$\frac{e^{-a\sqrt{s}}}{s}$
$2\sqrt{\frac{t}{\pi}}\, e^{-a^2/(4t)} - a\left\{erfc\left(\frac{a}{2\sqrt{t}}\right)\right\}$	$\frac{e^{-a\sqrt{s}}}{s\sqrt{s}}$
$e^{b^2t+ab}\left\{efrc\left(b\sqrt{t}+\frac{a}{2\sqrt{t}}\right)\right\}$	$\frac{e^{-a\sqrt{s}}}{\sqrt{s}(\sqrt{s}+b)}$

APPENDIX III

SOLUTIONS OF HOMOGENOUS PROBLEMS

In (4.21), considering the homogeneous problem of the LHS, i.e

$$\frac{\partial^2\bar{\theta}}{\partial y^2} - P_r s\bar{\theta}(y,s) - F_1\bar{\theta}(y,s) = 0 \qquad \text{(A3.1)}$$

$$\frac{d^2\bar{\theta}}{dy^2} - (P_r s + F_1)\bar{\theta} = 0. \qquad \text{(A3.2)}$$

The characteristic equation of the ODE is determined from the ansatz

$\bar{\theta} = e^{ry}$ and is

$$r^2 - (P_r s + F_1) = 0 \qquad \text{(A3.3)}$$

$$\Rightarrow \quad r = \pm\sqrt{P_r s + F_1.} \qquad \text{(A3.4)}$$

The general solution of the homogenous problem is

$$\bar{\theta}(y,s) = A(s)e^{-\sqrt{P_r s+F_1}\,y} + B(s)e^{\sqrt{P_r s+F_1}\,y}. \qquad \text{(A3.5)}$$

Where $A(s)$ and $B(s)$ are constants.

Similarly, in (4.36), $\frac{1}{S_c}\frac{\partial^2\bar{\emptyset}}{\partial y^2} - s\bar{\emptyset}(y,s) = K_c\bar{\emptyset}(y,s)$, the general solution of the homogenous problem is

$$\bar{\emptyset}(y,s) = A(s)e^{-\sqrt{S_c s+S_c K_c}\,y} + B(s)e^{\sqrt{S_c s+S_c K_c}\,y}. \qquad \text{(A3.6)}$$

In (A2.5), $\frac{\partial^2\bar{u}}{\partial y^2} - s\bar{u} = -G_r\bar{\theta} - G_c\bar{\emptyset} + M_1\bar{u}$, the general solution of the homogenous problem is

$$\bar{u}(y,s) = A(s)e^{-y\sqrt{s+M_1}} + B(s)e^{y\sqrt{s+M_1}}. \quad \text{(A3.7)}$$

In (5.10), $\frac{1}{P_r}\frac{\partial^2\bar{\theta}}{\partial y^2} - s\bar{\theta}(y,s) = \frac{1}{P_r}F\bar{\theta}(y,s) - ME_cL(u^2)$, the general solution of the homogenous problem is

$$\bar{\theta}(y,s) = A(s)e^{-y\sqrt{P_r s+F}} + B(s)e^{y\sqrt{P_r s+F}}. \quad \text{(A3.8)}$$

In (5.24), $\frac{\partial^2\bar{u}}{\partial y^2} - s\bar{u} = -G_r\bar{\theta} - G_c\bar{\emptyset} + M\bar{u}$, homogenous problem is

$$\bar{u}(y,s) = A(s)e^{-y\sqrt{s+M}} + B(s)e^{y\sqrt{s+M}}. \quad \text{(A3.9)}$$

In (6.17), taking the homogeneous problem as

$$\frac{\partial^2\bar{\theta}}{\partial y^2} + P_r\frac{\partial\bar{\theta}}{\partial y} - (P_r s + F_1)\bar{\theta} = 0. \quad \text{(A3.10)}$$

The characteristics equation is determined from the ansatz $\bar{\theta} = e^{ry}$ which is

$r^2 + P_r r - (P_r s + F_1) = 0$ compare to $ar^2 + br + c = 0$

$a = 1,\ b = P_r,\ c = -(P_r s + F_1)$ $\qquad r = \frac{-P_r \pm \sqrt{{P_r}^2 + 4(P_r s + F_1)}}{2} y$

The general solution of the homogeneous problem

is $\bar{\theta}(y,s) = A(s)e^{\frac{-P_r - \sqrt{P_r^2 + 4(P_r s + F_1)}}{2}y} + B(s)e^{\frac{-P_r + \sqrt{P_r^2 + 4(P_r s + F_1)}}{2}y}$. (A3.11)

In (6.34), $\frac{\partial^2\bar{u}}{\partial y^2} - s\bar{u} + \frac{\partial\bar{u}}{\partial y} = -G_r\bar{\theta} - G_c\bar{\emptyset} + M_1\bar{u}$, the homogeneous problem is $\frac{\partial^2\bar{u}}{\partial y^2} + \frac{\partial\bar{u}}{\partial y} - (s + M_1)\bar{u} = 0.$ (A3.12)

The characteristic equation is determined from the ansatz

$\bar{u} = e^{ry}$ which is

$r^2 + r - (s + M_1) = 0$ compare to $ar^2 + br + c = 0$

$a = 1,\ b = 1,\ c = -(s + M_1)$ $\qquad r = \frac{-1 \pm \sqrt{1-4s}}{2}$

The general solution of the homogeneous problem is

$$\bar{u}(y, s) = A(s)e^{\frac{-1-\sqrt{1+4(s+M_1)}}{2}y} + B(s)e^{\frac{-1+\sqrt{1+4(s+M_1)}}{2}y}. \qquad \text{(A3.13)}$$

In the homogeneous problem in (6.27) which is

$$\frac{\partial^2 \bar{\emptyset}}{\partial y^2} + S_c \frac{\partial \bar{\emptyset}}{\partial y} - S_c(s + K_c)\bar{\emptyset} = 0$$

The characteristic equation is determined from the ansatz

$\bar{\emptyset} = e^{ry}$ which is

$r^2 + S_c r - S_c(s + K_c) = 0$ compare to $ar^2 + br + c = 0$

$a = 1,\ b = S_c,\ c = -S_c(s + K_c)$ $\qquad r = \frac{-S_c \pm \sqrt{S_c{}^2 + 4S_c(s+K_c)}}{2}$

The general solution of the homogeneous problem is

$$\bar{\emptyset}(y, s) = A(s)e^{\frac{-S_c-\sqrt{S_c{}^2+4S_c(s+K_c)}}{2}y} + B(s)e^{\frac{-S_c+\sqrt{c^2+4S_c(s+K_c)}}{2}y}. \qquad \text{(A3.14)}$$

APPENDIX IV

CONVOLUTION THEOREM

If $L^{-1}[f(x)] = f(t)$ and$L^{-1}[g(x)] = g(t)$ then by convolution theorem;

$$(f.g)_{(x)} = \int_0^t f(t-x)g(x)dx \qquad \text{(A4.1)}$$

In the concentration equation in (4.39), using the convolution theorem;

$$f(t) = L^{-1}\left[\frac{1}{s}e^{-y\sqrt{S_c s + S_c K_c}}\right]$$

$$= L^{-1}\left[\frac{1}{s}\right] * L^{-1}\left[e^{-y\sqrt{S_c s + S_c K_c}}\right]$$

$$= 1 * \left(\frac{y\sqrt{S_c}}{2\sqrt{\pi t^3}}e^{\frac{-S_c y^2}{4t} - K_c t}\right). \qquad \text{(A4.2)}$$

$$f(t) = \int_0^t 1 * \frac{y\sqrt{S_c}}{2\sqrt{\pi x^3}}e^{\frac{-S_c y^2}{4x} - K_c x}dx$$

$$= \frac{y\sqrt{S_c}}{2\sqrt{\pi}}\int_0^t \frac{1}{\sqrt{x^3}}e^{\frac{-S_c y^2}{4x} - K_c x}dx$$

$$= \frac{y\sqrt{S_c}}{2\sqrt{\pi}}\left[\frac{\sqrt{\pi}}{y\sqrt{S_c}}\left[-e^{-y\sqrt{S_c K_c}}erfc\left(\frac{2x\sqrt{K_c} - y\sqrt{S_c}}{2\sqrt{x}}\right) + e^{y\sqrt{S_c K_c}}erfc\left(\frac{2x\sqrt{K_c} + y\sqrt{S_c}}{2\sqrt{x}}\right)\right]_0^t\right]$$

$$= -\frac{1}{2}\left[-e^{-y\sqrt{S_cK_c}}erfc\left(\frac{2t\sqrt{K_c}-y\sqrt{S_c}}{2\sqrt{t}}\right)+e^{y\sqrt{S_cK_c}}erfc\left(\frac{2t\sqrt{K_c}+y\sqrt{S_c}}{2\sqrt{t}}\right)\right].$$

(A4.3)

In the momentum equation in (4.48), applying convolution theorem;

$$f(t) = L^{-1}\left[\frac{1}{s-a}e^{-y\sqrt{s+M_1}}\right]$$

$$= L^{-1}\left[\frac{1}{s-a}\right] * L^{-1}\left[e^{-y\sqrt{s+M_1}}\right]$$

$$= e^{at} * \frac{y}{2\sqrt{\pi t^3}}e^{\frac{-y^2}{4t}-tM_1} \quad \text{(A4.4)}$$

$$f(t) = \int_0^t e^{a(t-x)}\frac{ye^{\frac{-y^2}{4x}-xM_1}}{2\sqrt{\pi x^3}}dx \quad \text{(A4.5)}$$

$$= \frac{y}{2\sqrt{\pi}}\int_0^t \frac{1}{\sqrt{x^3}}e^{at-(a+M_1)x-\frac{y^2}{4x}}$$

$$= \frac{y}{2\sqrt{\pi}}\left[\frac{\sqrt{\pi}}{y}e^{at}\left[-e^{-y\sqrt{a+M_1}}\left(erfc\left(\frac{2x\sqrt{a+M_1}-y}{2\sqrt{x}}\right)\right)+\right.\right.$$

$$\left.\left.e^{y\sqrt{a+M_1}}\left(erfc\left(\frac{2x\sqrt{a+M_1}+y}{2\sqrt{x}}\right)\right)\right]_0^t\right]$$

$$= \frac{1}{2} e^{at} \left[-e^{-y\sqrt{a+M_1}} \left(erfc \left(\frac{2t\sqrt{a+M_1} - y}{2\sqrt{t}} \right) \right) + e^{y\sqrt{a+M_1}} \left(erfc \left(\frac{2t\sqrt{a+M_1} + y}{2t} \right) \right) \right].$$

(A4.6)

Also, $f(t) = L^{-1}\left[\frac{1}{s+M_1} e^{-y\sqrt{s+M_1}} \right]$

$$= L^{-1}\left[\frac{1}{s+M_1} \right] * L^{-1}\left[e^{-y\sqrt{s+M_1}} \right]$$

$$= e^{-M_1 t} * \frac{y}{2\sqrt{\pi t^3}} e^{\frac{-y^2}{4t} - tM_1} \qquad \text{(A4.7)}$$

$$f(t) = \int_0^t e^{-M_1(t-x)} \frac{y e^{\frac{-y^2}{4x} - xM_1}}{2\sqrt{\pi x^3}} dx$$

$$= \frac{y}{2\sqrt{\pi}} \int_0^t \frac{1}{\sqrt{x^3}} e^{-M_1 t - \frac{y^2}{4x}}$$

$$= \frac{y}{2\sqrt{\pi}} \left[-\frac{2\sqrt{\pi} e^{-M_1 t} erf\left(\frac{y}{2\sqrt{x}}\right)}{y} \right]_0^t$$

$$= e^{-M_1 t} erfc \left(\frac{y}{2\sqrt{t}} \right). \qquad \text{(A4.8)}$$

Considering the temperature equation in (4.50), using the convolution theorem;

$$f(t) = L^{-1}\left[\frac{1}{s} e^{-y\sqrt{P_r s + F_1}\, y} \right]$$

$$= L^{-1}\left[\frac{1}{s} \right] * L^{-1}\left[e^{-y\sqrt{P_r s + F_1}\, y} \right]$$

$$= 1 * \frac{y\sqrt{P_r}}{2\sqrt{\pi t^3}} e^{\frac{-F_1 t}{P_r} - \frac{P_r y^2}{4t}} \quad \text{(A4.9)}$$

$$= \frac{y\sqrt{P_r}}{2\sqrt{\pi}} \int_0^t 1 * \frac{1}{\sqrt{t^3}} e^{\frac{-F_1 x}{P_r} - \frac{P_r y^2}{4x}} dx \quad \text{(A4.10)}$$

$$= \frac{1}{2}\left[-e^{-y\sqrt{F_1}}\left(erfc\left(\frac{2t\sqrt{\frac{F_1}{P_r}} - y\sqrt{P_r}}{2\sqrt{t}}\right)\right) + e^{y\sqrt{F_1}}\left(erfc\left(\frac{2t\sqrt{\frac{F_1}{P_r}} + y\sqrt{P_r}}{2\sqrt{t}}\right)\right)\right]. \quad \text{(A4.11)}$$

$$f(t) = L^{-1}\left[\frac{1}{P_r s + F_1} e^{-y\sqrt{P_r s + F_1}}\right]$$

Using convolution theorem;

$$f(t) = L^{-1}\left[\frac{1}{P_r s + F_1}\right] * L^{-1}\left[e^{-y\sqrt{P_r s + F_1}}\right]. \quad \text{(A4.12)}$$

$$= \frac{e^{-\frac{F_1 t}{P_r}}}{P_r} * \frac{y\sqrt{P_r}}{2\sqrt{\pi t^3}} e^{\frac{-F_1 t}{P_r} - \frac{P_r y^2}{4t}} \quad \text{(A4.13)}$$

$$= \frac{y\sqrt{P_r}}{2P_r\sqrt{\pi}} \int_0^t e^{-\frac{F_1(t-x)}{P_r}} * \frac{1}{\sqrt{x^3}} e^{\frac{-F_1 x}{P_r} - \frac{P_r y^2}{4x}} \quad \text{(A4.14)}$$

$$= \frac{1}{P_r}\left[-e^{-\frac{F_1 t}{P_r}} erf\left(\frac{y\sqrt{P_r}}{2\sqrt{x}}\right)\right]_0^t \quad \text{(A4.15)}$$

$$= \frac{1}{P_r} e^{-\frac{F_1 t}{P_r}} erfc\left(\frac{y\sqrt{P_r}}{2\sqrt{t}}\right). \quad \text{(A4.16)}$$

The velocity term (u^2) in the temperature model in (4.51) is expanded as

$$u^2 = \frac{1}{4}e^{2(at-y\sqrt{a+M_1})}\left(erfc\left(\frac{2t\sqrt{a+M_1}}{2\sqrt{t}}\right)\right)^2 +$$

$$\frac{1}{4}e^{2(at+y\sqrt{a+M_1})}\left(erfc\left(\frac{2t\sqrt{a+M_1}}{2\sqrt{t}}\right)\right)^2 + ((G_r\theta(y,t))^2 + 2G_r\theta(y,t)G_c\emptyset(y,t) +$$

$$(G_c\emptyset(y,t))^2)e^{-2M_1t}\left[1 - 2erfc\left(\frac{y}{2\sqrt{t}}\right) + \left(erfc\left(\frac{y}{2\sqrt{t}}\right)\right)^2\right] +$$

$$2\left[-\frac{1}{4}e^{at}erfc\left(\frac{2t\sqrt{a+M_1}-y}{2\sqrt{t}}\right)erfc\left(\frac{2t\sqrt{a+M_1}+y}{2\sqrt{t}}\right) -\right.$$

$$\frac{1}{2}e^{at-y\sqrt{a+M_1}}erfc\left(\frac{2t\sqrt{a+M_1}-y}{2\sqrt{t}}\right)\left(G_r\theta(y,t) + G_c\emptyset(y,t)\right)\left(e^{-M_1t} -\right.$$

$$e^{-M_1t}erfc\left(\frac{y}{2\sqrt{t}}\right)\Big) + \frac{1}{2}e^{at+y\sqrt{a+M_1}}erfc\left(\frac{2t\sqrt{a+M_1}+y}{2\sqrt{t}}\right)\left(G_r\theta(y,t) +\right.$$

$$\left.\left.G_c\emptyset(y,t)\right)\left(e^{-M_1t} - e^{-M_1t}erfc\left(\frac{y}{2\sqrt{t}}\right)\right)\right]. \qquad \text{(A4.17)}$$

Similarly, the velocity term (u^2) in the temperature model in (5.25) is expanded as

$$u^2 = \frac{y^2e^{-\frac{y^2}{2t}-2tM}}{4\pi t^3} + \frac{ye^{-\frac{y^2}{4t}-tM}}{\sqrt{\pi t^3}}\left(G_r\theta(y,t) + G_c\emptyset(y,t)\right)\left(e^{-Mt} -\right.$$

$$e^{-Mt}erfc\left(\frac{y}{2\sqrt{t}}\right)\Big) + (G_r^2\theta^2(y,t) + 2G_r\theta(y,t)G_c\emptyset(y,t) +$$

$$G_c^2\emptyset^2(y,t))e^{-2Mt}\left(1 - erfc\left(\frac{y}{2\sqrt{t}}\right)\right)^2. \qquad \text{(A4.19)}$$

Considering the concentration equation in (6.30), using the convolution theorem

$$f(t) = L^{-1}\left[\frac{1}{s}e^{\frac{-S_c-\sqrt{S_c^2+4S_c(s+k_c)}}{2}y}\right]$$

$$= L^{-1}\left[\frac{1}{s}\right] * L^{-1}\left[e^{\frac{-S_c-\sqrt{S_c^2+4S_c(s+k_c)}}{2}y}\right] \quad \text{(A4.20)}$$

$$= 1 * \frac{y\sqrt{S_c^3}}{2S_c\sqrt{\pi t^3}}e^{\frac{-S_c y^2}{4t}-\frac{S_c t}{4}-\frac{S_c y}{2}-K_c t} \quad \text{(A4.21)}$$

$$= \frac{y\sqrt{S_c^3}}{2S_c\sqrt{\pi}}\int_0^t 1 * \frac{1}{\sqrt{x^3}}e^{\frac{-S_c y^2}{4x}-\frac{S_c x}{4}-\frac{S_c y}{2}-K_c x}dx \quad \text{(A4.22)}$$

$$= \frac{1}{2}e^{\frac{-yS_c-y\sqrt{S_c^2+4S_cK_c}}{2}}\left(-erfc\left(\frac{t\sqrt{S_c+4K_c}-y\sqrt{S_c}}{2\sqrt{t}}\right)+\right.$$

$$\left.e^{y\sqrt{S_c^2+4S_cK_c}}erfc\left(\frac{t\sqrt{S_c+4K_c}+y\sqrt{S_c}}{2\sqrt{t}}\right)\right). \quad \text{(A4.23)}$$

In the velocity equation in (6.40), using the convolution theorem;

$$f(t) = L^{-1}\left[\frac{\lambda}{s}\mathrm{e}^{\frac{-1-\sqrt{1+4(s+M_1)}}{2}\mathrm{y}}\right] \quad \text{(A4.24)}$$

$$= \frac{\lambda}{2}\mathrm{e}^{\frac{-\mathrm{y}-\mathrm{y}\sqrt{1+4M_1}}{2}}\left[-erfc\left(\frac{-\mathrm{y}+\mathrm{t}\sqrt{1+4M_1}}{2\sqrt{t}}\right) + \mathrm{e}^{\mathrm{y}\sqrt{1+4M_1}}erfc\left(\frac{\mathrm{y}+\mathrm{t}\sqrt{1+4M_1}}{2\sqrt{t}}\right)\right].$$

(A4.25)

Also, $f(t) = L^{-1}\left[\frac{\lambda}{s+1}\mathrm{e}^{\frac{-1-\sqrt{1+4(s+M_1)}}{2}\mathrm{y}}\right]$

$$= L^{-1}\left[\frac{\lambda}{s+m}\right] * L^{-1}\left[\mathrm{e}^{\frac{-1-\sqrt{1+4(s+M_1)}}{2}\mathrm{y}}\right] \quad \text{(A4.26)}$$

$$= \lambda\, e^{-mt} * \frac{y}{2\sqrt{\pi t^3}} e^{\frac{-y^2}{4t}-\frac{t}{4}-\frac{y}{2}-M_1 t} \quad \text{(A4.27)}$$

$$= \frac{\lambda\, y}{2\sqrt{\pi}}\int_0^t e^{-m(t-x)}\frac{1}{\sqrt{x^3}} e^{\frac{-y^2}{4x}-\frac{x}{4}-\frac{y}{2}-M_1 x}dx \quad \text{(A4.28)}$$

$f(t)$

$$= \frac{\lambda}{2}\mathrm{e}^{\frac{-\mathrm{y}-\mathrm{y}\sqrt{1+4(m+M_1)+1}}{2}-mt}\left[-erfc\left(\frac{-\mathrm{y}+\mathrm{t}\sqrt{-4(m+M_1)+1}}{2\sqrt{t}}\right)\right.$$

$$\left. + \mathrm{e}^{\mathrm{y}\sqrt{-4(m+M_1)+1}}erfc\left(\frac{\mathrm{y}+\mathrm{t}\sqrt{-4(m+M_1)+1}}{2\sqrt{t}}\right)\right]. \quad \text{(A4.29)}$$

Also, $f(t) = L^{-1}\left[\frac{1}{s+M_1}\mathrm{e}^{\frac{-1-\sqrt{1+4(s+M_1)}}{2}\mathrm{y}}\right]$.

$$= L^{-1}\left[\frac{1}{s+M_1}\right] * L^{-1}\left[\mathrm{e}^{\frac{-1-\sqrt{1+4(s+M_1)}}{2}\mathrm{y}}\right] \quad \text{(A4.30)}$$

$$= e^{-M_1 t} * \frac{y}{2\sqrt{\pi t^3}} e^{\frac{-y^2}{4t}-\frac{t}{4}-\frac{y}{2}-M_1 t}$$

$$= \frac{y}{2\sqrt{\pi}} \int_0^t e^{-M_1(t-x)} \frac{1}{\sqrt{x^3}} e^{\frac{-y^2}{4x}-\frac{x}{4}-\frac{y}{2}-M_1 x} dx \quad \text{(A4.31)}$$

$$f(t) = \frac{1}{2}\mathrm{e}^{-M_1 t-y}\left[-erfc\left(\frac{\mathrm{t}-\mathrm{y}}{2\sqrt{t}}\right)\right.$$

$$\left. + \mathrm{e}^{\mathrm{y}} erfc\left(\frac{\mathrm{t}+\mathrm{y}}{2\sqrt{t}}\right)\right]. \quad \text{(A4.32)}$$

In the temperature equation in (6.24), using the convolution theorem;

$$f(t) = L^{-1}\left[\frac{1}{s}\mathrm{e}^{\frac{-P_r-\sqrt{P_r^2+4(P_r s+F_1)}}{2}\mathrm{y}}\right]$$

$$= L^{-1}\left[\frac{1}{s}\right] * L^{-1}\left[\mathrm{e}^{\frac{-P_r-\sqrt{P_r^2+4(P_r s+F_1)}}{2}\mathrm{y}}\right]$$

$$= 1 * \frac{y\sqrt{P_r}}{2\sqrt{\pi t^3}} e^{\frac{-P_r y^2}{4t}-\frac{F_1 t}{P_r}-\frac{P_r t}{4}-\frac{P_r y}{2}} \quad \text{(A4.33)}$$

$$= \frac{y\sqrt{P_r}}{2\sqrt{\pi}} \int_0^t 1 * \frac{1}{\sqrt{x^3}} e^{\frac{-P_r y^2}{4x}-\frac{F_1 x}{P_r}-\frac{P_r x}{4}-\frac{P_r y}{2}} dx \quad \text{(A4.34)}$$

$$= -\frac{1}{2}e^{\frac{-P_r}{2}-y\sqrt{4F_1+P_r^2}}erfc\left(\frac{t\sqrt{\frac{4F_1}{P_r}+P_r}-y\sqrt{P_r}}{2\sqrt{t}}\right)+$$

$$\frac{1}{2}e^{\frac{-P_r}{2}+y\sqrt{F_1+\frac{1}{4}P_r^2}}erfc\left(\frac{t\sqrt{\frac{4F_1}{P_r}+P_r}+y\sqrt{P_r}}{2\sqrt{t}}\right). \quad \text{(A4.35)}$$

Also, $L^{-1}\left[\frac{1}{P_rs+F_1}\mathrm{e}^{\frac{-P_r-\sqrt{P_r^2+4(P_rs+F_1)}}{2}\mathrm{y}}\right]$ (A4.36)

$$= L^{-1}\left[\frac{1}{P_rs+F_1}\right] * L^{-1}\left[\mathrm{e}^{\frac{-P_r-\sqrt{P_r^2+4(P_rs+F_1)}}{2}\mathrm{y}}\right]$$

$$= \frac{1}{P_r}e^{\frac{-F_1t}{P_r}} * \frac{y\sqrt{P_r}}{2\sqrt{\pi t^3}}e^{\frac{-P_ry^2}{4t}-\frac{F_1t}{P_r}-\frac{P_rt}{4}-\frac{P_ry}{2}}$$

$$f(t) = \frac{y\sqrt{P_r}}{2P_r\sqrt{\pi}}\int_0^t e^{\frac{-F_1t(t-x)}{P_r}} * \frac{1}{\sqrt{x^3}}e^{\frac{-P_ry^2}{4x}-\frac{F_1x}{P_r}-\frac{P_rx}{4}-\frac{P_ry}{2}}dx \quad \text{(A4.37)}$$

$$= -\frac{1}{2P_r}e^{\frac{-F_1}{P_r}+yP_r}erfc\left(\frac{t\sqrt{P_r}-y\sqrt{P_r}}{2\sqrt{t}}\right)+\frac{1}{2}e^{\frac{-F_1}{P_r}+2yP_r}erfc\left(\frac{t\sqrt{P_r}+y\sqrt{P_r}}{2\sqrt{t}}\right).$$

(A4.38)

The velocity term $u^2(y,t)$ in the temperature equation (6.42) is expanded as follows;

$$u^2(y,t) = \frac{\lambda}{4}^2 e^{-y+y\sqrt{1+4M_1}}\left(erfc\left(\frac{-y+t\sqrt{1+4M_1}}{2\sqrt{t}}\right)\right)^2 -$$

$$\frac{\lambda}{2}^2 e^{-y} erfc\left(\frac{-y+t\sqrt{1+4M_1}}{2\sqrt{t}}\right) erfc\left(\frac{y+t\sqrt{1+4M_1}}{2\sqrt{t}}\right) +$$

$$\frac{\lambda}{4}^2 e^{-y-y\sqrt{1+4M_1}}\left(erfc\left(\frac{y+t\sqrt{1+4M_1}}{2\sqrt{t}}\right)\right)^2 +$$

$$\frac{\lambda}{4}^2 e^{-2mt-y-y\sqrt{-4(m+M_1)+1}}\left(erfc\left(\frac{-y+t\sqrt{-4(m+M_1)+1}}{2\sqrt{t}}\right)\right)^2 -$$

$$\frac{\lambda}{2}^2 e^{-2mt-y} erfc\left(\frac{-y+t\sqrt{-4(m+M_1)+1}}{2\sqrt{t}}\right) erfc\left(\frac{y+t\sqrt{-4(m+M_1)+1}}{2\sqrt{t}}\right) +$$

$$\frac{\lambda}{4}^2 e^{-2mt-y+y\sqrt{-4(m+M_1)+1}}\left(erfc\left(\frac{y+t\sqrt{-4(m+M_1)+1}}{2\sqrt{t}}\right)\right)^2 + (G_r^2\theta^2(y,t) +$$

$$2G_r\theta(y,t)G_c\emptyset(y,t) + G_c^2\emptyset^2(y,t))\left[-\frac{1}{4}(-2e^{-M_1 t} -\right.$$

$$e^{-M_1 t-y})^2\left(-erfc\left(\frac{t-y}{2\sqrt{t}}\right) + erfc\left(\frac{t+y}{2\sqrt{t}}\right)\right)^2\Bigg] + \Bigg[\Bigg[-\lambda$$

$$e^{\frac{-y-y\sqrt{1+4M_1}}{2}} erfc\left(\frac{-y+t\sqrt{1+4M_1}}{2\sqrt{t}}\right) + \lambda$$

$$e^{\frac{-y+y\sqrt{1+4M_1}}{2}} erfc\left(\frac{y+t\sqrt{1+4M_1}}{2\sqrt{t}}\right)\Bigg]\Bigg[-\frac{\lambda}{2} e^{\frac{-2mt-y-y\sqrt{-4(m+M_1)+1}}{2}} erfc\left(\frac{-y+t\sqrt{-4(m+M_1)+1}}{2\sqrt{t}}\right) +$$

$$\frac{\lambda}{2} e^{\frac{-2mt-y+y\sqrt{-4(m+M_1)+1}}{2}} erfc\left(\frac{y+t\sqrt{-4(m+M_1)+1}}{2\sqrt{t}}\right)\Bigg]\Bigg] + (G_r\theta(y,t) +$$

$$G_c\emptyset(y,t))\frac{\lambda}{2} e^{\frac{-y-y\sqrt{1+4M_1}}{2}}\left[-erfc\left(\frac{-y+t\sqrt{1+4M_1}}{2\sqrt{t}}\right) +\right.$$

$$e^{y\sqrt{1+4M_1}}erfc\left(\frac{y+t\sqrt{1+4M_1}}{2\sqrt{t}}\right)\Big]\left[\frac{2e^{-M_1t}-e^{-M_1t-y}}{2}\left(-erfc\left(\frac{t-y}{2\sqrt{t}}\right)+\right.\right.$$

$$\left.\left.erfc\left(\frac{t+y}{2\sqrt{t}}\right)e^{y}\right)\right]+\left(G_r\theta(y,t)+\right.$$

$$\left.G_c\emptyset(y,t)\right)\frac{\lambda}{2}e^{\frac{-2mt-y-y\sqrt{-4(m+M_1)+1}}{2}}\left[-erfc\left(\frac{-y+t\sqrt{-4(m+M_1)+1}}{2\sqrt{t}}\right)+\right.$$

$$\left.e^{y\sqrt{-4(m+M_1)+1}}erfc\left(\frac{y+t\sqrt{-4(m+M_1)+1}}{2\sqrt{t}}\right)\right]\left[\frac{2e^{-M_1t}-e^{-M_1t-y}}{2}\left(-erfc\left(\frac{t-y}{2\sqrt{t}}\right)+\right.\right.$$

$$\left.\left.erfc\left(\frac{t+y}{2\sqrt{t}}\right)e^{y}\right)\right]. \qquad \text{(A4.39)}$$

The term $\left(\frac{\partial u(y,t)}{\partial y}\right)^2$ in the temperature equation (6.42) is obtained as;

$$\frac{\partial u(y,t)}{\partial y}=\left[-\frac{\lambda}{2\sqrt{\pi t}}e^{\frac{-y-y\sqrt{1+4M_1}}{2}-\frac{\left(-y+t\sqrt{4M_1+1}\right)^2}{4t}}-\frac{\lambda}{4}\left(-1-\right.\right.$$

$$\left.\sqrt{4M_1+1}\right)e^{\frac{-y-y\sqrt{1+4M_1}}{2}}erfc\left(\frac{-y+t\sqrt{4M_1+1}}{2\sqrt{t}}\right)-\frac{\lambda}{2\sqrt{\pi t}}e^{\frac{-y+y\sqrt{1+4M_1}}{2}-\frac{\left(y+t\sqrt{4M_1+1}\right)^2}{4t}}+$$

$$\left.\frac{\lambda}{4}\left(-1+\sqrt{4M_1+1}\right)e^{\frac{-y+y\sqrt{1+4M_1}}{2}}erfc\left(\frac{y+t\sqrt{4M_1+1}}{2\sqrt{t}}\right)\right]+\left[\frac{\lambda}{4}\left(-1-\right.\right.$$

$$\left.\sqrt{1-4(m+M_1)}\right)e^{\frac{-2mt-y-y\sqrt{1-4(m+M_1)}}{2}}erfc\left(\frac{-y+t\sqrt{1-4(m+M_1)}}{2\sqrt{t}}\right)+$$

$$\frac{\lambda}{2\sqrt{\pi t}}e^{\frac{-2mt-y-y\sqrt{1-4(m+M_1)}}{2}-\frac{\left(-y+t\sqrt{1-4(m+M_1)}\right)^2}{4t}}+$$

$$\frac{\lambda}{2\sqrt{\pi t}}e^{\frac{-2mt-y+y\sqrt{1-4(m+M_1)}}{2}-\frac{\left(y+t\sqrt{1-4(m+M_1)}\right)^2}{4t}}-\frac{\lambda}{4}\left(-1+\right.$$

$$\sqrt{1-4(m+M_1)}\mathrm{e}^{\frac{-2\mathrm{mt}-\mathrm{y}+\mathrm{y}\sqrt{1-4(m+M_1)}}{2}}erfc\left(\frac{y+t\sqrt{1-4(m+M_1)}}{2\sqrt{t}}\right)\Bigg] +$$

$$(G_r\theta(y,t)+G_c\emptyset(y,t))\left[\frac{1}{2\sqrt{\pi t}}e^{\frac{-M_1t-(t-y)^2}{4t-y}}-\frac{1}{2}erfc\left(\frac{t-y}{2\sqrt{t}}\right)e^{-M_1t-y}+\right.$$

$$\left.\frac{1}{2\sqrt{\pi t}}e^{\frac{-M_1t-(t-y)^2}{4t-y}}\right]. \qquad \text{(A4.40)}$$

$$\left(\frac{\partial u(y,t)}{\partial y}\right)^2=\left[-\frac{\lambda}{2\sqrt{\pi t}}\mathrm{e}^{\frac{-\mathrm{y}-\mathrm{y}\sqrt{1+4M_1}}{2}-\frac{\left(-y+t\sqrt{4M_1+1}\right)^2}{4t}}-\frac{\lambda}{4}(-1-\right.$$

$$\sqrt{4M_1+1}\mathrm{e}^{\frac{-\mathrm{y}-\mathrm{y}\sqrt{1+4M_1}}{2}}erfc\left(\frac{-y+t\sqrt{4M_1+1}}{2\sqrt{t}}\right)-\frac{\lambda}{2\sqrt{\pi t}}\mathrm{e}^{\frac{-\mathrm{y}+\mathrm{y}\sqrt{1+4M_1}}{2}-\frac{\left(y+t\sqrt{4M_1+1}\right)^2}{4t}}+$$

$$\frac{\lambda}{4}(-1+\sqrt{4M_1+1})\mathrm{e}^{\frac{-\mathrm{y}+\mathrm{y}\sqrt{1+4M_1}}{2}}erfc\left(\frac{y+t\sqrt{4M_1+1}}{2\sqrt{t}}\right)\Bigg]^2+\left[\frac{\lambda}{4}(-1-\right.$$

$$\sqrt{1-4(m+M_1)}\mathrm{e}^{\frac{-2\mathrm{mt}-\mathrm{y}-\mathrm{y}\sqrt{1-4(m+M_1)}}{2}}erfc\left(\frac{-y+t\sqrt{1-4(m+M_1)}}{2\sqrt{t}}\right)+$$

$$\frac{\lambda}{2\sqrt{\pi t}}\mathrm{e}^{\frac{-2\mathrm{mt}-\mathrm{y}-\mathrm{y}\sqrt{1-4(m+M_1)}}{2}-\frac{\left(-y+t\sqrt{1-4(m+M_1)}\right)^2}{4t}}+$$

$$\frac{\lambda}{2\sqrt{\pi t}}\mathrm{e}^{\frac{-2\mathrm{mt}-\mathrm{y}+\mathrm{y}\sqrt{1-4(m+M_1)}}{2}-\frac{\left(y+t\sqrt{1-4(m+M_1)}\right)^2}{4t}}-\frac{\lambda}{4}(-1+$$

$$\sqrt{1-4(m+M_1)}\mathrm{e}^{\frac{-2\mathrm{mt}-\mathrm{y}+\mathrm{y}\sqrt{1-4(m+M_1)}}{2}}erfc\left(\frac{y+t\sqrt{1-4(m+M_1)}}{2\sqrt{t}}\right)\Bigg]^2+$$

$$\left[(G_r\theta(y,t)+G_c\emptyset(y,t))\left[\frac{1}{2\sqrt{\pi t}}e^{\frac{-M_1t-(t-y)^2}{4t-y}}-\frac{1}{2}erfc\left(\frac{t-y}{2\sqrt{t}}\right)e^{-M_1t-y}+\right.\right.$$

$$\left.\left.\frac{1}{2\sqrt{\pi t}}e^{\frac{-M_1t-(t-y)^2}{4t-y}}\right]\right]^2+2\left[\left[-\frac{\lambda}{2\sqrt{\pi t}}\mathrm{e}^{\frac{-\mathrm{y}-\mathrm{y}\sqrt{1+4M_1}}{2}-\frac{\left(-y+t\sqrt{4M_1+1}\right)^2}{4t}}-\frac{\lambda}{4}(-1-\right.\right.$$

$$\sqrt{4M_1+1}\Big)\mathrm{e}^{\frac{-\mathrm{y}-\mathrm{y}\sqrt{1+4M_1}}{2}}erfc\left(\frac{-y+t\sqrt{4M_1+1}}{2\sqrt{t}}\right)-\frac{\lambda}{2\sqrt{\pi t}}\mathrm{e}^{\frac{-\mathrm{y}+\mathrm{y}\sqrt{1+4M_1}}{2}-\frac{(y+t\sqrt{4M_1+1})^2}{4t}}+$$

$$\frac{\lambda}{4}\left(-1+\sqrt{4M_1+1}\right)\mathrm{e}^{\frac{-\mathrm{y}+\mathrm{y}\sqrt{1+4M_1}}{2}}erfc\left(\frac{y+t\sqrt{4M_1+1}}{2\sqrt{t}}\right)\Bigg]\Bigg[\frac{\lambda}{4}\Big(-1-$$

$$\sqrt{1-4(m+M_1)}\Big)\mathrm{e}^{\frac{-2\mathrm{mt}-\mathrm{y}-\mathrm{y}\sqrt{1-4(m+M_1)}}{2}}erfc\left(\frac{-y+t\sqrt{1-4(m+M_1)}}{2\sqrt{t}}\right)+$$

$$\frac{\lambda}{2\sqrt{\pi t}}\mathrm{e}^{\frac{-2\mathrm{mt}-\mathrm{y}-\mathrm{y}\sqrt{1-4(m+M_1)}}{2}-\frac{(-y+t\sqrt{1-4(m+M_1)})^2}{4t}}+$$

$$\frac{\lambda}{2\sqrt{\pi t}}\mathrm{e}^{\frac{-2\mathrm{mt}-\mathrm{y}+\mathrm{y}\sqrt{1-4(m+M_1)}}{2}-\frac{(y+t\sqrt{1-4(m+M_1)})^2}{4t}}-\frac{\lambda}{4}\Big(-1+$$

$$\sqrt{1-4(m+M_1)}\Big)\mathrm{e}^{\frac{-2\mathrm{mt}-\mathrm{y}+\mathrm{y}\sqrt{1-4(m+M_1)}}{2}}erfc\left(\frac{y+t\sqrt{1-4(m+M_1)}}{2\sqrt{t}}\right)\Bigg]+$$

$$\Bigg[-\frac{\lambda}{2\sqrt{\pi t}}\mathrm{e}^{\frac{-\mathrm{y}-\mathrm{y}\sqrt{1+4M_1}}{2}-\frac{(-y+t\sqrt{4M_1+1})^2}{4t}}-\frac{\lambda}{4}\Big(-1-$$

$$\sqrt{4M_1+1}\Big)\mathrm{e}^{\frac{-\mathrm{y}-\mathrm{y}\sqrt{1+4M_1}}{2}}erfc\left(\frac{-y+t\sqrt{4M_1+1}}{2\sqrt{t}}\right)-\frac{\lambda}{2\sqrt{\pi t}}\mathrm{e}^{\frac{-\mathrm{y}+\mathrm{y}\sqrt{1+4M_1}}{2}-\frac{(y+t\sqrt{4M_1+1})^2}{4t}}+$$

$$\frac{\lambda}{4}\left(-1+\sqrt{4M_1+1}\right)\mathrm{e}^{\frac{-\mathrm{y}+\mathrm{y}\sqrt{1+4M_1}}{2}}erfc\left(\frac{y+t\sqrt{4M_1+1}}{2\sqrt{t}}\right)\Bigg]\Bigg[(G_r\theta(y,t)+$$

$$G_c\emptyset(y,t))\left[\frac{1}{2\sqrt{\pi t}}e^{\frac{-M_1t-(t-y)^2}{4t-y}}-\frac{1}{2}erfc\left(\frac{t-y}{2\sqrt{t}}\right)e^{-M_1t-y}+\frac{1}{2\sqrt{\pi t}}e^{\frac{-M_1t-(t-y)^2}{4t-y}}\right]\Bigg]+$$

$$\left[\frac{\lambda}{4}\left(-1-\sqrt{1-4(m+M_1)}\right)\mathrm{e}^{\frac{-2\mathrm{mt}-\mathrm{y}-\mathrm{y}\sqrt{1-4(m+M_1)}}{2}}erfc\left(\frac{-y+t\sqrt{1-4(m+M_1)}}{2\sqrt{t}}\right)+\right.$$

$$\frac{\lambda}{2\sqrt{\pi t}}\mathrm{e}^{\frac{-2\mathrm{mt}-\mathrm{y}-\mathrm{y}\sqrt{1-4(m+M_1)}}{2}-\frac{(-y+t\sqrt{1-4(m+M_1)})^2}{4t}}+$$

$$\frac{\lambda}{2\sqrt{\pi t}}\mathrm{e}^{\frac{-2\mathrm{mt}-\mathrm{y}+\mathrm{y}\sqrt{1-4(m+M_1)}}{2}-\frac{\left(y+t\sqrt{1-4(m+M_1)}\right)^2}{4t}}-\frac{\lambda}{4}\left(-1+\right.$$

$$\left.\sqrt{1-4(m+M_1)}\mathrm{e}^{\frac{-2\mathrm{mt}-\mathrm{y}+\mathrm{y}\sqrt{1-4(m+M_1)}}{2}}erfc\left(\frac{y+t\sqrt{1-4(m+M_1)}}{2\sqrt{t}}\right)\right]\left[\left(G_r\theta(y,t)+\right.\right.$$

$$\left.\left.G_c\emptyset(y,t)\right)\left[\frac{1}{2\sqrt{\pi t}}e^{\frac{-M_1t-(t-y)^2}{4t-y}}-\frac{1}{2}erfc\left(\frac{t-y}{2\sqrt{t}}\right)e^{-M_1t-y}+\frac{1}{2\sqrt{\pi t}}e^{\frac{-M_1t-(t-y)^2}{4t-y}}\right]\right].$$

(A4.41)

From the temperature equation (6.43), the terms *b2* and $b3$ are

$$b_2=\left[-\frac{\lambda}{2\sqrt{\pi t}}\mathrm{e}^{\frac{-\mathrm{y}-\mathrm{y}\sqrt{1+4M_1}}{2}-\frac{\left(-y+t\sqrt{4M_1+1}\right)^2}{4t}}-\frac{\lambda}{4}\left(-1-\right.\right.$$

$$\left.\sqrt{4M_1+1}\mathrm{e}^{\frac{-\mathrm{y}-\mathrm{y}\sqrt{1+4M_1}}{2}}erfc\left(\frac{-y+t\sqrt{4M_1+1}}{2\sqrt{t}}\right)-\frac{\lambda}{2\sqrt{\pi t}}\mathrm{e}^{\frac{-\mathrm{y}+\mathrm{y}\sqrt{1+4M_1}}{2}-\frac{\left(y+t\sqrt{4M_1+1}\right)^2}{4t}}+\right.$$

$$\frac{\lambda}{4}\left(-1+\sqrt{4M_1+1}\right)\mathrm{e}^{\frac{-\mathrm{y}+\mathrm{y}\sqrt{1+4M_1}}{2}}erfc\left(\frac{y+t\sqrt{4M_1+1}}{2\sqrt{t}}\right)\Bigg]^2+\left[\frac{\lambda}{4}\left(-1-\right.\right.$$

$$\left.\sqrt{1-4(m+M_1)}\mathrm{e}^{\frac{-2\mathrm{mt}-\mathrm{y}-\mathrm{y}\sqrt{1-4(m+M_1)}}{2}}erfc\left(\frac{-y+t\sqrt{1-4(m+M_1)}}{2\sqrt{t}}\right)+\right.$$

$$\frac{\lambda}{2\sqrt{\pi t}}\mathrm{e}^{\frac{-2\mathrm{mt}-\mathrm{y}-\mathrm{y}\sqrt{1-4(m+M_1)}}{2}-\frac{\left(-y+t\sqrt{1-4(m+M_1)}\right)^2}{4t}}+$$

$$\frac{\lambda}{2\sqrt{\pi t}}\mathrm{e}^{\frac{-2\mathrm{mt}-\mathrm{y}+\mathrm{y}\sqrt{1-4(m+M_1)}}{2}-\frac{\left(y+t\sqrt{1-4(m+M_1)}\right)^2}{4t}}-\frac{\lambda}{4}\left(-1+\right.$$

$$\sqrt{1-4(m+M_1)}\mathrm{e}^{\frac{-2\mathrm{mt}-\mathrm{y}+\mathrm{y}\sqrt{1-4(m+M_1)}}{2}}erfc\left(\frac{y+t\sqrt{1-4(m+M_1)}}{2\sqrt{t}}\right)\Bigg]^2+$$

$$\left[(G_c\emptyset(y,t))\left[\frac{1}{2\sqrt{\pi t}}e^{\frac{-M_1t-(t-y)^2}{4t-y}}-\frac{1}{2}erfc\left(\frac{t-y}{2\sqrt{t}}\right)e^{-M_1t-y}+\frac{1}{2\sqrt{\pi t}}e^{\frac{-M_1t-(t-y)^2}{4t-y}}\right]\right]^2$$

$$+2\Bigg[\Bigg[-\frac{\lambda}{2\sqrt{\pi t}}\mathrm{e}^{\frac{-\mathrm{y}-\mathrm{y}\sqrt{1+4M_1}}{2}-\frac{(-y+t\sqrt{4M_1+1})^2}{4t}}-\frac{\lambda}{4}(-1-$$

$$\sqrt{4M_1+1}\mathrm{e}^{\frac{-\mathrm{y}-\mathrm{y}\sqrt{1+4M_1}}{2}}erfc\left(\frac{-y+t\sqrt{4M_1+1}}{2\sqrt{t}}\right)-\frac{\lambda}{2\sqrt{\pi t}}\mathrm{e}^{\frac{-\mathrm{y}+\mathrm{y}\sqrt{1+4M_1}}{2}-\frac{(y+t\sqrt{4M_1+1})^2}{4t}}+$$

$$\frac{\lambda}{4}(-1+\sqrt{4M_1+1})\mathrm{e}^{\frac{-\mathrm{y}+\mathrm{y}\sqrt{1+4M_1}}{2}}erfc\left(\frac{y+t\sqrt{4M_1+1}}{2\sqrt{t}}\right)\Bigg]\Bigg[\frac{\lambda}{4}(-1-$$

$$\sqrt{1-4(m+M_1)}\mathrm{e}^{\frac{-2\mathrm{mt}-\mathrm{y}-\mathrm{y}\sqrt{1-4(m+M_1)}}{2}}erfc\left(\frac{-y+t\sqrt{1-4(m+M_1)}}{2\sqrt{t}}\right)+$$

$$\frac{\lambda}{2\sqrt{\pi t}}\mathrm{e}^{\frac{-2\mathrm{mt}-\mathrm{y}-\mathrm{y}\sqrt{1-4(m+M_1)}}{2}-\frac{(-y+t\sqrt{1-4(m+M_1)})^2}{4t}}+$$

$$\frac{\lambda}{2\sqrt{\pi t}}\mathrm{e}^{\frac{-2\mathrm{mt}-\mathrm{y}+\mathrm{y}\sqrt{1-4(m+M_1)}}{2}-\frac{(y+t\sqrt{1-4(m+M_1)})^2}{4t}}-\frac{\lambda}{4}(-1+$$

$$\sqrt{1-4(m+M_1)}\mathrm{e}^{\frac{-2\mathrm{mt}-\mathrm{y}+\mathrm{y}\sqrt{1-4(m+M_1)}}{2}}erfc\left(\frac{y+t\sqrt{1-4(m+M_1)}}{2\sqrt{t}}\right)\Bigg]+$$

$$\left[-\frac{\lambda}{2\sqrt{\pi t}}\mathrm{e}^{\frac{-\mathrm{y}-\mathrm{y}\sqrt{1+4M_1}}{2}-\frac{(-y+t\sqrt{4M_1+1})^2}{4t}}-\frac{\lambda}{4}(-1-\right.$$

$$\sqrt{4M_1+1}\mathrm{e}^{\frac{-\mathrm{y}-\mathrm{y}\sqrt{1+4M_1}}{2}}erfc\left(\frac{-y+t\sqrt{4M_1+1}}{2\sqrt{t}}\right)-\frac{\lambda}{2\sqrt{\pi t}}\mathrm{e}^{\frac{-\mathrm{y}+\mathrm{y}\sqrt{1+4M_1}}{2}-\frac{(y+t\sqrt{4M_1+1})^2}{4t}}+$$

$$\frac{\lambda}{4}(-1+$$

$$\sqrt{4M_1+1}\mathrm{e}^{\frac{-\mathrm{y}+\mathrm{y}\sqrt{1+4M_1}}{2}}erfc\left(\frac{y+t\sqrt{4M_1+1}}{2\sqrt{t}}\right)\Bigg]\Bigg[(G_c\emptyset(y,t))\left[\frac{1}{2\sqrt{\pi t}}e^{\frac{-M_1t-(t-y)^2}{4t-y}}-\right.$$

$$\left.\frac{1}{2}erfc\left(\frac{t-y}{2\sqrt{t}}\right)e^{-M_1t-y}+\frac{1}{2\sqrt{\pi t}}e^{\frac{-M_1t-(t-y)^2}{4t-y}}\right]\Bigg]+\Bigg[\frac{\lambda}{4}(-1-$$

$$\sqrt{1-4(m+M_1)}\mathrm{e}^{\frac{-2\mathrm{mt}-\mathrm{y}-\mathrm{y}\sqrt{1-4(m+M_1)}}{2}}erfc\left(\frac{-y+t\sqrt{1-4(m+M_1)}}{2\sqrt{t}}\right)+$$

$$\frac{\lambda}{2\sqrt{\pi t}}\mathrm{e}^{\frac{-2\mathrm{mt}-\mathrm{y}-\mathrm{y}\sqrt{1-4(m+M_1)}}{2}-\frac{\left(-y+t\sqrt{1-4(m+M_1)}\right)^2}{4t}}+$$

$$\frac{\lambda}{2\sqrt{\pi t}}\mathrm{e}^{\frac{-2\mathrm{mt}-\mathrm{y}+\mathrm{y}\sqrt{1-4(m+M_1)}}{2}-\frac{\left(y+t\sqrt{1-4(m+M_1)}\right)^2}{4t}}-\frac{\lambda}{4}(-1+$$

$$\sqrt{1-4(m+M_1)}\mathrm{e}^{\frac{-2\mathrm{mt}-\mathrm{y}+\mathrm{y}\sqrt{1-4(m+M_1)}}{2}}erfc\left(\frac{y+t\sqrt{1-4(m+M_1)}}{2\sqrt{t}}\right)\Bigg]\Bigg[(G_c\emptyset(y,t))\left[\frac{1}{2\sqrt{\pi t}}e^{\frac{-M_1t-(t-y)^2}{4t-y}}-\right.$$

$$\left.\left.\frac{1}{2}erfc\left(\frac{t-y}{2\sqrt{t}}\right)e^{-M_1t-y}+\frac{1}{2\sqrt{\pi t}}e^{\frac{-M_1t-(t-y)^2}{4t-y}}\right]\right]\Bigg]. \qquad \text{(A4.42)}$$

$$b_3=\frac{\lambda}{4}^2e^{-y+y\sqrt{1+4M_1}}\left(erfc\left(\frac{-\mathrm{y}+\mathrm{t}\sqrt{1+4M_1}}{2\sqrt{t}}\right)\right)^2-$$

$$\frac{\lambda}{2}^2e^{-y}erfc\left(\frac{-\mathrm{y}+\mathrm{t}\sqrt{1+4M_1}}{2\sqrt{t}}\right)erfc\left(\frac{\mathrm{y}+\mathrm{t}\sqrt{1+4M_1}}{2\sqrt{t}}\right)+$$

$$\frac{\lambda}{4}^2e^{-y-y\sqrt{1+4M_1}}\left(erfc\left(\frac{\mathrm{y}+\mathrm{t}\sqrt{1+4M_1}}{2\sqrt{t}}\right)\right)^2+$$

$$\frac{\lambda}{4}^2e^{-2mt-y-y\sqrt{-4(m+M_1)+1}}\left(erfc\left(\frac{-\mathrm{y}+\mathrm{t}\sqrt{-4(m+M_1)+1}}{2\sqrt{t}}\right)\right)^2-$$

$$\frac{\lambda}{2}^{2} e^{-2mt-y} erfc\left(\frac{-y+t\sqrt{-4(m+M_1)+1}}{2\sqrt{t}}\right) erfc\left(\frac{y+t\sqrt{-4(m+M_1)+1}}{2\sqrt{t}}\right) +$$

$$(G_c^2 \emptyset^2(y,t)) \frac{\lambda}{4}^{2} e^{-2mt-y+y\sqrt{-4(m+M_1)+1}} \left(erfc\left(\frac{y+t\sqrt{-4(m+M_1)+1}}{2\sqrt{t}}\right)\right)^2 \left[-\frac{1}{4}(-2e^{-M_1 t} -\right.$$

$$\left. e^{-M_1 t-y})^2 \left(-erfc\left(\frac{t-y}{2\sqrt{t}}\right) + erfc\left(\frac{t+y}{2\sqrt{t}}\right)\right)^2\right] + \left[\left[-\lambda\right.\right.$$

$$e^{\frac{-y-y\sqrt{1+4M_1}}{2}} erfc\left(\frac{-y+t\sqrt{1+4M_1}}{2\sqrt{t}}\right) + \lambda$$

$$\left.\left. e^{\frac{-y+y\sqrt{1+4M_1}}{2}} erfc\left(\frac{y+t\sqrt{1+4M_1}}{2\sqrt{t}}\right)\right]\left[\frac{-\lambda}{2} e^{\frac{-2mt-y-y\sqrt{-4(m+M_1)+1}}{2}} erfc\left(\frac{-y+t\sqrt{-4(m+M_1)+1}}{2\sqrt{t}}\right) +\right.\right.$$

$$\left.\left.\frac{\lambda}{2} e^{\frac{-2mt-y+y\sqrt{-4(m+M_1)+1}}{2}} erfc\left(\frac{y+t\sqrt{-4(m+M_1)+1}}{2\sqrt{t}}\right)\right]\right] +$$

$$(G_c \emptyset(y,t)) \frac{\lambda}{2} e^{\frac{-y-y\sqrt{1+4M_1}}{2}} \left[-erfc\left(\frac{-y+t\sqrt{1+4M_1}}{2\sqrt{t}}\right) +\right.$$

$$\left. e^{y\sqrt{1+4M_1}} erfc\left(\frac{y+t\sqrt{1+4M_1}}{2\sqrt{t}}\right)\right]\left[\frac{2e^{-M_1 t}-e^{-M_1 t-y}}{2}\left(-erfc\left(\frac{t-y}{2\sqrt{t}}\right) +\right.\right.$$

$$\left.\left. erfc\left(\frac{t+y}{2\sqrt{t}}\right) e^{y}\right)\right] +$$

$$(G_c \emptyset(y,t)) \frac{\lambda}{2} e^{\frac{-2mt-y-y\sqrt{-4(m+M_1)+1}}{2}} \left[-erfc\left(\frac{-y+t\sqrt{-4(m+M_1)+1}}{2\sqrt{t}}\right) +\right.$$

$$\left. e^{y\sqrt{-4(m+M_1)+1}} erfc\left(\frac{y+t\sqrt{-4(m+M_1)+1}}{2\sqrt{t}}\right)\right]\left[\frac{2e^{-M_1 t}-e^{-M_1 t-y}}{2}\left(-erfc\left(\frac{t-y}{2\sqrt{t}}\right) +\right.\right.$$

$$\left.\left. erfc\left(\frac{t+y}{2\sqrt{t}}\right) e^{y}\right)\right].$$

(A4.43)

APPENDIX V

MATLAB CODES

Concentration profile for air (Sc=0.24), electrolyte solution (Sc=0.67) and water (Sc=0.62) when Kc=1

```
>> syms phi1 phi2 phi3 phi4 phi5 phi6 y
>>phi1=0.5*exp(-0.4899*y)*erfc(0.4472-0.5477*y)+

0.5*exp(0.4899*y)*erfc(0.4472+0.5477*y)


>>phi2=0.5*exp(-0.4899*y)*erfc(0.6325-0.3873*y)+

0.5*exp(0.4899*y)*erfc(0.6325+0.3873*y)


>>phi3=0.5*exp(-0.8185*y)*erfc(0.4472-0.9152*y)+

0.5*exp(0.8185*y)*erfc(0.4472+0.9152*y)


>>phi4=0.5*exp(-0.8185*y)*erfc(0.6325-0.6471*y)+

0.5*exp(0.8185*y)*erfc(0.6325+0.6471*y)


>>phi5=0.5*exp(-0.7874*y)*erfc(0.4472-0.8803*y)+

0.5*exp(0.7874*y)*erfc(0.4472+0.8803*y)


>>phi6=0.5*exp(-0.7874*y)*erfc(0.6325-

0.6225*y)+.5*exp(0.7874*y)*erfc(0.6325+0.6225*y)


>> a=ezplot(phi1,0,2)
>> set(a,'color','g','LineStyle','--')
>> hold on
```

```
>> b=ezplot(phi2,0,2)
>> set(b,'color','k','LineStyle','--')
>> hold on
>> c=ezplot(phi3,0,2)
>> set(c,'color','y','LineStyle','-')
>> hold on
>> d=ezplot(phi4,0,2)
>> set(d,'color','r','LineStyle','-')
>> hold on
 >> set(e,'color','c','LineStyle',':')
>> hold on
>> f=ezplot(phi6,0,2)
>> set(f,'color','b','LineStyle',':')
>> ylabel('phi')
>> title('')
>> Legend('a','b','c','d','e','f','Location','northwest')
```


APPENDIX VI

LIST OF PUBLICATIONS

Sulemana M., Seini I.Y., Daabo M.I. (2017), Unsteady Boundary Layer Flow Past a Vertical Plate in the Presence of Transverse Magnetic Field and Heat Source Embedded in a Porous Medium, Journal of Mathematical and Computational Science, Vol. 7, No 3, 564-582.

Sulemana M., Seini I.Y., Daabo M.I. (2017), Unsteady hydromagnetic convective heat and mass transfer past an impulsively started infinite vertical surface with Newtonian heating in a porous medium, Journal of Engineering and Applied Sciences, Vol. 12(1), 5767-5776.